Life cycle, biochemistry and chemotherapy of *Spironucleus vortens*

CARDIFF UNIVERSITY

PRIFYSGOL CAERDYD

A thesis submitted for the degree of

Philosophiae Doctor **(Ph.D)**

by

Catrin Ffion Williams

April 2013

School of Biosciences

Cardiff University

ACKNOWLEDGEMENTS

DECLARATION AND STATEMENTS

DECLARATION

This work has not been submitted in substance for any other degree or award at this or any other university or place of learning, nor is being submitted concurrently in candidature for any degree or other award.

Signed …………………………………… (candidate) Date …………………………

STATEMENT 1

This thesis is being submitted in partial fulfilment of the requirements for the degree of PhD.

Signed …………………………………… (candidate)   Date …………………………

STATEMENT 2

This thesis is the result of my own independent work/investigation, except where otherwise stated. Other sources are acknowledged by explicit references. The views expressed are my own.

Signed …………………………………… (candidate)   Date …………………………

STATEMENT 3

I hereby give consent for my thesis, if accepted, to be available for photocopying and for inter-library loan, and for the title and summary to be made available to outside organisations.

Signed …………………………………… (candidate)   Date …………………………

STATEMENT 4: PREVIOUSLY APPROVED BAR ON ACCESS

I hereby give consent for my thesis, if accepted, to be available for photocopying and for inter-library loans after expiry of a bar on access previously approved by the Academic Standards & Quality Committee.

Signed …………………………………… (candidate)   Date …………………………

CONTENTS

CHAPTER 7: Antioxidant defences of *Spironucleus vortens*: an aerotolerant anaerobic diplomonad parasite.. 141

LIST OF FIGURES

LIST OF TABLES

ABBREVIATIONS

$[O_2]_{V=0}$	Lower O_2 tension at which O_2 consumption ceased
$[O_2]_{V=i}$	Upper O_2 tension which was inhibitory to O_2 consumption
16S	Small ribosomal RNA subunit
AA	Allyl alcohol
AD	Allyl disulphide
ADH	Arginine dihydrolase
ADH	Alcohol dehydrogenase
AF	Auranofin
AIC	Akaike information criterion
Aj	Ajoene
Al	Allicin
ALT	Alanine aminotransferase
AMD	Allyl methyl disulphide
AMS	Allyl methyl sulphide
ANOVA	Analysis of variance
AS	Allyl sulphide
AST	Aspartate aminotransferase
ATCC	American Tissue Culture Collection
ATM	Sodium aurothiomalate
ATP	Adenosine triphosphate
AZO	Azomycin
bp	Base pair(s)
BSA	Bovine serum albumin
c	Concentration (moles/L)
CM	Culture medium
CWP1	Cyst wall protein 1
DADS	Diallyl disulphide
DATS	Diallyl trisulphide
dH_2O	Distilled water
DIC	Differential interference contrast
DMSO	Dimethyl sulfoxide
DTNB	Ellman's reagens 5-5'-dithiobis-(2-nitrobenzoic acid)

e	Molar extinction coefficient
EC	Enzyme commission
EDTA	Ethylenediaminetetraacetic acid
E_t	Efficacy of treatment
FAC	Ferric ammonium citrate
FAD	Oxidised flavin adenine dinucleotide
$FADH_2$	Reduced flavin adenine dinucleotide
FDI	Flavodiiron protein
Fd_{ox}	Oxidized ferredoxin
Fd_{red}	Reduced ferredoxin
FIC	Fractional inhibitory concentration
FR	Fenton reaction
FTIC	Fluorescein isothiocyanate
GC-MS	Gas Chromatography Mass Spectrometry
GDH	Glutamate dehydrogenase
gdh	Glutamate dehydrogenase (gene)
GLM	General linear model
GLMM	Generalized linear model
GSH	Reduced glutathione
GSR	Glutathione reductase
GSSG	Oxidized glutathione
GST	Glutathione-S-transferase
Gtm	Glutamate
HEPES	4-(2-hydroxyethyl)-1-piperazineethanesulfonic acid
HEPPS	3-[4-(2-hydroxyethyl)-1-piperazinyl]-propanesulfonic acid
HITH	Hole-in-the-head
HPLC	High Performance Liquid Chromatography
HWR	Harber-Weiss reaction
Hyd	Hydrogenase
IC_{50}	Concentration which inhibits growth by 50%
IEF	Isoelectric focusing
IND	Indifferent
K_m	O_2 affinity
K_t	O_2 tolerance

l	Path length (1 cm)
L_0	Faecal trophozoite count before treatment
LDH	Lactate dehydrogenase
L_t	Faecal trophozoite count after treatment
Mal	Malate
MALDI TOF MS/MS	Matrix Assisted Laser Desorption Ionization Tandem Mass Spectrometry
MBB	Monobromobimane
MBC	Monochlorobimane
MD	Methyl disulphide
MDH	Malate dehydrogenase
MDO	Mitochondria-derived organelle(s)
ME	Malic enzyme
MIC	Minimum inhibitory concentration
MTZ	Metronidazole
N	Number of replicates/samples
$NAD(P)^+$	Oxidised nicotinamide adenine dinucleotide (phosphate)
NAD(P)H	Reduced nicotinamide adenine dinucleotide (phosphate)
NBCS	New born calf serum
NC	Negative control
ND	Not determined
NMR	Nuclear magnetic resonance
NO	NADH oxidase
OD	Optical density
PBS	Phosphate buffered saline
PC	Positive control
PCR	Polymerase Chain Reaction
PD	Propyl disulphide
PDC	Pyruvate decarboxylase
PDI	Protein disulphide isomerase
PFOR	Pyruvate:ferredoxin oxidoreductase
pI	Isoelectric point
PIPES	Piperazine-N,N′-bis(2-ethanesulfonic acid)
Prx	Peroxiredoxin

PS	Propyl sulphide
Pyr	Pyruvate
R_0	Basic reproduction number
RBR	Rubrerythrin
rDNA	Ribosomal DNA
ROS	Reactive O_2 species
RP-HPLC	Reverse Phase High Performance Liquid Chromatography
rRNA	Ribosomal RNA
SEM	Scanning Electron Microscopy
SOD	Superoxide dismutase
SSU	Small subunit
Sv1	New *Spironucleus vortens* isolate
SvP1-8	*Spironucleus vortens* proteins
SYN	Synergy
TCA	Trichloroacetic acid
TFC	Trophozoite faecal count
TNB	2-nitro-5-thiobenzoate
Trx	Thioredoxin
$Trx(S)_2$	Oxidized thioredoxin
$Trx(SH)_2$	Reduced thioredoxin
TrxR	Thioredoxin reductase
TZ	Tinidazole
WST-1	2-(4-iodophenyl)-3-(4-nitrophenyl)-5-(2, 4-disulphophenyl)-2H-tetrazolium, monosodium salt
ΔA	Abosbance/min
$\mu 1$	First logarithmic growth phase
$\mu 2$	Second logarithmic growth phase

PUBLICATIONS

Refereed and submitted papers

1. Fernández-Moreia V, Thorpe-Greenwood FL, Amoroso AJ, Cable J, Court JB, Grey V, Hayes AJ, Jenkins RL, Karriuki BM, Lloyd D, Millet COM, **Williams CF**, Coogan MP (2010). Uptake, localisation, toxicity and stability of rhenium *fac*-tricarbonyl bisimine pyridine derivatives as fluorophores in cell imaging studies in yeast and human breast cancer cells. OBC 8: 3888-3891

2. Millet COM, Lloyd D, **Williams CF**, Williams D, Evans G, Saunders RA, Cable J (2010). Effect of garlic and allium-derived products on the growth and metabolism of *Spironucleus vortens.* Exp Parasitol 127: 490-499

3. Millet COM, Lloyd D, **Williams CF**, Cable J (2011). *In vitro* culture of the diplomonad fish parasite *Spironucleus vortens* reveals unusually fast doubling time and atypical biphasic growth. J Fish Dis 34: 71-73

4. Thorpe-Greenwood FL, Fernández-Moreira V, Millet CO, **Williams CF**, Cable J, Court JB, Hayes AJ, Lloyd D, Coogan MP (2011). A 'Sleeping Trojan Horse' which transports metal ions into cells, localises in the nucleoli, and has potential for bimodal fluorescence/PET imaging. Chem Commun 47: 3096-3098

5. **Williams CF,** Lloyd D, Poynton SL, Jørgensen A, Millet COM, Cable J (2011). *Spironucleus* species: economically-important fish pathogens and enigmatic single-celled eukaryote*s.* J Aquac Res Development S2-002

6. Balasingham RG, Thorp-Greenwood FL, **Williams CF**, Coogan MP, Pope SJA (2012). Biologically compatible, phosphorescent dimetallic rhenium complexes linked through functionalized alkyl chains: syntheses, spectroscopic properties, and applications in imagining microscopy. Inorg Chem 51: 1419-1426

7. **Williams CF**, Lloyd D (2012). Composition and antimicrobial properties of sulphur-containing constituents of garlic (*Allium sativum*). In: Essential Oils as Natural Food Additives: Composition, Quality and Antimicrobial Activity. Ed. Valgimigli L. Nova Publishers, Inc. NY, USA, pp. 287-304

8. **Williams CF**, Lloyd D, Kolarich D, Alagesan K, Duchene D, Cable J, Williams D, Leitsch D (2012). Disrupted intracellular redox balance of the diplomonad fish parasite *Spironucleus vortens* by 5-nitroimidazoles and garlic-derived compounds. Vet Parasitol 190: 62-73

9. Fernández-Moreira V, Ortego ML, **Williams CF**, Coogan MP, Villacampa MD, Gimeno MC (2012). Bioconjugated rhenium(I) complexes with amino acid derivatives: synthesis, photophysical properties, and cell imaging studies. Organometallics 31: 5950-5957

10. Balasingham RG, **Williams CF**, Mottram HJ, Coogan MP, Pope SJA (2012). Gold(I) complexes derived from alkynyloxy-substituted anthraquinones: syntheses, luminescence, preliminary cytotoxicity, and cell imaging studies. Organometallics 31: 5835-5843

11. **Williams CF**, Kombrabail M, Vijayalakshmi K, White N, Krishnamoorthy G, Lloyd D (2012). Evaluation of two novel methods for assessing intracellular O_2. Meas Sci Technol 23: 084005

12. Joshi LT, Phillips DS, **Williams CF**, Alyousef A, Baillie L (2012). Contribution of spores to the ability of *Clostridium difficile* to adhere surfaces. Appl Environ Microbiol 78: 7671-7679

13. Leitsch D, **Williams CF**, Lloyd D, Duchêne M (2013). Unexpected properties of NADP-dependent secondary alcohol dehydrogenase (ADH-1) in *Trichomonas vaginalis* and other microaerophilic parasites. Exp Parasitol 134: 374-380

14. **Williams CF**, Vacca AR, Lloyd D, Schelkle B, Cable J (in press). Non-invasive estimation of *Spironucleus vortens* in angelfish provides novel insights on the transmission of this diplomonad parasite. Dis Aquat Organ DOI: 10.3354/dao02618

15. **Williams CF**, Millet COM, Hayes AJ, Hann AC, Cable J, Lloyd D (in press). Diversity in mitochondria-derived organelles of the parasitic diplomonads *Spironucleus* and *Giardia*. Trends Parasitol DOI: 10.1016/j.pt.2013.04.004

16. Pritchard V, Thorp-Greenwood F, Balasingham R, **Williams CF**, Kariuki B, Platts J, Hallett A, Coogan MP (submitted). Simple polyphenyl zirconium and hafnium metallocene room-temperature lumophores for cell imaging.

17. Williams CF, Cable J, Yarlett N, Aon MA, Lloyd D (submitted). Antioxidant defences of *Spironucleus vortens*: glutathione is the major non-protein thiol.

Oral presentations

1. **Williams CF**, Millet COM, Cable J, Coogan M, Lloyd D, Williams D. (2010). Garlic: a potential cure for 'hole-in-the-head' disease in fish? Presented at: Plant-Micro Wales Meeting, 12-13 July, 2010 and International Society of Protistologists (ISOP), Canterbury 18-23 July, 2010.

2. **Williams CF**, Aon MA, Yarlett N, Cable J, Lloyd D (2011). Effects of inhibitors on the redox dynamics of *Spironucleus vortens*. Presented at: Plant-Micro Wales Meeting, Bangor, 11-12 July, 2011 (awarded 2nd prize for student presentations) and European Congress of Protistologists (ECOP), Berlin, 25-29 July, 2011.

Poster presentations

1. **Williams CF**, Millet COM, Cable J, Coogan M, Lloyd D, Williams D. (2010). Garlic: a potential cure for 'hole-in-the-head' disease in fish? Presented at: British Society for Parasitology Spring Meeting, Cardiff, 30 March-1 April, 2010 and South Wales and South West Microbiology Forum, Cardiff, 23 September, 2010.

2. **Williams CF**, Leitsch D, Dunham L, Cable J, Coogan MP, Williams D, Lloyd D (2011). *Spironucleus vortens*: a proteomic study of novel and traditional chemotherapeutic

agents. Presented at: European Congress of Protistologists (ECOP), Berlin, 25-29 July, 2011.

3. **Williams CF**, Kombrabail M, Vijayalakshmi K, White N, Krishnamoorthy G & Lloyd D (2011). Evaluation of two novel methods for assessing intracellular O_2. Presented at: Nano Meets Spectroscopy, London, 15-16 September, 2011.

4. **Williams CF**, Millet COM, Cable J, Coogan MP, Lloyd D (2012). *Spironucleus vortens*: economically-important fish pathogens and enigmatic diplomonad flagellates. Presented at: 5th International Conference on Anaerobic Protists (ICAP), Los Angeles, 6-9 September, 2012 and All Wales and South West Microbiology Forum, Swansea, 13-14 September, 2012 (awarded 1st prize for student presentations).

SUMMARY

Spironucleus is an opportunistic protozoan parasite capable of causing devastating losses in the production of both ornamental and food fish. Control of infection outbreaks is problematic due to restrictions on the use of chemotherapeutics and rapid parasite transmission amongst fish. This PhD investigated the life cycle, biochemistry and chemotherapy of *Spironucleus vortens*. Direct transmission of *S. vortens* was found to be facilitated by the trophozoite form, information which may be applied in aquaculture to prevent infection outbreaks. No *S. vortens* cysts were observed *in vitro* or *in vivo* and trophozoites were able to survive for prolonged periods in the faeces of angelfish. This novel finding facilitated development of a non-invasive method to quantify the degree of intestinal colonization in the host, which was then applied to determine the efficacy of new and existing chemotherapeutics against *S. vortens in vivo*. Garlic-derived compounds were shown to be realistic alternatives to the current drug of choice, metronidazole, in the treatment of Spironucleosis in fish. Synergy between metronidazole and the garlic-derived compound, ajoene, was also observed *in vitro* and *in vivo*. The mode of action of metronidazole and garlic-derivatives involved disruption of *S. vortens* intracellular redox balance, a pivotal cellular process which ensures normal cellular function and survival. Further biochemical investigations into the antioxidant defence system (consisting of glutathione, thioredoxin and superoxide dismutase) as well as the carbohydrate and amino acid metabolism of *S. vortens* provided greater understanding of the success of this organism as a parasite. This is reflected in its ability to withstand fluctuations in O_2 and nutrition during key pathogenic stages of its life cycle, including extra-intestinal systemic infection and transmission to a new host.

Chapter 1

Introduction

CHAPTER 1: INTRODUCTION

Adapted from:

Spironucleus species: Economically-Important Fish Pathogens and Enigmatic Single-Celled Eukaryotes

Catrin F Williams[1]*, David Lloyd[1], Sarah L Poynton[2], Anders Jorgensen[3], Coralie OM Millet[1] and Joanne Cable[1]*

[1]*School of Biosciences, Cardiff University, Cardiff CF10 3AT, Wales, UK*
[2]*Comparative Medicine, Johns Hopkins University, School of Medicine, Baltimore, MD, USA*
[3]*Norwegian Veterinary Institute, Oslo, Norway*

1.1. OVERVIEW

Diplomonads (suborder Diplomonadida, family Hexamitidae) are a group of aerotolerant anaerobic or microaerophilic flagellates, which possess a double set of cellular organelles. Amongst the diplomonad genera are *Hexamita*, *Octomitus*, *Giardia* and *Spironucleus* (Poynton & Sterud 2002). Species of *Hexamita* are mostly free-living organisms that reside in anaerobic water sediments (Fenchel et al. 1995), whereas the other taxa are almost exclusively parasites, which commonly occur in the intestinal tract of mammals, birds, reptiles, amphibians and fish (Brugerolle 1975; Poynton et al. 1995; Sterud et al. 1998; Adam 2001; Cooper et al. 2004; Fain et al. 2008).

Spironucleus spp. are of particular importance in the aquaculture industry due to their ability to cause systemic infections in both ornamental and food fish (Nigrelli & Hafter 1947; O'Brien et al. 1993; Sterud 1998a; Sterud et al. 1998; Tojo & Santamarina 1998; Paull & Matthews 2001; Guo & Woo 2004a,b; Jørgensen & Sterud 2006). In 2009, fish accounted for 16.6% of the world population's intake of animal protein and 6.5% of all protein consumed (FAO 2012). Hence, as wild fish stocks become increasingly depleted, fish farming is becoming a popular alternative to supply the ever increasing global demand for fish. Aquaculture is a multi-billion dollar industry which has been expanding at an average rate of 3.2% per year in the period of 1961-2009, outpacing the annual 1.7% increase in the world's population (FAO 2012). Globally, capture fisheries and aquaculture supplied 148 million tonnes of fish in 2010, with a total value of US$217.5 billion (FAO 2012). Disease is a major limiting factor to aquaculture production, resulting in losses of 45% to the industry per annum (FDA 2012). *Spironucleus* spp. are ubiquitously found in tropical, temperate and cold waters and have

a broad host-range encompassing freshwater (O'Brien et al. 1993; Tojo & Santamarina 1998; Paull & Matthews 2001) and marine fish (Poynton & Morrison 1990; Sterud 1998b; Sterud et al. 2003; Jørgensen & Sterud 2004, 2006). *Spironucleus salmonicida* causes significant outbreaks of systemic Spironucleosis in Norwegian *Salmo salar* (Atlantic salmon) (Mo et al. 1990; Poppe et al. 1992; Poppe & Mo 1993; Sterud et al. 1998) and British Columbian *Oncorhynchus tshawytscha* (Chinook salmon) (Kent et al 1992). In ornamental fish farms, *Spironucleus vortens* also causes outbreaks of systemic infections, which have been linked to a manifestation referred to as hole-in-the-head disease in aquaculture (Paull & Matthews 2001). Outbreaks of Spironucleosis results in significant host mortality (Guo and Woo 2004a&b).

Although the pathogenic potential of some *Spironucleus* spp. is widely accepted (Mo et al. 1990; Poppe et al. 1992; Poppe & Mo 1993; Sterud et al. 1998; Paull & Matthews 2001), it has been suggested that *Spironucleus* spp. are putative intestinal commensals, which become invasive in fish hosts with a compromised immune system or those which lack acquired immunity, under aquacultural conditions (Woo & Poynton 1995; Dawson et al. 2008). This is reflected in the observation that *Spironucleus* infections in wild fish are generally non-pathogenic (e.g. *S. barkhanus* in wild grayling, Sterud et al. 1997, and *S. torosa* in wild gadids, Poynton & Morrison 1990). Stressful conditions sometimes observed in aquaculture, including poor water quality, temperature fluctuations and overcrowding, have thus been implicated as triggers of *Spironucleus* pathogenesis (Bassleer 1983; Whaley & Francis-Floyd 1991; Woo & Poynton 1995).

Disease management and chemotherapy of Spironucleosis is problematic as important aspects of parasite transmission, host/geographical range and pathogenicity are poorly understood. Identification of infection outbreaks is especially difficult as is accurate diagnosis, due to the need for expert morphological investigations (using electron microscopy) or molecular techniques (such as 16S rDNA PCR) for species-level identification (Jørgensen & Sterud 2006). Confusion in the nomenclature, incomplete species descriptions and species misidentifications of hexamitid parasites further hinders advances in the field and inter- or intra-species comparisons are difficult as few specimens were deposited in reference collections. An added complication in infection control is the ban on use of the drug of choice, metronidazole, on European and American food fish farms (Commission Regulation No. 613/98, 1998; FARAD, 2010).

Research on many fish microparasites is hampered by an inability to fulfil Koch's postulates. However, recent advances in our ability to identify cryptic species of

Spironucleus, to culture the pathogens and accurately monitor their biochemistry paves the way for a better understanding of diplomonad biology and subsequent parasite chemotherapy.

1.2. LIFE CYCLE

Identification of piscine diplomonads relies on the characterisation of two distinct stages of the life cycle; the easily recognized and actively swimming trophozoite, and the non-motile cyst form (Fig 1.1). The trophozoite is the feeding stage of the parasite (see Section 1.5 for nutritional requirements), which also undergoes asexual reproduction by longitudinal binary fission, as is typical for flagellates. This stage is most familiar to fish health investigators, since it is commonly encountered in the intestinal lumen, and less commonly in bile, blood, and organs (O'Brien et al. 1993; Poppe & Mo 1993; Poynton et al. 1995; Sterud et al. 1998; Paull & Matthews 2001; Guo & Woo 2004a). Prolonged *in vitro* culture of the trophozoite stage has been achieved in trypticase-yeast extract-iron (TY-I-S33) culture medium (Poynton et al. 1995; Sterud 1998a; Sangmaneedet & Smith 1999; Millet et al. 2010a).

Trophozoites typically do not survive for long periods in freshwater (Kent et al. 1992), but have been detected in fresh faecal samples from *Oncorhynchus mykiss* (rainbow trout) infected with *S. salmonis* (see Tojo & Santamarina 1998). The same study reported lack of *S. salmonis* cysts in the faeces of heavily infected fish, highlighting the rarity of these forms. Despite this, *S. salmonis* cysts have been observed *in vivo* (Moore 1922; David 1926) as well as *in vitro* (Uldal 1996). Cysts of other piscine *Spironucleus* spp. are poorly characterized. The cyst form facilitates direct transmission through the aquatic environment via the faecal-oral route (Woo & Poynton 1995); however transmission via skin lesions (Poppe et al. 1992) as well as through the rectal route by both cyst and trophozoite (Kent et al. 1992) has also been suggested. For those *Spironucleus* spp. where cysts have been documented, the resilience of the cyst wall confers protection against harsh external conditions including osmotic changes, high O_2 tensions and temperature fluctuations (Corliss 2001). After ingestion by a new host, the cyst passes along the digestive tract, and excysts releasing trophozoites and completing the life cycle (Woo & Poynton 1995).
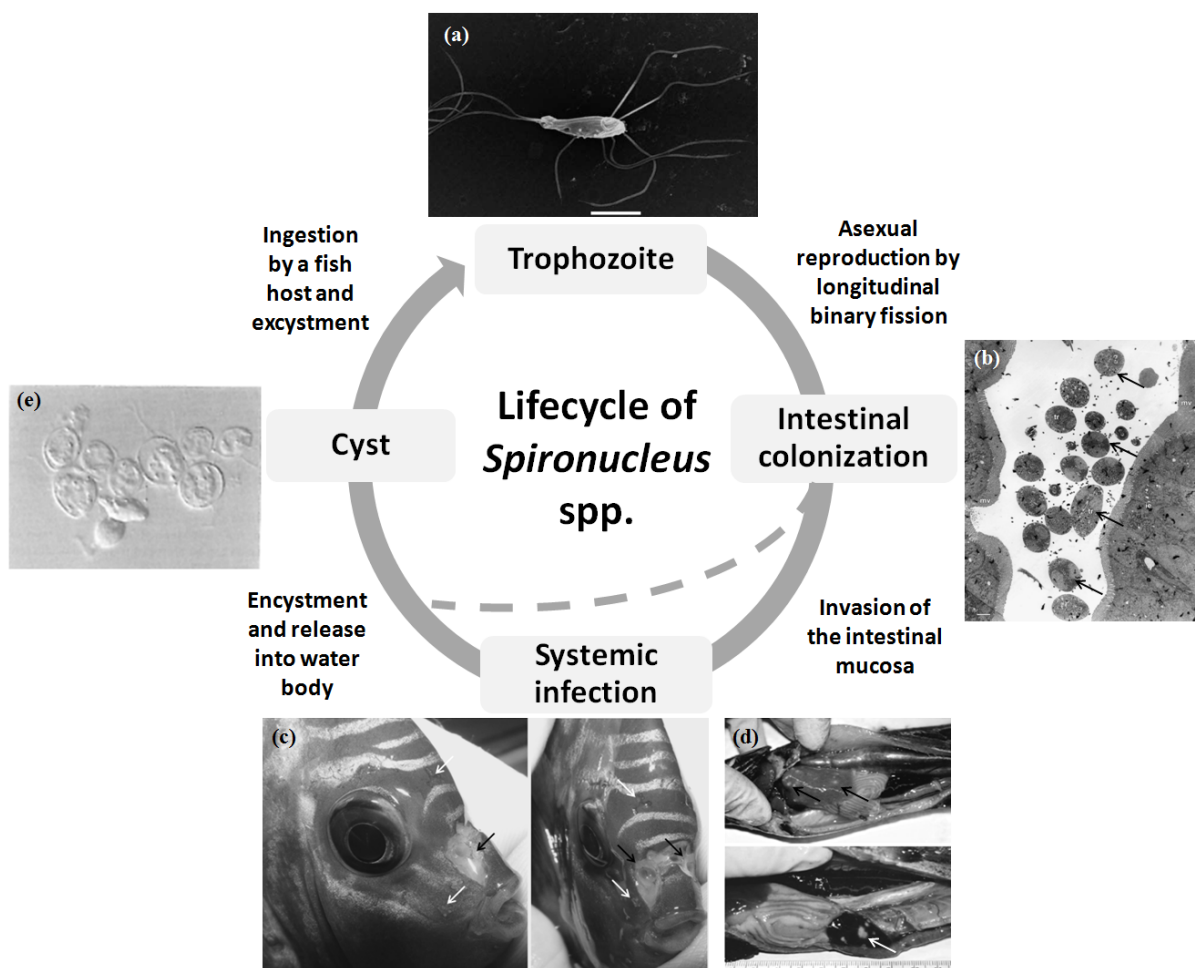
Fig. 1.1. Depiction of the typical life cycle of *Spironucleus* spp. A flagellated *Spironucleus* trophozoite resides in the intestinal tract of the fish host, scale bar = 5 µm (a). Multiplication of the parasite leads to intestinal colonization (b), arrows indicate presence of numerous trophozoites in the intestinal lumen (transverse section). Invasion of the intestinal mucosa leads to systemic infection, manifesting as hole-in-the-head disease in ornamental fish (c), white arrows indicate small, bilaterally symmetrical lesions, black arrows indicate larger lesions which have coalesced (pers. obs.). Granulomatous nodules (indicated by arrows) in the liver and spleen are associated with systemic Spironucleosis in *Salmo salar* (d). Transmission of the parasite through the water body is facilitated via an encysted form (e), following intestinal colonisation (dashed line) or systemic infection. Images adapted from Paull and Matthews (2001) with permission from Inter-Research (a), Poynton et al. 2004 with permission from Inter-Research (b), pers. obs. (c) Guo and Woo 2004b with permission from Inter-Research (d) and Uldal 1996 with permission from The European Association of Fish Pathologists (e).

Details of the transformation from trophozoite to cyst (encystment), and from cyst to trophozoite (excystment) are poorly understood for piscine *Spironucleus*. As a result most details of the life cycle are inferred from avian (Wood & Smith 2005) and mammalian (Januschka et al. 1988; Koudela et al. 1996) *Spironucleus* spp., as well as the related genus *Giardia* in mammals (Kunstýr 1977; Kunstýr & Ammerpohl 1978; Brugerolle et al. 1980; Januschka et al. 1988). Common features of encystment in diplomonads are the quiescence of the trophozoite, production of cyst wall material in the cytoplasm and its trafficking to the surface, formation of the cyst wall and doubling of the flagellate within the cyst (Moore 1922; Kulda & Nohynkova 1978; Siddall et al. 1992). *In vitro* encystment of *S. salmonis* has been induced by starvation of trophozoites in spent culture medium (Uldal 1996). Furthermore, *in vitro* excystment of *S. muris* from mouse faeces was achieved by a low pH induction medium, followed by transfer to a neutral pH buffer or TY-I-S33 culture medium, mimicking passage of the cyst through the gastrointestinal tract (Koudela et al. 1996). Fundamental questions remain about the life cycle of *Spironucleus* in fish, including triggers for encystment, duration of infectivity, minimum infective dose and triggers for excystment.

1.3. TAXONOMY AND IDENTIFICATION

Although taxonomic confusion in the literature regarding the genera of diplomonads that infect fish remains, ultrastructural characterization has brought much needed clarity. Studies using only light microscopy have assigned the piscine diplomonads to *Hexamita*, *Octomitus* and *Spironucleus*. However, transmission electron microscopy has confirmed that all piscine diplomonads examined to date, belong unequivocally to the genus *Spironucleus*. Using this approach, 5 species of piscine diplomonads are currently recognized: *S. barkhanus, S. salmonicida, S. salmonis, S. torosa* and *S. vortens*. All of these species have only been comprehensively characterized from fishes in northwest Europe. However, given the global diversity of fish species, and the importance of aquaculture in Asia, it is likely that additional distinct species will be described from other parts of the world in the future.

1.3.1. Reference Specimens

Table 1.1 summarises the type host, type locality, type material and Accession Numbers of the best described *Spironucleus* spp. from fish, although even this is

incomplete. This is exemplified in a recent study, which demonstrates that *S. salmonicida* can be found in the intestine of wild *Salmo trutta* (Brown trout) and *Salvelinus alpinus* (Arctic charr) (Jørgensen et al. 2011). However, farmed *Salmo salar* (Atlantic salmon) were designated the type host of *Spironucleus salmonicida* due to the lack of a wild host (Jørgensen & Sterud 2006). Based on current knowledge, Brown trout or Arctic charr should probably have been chosen as type host of *S. salmonicida*; however a formal re-description must then be undertaken. No reference material or sequence data are available from the original description of *S. elegans* (type host: amphibians) (Lavier 1936), although Brugerolle et al. (1973) provided a valuable ultrastructural description. Based on morphology, Poynton et al. (1995) considered a hexamitid isolated from angelfish to be different from *S. elegans* and thus described *S. vortens*. The conspecificity of *S. vortens* and *S. elegans* was later questioned due to the remarkable ultrastructural similarities between the two species (Sterud & Poynton 2002), but has not been resolved. *S. vortens* (type host: *Pterophyllum scalare*, angelfish) has been described from several species of aquarium fish and also from wild *Leuciscus idus* (ide) in Norway (Sterud & Poynton 2002). Subsequently, sequencing of the small subunit ribosomal RNA (SSU rRNA) gene revealed that the isolates from angelfish and ide were genetically more distant than *S. salmonicida* and *S. barkhanus* and therefore should be regarded as separate species (Jørgensen & Sterud 2007). However, again no formal description has been made.

1.3.2. Morphological Identification

The genus *Spironucleus* have been subjected to considerable taxonomic confusion due to limited species descriptions based on light microscopy only. An example of this is illustrated by four Chinese studies which reported a total of 25 new species of *Spironucleus* and *Hexamita* from various fish species (Xiao & Li 1993, 1994; Li & Nie 1995; Xiao et al. 2002). Most of these descriptions were based on light microscopy and/or poorly resolved ultrastructural data, thus these species should be regarded as insufficiently characterized. Detailed ultrastructural investigation, described below, using scanning and transmission electron microscopy is required in order to accurately distinguish between *Spironucleus* spp. Table 1.2 summarizes genus and species-specific morphological characteristics of piscine diplomonads.

Morphological characterization of *Spironucleus* is based upon the trophozoite form which is easily recognized, even by non-specialists. The cyst form has rarely been reported from fish, and ultrastructure information of this stage from fish hosts is not

available (Poynton & Sterud 2002). Trophozoites are characterised according to their distinct spherical to pyriform body, approximately 10–20 µm long and 5–10 µm wide, which is actively propelled through the water by the six anterior locomotory flagella. From the posterior of the body trail two additional flagella. Observation of actively swimming trophozoites shows that the six locomotory flagella are approximately 1.5 times the body length and emerge from the anterior body in two groups of three. The two trailing flagella are approximately twice the body length, and emerge from the posterior of the body close to each other. The six anterior flagella originate anterio-medially, near the meeting of the nuclei, and travel just a short distance before emerging anterio-laterally. In contrast, the two posterior flagella, which also originate near the meeting of the nuclei, run within the body from the anterior to the posterior (through an invagination of the cell membrane called the flagellar pocket), and then emerge as trailing flagella (Poynton & Sterud 2002).

1.3.2.1. Light Microscopy

All genera of diplomonads have paired anterior nuclei, the exact shape and location of which are diagnostic for the genus. The nuclei of *Spironucleus* are elongate and taper anteriorly, lying very close to each other at the extreme anterior of the cell. Both *S. torosa* and *S. vortens* have an accessory cytoskeleton, composed of microtubular bands supporting surface ornamentation. In *S. torosa* these microtubular bands appear as two loops at the posterior of the cell, each representing the microtubules in a torus (raised round structure) surrounding the opening of the flagellar pocket (Poynton & Sterud 1990). Conversely, in *S. vortens*, the accessory cytoskeleton is evident as a dark staining area at the extreme posterior of the cell, representing the complex of counter-crossing microtubular bands supporting the elaborate folds between the emerging posterior flagella (Poynton et al. 1995).

Table 1.1. Host-range, geographical location and micro-habitat of cultured *Spironucleus* spp.

Species	Type host	Additional hosts	Type locality	Location in host	Type material	Reference culture	Reference sequence (GenBank Acc.)
S. barkhanus[1]	*Thymallus thymallus*	*Salvelinus alpinus* *Salmo trutta*	River Glomma, Norway	Lumen of gut and gall bladder	B	ATCC 50467	DQ186581
S. elegans[2]	*Triturus alpestris* *Rana rana*	*Pterophyllum scalare*	NA	Intestine	NA	NA	NA
S. salmonicida[3]	*Salvelinus alpines*	*Oncorhychus namaykush* *Salmo salar*	Fiskfjorden, Norway (68°N, 15°E)	Systemic infection	C	ATCC 50377	DQ181595
S. salmonis[4]	*Salvelinus fontinalis*	*Oncorhynchus mykiss*	Bath, New York State, USA	Digestive tract, upper intestinal region	NA	NA	DQ394703
S. torosus[5]	*Gadus morhua*	*Melanogrammus aeglefinus* *Lota lota*	Chebucto Head approach to Halifax Harbour, Nova Scotia, Canada	Digestive tract, rectum in cod	D	NA	EF050055
S. vortens[6]	*Pterophyllum scalare*	*Leuciscus idus* *Symphysodon discus*	Archer, Florida, USA (29° 32'N, 82° 31W)	Lumen of intestine	A	ATCC 50386	U93085

[A] Holotype slide of protargol-impregnated specimens and TEM block in the International Protozoan Slide collection at the National Museum of Natural History, Smithsonian Institution, Washington D.C. Accession number USNM #47820.

[B] TEM blocks and SEM stubs kept at the Norwegian School of Veterinary Science, Oslo, Norway,

[C] SEM stub: 180-1 (hapantotype) deposited in the International Protozoan Slide collection at the National Museum of Natural History, Smithsonian Institution, Washington. D.C. Accession number USNM 1093603. TEM blocks: 2718-3, 2718-5, 2618-25 and 2618-30 representing paratypes are deposited at Norwegian School of Veterinary Science, Oslo.

[D] Holotype and numerous paratypes deposited in the Invertebrate Collection (Parasites), National Museum of Natural Sciences, Ottawa, Canada. Accession number NMCP 1988-0899.

Citations: [1]Sterud et al. 1997; [2]Lavier 1936; [3]Jørgensen & Sterud 2006; [4]Moore 1922; [5]Poynton & Morrison 1990; [6]Poynton et al. 1995.

1.3.2.2. Electron Microscopy

The surface of a *Spironucleus* trophozoite is mostly smooth, although discharging vacuoles undergoing exocytosis may be seen. In 4 out of the 5 well described *Spironucleus* spp. from fish, surface ornamentation is distinctive. Its function is unknown, but is useful for species identification (Fig 1.2). *S. barkhanus* and *S. salmonicida* have a crescent-shaped ridge (barkhan) around the opening of each flagellar pocket (Sterud et al. 1997), while *S. torosa* has a ring-shaped swelling (torus) around the flagellar pocket (Poynton & Morrison 1990) and *S. vortens* is characterised by lateral ridges bearing tufts of microfibrils, which then form counter-crossing ridges between the opening of the flagellar pockets (Poynton et al. 1995). The presence of posterior papillae is also characteristic of *S. vortens* (Poynton et al. 1995). *S. salmonis* lacks ornamentation (Poynton et al. 2004).

Internal ultrastructure reveals that the *Spironucleus* trophozoite is rotationally symmetrical about its long axis, with each cell having a double set of organelles (Brugerolle et al. 1973). The paired nuclei taper anteriorly and are wrapped around each other at their apices, forming an S-shape when viewed in transverse section of the anterior end of the cell. The cytoplasm of piscine diplomonads typically comprises a homogenous area at the apex of the cell, but elsewhere it is heterogeneous and organelle-rich. The latter contains a variety of organelles, which may include (depending upon species) electron-dense bodies, endoplasmic reticulum, membranous structures and ribosomes. *S. salmonis* is characterised by the presence of electron-dense bodies and a membrane-bound sac of free ribosomes around the opening of the flagellar pockets (Poynton et al. 2004; Sanghari-Fard et al. 2007a). Interestingly, the appearance of these cytoplasmic organelles can vary between *Spironucleus* harvested directly from the fish, and those maintained in culture (Poynton & Sterud 2002). Glycogen granules, vacuoles and bacteria may also be present in the cytoplasm (Poynton & Morrison 19990; Poynton & Sterud 2002). There are no Golgi or mitochondria present. However, recent studies suggest the presence of degenerate mitochondria, called hydrogenosomes, present within *S. vortens* (see Millet 2009) and *S. salmonicida* (see Jelström-Hultqvist 2012). Unlike mitochondria, these organelles lack DNA and cytochromes, thus oxidative phosphorylation does not take place. They do however retain some key mitochondrial features, including a double membrane, ATP production by substrate level phosphorylation of pyruvate and iron sulphur cluster assembly (see review by Shiflett &

Johnson 2010). As the name suggests, the main role of hydrogenosomes within the cell is to produce H_2 (discussed further in Section 1.5) (Bui et al. 1996).

1.3.3. Molecular identification and genetics

Until recently ultrastructure was considered sufficient to differentiate species of piscine diplomonads; however this is not entirely the case. New species descriptions of *Spironucleus* spp. should include both ultrastructural and molecular data. Guidelines for ultrastructural description of diplomonad flagellates have been presented by Poynton and Sterud (2002) and 16S PCR primers have now been developed for several taxa (Table 1.3). Sequence data of other genes, such as glutamate dehydrogenase (gdh) and α-tubulin are also available for *S. vortens*, *S. barkhanus* and *S. salmonicida* (see Andersson & Roger 2002; Andersson et al. 2003, 2007; Jørgensen & Sterud 2004, 2006, 2007; Kolisko et al. 2008). However, the SSU rRNA gene appears to be a suitable marker for species identification in the genus *Spironucleus*, even for morphologically cryptic species. This is exemplified by *S. salmonicida* and *S. barkhanus,* which are morphologically identical, but display only 92.7% similarity in 1154 bp of the SSU rRNA gene. For *S. torosa*, variation in the SSU rRNA gene separates the species into two genotypes that may be related to the two different morphologies observed (Jørgensen et al. 2007). However this genetic variation was not considered sufficient to warrant species status for the two clades (Jørgensen et al. 2007). Phenotypic differences also exist between isolates of *S. salmonicida*. The isolate causing disease in Canadian *Oncorhynchus tshawytscha* (Chinook salmon) could not establish in Atlantic salmon (Kent et al. 1992; Guo & Woo 2004b). Clinical signs and pathology in Chinook salmon also differed from those observed in *S. salmonicida* infections of Atlantic salmon in Norway. No sequence differences in the SSU rRNA, α-tubulin or gdh genes have been identified between these isolates. Completion of ongoing genome projects of *S. barkhanus* and *S. vortens* will reveal a wide range of markers for diagnostic, taxonomic, systematic and for functional studies (Andersson et al. 2007; Dawson et al. 2008; Roxström-Lindquist et al. 2010). An episomal protein-tagging shuttle vector system has already been developed for *S. vortens* (see Dawson et al. 2008) and stable transfection of *S. salmonicida* has been achieved (Jerlström-Hultqvist et al. 2012); enabling studies of protein expression, intracellular trafficking and cell signalling in *Spironucleus*.

Table 1.2. Morphological identification of diplomonads. Important ultrastructural aspects for genus and species level identification of diplomonad genera and *Spironucleus* spp. respectively. Adapted from Poynton and Sterud (2002) with permission from John Wiley & Sons Ltd.

	GENUS-LEVEL IDENTIFICATION		
Genera	*Spironucleus*	*Hexamita*	*Octomitus*
Flagellar pockets (cytostomal canals)[a]	+	+	-
Central axis formed by recurrent axonemes, microtubular bands, endoplasmic reticulum	-	-	+
Two terminal spikes	-	-	+
Shape of nuclei	S-shaped	Spherical	Reniform
Location of kinetosomes relative to nuclei	Sub-apical	External structure	Between
Position of recurrent flagella relative to nuclei	Medial	Lateral	Medial
Supra-nuclear microtubular band	+	+	Reduced
Infra-nuclear microtubular band	+	+	Reduced

	SPECIES-LEVEL IDENTIFICATION		
Species	*S. barkhanus / S. salmonicida*	*S. salmonis*	*S. torosa*	*S. vortens*
Flagellar pocket ornamentation	Crescent-shaped (barkhan)	No ornamentation	Ring-shaped swellings (torus)	Counter-crossing ridges
Microtubular pattern around flagellar pocket	3 radiate bands	-	3 concentric bands	3 staggard bands
Distinctive organelles	Hydrogenosomes[b]	Electron-dense bodies / membrane-bound sac of free ribosomes	-	Hydrogenosomes[b]

[a]When present, the recurrent flagella are ensheathed
[b]May also be present in other *Spironucleus* spp. but currently only documented in *S. vortens* and *S. salmonicida*
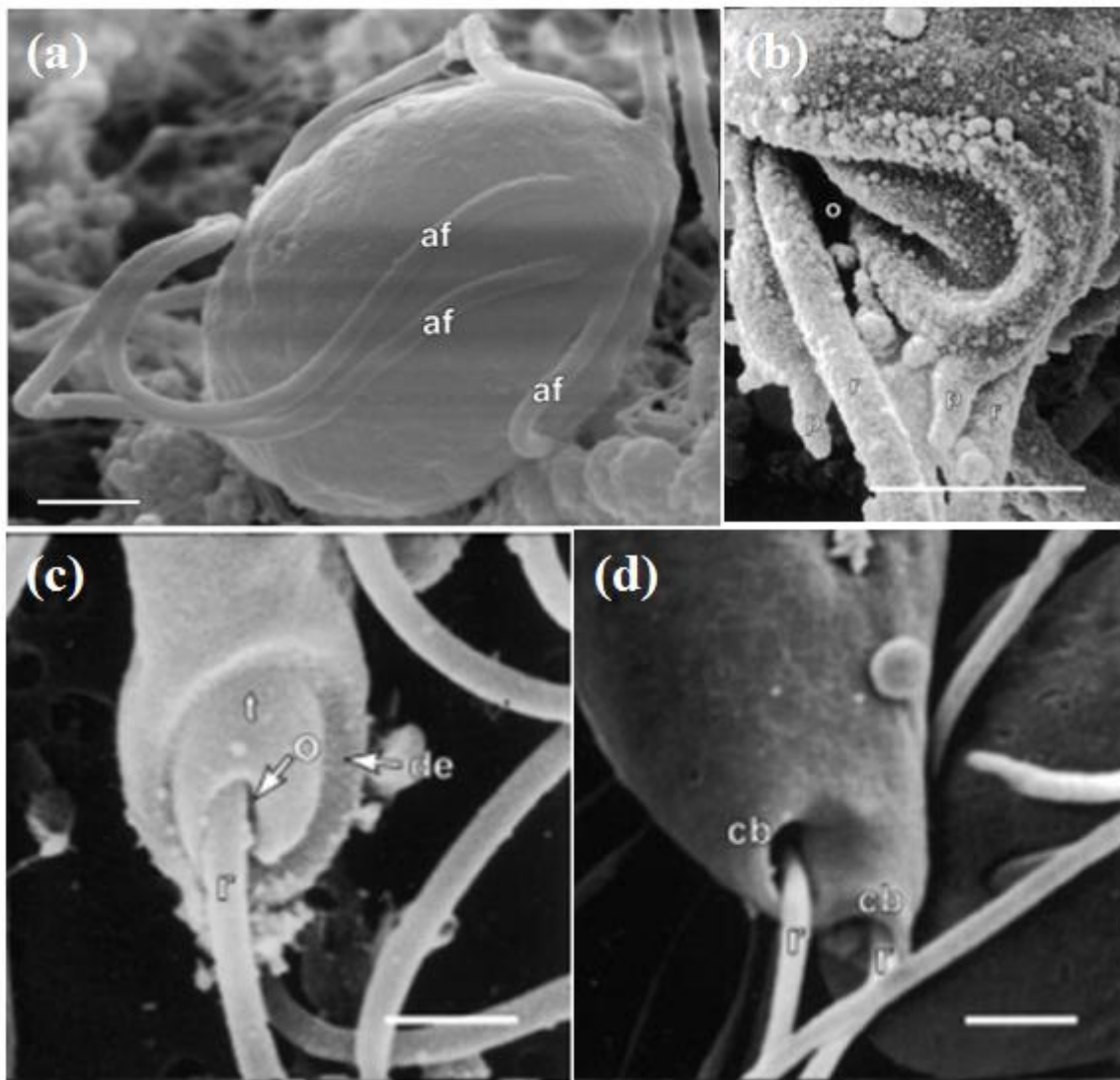
Fig. 1.2. Distinctive surface ornamentation of piscine diplomonads. Anterior-lateral view of *Spironucleus salmonis* showing emergence of anterior flagella and unadorned surface (a). Ventral or dorsal view of *S. vortens* posterior end, with counter-crossing of right peripheral ridges around exits of recurrent flagella. Presence of papillae is also of diagnostic value (b). Lateral view of *S. torosa* which has ring-shaped swellings (tori) surrounding the exits of recurrent flagella (c). Oblique view of *S. barkhanus* recurrent flagella surrounded by crescent shaped ridges (barkhans), this is also found in the the morphologically indistinguishable *S. salmonicida* (d). Abbreviations: (af) anterior flagella; (cb) crescent-shaped ridge (barkhan); (de) depression; (o) opening of flagellar pockets (cytostomal canals); (p) papilla (r) recurrent flagellum; (t) torus (scale bars = 1 µm). Adapted from Saghari-Fard et al. 2007a with permission from Inter-Research (a), Poynton et al. (1995) with permission from John Wiley & Sons Ltd (b), Sterud 1998b with permission from American Society of Parasitologists (c) and Sterud et al. 1998 with permission from Inter-Research (d).

Although genome sequencing of *S. salmonicida* has not yet been completed, genomic surveys of this parasite has revealed a reduced and compact genome with genes lacking introns, and several genes had apparently been acquired from different bacteria (Andersson & Roger 2003; Andersson et al. 2003, 2004, 2007). The genome of *S. salmonicida* has also been compared to more than 5000 expressed sequence tags (ESTs) from the morphological indistinguishable species *S. barkhanus*. The genome size of *S. salmonicida* and *S. barkhanus* is ~12 Mb and 16 Mb, respectively. In addition, codon usage and frequency of allelic variation also differs in the two species. This indicates that at least parts of the *S. barkhanus* genome have been duplicated and that these morphological indistinguishable species have been subjected to extensive divergent evolution (Roxström-Lindquist et al. 2010).

1.3.4. Phylogeny of *Spironucleus*

The diplomonads have been considered to be amongst the earliest eukaryote lineages and true intermediates in the prokaryote-eukaryote transition (Cavalier-Smith 1983). The apparent lack of eukaryotic organelles within diplomonads suggested that they diverged from other eukaryotes prior to acquisition of the mitochondrial endosymbiont. As a result, these organisms were included as members of the paraphyletic Archezoa Kingdom (Cavalier-Smith 1983). However, it was later shown that the diplomonads contained remnants of mitochondrial symbiosis. Furthermore, several mitochondrial genes were discovered in the genomes of other Archezoa (including *Giardia*) (Clark & Roger 1995; Germot et al. 1997; Embley & Hirt 1998; Hashimoto et al. 1998) suggesting that ancestors of the diplomonads once harboured the α-proteobacteria endosymbiont. Later, mitochondrion-like organelles, hydrogenosomes and mitosomes, were found in several amitochondriate eukaryotes, including *Giardia* and *Spironucleus* (see Tovar et al. 1999, 2003; Maiden 2006; Millet 2009; Jelström-Hultqvist 2012). As a result, the diplomonads have recently been re-classified into the Fornicata clade of the eukaryotic supergroup Excavata (Simpson 2003).

Currently, the genus *Spironucleus* is a member of the Diplomonadida which also contains the genera *Giardia*, *Octomitus*, *Hexamita*, *Enteromonas*, *Trimitus* and *Trepomonas* (see Kolisko et al. 2008). Phylogenetic analysis of the genus *Spironucleus* has been based on SSU rRNA gene data (Keeling & Doolittle 1996a,b; Keeling & Brugerolle 2006; Jørgensen & Sterud 2007; Kolisko et al. 2005, 2008). *Spironucleus* constitutes three branches in the Hexamitinae sub-tree (Fig 1.3). The clade containing *S.*

salmonicida, *S. barkhanus, S. torosa* and also the tortoise *Spironucleus* sp. isolate GEPA2H seems to be the most basal in the genus *Spironucleus*. *S. salmonis* and *S. vortens* are sister taxa in all SSU analyses and branch off secondary to the clade containing marine *Spironucleus* and the tortoise isolate. Both these clades are well supported. The position of the clade consisting of *S. meleagridis* (type host: birds) and *S. muris* (type host: rodents) varies and is never well supported by any tree-building method (Poynton et al. 1995; Kolisko et al. 2005, 2008).

Table 1.3. *Spironucleus* primers. These allow amplification of the small subunit ribosomal RNA (SSU rRNA) gene for identification of fish diplomonads to the genus or species level using PCR or sequencing. Spiro-1 and Spiro-2 primers will amplify most members of the genus *Spironucleus* and *Hexamita*. Spiro-3 to Spiro-6 may be used as sequencing primers for most species of *Spironucleus* and *Hexamita*. The Spironucleosis, Salmonis and Torosa primers are specific for *S. salmonicida*, *S. salmonis* and *S. torosa*, respectively.

Primer name	Sequence	Application	Reference
Spiro-1f	AAGATTAAGCCATGCATGCC	PCR/Seq	
Spiro-2r	GCAGCCTTGTTACGACTTCTC	PCR/Seq	
Spiro-3r	CATTGGGYAATYTYCCGCCCT	Sequencing	Jørgensen & Sterud 2004
Spiro-4f	GAYTCYGGAGAVTGRGCAYGAG	Sequencing	
Spiro-5r	STYTCCGTCAATMCYTTMAAGTTTC	Sequencing	
Spiro-6f	AAGRYTGAAACTTKAARGKATTGACGG	Sequencing	
Spironucleosis-1f	TCATTTATCAGTGGTTAGTACATGC	PCR/Seq	
Spironucleosis-2r	TTCAAGCCTAACCACGACAAG	PCR/Seq	
Salmonis-1f	TTGTGTACGAGGCAGTGACG	PCR/Seq	Fard et al. 2007a
Salmonis-2r	TCCCCGGTTCGTTGGTCAAG	PCR/Seq	
Torosa 16sf	CTCTTGAGTGAGGTAGTCACCAGC	PCR/Seq	Jørgensen et al. 2007
Torosa 16sr	GTGTCCGAATAACTCACCAAAACC	PCR/Seq	

Based on the habitat of their hosts, it was suggested by Jørgensen and Sterud (2007) that the three *Spironucleus* clades may have evolved separately in the sea, in freshwater and on land. This was later refuted by Kolisko et al. (2008), due to presence of the terrestrial GEPA2H tortoise isolate in the 'marine' *Spironucleus* clade. However, the phylogeny of the diplomonads and *Spironucleus* probably suffers from low taxon sampling with only 8 *Spironucleus* species included in the most recent studies (Jørgensen

& Sterud 2007; Kolisko et al. 2008). This speculation is strongly supported by the aforementioned Chinese studies, describing a total of 25 new species of *Spironucleus* and *Hexamita* from fish (Xiao & Li 1993, 1994; Li & Nie 1995; Xiao et al. 2002). As with most fish pathogens, present records do not reveal the complexity of diplomonad diversity. More sampling of diplomonads from a broader geographical and host range is required in order to understand the evolutionary processes which led to the adaptation of these organisms to such different environments and resulted in the morphological and genetic diversity seen today.

1.4. HOST-PATHOGEN INTERACTIONS

1.4.1. Distribution and Host Specificity

Piscine diplomonads infect both wild and farmed fishes globally, encompassing marine to freshwater habitats, and arctic to tropical climates. The diplomonad fauna of fishes is best known from regions of the world where fisheries and aquaculture provide key sources of protein for human consumption, such as Europe (Kulda & Lom 1964; Sterud et al. 1998; Tojo & Santamarina 1998), North America (Kent et al. 1992) and increasingly China (Xiao & Li 1993, 1994; Li & Nie 1995; Xiao et al. 2002). Most of the recent reports of *Spironucleus* are in commercially important species of fish, particularly those in aquaculture that are raised as food fish or as ornamentals. Thus, there is a sense that this genus of flagellates is primarily found in cichlids, cyprinids, gadids and salmonids. However a broader consideration of the literature, including numerous older publications focusing on ecological parasitology and surveys, shows that diplomonads are commonly encountered in many more families of fish.

Since reliable species identification of *Spironucleus* is rare, a sound understanding of host range has not yet been achieved. Some species of *Spironucleus* have a broad host range, being reported from a variety of host species. For example, *S. salmonis* infects *Salvelinus fontinalis* (brook trout), rainbow trout, brown trout, Arctic charr and *Gasterosteus aculeatus* (three-spined stickleback) (Moore 1922; Davis 1926; Sanghari-Fard et al. 2007a; Jørgensen et al. 2011). However, innate immunity may also play a role in host-susceptibility. Surveys show that not all species of fish in a given habitat are infected. In an infection trial conducted by Kent et al. (1992), Atlantic salmon were not susceptible to experimental infection with an isolate of *S. salmonicida* from Chinook salmon. Conversely, Guo and Woo (2004b) found that 3 different families of Atlantic salmon remained fully susceptible to experimental infection with *S. salmonicida* isolated

from Atlantic salmon. A genetic basis for susceptibility within host families has been suggested (Guo & Woo 2004b). Cross infection is even feasible across animal groups; with *S. elegans* from newts infecting angelfish (Kulda & Lom 1964). Moreover, individual fish may be co-infected, for instance with *S. salmonis* and *S. salmonicida* (see Jørgensen et al. 2011). This implies that in previous studies, clinical disease and pathology may have actually been caused by multiple hexamitid infections. This underlines the need to use molecular methods for identification of *Spironucleus* spp.

1.4.2. Pathogenicity in Wild versus Farmed Fish

Spironucleus spp. are found in high prevalence in both wild and farmed fish, however, the pathogenicity of isolates varies greatly between these two host habitats. For example, *S. barkhanus* and the morphologically indistinguishable *S. salmonicida* infect wild and farmed fish, respectively. However, systemic Spironucleosis has only ever been observed for *S. salmonicida* in aquaculture, whilst *S. barkhanus* infections in wild fish are generally commensal (Jørgensen & Sterud 2006). Furthermore, the *S. vortens* isolate recently characterized in wild Norwegian ide has not been associated with Spironucleosis in these fish; however, farmed cichlids are extremely susceptible to this parasite (Paull & Matthews 2001; Sterud & Poynton 2002). This difference in susceptibility between wild and farmed fish has led to the description of *Spironucleus* spp. as opportunistic pathogens, whereby pathogenesis is favoured over commensalism in an immunocompromised host. Factors such as poor water quality, malnutrition, temperature fluctuations, bad husbandry and overcrowding all have been associated with stress of the fish host, and subsequent reduction in host immunity (Bassleer 1983; Rottmann et al. 1992; Francis-Floyd & Reen 1994; Woo & Poynton 1995). Some of these factors are unavoidable in aquaculture, which explains why farmed fish are more susceptible to disease than wild fish. However, a recent study by Meseck et al. (2007) has documented systemic Spironucleosis in Chinook salmon from Lake Ontario, meaning that disease outbreaks in wild fish cannot be ruled out.
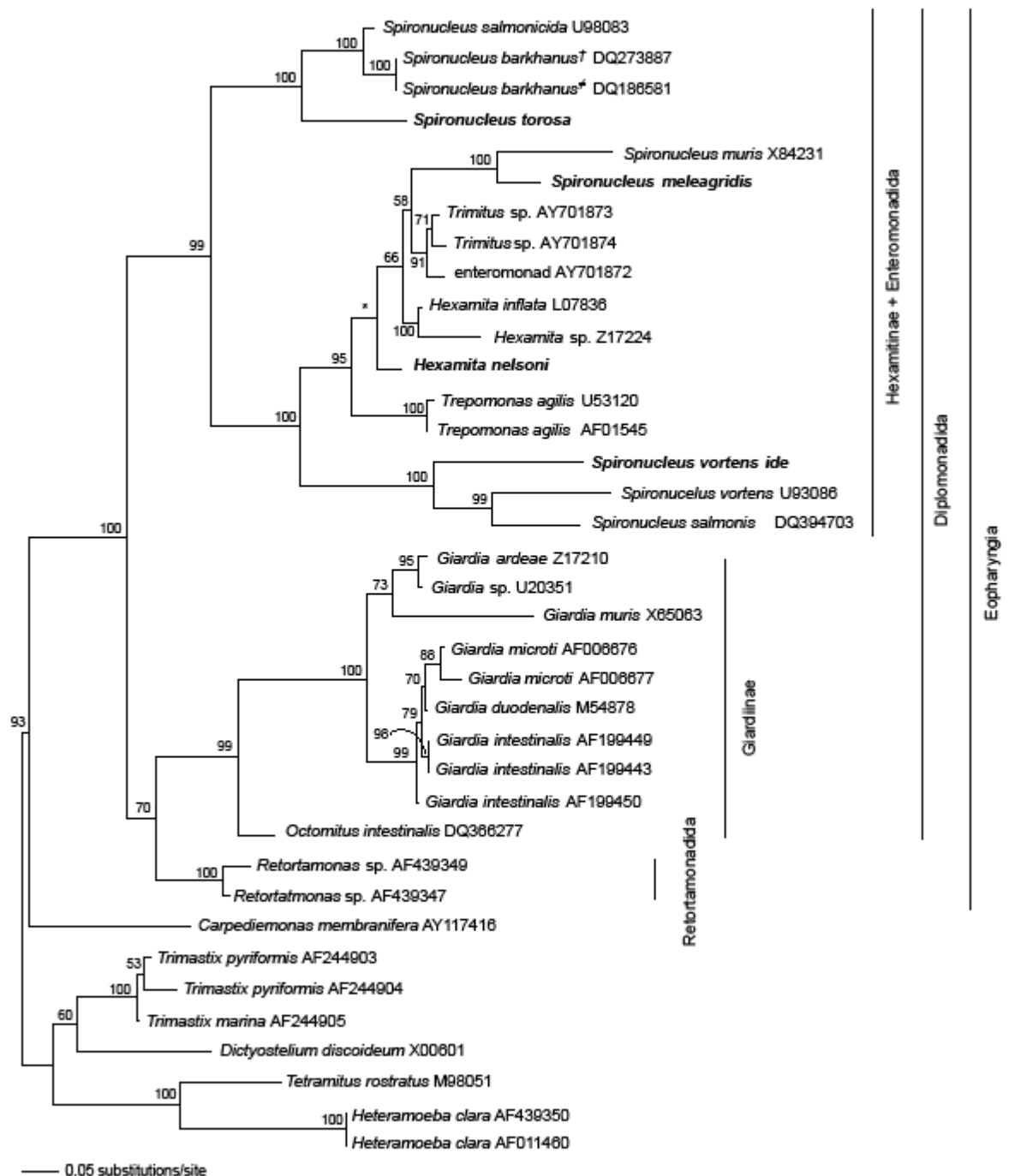
Fig. 1.3. Phylogeny of diplomonads. Maximum likelihood phylogeny of Diplomonadida, Eopharyngia, constructed according to partial SSU rRNA gene sequence data. At each node, bootstrap support analysis values are given. Asterisks indicate unresolved bootstrap analyses. Reproduced from Jørgensen and Sterud 2007 with permission from Elsevier.

17

It is plausible that wild fish may serve as a reservoir of infection for farmed fish. For example, following a series of systemic Spironucleosis outbreaks in Norwegian fish farms (Mo et al. 1990; Poppe et al. 1992; Poppe & Mo 1993) it was hypothesised that wild feral Arctic charr were the source of parasite transmission to the sea-caged Atlantic salmon (Sterud et al. 1998). A more recent outbreak was observed in farmed Arctic charr, found in northern Norway (Sterud et al. 2003). The affected fish farm sourced their charr smolt from a hatchery which utilized water possibly infected with *S. barkhanus* from wild Arctic charr outside the farm. Despite the fact that no fish within the hatchery were found to harbour *S. barkhanus*, it was suggested that transmission of flagellates from wild to farmed char was the most likely source of the outbreak (Sterud et al. 2003). However, molecular analysis revealed large genetic differences in the isolates from wild and farmed fish, resulting in species reassignment of the farmed isolate to *S. salmonicida*. This led to a further reappraisal of the likely transmission route from wild feral populations to farmed stocks after their transfer to seawater (Jørgensen & Sterud 2004). Transmission of *S. vortens* from aquarium cichlids to wild ide has also been suggested, as a result of improper disposal of moribund or dead fish into domestic waste systems and/or dumping in lakes (Sterud & Poynton 2002). However, the large genetic differences between *S. vortens* isolated from wild and farmed fish implies a similar scenario to that of *S. salmonicida*, whereby species reassignment may be required (Jørgensen & Sterud 2007). Prevalence and intensity of *Spironucleus* infections have also been associated with fish age. This has particular importance for infections in aquaculture, where disease may only manifest at certain stages of the production cycle. For example the chronic disease associated with *S. salmonis* typically affects young fish, suggesting that there is acquired immunity to infection (Uldal & Buchmann 1996). In contrast, *S. salmonicida* causes disease in adult fish (Poppe et al. 1992; Kent et al. 1992; Sterud et al. 2003).

1.4.3. Microhabitat Preferences

In both wild and farmed fish, the intestinal tract is believed to be the natural habitat for piscine diplomonads. Most reports of *Spironucleus* in wild fish document the flagellates in the intestine, and less commonly in the gall bladder. Only in rare cases are wild fish reported to carry *Spironucleus* infections elsewhere; a particular case of note being the presence of *Spironucleus* spp. in abscess lesions in the somatic muscle adjacent to the dorsal fin of adult Chinook salmon from Lake Ontario (Meseck et al. 2007).

However, in farmed fish, systemic infections (including the presence of the flagellates in the blood) are common (discussed further in Section 1.4.4).

Certain species of piscine *Spironucleus* have particular microhabitat preferences within the intestine. For example, *S. salmonis*, commonly infecting farmed rainbow trout, is concentrated in the pyloric region (Sanghari-Fard et al. 2007a), while *S. torosa*, in wild gadids, clusters posterior to the ileo-rectal valve in the most posterior section of the intestine (Poynton & Morrison 1990). Different *Spironucleus* species may have different metabolic requirements, based on differences in the organelles in the heterogeneous cytoplasm (see Section 1.5). Along the length of the intestine, there are gradients in morphology, physiology and metabolic activity. In *S. salmonis*, the optimum and tolerable pH have been studied *in vivo* (Sanghari-Fard et al. 2007b) and *in vitro* (Buchmann & Uldal 1996). Flagellates survive within a pH range of 5.5-9.0, with optimal pH for population increase being between 7.5-8.0 (Buchmann & Uldal 1996). *In vivo*, however, parasite density within the intestinal tract did not correlate with optimal pH, suggesting that microhabitat preference is not dependent on this factor (Sanghari-Fard et al. 2007b).

Parasite-host interactions of *Spironucleus* spp. are poorly characterised. Of the few studies which address this topic it has been observed that *S. torosa,* which usually swims free in the lumen, can attach to the intestinal microvilli, with apparent cytoplasmic connections between the flagellates and fish cells (Poynton & Morrison 1990). There are also marked differences in the cytoplasmic organelles of the free-swimming and attached forms (Poynton & Morrison 1990). In the case of *S. vortens*, another species that is usually found in the intestinal lumen, there is the capacity to become systemic, infecting kidney, liver, spleen and head lesions (Paull & Matthews 2001). *Spironucleus* in farmed Arctic charr may even occur intracellularly within the capillaries and sinusoids of the liver, spleen and kidney (Sterud et al. 2003). Although there may be numerous parasites, gross and histopathological lesions are rare and mortality is low (Sterud et al. 2003). One of the most challenging questions in understanding microhabitat preference of piscine diplomonads concerns identification of the factors involved in onset and establishment of systemic infections.

1.4.4. Pathology and Clinical Manifestation

Spironucleosis ranges from an asymptomatic to chronic disease, with the main clinical symptoms consisting of anorexia, weight loss, lethargy, enteritis, dark

colouration, pale gills and egestion of stringy faeces (Woo & Poynton 1995; Uldal & Buchmann 1996). Infected fish also exhibit unusual swimming behaviour such as corkscrew movements, a tendency to swim on their side and to linger in the corner of tanks (Tojo & Santamarina 1998). In addition to direct morphological and molecular identification from tissues (see Sections 1.3.2 and 1.3.3), microscopic analysis of the host's faeces provides a convenient method of non-invasively diagnosing Spironucleosis. Enumeration of parasites per field of view, allows an assessment of the severity of infection (Tojo & Santamarina 1998). Although both cysts and trophozoites have been isolated from the faeces of infected fish (Lom & Dyková 1992; Uldal 1996), the motile trophozoite form is more easily identified, with the cyst form being exceptionally rare (Kulda & Lom 1964; Kent et al. 1992; Tojo & Santamarina 1998).

Two main forms of Spironucleosis are described causing coelozoic (intestinal) and histozoic (systemic) infections. In both cases, fish may appear asymptomatic; however, severe clinical signs and pathology are observed in relation to disease outbreaks.

1.4.4.1. Intestinal Spironucleosis

The intestinal form of Spironucleosis (originally described as hexamitosis) in salmonid fingerlings and aquarium fish is generally considered to be benign (Uzmann & Jesse 1963; Uzmann et al. 1965). There is no doubt, however, that the occurrence of vast numbers of the parasite in the gut may lead to severe enteritis with emaciation, exophthalmia, ascites and faecal casts (Moore 1922; Davis, 1926; Ferguson & Moccia 1980). Symptoms are non-specific, but often include locomotive disorders and increasing mortalities.

1.4.4.2. Systemic Spironucleosis

Several diplomonad species may cause systemic infections in fish (Ferguson & Moccia 1980; Mo et al. 1990; Kent et al. 1992; Poppe et al. 1993; Fagerholm & Bylund 1997; Sterud et al. 1998; Paull & Matthews 2001). *S. vortens* infects a variety of fish species and is associated with hole-in-the-head (HITH) diseases in cichlids, e.g. angelfish and discus (Poynton et al. 1995; Paull & Matthews 2001). The disease is characterized by parasite-filled necrotic lesions in the head region, sometimes also extending posteriorly along the lateral line. Lesions are usually bilaterally symmetrical and may coalesce into larger lesions, discharging yellow mucus (Woo & Poynton 1995; Paull & Matthews

2001). Large numbers of flagellates have been found in internal organs such as the heart, liver and kidney (Mo et al. 1990; Poppe et al. 1992; Poppe & Mo 1993). In addition, trophozoites of *S. vortens* were detected in the intestine of fish with systemic infections and it was suggested by Paull and Mathews (2001) that the infection had an intestinal origin.

Systemic infections caused by *S. salmonicida* in Atlantic salmon, are marked by parasite filled abscesses and pustules in subcutaneous muscle tissue, in necrotic tissue of the heart, kidney, liver and spleen, but never in the intestine (Mo et al. 1990; Poppe & Mo 1993; Sterud et al. 1998; Jørgensen & Sterud 2004, 2006). Typical histopathology of systemic infections with *S. salmonicida* in Atlantic salmon reveals severe epicarditis, large caseonecrotic areas with, at times, formation of granulomatous response in the kidney, liver and spleen. The characteristic paired anterior nuclei of the flagellates are usually observed centrally in the granulomas and foci of necrotic tissue (Poppe et al. 1992; Poppe & Mo 1993). *S. salmonicida* also causes systemic Spironucleosis in farmed Arctic charr and Chinook salmon. In these hosts the symptoms are somewhat different compared to the infection in Atlantic salmon. Granulomas in muscle tissues and internal organs are not apparent, but vast aggregates of parasites occur in the vasculature of most organs (Kent et al. 1992; Sterud et al. 2003).

Specific triggers for pathogenicity and onset of systemic infection are currently unknown, and may vary greatly between *Spironucleus* spp. due to differences in microhabitat preferences. The host immune system is likely to play a key role in protecting against Spironucleosis, however further work is required in order to categorise the immune response to *Spironucleus* infection, and understand subsequent methods of parasite evasion.

1.5. PHYSIOLOGY AND BIOCHEMISTRY

Knowledge regarding the biochemistry and physiology of *Spironucleus* spp. is paramount in order to understand mechanisms of pathogenicity, and consequent exploitation of novel molecular pathways for chemotherapeutic control. This has been made possible as a result of optimisation of *in vitro* culture for several *Spironucleus* isolates (see Table 1.4).

Table 1.4. *In vitro* culturing conditions of *Spironucleus* spp. This includes the source of the species and corresponding optimal culture medium composition and temperature (temperature range given in brackets). Reproduced from Millet 2009.

Species	Source	Culture medium	Temp. (ºC)	Reference
Spironucleus vortens	Lip lesion, angelfish, Florida (ATCC 50386)	Keister's modified TY-I-S33	25 (22-34)	Sangmaneedet & Smith 2000
	Intestine, internal organs and head lesions of cichlids with hole in the head disease, UK	Keister's modified TY-I-S33 supplemented with fresh *Oreochromis niloticus* liver	25	Paull & Matthews 2001
	Intestine of wild Ide, river Leira, Norway	Keister's modified, TY-I-S33	15 (5-15)	Sterud & Poynton 2002
Spironucleus barkhanus	Gall bladder of wild grayling, Norway	Keister's modified TY-I-S33	15 (5-20)	Sterud 1998a
	Muscle abscess of farmed Atlantic salmon, Norway	Keister's modified TY-I-S33	10 (5-20)	Sterud 1998a
	Blood, liver and kidney of farmed Atlantic char, Norway	Growth not supported by Keister's modified TY-I-S33	NA	Sterud et al. 2003
Spironucleus salmonis (*Hexamita salmonis*)	Intestine of wild rainbow trout, Dennmark	MEM with 10% bovine serum. Not supported by Keister's modified TY-I-S33	10 (5-10)	Buchmann & Uldal 1996

Although detailed information on nutrient uptake, and pathways of carbon and nitrogen metabolism have not been investigated, a great deal on the physiology of fish diplomonads can be inferred from studies of nutritional and environmental conditions necessary for growth. This is especially true for *S. vortens* grown *in vitro* under anaerobic conditions in stoppered tubes with ascorbate and cysteine to ensure removal of traces of O_2 (Sangmaneedet & Smith 2000). Extremely rapid trophozoite multiplication corresponds to a mean generation time of 1.79 h at 25ºC (Millet et al. 2010a). Their copious production of H_2 (Fig 1.4), a metabolic product rare amongst eukaryotes, strongly suggests similarities to other flagellate parasitic protists that thrive in low O_2 environments, i.e. the parabasalid trichomonads and many diplomonads (Millet et al. 2010b). The progressive diminution of the aerobic life-style typical of their free-living ancestors, together with multiple lateral transfer of genes of bacterial origins have

enabled these parasitic organisms to prosper energetically without the traits of their mitochondriate free-living counterparts (Horner et al. 1996). Loss of a cytochrome-mediated respiratory chain driven by an electron transport system and its coupled proton driven ATP synthase, along with the acquisition of hydrogenases, characterizes a novel redox-active organelle, the hydrogenosome (Lloyd et al. 1979a,b) recently found in *S. vortens* and *S. salmonicida* (see Millet 2009; Jerlström-Hultqvist 2012).
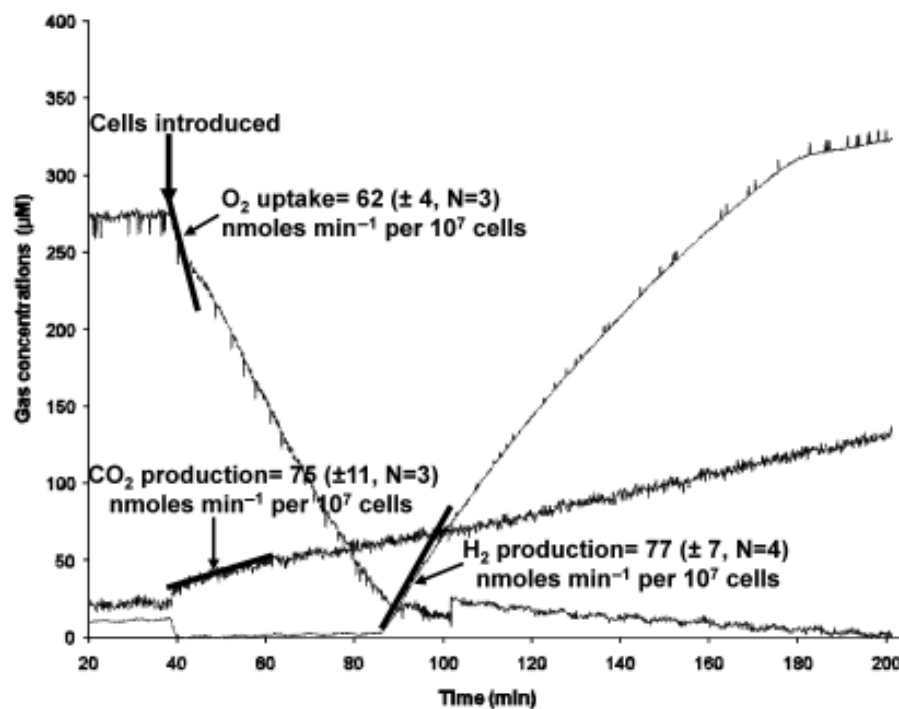
Fig. 1.4. Gas metabolism of *Spironucleus vortens*. Cells were assayed in a stirred suspension of 7.4 x 10^5 cells/ml in air-saturated phosphate buffered saline at 20ºC, analysed by membrane-inlet mass spectrometry. Rates of O_2 consumption, H_2 production and CO_2 production were derived from linear regression at the indicated tangents (standard deviation and number of replicates are denoted in brackets). Reproduced from Millet et al. (2010b) with permission from John Wiley & Sons Ltd.

H_2 production in *S. vortens* is even more rapid than in *Trichomonas vaginalis*, a protozoan parasite with well-defined hydrogenosomes (Lindmark et al. 1975), and is similarly inhibited under microaerobic conditions. Cyanide- and CO-sensitivity in both organisms strongly suggests that the hydrogenase responsible is of the Fe-only category (Horner et al. 2000). This conclusion has been validated for *T. vaginalis* by redox

properties and furthermore by electron paramagnetic resonance spectroscopy, a powerful technique frequently employed in the characterization of metal centres in iron-sulphur proteins, such as hydrogenase (Chapman et al. 1986). Identification of a Fe-hydrogenase-like sequence in the genome of *S. barkhanus* strongly supports these conclusions (Millet et al. 2010b).

As in the trichomonads, well-washed, non-proliferating *S. vortens* from anaerobic cultures avidly consume O_2 (Fig 1.4) over periods of several hours even in the absence of added substrates (Millet 2009). This denotes an exceptional O_2 scavenging ability for these parasites, which in turn suggests that they are well-equipped to cope with large fluctuations in O_2 levels during the course of infection or transmission. Their endogenous capacity must reflect a considerable reserve of reduced carbon analogues, e.g. glycogen as in *G. intestinalis* (see Pradhan et al. 2012), although the biochemical identity remains to be established for *S. vortens*. As this O_2 consumption does not directly provide energy it should be regarded as an O_2-scavenging function rather than as respiration.

Both endogenous and glucose-driven metabolism in *S. vortens* yield CO_2, ethanol, acetate, alanine and lactate as revealed by membrane inlet mass spectrometry, ^{1}H NMR and ^{13}C NMR (Millet et al. 2011). Ethanol can also be utilized, but like glucose is not as favoured as amino acids. In this respect, cultures of *S. vortens* show characteristics similar to those of some cultured mammalian cell lines where glucose uptake is slow and amino acids are the favoured substrate (Millet et al. 2011). Cultures of *S. vortens* analysed by ion-exchange chromatography at intervals over a period of 6 days indicate that despite the presence of high concentrations of free amino acids, peptides and proteins become depleted (Millet et al. 2011). Production of extracellular peptidases and proteases is likely to be an essential aspect of their invasiveness potential during pathogenesis. Free amino acids showing net gains during culture growth include glutamate, alanine and aspartate, whereas lysine, arginine, leucine, cysteine and urea are extensively utilised. Unlike *T. vaginalis, G. intestinalis* or *Hexamita inflata* (see Biagini et al. 2003)*, S. vortens* appears not to have the arginine dihydrolase (ADH) pathway for energy production, as no ornithine has been detected. Addition of arginine to non-proliferating cells has resulted in no detectable ammonia or nitric oxide production. However, many homologues of the ADH pathway can be found in the *S. vortens* genome, thus the presence of such an energy generation pathway in this organism cannot be completely ruled out (Millet et al. 2011).

It should be emphasised that the physiology and underlying biochemical properties of *Spironucleus* species may vary widely, between and within species in relation to short time-scale changes of *in situ* microenvironments as well as the more profound changes expected at different life cycle stages. Factors pivotal in these respects include nutrient supplies and environmental O_2 concentrations. Central to the extreme limits for parasite viability and persistence is the intracellular redox potential which must be maintained for normal metabolic function and redox signalling. This in turn depends on adequate supplies of host-derived reduced carbon compounds for growth and energy production. Further research in these areas will improve our knowledge of key parasite biochemical processes relating to pathogenicity and transmission, and will provide an insight into the phenotypic diversity of diplomonads.

1.6. DISEASE MANAGEMENT

In vitro culture methods for routine maintenance of *Spironucleus* spp. provides convenient means of screening new and existing chemotherapeutic agents. Furthermore, recent developments in our understanding of piscine diplomonad biochemistry show potential for the development of novel strategies of disease management.

1.6.1. Treatment

Treatment of salmonid infection is recommended when 15-20 trophozoites are counted microscopically per field of view (using 100 X total magnification) (Post 1987 cited in Woo & Poynton 1995). The most common chemotherapeutic means of eradicating human and veterinary diplomonad infections is metronidazole (Flagyl, Fish-zole) (Tojo & Santamarina 1998; Sangmaneedet & Smith 1999). This is an unique, limited spectrum antibiotic that is used to combat anaerobic or microaerophilic, pathogenic microorganisms. When administered, the metronidazole pro-drug acts as a high affinity electron acceptor and is activated by reduction at the drug nitro group by the low redox potential electron transfer systems present in anaerobic/microaerophilic organisms (see review by Freeman et al. 1997). This in turn results in cytotoxic reduction products including nitro-radical anions which are suggested to cause cell death via DNA damage, leaving the aerobic host unaffected (Edwards 1993).

Metronidazole has a minimum inhibitory concentration of 1 µg/ml against *S. vortens in vitro*, with the recommended dose in ornamental fish being 10 mg per 1 g fish

food (Millet 2009). For the treatment of food fish, 2-5 g/kg feed or 4 mg/L bath treatment is recommended (Tojo & Santamarina 1998), with oral administration being more effective than bathing (Whaley & Francis-Floyd 1991). However in 1998, European Council Regulation 613/98/EEC (Commission Regulation No. 613/98, 1998) banned the use of metronidazole on outdoor European fish farms, due to its environmental side effects (Lanzky & Halting-Sørensen 1997; Kümmerer et al. 2000; Jjemba 2002), cytotoxicity and genotoxicity in fish (Cavaş & Ergene-Gözükara 2005; Khalil et al. 2007), and it being listed as a potential human carcinogen by the International Agency for Research on Cancer (IARC 1987). Administration of metronidazole to food animals is also banned in the US (FARAD 2010). As a further complication, resistance to metronidazole has been documented on some fish farms (Tojo & Santamarina 1998).

Other effective nitroimidazoles include benznidazole, ronidazole, secnidazole (Tojo & Santamarina 1998) and dimetridazole (Woo & Poynton 1995), the latter, however, has severe toxic side effects in fish (Tojo & Santamarina 1998). Some non-nitroimidazoles are also effective, including albendazole, aminosidine, diethylcarbamazine and nitroscanate, all at doses of 40 g/kg feed for a 10 day period (Tojo & Santamarina 1998). Furthermore, mebendazole, a highly active benzimidazole, has been shown to inhibit *S. vortens* growth *in vitro* at a concentration of 0.5 µg/ml (Millet 2009).

More recently, the inhibitory effect of *Allium sativum* (garlic) has been investigated as an alternative therapy for the treatment of Spironucleosis. *Allium*-derived compounds are broad-spectrum antimicrobial agents and thus are effective against a wide range of human and veterinary pathogens (see review by Williams & Lloyd 2012, Appendix 3). *In vitro*, ajoene and a mixture of vinyl dithiins and thiosulphinates extracted from garlic are highly effective at inhibiting *S. vortens* growth, having minimum inhibitory concentrations of 107 and 83 µg/ml respectively (Millet et al. 2010c). *In vivo* assays are required in order to determine the efficacy of garlic in fish. However, if successful, garlic-based therapy has the potential to provide a less toxic and more environmentally friendly alternative to metronidazole in the treatment of fish diplomonad infections.

1.6.2. Preventative Measures

Due to our current lack of knowledge regarding the transmission of *Spironucleus* to fish farms, along with the possibility of sub-clinical infections, eliminating this parasite

from aquaculture will not be possible in the short term. However, preventative measures can be employed in order to minimise the occurrence of an outbreak. These include, quarantine of new stock, use of appropriate under-gravel filters, frequent cleaning of tanks, good husbandry and healthy nutrition (Woo & Poynton 1995). Furthermore, ozonization and UV irradiation of inlet water greatly reduces pathogen entry into tanks (Litved et al. 1995). As outbreaks are associated with 'stress' of the host, care should be taken to ensure that water quality, aeration and temperature are maintained at an optimal level, especially when fish are under crowded conditions (Woo & Poynton 1995; Whaley & Francis-Floyd 1991). These are all factors which may contribute towards an outbreak (of this and other infectious diseases) by decreasing the efficiency of the fish immune system and thereby increasing susceptibility (Bassleer 1983). Identifying the source and method of transmission of *Spironucleus* into fish farms will lead to more specific measures to prevent outbreaks in aquaculture.

1.6.3. Economical Impact

Failures in prevention and control of Spironucleosis may cause severe economic losses both to fish farmers and the aquarium industry as a whole. Systemic Spironucleosis caused by *S. salmonicida* in Norwegian farms of Atlantic salmon has resulted in near or complete loss of all stocks at some farms (Mo et al. 1990; Poppe et al. 1992; Sterud et al. 1997). However, most infections reduced profits due to downgrading at slaughter and increased labour costs during the filleting process. *S. salmonis* may also have an economical impact on farming of rainbow trout due to reduced growth and increased mortality of young fry. *S. vortens* has a similar effect in the production of ornamental fish, resulting in loss of highly valuable specimens, including angelfish and discus *Symphysodon discus*, the trade of which is a multi-million dollar industry per annum (Andrews 1990).

1.7. CONCLUSIONS

Although piscine diplomonads have been described since the late 19th Century (Seligo 1887), our appreciation of the basic biology of these organisms remains in its infancy. However, our understanding of their taxonomy, biochemistry and pathogenicity has greatly increased in the last few years. Identification of morphologically cryptic *Spironucleus* spp. through SSU rDNA sequencing (Jørgensen & Sterud 2007) has considerably clarified fish diplomonad taxonomy. Furthermore, optimisation of *in vitro*

27

Spironucleus cultures has provided a convenient source of flagellates, allowing complete replacement of animal models for biochemical and physiological investigations of parasite pathogenicity. Such studies have revealed novel molecular pathways of gas metabolism, redox control and nutrition (Millet et al. 2010a, b; Millet et al. 2011), which are essential for our understanding of parasite pathogenicity and consequent exploitation of novel molecular pathways for chemotherapeutic control. This is especially important in light of restrictions on the use of metronidazole in aquaculture. *Allium*-derived compounds show great potential as alternative antiparasitic agents, although *in vivo* investigations are required to confirm efficiency at eradicating Spironucleosis in fish (Millet et al. 2010c).

1.8. THESIS AIMS

- Determine the mode of transmission of *S. vortens* between hosts and to specifically address the presence of an encysted stage

- Develop a non-invasive method of quantifying intestinal colonization by *S. vortens* in angelfish as a means of testing new and existing chemotherapeutics *in vivo*

- Evaluate the *in vitro* and *in vivo* inhibitory effects of metronidazole and garlic-derived compounds against *S. vortens*

- Investigate the mode of action of metronidazole and garlic-derivatives against *S. vortens* using microscopic, proteomic and fluorescence techniques

- Further investigate the role of glucose and glutamate as carbohydrate and amino acid metabolic substrates of *S. vortens*

- Characterize biochemical aspects of the antioxidant defence system of *S. vortens*, including the identity of the major protein and non-protein thiols

1.9. THESIS HYPOTHESES

- Piscine *Spironucleus* cysts are rarely seen *in vivo*, and have never been characterized for *Spironucleus vortens*, hence transmission of *S. vortens* is predicted to occur via the trophozoite form (Chapter 3)

- As *Spironucleus* spp. are transmitted via the faecal-oral route, enumeration of parasites in the host's faeces is hypothesised to provide a non-invasive approach to estimating the degree of intestinal colonization by *S. vortens* in angelfish (Chapter 3)

- Metronidazole and garlic-derivatives act synergistically against *S. vortens* (Chapter 4)

- The mode of action of metronidazole and garlic-derivatives involves disruption of *S. vortens* intracellular redox balance (Chapter 5)

- Glucose is a secondary substrate of *S. vortens*, the primary substrate is hypothesised to be the amino acid glutamate, which is incorporated from the culture medium in high quantities (Chapter 6)

- The aerotolerant nature of *S. vortens*, an anaerobic organism, must reflect a sophisticated antioxidant defence system which detoxifies reactive O_2 species (Chapter 7)

1.10. THESIS LAYOUT

This thesis consists of a general introduction (Chapter 1) of *Spironucleus* spp., which has already been published as a review article in the Journal of Aquaculture Research and Development. This is followed by the general methodologies employed during the subsequent experimental chapters (Chapter 2). There are 5 experimental chapters in total (Chapters 3-7). These are self-contained chapters, some of which are in press (Chapter 3, Diseases of Aquatic Organisms), are already published (Chapter 5, Veterinary Parasitology) or have been submitted for peer review (Chapter 7). The remaining experimental chapters (Chapters 4 and 6) are in preparation for submission. The experimental chapters are followed by a general discussion (Chapter 8) which summarises the findings of the thesis and highlights important implications of the research as well as opportunities for future investigations. The appendix contains raw data from growth curve experiments as well as other published works which were side-projects to this PhD.

1.11. REFERENCES

Adam RD (2001). Biology of *Giardia lamblia*. Clin Microbiol Rev 14: 447-475

Andersson JO, Roger AJ (2002). Evolutionary analyses of the small subunit of glutamate synthase: gene order conservation, gene fusions, and prokaryote-to-eukaryote lateral gene transfers. Eukaryot Cell 1: 304-310

Andersson JO, Roger AJ (2003). Evolution of glutamate dehydrogenase genes: evidence for lateral gene transfer within and between prokaryotes and eukaryotes. BMC Evol Biol 3: 14

Andersson JO, Sjögren ÅM, Davis LA, Embley TM, Roger AJ (2003). Phylogenetic analyses of diplomonad genes reveal frequent lateral gene transfers affecting eukaryotes. Curr Biol 13: 94-104

Andersson JO, Sarchfield SW, Roger AJ (2004). Gene transfers from nanoarchaeota to an ancestor of diplomonads and parabasalids. Mol Biol Evol 22: 85-90

Andersson JO, Sjögren ÅM, Horner DS, Murphy CA, Dyal PL, Svärd SG, Logsdon JM, Raglan MA, Hirt RP, Roger AJ (2007). A genomic survey of the fish parasite *Spironucleus salmonicida* indicates genomic plasticity among diplomonads and significant lateral gene transfer in eukaryote genome evolution. BMC Genomics 8: 51

Andrews C (1990). The ornamental fish trade and fish conservation. J Fish Biol 37: 53-59

Bassleer G (1983). Disease prevention and control. *Spironculeus/Hexamita* infection, hole-in-the-head disease. FAMA 6: 38-60

Biagini GA, Yarlett N, Ball GE, Billetz AC, Lindmark DG, Martinez MP, Lloyd D, Edwards MR (2003). Bacterial-like energy metabolism in the amitochondriate protozoon *Hexamita inflata*. Mol Biol Parasitol 128: 11-19

Brugerolle G, Joyon L, Oktem N (1973). Contribution a l'étude cytologique et phylétique des diplozoaires (Zoomastigophorea, Diplozoa, Dangeard 1910). II Etude ultrastructurale du genre *Spironucleus* (Lavier 1936). Protistologica IX: 495-502

Brugerolle G (1975). Contribution a l'étude cytologique et phylétique des diplozoaires (Zoomastigophorea, Diplozooa, Dangeard 1910). VI. Caractères généraux des diplozoaires. Protistologica XI: 111-118

Brugerolle G, Kunstýr I, Senaud J, Friedhoff KT (1980). Fine structure of trophozoites and cysts of the pathogenic diplomonad *Spironucleus muris*. Z Parasitenkd 62: 47-61

Buchmann K, Uldal A (1996). Temperature, pH and bile dependent *in vitro* cultivation of *Hexamita salmonis* from rainbow trout *Oncorhynchus mykiss* intestine. Dis Aquat Org 24: 169-172

Bui ETN, Bradley PJ, Johnson PJ (1996). A common evolutionary origin for mitochondria and hydrogenosomes. Proc Natl Acad Sci 93: 9651-9656

Cavalier-Smith T (1983). A 6-kingdom classification and a unified phylogeny. In: Schwemmler W, Schenk HEA (eds.), Endocytobiology, Berlin: Walter de Gruyter & Co, pp 1027-1034

Cavaş T, Ergene-Gözükara S (2005). Genotoxicity evaluation of metronidazole using the piscine micronucleus test by acridine orange staining. Environ Toxicol Phar 1: 107-111

Chapman A, Cammack R, Linstead DJ, Lloyd D (1986). Respiration of *Trichomonas vaginalis*: components detected by electron paramagnetic resonance spectroscopy. Eur J Biochem 156: 193-198

Clark CG, Roger AJ (1995). Direct evidence for secondary loss of mitochondria in *Entamoeba histolytica*. Proc Natl Acad Sci USA 92: 6518-6521

Commission Regulation (EC) No. 613/98 (1998). Off J Eur Commun L82/14-17 [Cited 18 February 2013] URL: http://ec.europa.eu/health/files/mrl/regpdf/1998_03_18-0613_en.pdf

Cooper GL, Charlton BR, Bickford AA, Nordhausen R (2004). *Hexamita meleagridis* (*Spironucleus meleagridis*) infection in chukar partridges associated with high mortality and intracellular trophozoites. Avian Dis 48: 706-710

Corliss JO (2001). Protozoan Cysts and Spores. Encyclopedia of Life Sciences, John Wiley and Sons Ltd. [Cited 2 April 2013] URL: http://onlinelibrary.wiley.com/doi/10.1038/npg.els.0001934/pdf

Davis HS (1926). *Octomitus salmonis*, a parasitic flagellate of trout. Bull US Bur Fish 42: 9-26

Dawson SC, Pham JK, House SA, Slawson EE, Cronembold D, Cande WZ (2008). Stable transformation of an episomal protein-tagging shuttle vector in the piscine diplomonad *Spironucleus vortens*. BMC Microbiol 8: 71

Edwards DI (1993). Nitroimidazole drugs - action and resistance mechanisms. II. Mechanism of resistance. JAC 31: 201-210

Embley TM, Hirt RP (1998). Early branching eukaryotes? Curr Opin Genet Dev 8: 624-629

Fagerholm HP, Bylund G (1997). Is *Hexamita salmonis* (flagellata) causing widespread systemic disease in fish? Bull Scand Soc Parasitol 5: 33-34

Fain MA, Karjala Z, Perdue KA, Copeland MK, Cheng LI, Elkins WR (2008). Detection of *Spironucleus muris* in unpreserved mouse tissue and fecal samples by using a PCR assay. J Am Assoc Lab Anim Sci 47: 39-43

FAO (2005) Fisheries and aquaculture topics. Ornamental fish. Topics fact sheets. In: FAO Fisheries and Aquaculture Department [online]. Rome, Italy. Updated 27 May 2005 [Cited 8 January 2013] URL: http://www.fao.org/fishery/topic/13611/en

FARAD (2010). Restricted and prohibited drugs in food animals. USA Food and Drug Administration [online]. Updated 2 August 2012 [Cited 18 February 2013] URL: http://www.farad.org/eldu/prohibit.asp

FDA (2012) Safety & health. Antimicrobial resistance. Animal husbandry and disease control: aquaculture. In: FDA Animal & Veterinary [online]. Maryland, USA. Updated 5 September 2012 [Cited 8 January 2013], URL: http://www.fda.gov/AnimalVeterinary/SafetyHealth/AntimicrobialResistance/ucm08209 9.htm

Fenchel T, Bernard C, Esteban G, Finlay BJ, Hansen PJ, Iversen N (1995). Microbial diversity and activity in a Danish fjord with anoxic deep water. Ophelia 43: 45-100

Ferguson HW, Moccia RD (1980). Disseminated hexamitosis in Siamese fighting fish. J Am Vet Med Assoc 177: 854-857

Francis-Floyd R, Reed P (1994). Management of *Hexamita* in Ornamental Cichlids. UF/IFAS Fact Sheet VM-67

Freeman CD, Klutman NE, Lamp KC (1997). Metronidazole. A therapeutic review and update. Drugs 54: 679-708

Germot A, Philippe H, Le GH (1997). Evidence for loss of mitochondria in *Microsporidia* from a mitochondrial-type HSP70 in Nosema locustae. Mol Biochem Parasitol 87: 159-168

Guo FC, Woo PT (2004a). Detection and quantification of *Spironucleus barkhanus* in experimentally infected Atlantic salmon *Salmo salar*. Dis Aquat Org 61: 175-178

Guo FC, Woo PT (2004b). Experimental infections of Atlantic salmon *Salmo salar* with *Spironucleus barkhanus*. Dis Aquat Org 61: 59-66

Hashimoto T, Sanchez LB, Shirakura T, Müller M, Hasegawa M (1998). Secondary absence of mitochondria in *Giardia lamblia* and *Trichomonas vaginalis* revealed by valyl-tRNA synthetase phylogeny. Proc Natl Acad Sci USA 95: 6860-6865

Horner DS, Hirt RP, Kilvington S, Lloyd D, Embley TM (1996). Molecular data suggest an early acquisition of the mitochondrion endosymbiont. Proc Roy Soc B 263: 1053-1059

Horner DS, Foster PG, Embley TM (2000). Iron hydrogenases and the evolution of anaerobic eukaryotes. Mol Biol Evol 17: 1695-1709

IARC (1987). Evaluation of carcinogenetic risk to humans. IARC 7: 250-251 [Cited12 April 2013], URL: http://monographs.iarc.fr/ENG/Monographs/suppl7/suppl7.pdf

Januschka MM, Erlandsen SL, Bemrick WJ, Schupp DG, Feely DE (1988). A comparison of *Giardia microti* and *Spironucleus muris* cysts in the vole: an immunocytochemical, light, and electron microscopic study. J Parasitol 74: 452-458

Jerlström-Hultqvist J (2012). Hidden diversity revealed. Genomic, transcriptomic and functional studies of diplomonads. Unpublished PhD Thesis, Uppsala University [Cited 26 February 2013] URL: http://uu.diva-portal.org/smash/get/diva2:562514/FULLTEXT01

Jerlström-Hultqvist J, Einarsson E, Svärd SG (2012). Stable transfection of the diplomonad parasite *Spironucleus salmonicida*. Eukaryot Cell 11: 1353-1361

Jjemba PK (2002). The effect of chloroquine, quinacrine and metronidazole on both soybean plants and soil microbiota. Chemosphere 46: 1019-1025

Jørgensen A, Sterud E (2004). SSU rRNA gene sequence reveals two genotypes of *Spironucleus barkhanus* (Diplomonadida) from farmed and wild Arctic charr *Salvelinus alpinus*. Dis Aquat Org 62: 93-96

Jørgensen A, Sterud D (2006). The marine pathogenic genotype of *Spironucleus barkhanus* from farmed salmonids redescribed as *Spironucleus salmonicida* n. sp. J Eukaryot Microbiol 53: 531-541

Jørgensen A, Sterud E (2007). Phylogeny of *Spironucleus* (Eopharyngia: Diplomonadida: Hexamitinae). Protist 158: 247-254

Jørgensen A, Alfjorden A, Henriksen K, Sterud E (2007). Phylogenetic analysis of the SSU rRNA gene from the piscine diplomonad *Spironucleus torosus* (Diplomonadida: Hexamitinae). Folia Parasitol 54: 277-282

Jørgensen A, Torp K, Bjørland MA, Poppe TT (2011). Wild Arctic char *Salvelinus alpinus* and trout *Salmo trutta*; hosts and reservoir of the salmonid pathogen *Spironucleus salmonicida* (Diplomonadida; Hexamitidae). Dis Aquat Org 97: 57-63

Keeling PJ, Doolittle WF (1996a). A non-canonical genetic code in an early diverging eukaryotic lineage. Embo Journal 15: 2285-2290

Keeling PJ, Doolittle WF (1996b). Alpha-tubulin from early-diverging eukaryotic lineages and the evolution of the tubulin family. Mol Biol Evol 13: 1297-1305

Keeling PJ, Brugerolle G (2006). Evidence from SSU rRNA phylogeny that *Octomitus* is a sister lineage to *Giardia.* Protist 157: 205-212

Kent ML, Ellis J, Fournie JW, Dawe SC, Bagshaw JW, Whitaker DJ (1992). Systemic hexamitid infection in seawater pen-reared chinook salmon. Dis Aquat Org 14: 81-89

Khalil WKB, Mahmoud MA, Zahran MM, Mahrous KF (2007). A sub-acute study of metronidazole toxicity assessed in Egyptian *Tilapia zillii*. J Appl Toxicol 27: 380-390

Kolisko M, Cepicka I, Hampl V, Kulda J, Flegr J (2005). The phylogenetic position of enteromonads: a challenge for the present models of diplomonad evolution. Int J Syst Evol Microbiol 55: 1729-1733

Kolisko M, Cepicka I, Hampl V, Leigh J, Roger AJ, Kulda J, Simpson AGB, Flegr J (2008). Molecular phylogeny of diplomonads and enteromonads based on SSU rRNA, alpha-tubulin and HSP90 genes: Implications for the evolutionary history of the double karyomastigont of diplomonads. BMC Evol Biol 8: 205

Koudela B, Karr CD, Meyer EA, Meyer B, Jarroll EL (1996). *In vitro* excystation of *Spironucleus muris*. J Euk Microbiol 43: 61-64

Kulda J, Lom J (1964). Remarks on the diplomastigine flagellates from the intestine of fishes. Parasitology 54: 753-762

Kulda J, Nohynkova E (1978). Flagellates of human intestine and of intestines of other species. In: Kreier JP (ed), Parasitic Protozoa, Vol 2, Academic Press, New York, pp 2-138

Kümmerer K, Al-Ahmad A, Mersch-Sundermann V (2000). Biodegradability of some antibiotics, elimination of the genotoxicity and affection of waste water bacteria in a simple test. Chemosphere 40: 701-710

Kunstýr I (1977). Infectious form of *Spironucleus* (*Hexamita*) *muris*: banded cysts. Lab Anim 11: 185-188

Kunstýr I, Ammerpohl E (1978). Resistance of faecal cysts of *Spironucleus muris* to some physical factors and chemical substances. Lab Anim 12: 95-97

Lanzky PF, Halting-Sørensen B (1997). The toxic effect of the antibiotic metronidazole on aquatic organisms. Chemosphere 11: 2553-2561

Lavier G (1936). Sur la structure des flagellès du genre *Hexamita* Duj. Societe De Biologie, Paris Comptes Rendus 121: 1177-1180

Li L, Nie D (1995). Notes on parasitic hexamitids of fishes with descriptions of 18 new species (Zoomastigophores: Diplomonadida: Hexamitidae). Acta Zootaxonomica Sinica 20: 6-28

Liltved H, Hektoen H, Efraimsen H (1995). Inactivation of bacterial and viral fish pathogens by ozonation or UV irradiation in water of different salinity. Aquacult Eng 13: 107-122

Lindmark DG, Müller M, Shio H (1975). Hydrogenosomes in *Trichomonas vaginalis*. J Parasitol 61: 552-554

Lloyd D, Lindmark DG, Müller M (1979a). Respiration of *Tritrichomonas foetus*: absence of detectable cytochromes. J Parasitol 65: 466-469

Lloyd D, Lindmark DG, Müller M (1979b). Adenosine triphosphatase activity of *Tritrichomonas foetus*. J Gen Microbiol 115: 301-307

Lloyd D, Kristensen B (1985). Metronidazole inhibition of hydrogen production *in vivo* in drug-sensitive and resistant strains of *Trichomonas vaginalis*. J Gen Microbiol 131: 849-853

Lom J, Dyková I (1992). Developments in aquaculture and fisheries science, Vol 26. Protozoan parasites of fishes. Elsevier, Amsterdam

Maiden MC (2006). Multilocus sequence typing of bacteria. Annu Rev Microbiol 60: 561-588

Meseck EK, French TW, Grimmett SG, Bartlett SL, Wooster GA, Getchell RG, Schachte JH Jr, Bowser PR (2007). Gross and microscopic pathology associated with large cavernous lesions in muscle of chinook salmon from Lake Ontario. J Wildl Dis 43: 111-115

Millet COM (2009). Growth, metabolism, ultrastructure and chemotherapy of *Spironucleus vortens*. Unpublished PhD thesis, Cardiff University

Millet COM, Lloyd D, Williams C, Cable J (2010a). *In vitro* culture of the diplomonad fish parasite *Spironucleus vortens* reveals unusually fast doubling time and a typical biphasic growth. J Fish Dis 34: 71-73

Millet COM, Cable J, Lloyd D (2010b). The diplomonad fish parasite *Spironucleus vortens* produces hydrogen. J Euk Microbiol 57: 400-404

Millet COM, Lloyd D, Williams CF, Williams D, Evans G, Saunders RA, Cable J (2010c). Effect of garlic and *Allium*-derived products on the growth and metabolism of *Spironucleus vortens*. Exp Parasitol 127: 490-499

Millet COM, Lloyd D, Coogan MP, Rumsey J, Cable J (2011). Carbohydrate and amino acid metabolism of *Spironucleus vortens*. Exp Parasitol 129: 17-26

Mo TA, Poppe T, Iversen L (1990). Systemic hexamitosis in salt-water reared Atlantic salmon. Bull Eur Assoc Fish Pathol 10: 69

Moore E (1922). *Octomitus salmonis*, a new species of intestinal parasite in trout. Trans Am Fisheries Soc 52: 74-97

Nigrelli RF, Hafter E (1947). A species of *Hexamita* from the skin of two cichlids. Anat Rec 99: 683

O'Brien GM, Ostland VE, Ferguson H (1993). *Spironucleus*-associated necrotic enteritis in angelfish (*Pterophyllum scalare*). Can Vet J 34: 301-303

Paull GC, Matthews RA (2001). *Spironucleus vortens*, a possible cause of hole-in-the-head disease in cichlids. Dis Aquat Org 45: 197-202

Poppe T, Mo TA, Iversen L (1992). Disseminated hexamitosis in sea-caged Atlantic salmon. Dis Aquat Org 14: 91-97

Poppe T, Mo TA (1993). Systemic, granulomatous hexamitosis of farmed Atlantic salmon: interactions with wild fish. Fish Res 17: 147-152

Post G (1987). Textbook of fish health. TFH Publications, Neptune City, New Jersey

Poynton SL, Morrison CM (1990). Morphology of diplomonad flagellates: *Spironucleus torosa* n. sp. from Atlantic cod *Gadus morhua* L., and haddock *Melanogrammus aeglefinus* (L.) and *Hexamita salmonis* Moore from brook trout *Salvelinus fontinalis* (Mitchill). J Protozool 37: 369-383

Poynton SL, Fraser W, Francis-Floyd R, Rutledge P, Reed P, Nerad TA (1995). *Spironucleus vortens* n. sp. from the fresh-water Angelfish *Pterophyllum scalare*: morphology and culture. J Euk Microbiol 42: 731-742

Poynton SL, Sterud E (2002). Guidelines for species description of diplomonad flagellates in fish. J Fish Dis 25: 15-31

Poynton SL, Fard MR, Jenkins J, Ferguson HW (2004). Ultrastructure of *Spironucleus salmonis* n. comb. (formerly *Octomitus salmonis* sensu Moore 1922, Davis 1926, and *Hexamita salmonis* sensu Ferguson 1979), with a guide to *Spironucleus* species. Dis Aquat Org 60: 49-64

Pradhan P, Lundgren SW, Wilson WA, Brittingham A (2012). Glycogen storage and degradation during in vitro growth and differentiation of *Giardia intestinalis*. J Parasitol 98: 442-444

Rottmann RE, Francis-Floyd, Durborow R (1992). The role of stress in fish disease. SRAC Publication No. 474

Roxström-Lindquist K, Jerlström-Hultqvist J, Jørgensen A, Troell K, Svärd SG (2010). Large genomic differences between the morphologically indistinguishable diplomonads *Spironucleus barkhanus* and *Spironucleus salmonicida*. BMC Genomics 11: 258

Sanghari-Fard MR, Jørgensen A, Sterud E, Bleiss W, Poynton SL (2007a). Ultrastructure and molecular diagnosis of *Spironucleus salmonis* (Diplomonadida) from rainbow trout *Oncorhynchus mykiss* in Germany. Dis Aquat Org 75: 37-50

Saghari-Fard MR, Weisheit C, Poynton SL (2007b). Intestinal pH profile in rainbow trout *Oncorhynchus mykiss* and microhabitat preference of the flagellate *Spironucleus salmonis* (Diplomonadida). Dis Aquat Org 76: 241-249

Sangmaneedet S, Smith SA (1999). Efficacy of various chemotherapeutic agents on the growth of *Spironucleus vortens*, an intestinal parasite of the freshwater angelfish. Dis Aquat Org 38: 47-52.

Sangmaneedet S, Smith SA (2000). *In vitro* studies on the optimal requirements for the growth of *Spironucleus vortens*, an intestinal parasite of the freshwater angelfish. Dis Aquat Org 39: 135-141

Seligo A (1887). Untersuchungen über Flagellaten. Beitr Biol Pflz 4: 145-180

Shiflett A, Johnson PJ (2010). Mitochondrion-related organelles in parasitic eukaryotes. Annu Rev Microbiol 64: 409-429

Siddall ME, Hong H, Desser SS (1992). Phylogenetic analysis of the Diplomonadida (Wenyon, 1926) Brugerolle, 1975: evidence for heterochrony in protozoa and against *Giardia lamblia* as a 'missing link'. J Protozool 39: 361-367

Simpson AGB (2003). Cytoskeletal organization, phylogenetic affinities and systematics in the contentious taxon Excavata (Eukaryota). Int J Syst Evol Microbiol 53: 1759–1777

Sterud E, Mo TA, Poppe TT (1997). Ultrastructure of *Spironucleus barkhanus* n. sp. (Diplomonadida: Hexamitidae) from grayling *Thymallus thymallus* (L.) (Salmonidae) and Atlantic salmon *Salmon salar* L. (Salmonidae). J Euk Microbiol 44: 399-407

Sterud E (1998a). *In vitro* cultivation and temperature-dependent growth of two strains of *Spironucleus barkhanus* (Diplomonadida: Hexamitidae) from Atlantic salmon *Salmo salar* and grayling *Thymallus thymallus*. Dis Aquat Org 33: 57-61

Sterud E. (1998b). Electron microscopical identification of the flagellate *Spironucleus torosa* (Hexamitidae) from burbot *Lota lota* (Gadidae) with comments upon its probable introduction to this freshwater host. J Parasitol 84: 947-953

Sterud E, Mo TA, Poppe TT (1998). Systemic Spironucleosis in sea-farmed Atlantic salmon *Salmo salar*, caused by *Spironucleus barkhanus* transmitted from feral Arctic char *Salvelinus alpinus*? Dis Aquat Org 33: 63-66

Sterud E, Poynton SL (2002). *Spironucleus vortens* (Diplomonadida) in the Ide, *Leuciscus idus* (L.) (Cyprinidae): a warm water hexamitid flagellate found in northern Europe. J Euk Microbiol 49: 137-145

Sterud E, Poppe T, Borno G (2003). Intracellular infection with *Spironucleus barkhanus* (Diplomonadida: Hexamitidae) in farmed Arctic char *Salvelinus alpinus*. Dis Aquat Org 56: 155-161

Tojo JL, Santamarina MT (1998). Oral pharmacological treatments for parasitic diseases of rainbow trout *Oncorhynchus mykiss*. I: *Hexamita salmonis*. Dis Aquat Org 33: 51-56

Tovar J, Fischer A, Clark CG (1999). The mitosome, a novel organelle related to mitochondria in the amitochondrial parasite *Entamoeba histolytica*. Mol Microbiol 32: 1013-1021

Tovar J, León-Avila G, Sánchez LB, Sutak R, Tachezy J, van der Giezen M, Hernández M, Müller M, Lucocq JM (2003). Mitochondrial remnant organelles of *Giardia* function in iron-sulphur protein maturation. Nature 426: 172-176

Uldal A (1996). Life cycle observations on *Hexamita salmonis* from rainbow trout intestine. *In vitro* studies. Bull Eur Ass Fish Pathol 16: 112-14

Uldal A, Buchmann K (1996). Parasite host relations: *Hexamita salmonis* in rainbow trout *Oncorhynchus mykiss*. Dis Aquat Org 25: 229-231

Uzmann JR, Jesse JW (1963). The *Hexamita* (=*Octomitus*) problem: a preliminary report. Prog Fish Cult 25: 141-143

Uzmann, JR, Paulik GJ, Hayduk SH (1965). Experimental hexamitiasis in juvenile coho salmon (*Oncorhynchus kisutch*) and steelhead trout (*Salmo gairdneri*). Trans Am Fish Soc 94: 53-61

Whaley J, Francis-Floyd R (1991). A comparison of metronidazole treatments for hexamitiasis in angelfish. Proc IAAAM, pp 110-114

Williams CF, Lloyd D (2012). Composition and antimicrobial properties of sulphur-containing constituents of garlic (*Allium sativum*). In: Essential Oils as Natural Food Additives: Composition, Quality and Antimicrobial Activity. Ed. Valgimigli L. Nova Publishers, Inc. NY, USA, pp 287-304

Woo PTK, Poynton SL (1995). Diplomonadida, Kinetoplastida and Amoebida (Phylum Sarcomastigophora). In: Woo PTK (ed.), Fish Diseases and Disorders, Vol. 1, Protozoan and Metozoan Infections, CAB International, Wallingford, UK, pp 27-96

Wood AM, Smith HV (2005). Spironucleosis (Hexamitiasis, Hexamitosis) in the ring-necked pheasant (*Phasianus colchicus*): detection of cysts and description of *Spironucleus meleagridis* in stained smears. Avian Dis 49: 138-143

Xiao W, Li L (1993). *Hexamita transparentus* sp. nov. and its ultrastructure. Trans Res Fish Dis 1: 52-55

Xiao W, Li L (1994). A light and transmission electron microscopic study of *Hexamita capsularis* sp. nov. (Diplomonadida: *Hexamita*) in fish (*Xenocypris divide*). Chin J Oceanol Limnol 12: 208-212

Xiao W, Wang J, Li L (2002). Descriptions of five new species of parasitic flagellate belonging to Hexamitidae in fishes. Acta Hydrobiologica Sinica 26: 509-511

Chapter 2

General Methods

CHAPTER 2: GENERAL METHODS

To avoid repetition, methods that are common to more than one chapter are provided here and are referred to in subsequent experimental chapters.

2.1. Fish origin and general maintenance

Juvenile angelfish were obtained from J&K Aquatics (Taunton, UK). When received, fish were held individually for the duration of the experiment in 12 L plastic tanks, each filled with dechlorinated water, an air supply and a plastic tank decoration for cover. Fish were maintained at 24±1°C with a 12h: 12h light: dark cycle and fed on a flake food (TetraMin) diet. Complete water changes were performed at least once per week in order to maintain good water quality.

2.2. Parasite origin and general maintenance

Spironucleus vortens trophozoites were maintained in Keister's modified TYI-S-33 medium by a modified method employed by Millet et al. (2010), without bile supplementation. Keister's modified TYI-S-33 medium contained per 900 ml distilled H_2O: 20 g pancreatic digest of casein (Oxoid); 10 g yeast extract (Oxoid); 10 g glucose (Acros Organics); 2 g NaCl (Fisher Scientific); 2 g L-cysteine HCl (Sigma-Aldrich); 0.2 g ascorbic acid (Sigma-Aldrich); 1 g K_2HPO_4 (Fisher Scientific); 0.6 g KH_2PO_4 (Fisher Scientific) and 22.8 mg ferric ammonium citrate (Sigma-Aldrich). On dissolving these constituents, the pH of the medium was adjusted to 6.8 using NaOH (Fisher Scientific) and autoclaved, before adding 100 ml sterile, heat-inactivated new-born calf serum (Gibco). Trophozoites were routinely subcultured aseptically after 48 h incubation, by transferring 500 µl of a homogenous log-phase culture into 10 ml of culture medium, leaving a 5 ml head space in 15 ml screw capped Falcon tubes (Greiner Bio-one). When accurate cell counts were necessary, trophozoites were fixed using 1.5% (v/v) formaldehyde and counted using an Improved Neubauer haemocytometer (Weber Scientific International). To ensure axenic maintenance, cultures were regularly checked for microbial contamination by plating-out 100 µl of a log-phase culture on nutrient agar and incubating under the above conditions for 5 d.

2.3. Automated optical cell density monitoring

A Bioscreen C optical density reader (Labsystems, Finland) was employed to monitor the growth of *S. vortens* trophozoites in 100 well honeycomb plates (Thermo-Fisher), according to Millet et al. (2011). Each well of the honeycomb plate contained 290 μl Keister's modified TYI-S-33 medium, 10 μl log-phase cell suspension, at a final density of 10^4 cells/ well, and 3 μl of the required inhibitor or supplement concentration (as specified in the appropriate chapters). Positive (cells with no inhibitors), negative (no cells or inhibitors) and, if applicable, solvent (cells with 3 μl DMSO, Sigma-Aldrich) controls were also prepared. All treatments were performed in triplicate. Optical density (OD) values were recorded every 15 min on a vertical light path using a wideband filter (420-580 nm) at 24°C, with plates shaken at low amplitude for 10 s before each reading to ensure mixing of well contents. Logarithmic growth rates (μ) and final growth yields were calculated as follows from the resulting growth curves:

$$\mu=(OD_{t2}-OD_{t1})/(t_2-t_1)$$

$$\text{Final yield}= OD_{tf}- OD_{t0}$$

Where, OD_{t1} is the optical density at the beginning of log phase growth, OD_{t2} is the optical density at the end of log phase growth, OD_{t0} is the initial optical density at the beginning of the growth curve and OD_{tf} is the final optical density after entering the stationary phase.

2.4. Determination of protein content

The protein content of cell-free *S. vortens* extracts were quantified using the Bradford assay (Bradford 1976). A sample volume of 3 μl was added to 1 ml dH_2O and a 1/5 dilution of Bradford reagent (Bio-Rad) and the OD measured at 595 nm. A calibration curve was constructed using this method for a range of protein (BSA) concentrations, as demonstrated in Figure 2.1, and used to estimate the protein content of samples for subsequent assays.

OD (595 nm) = 0.01874 + 0.1289 BSA conc (mg/ml)

S	0.0318582
R-Sq	97.7%
R-Sq(adj)	95.3%
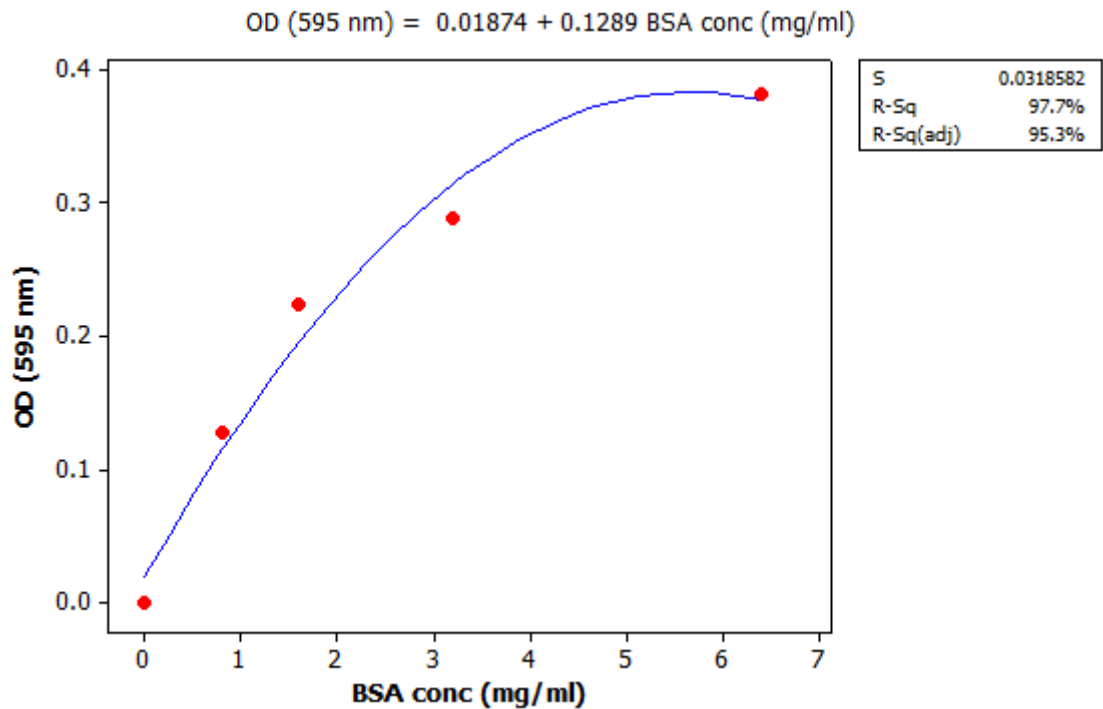
Fig. 2.1. Bradford assay calibration curve. Calibration curve used to determine protein concentration consisting of a fitted line plot constructed in Minitab (Version 16) of BSA concentration against optical density (OD) at 595 nm using the Bradford assay.

2.5. References

Bradford MM (1976). A rapid and sensitive method for the quantification of microgram quantities of protein utilizing the principle of protein-dye binding. Anal Biochem 72: 248-254

Millet COM, Cable J, Lloyd D (2010). The diplomonad fish parasite *Spironucleus vortens* produces hydrogen. J Euk Microbiol 57: 400-404

Millet CO, Lloyd D, Williams C, Williams D, Evans G, Saunders RA, Cable J (2011). Effect of garlic and *Allium*-derived products on the growth and metabolism of *Spironucleus vortens*. Exp Parasitol 127: 490-499

Chapter 3

Non-invasive estimation of *Spironucleus vortens* in angelfish provides novel insights on the transmission of this diplomonad parasite

CHAPTER 3:

Non-invasive estimation of *Spironucleus vortens* in angelfish provides novel insights on the transmission of this diplomonad parasite

Williams CF, Vacca AR, Lloyd D, Schelkle B & Cable J

3.1. ABSTRACT

Spironucleus vortens is a protozoan fish parasite of veterinary and economic importance in the ornamental aquaculture industry. Despite this, key aspects of the life cycle of this organism, including its mode of transmission, have not been fully elucidated. The current study developed a non-invasive method for quantifying *S. vortens* in angelfish, which was then used to investigate parasite transmission and aggregation within host populations. As previously observed for *S. meleagridis* and *S. salmonis*, motile *S. vortens* trophozoites were detected in host faeces using light microscopy. Species-level identification of these flagellates was confirmed using 16S rDNA PCR. Faecal trophozoite counts were significantly correlated with trophozoite counts from the posterior intestine, the primary habitat of the parasite. This novel finding allowed effective prediction of intestinal parasite load from faecal counts. Overall, faecal count data revealed 20% of hosts harbour 83% of parasites, conforming to the Pareto Principle (80/20 rule) of parasite aggregation with implications for parasite transmission. Trophozoites survived for ≥ 36 d outside the host within faecal pellets and remained motile at low pH (comparable to that of angelfish stomach). No putative *S. vortens* cysts were observed in cultures or faecal samples. This calls into question the commonly accepted hypothesis that a protective encysted stage is required in the life cycle of *S. vortens* to facilitate transmission to a new host.

3.2. INTRODUCTION

Ornamental aquaculture is a global multi-million dollar industry, which has been growing at an annual rate of 14% since 1985 (FAO 2005). Disease is a major limiting

factor in aquaculture production, causing losses of 45% to the industry (FDA 2012). Unfavourable conditions such as overcrowding, low dissolved O_2 tensions and aggression due to competition for resources, leads to animal stress which increases fish susceptibility to diseases. Accurate diagnosis of many fish diseases requires sophisticated equipment, such as electron microscopy, and consultation with fish health experts for pathogen identification (Sterud & Poynton 2002; Noga 2010). A further complication is the lack of available data into basic aspects of pathogen biology, including the life cycle and transmission of some disease-causing agents. Hence, infections are often undiagnosed, and may lead to disease outbreaks and significant mortality of fish if control measures fail.

Diplomonads are a group of aerotolerant anerobic or microaerophilic organisms which inhabit low O_2 environments such as the intestinal tract of animals and lake sediments (Biagini et al. 1998; Lloyd et al. 2002; Kolisko et al. 2010; Williams et al. 2011). *Spironucleus vortens* is a diplomonad parasite of freshwater ornamental fish. First isolated from an angelfish in Florida in 1991 (Poynton et al. 1995), *S. vortens* is particularly prevalent in cichlids and cyprinids, including angelfish, *Pterophyllum scalare*, and discus, *Symphysodon discus* (see review by Williams et al. 2011). The primary habitat of this parasite is the middle to posterior intestinal tract; however, motile trophozoites have also been isolated from other organs, including the liver, spleen and kidneys of infected hosts, indicating systemic infection. Recovery of this organism from head lesions has led to this parasite being described as the putative causative agent of hole-in-the-head disease (Paull & Matthews 2001).

Studies into the biology of *Spironucleus* spp. have been greatly hampered by lack of appropriate experimental methods. Earlier studies, which relied on the use of light microscopy alone to identify diplomonads, resulted in the assignation of piscine diplomonads to the genera *Hexamita*, *Octomitus* and *Spironucleus*. Recent detailed ultrastructural work and molecular tools, however, have confirmed that all piscine diplomonads belong to the genus *Spironucleus* (see Poynton & Sterud 2002, Jørgensen & Sterud 2007). PCR and/or sequencing primers have now been designed for most *Spironucleus* spp. (see review by Williams et al. 2011). In the case of *S. vortens*, however, the only available primers indiscriminately amplify the 16S rRNA gene of most *Spironucleus* species. Species-level identification of *S. vortens* therefore requires sequencing of 16S rDNA or transmission electron microscopy.

The life cycle of piscine *Spironucleus* spp. is poorly characterised, with most information being inferred from the distantly related mammalian diplomonad parasite *Giardia* (see review by Ankarklev et al. 2010). Like *Giardia*, the life cycle of *Spironucleus* spp. is thought to be direct, via the faecal-oral route, with transmission between hosts being facilitated by an infective encysted stage (Woo & Poynton 1995). The cyst form has been documented for *S. muris* (host: rodents), *S. meleagridis* (host: birds) and *S. salmonis* (host: salmon, trout), but has only rarely been seen *in vivo* for other piscine *Spironucleus* spp. and in the case of *S. vortens*, has never been documented (Sangmaneedet & Smith 2000; Williams et al. 2011). Likewise, the cyst form has not yet been reported for *S. salmonicida* (host: salmon, trout) but a recent genomic survey identified in this parasite a *Giardia lamblia* cyst wall protein homologue as well as two enzymes involved in cyst wall assembly, glucosamine-6-phosphate isomerase and UDP-N-acetylglucosamine pyrophosphorylase (Andersson et al. 2007). For *S. meleagridis* and *S. salmonis*, live trophozoites are expelled into fresh faeces without encystment (Tojo & Santamarina 1998; Philbey et al. 2002) and transmission of *S. salmonicida* trophozoites via skin lesions has been suggested (Poppe et al. 1992). The fact that *S. vortens*, *S. salmonicida* and *S. meleagridis* trophozoites are associated with extra-intestinal systemic infections, with parasites being identified in a number of different organs (Poppe et al. 1992; Paull & Matthews 2001; Bailey et al. 2010), indicates that trophozoites are able to tolerate fluctuations in O_2 tensions, pH and nutrition. Hence, it may be possible that some *Spironucleus* spp., including *S. vortens,* may not require an encysted stage, with the trophozoite form instead responsible for transmission.

The transmission potential of a pathogen is commonly measured using the basic reproduction rate, R_0. This represents the average number of secondary infections caused by an infected host during its lifetime. An R_0 value of >1 typically marks an epidemic outbreak, whereas if the calculated R_0 value is <1, the outbreak will become extinct (Woolhouse et al. 1997). The reliability of this epidemic threshold value, however, has recently been questioned as it can lead to misleading conclusions regarding the infectivity of the pathogen and lead to inappropriate medical interventions for pathogen control (Breban et al. 2007). For example, R_0 is affected by heterogeneities in pathogen transmission rates between individuals in a given population (Woolhouse et al. 1997). Such variation in pathogen transmission can be partially explained by the Pareto Principle, a statistical pattern known as the 80/20 rule, as proposed by Woolhouse et al. (1997). Host-parasite systems commonly abide to the 80/20 rule, whereby 20% of hosts

harbour *ca.* 80% of the parasites and hence transmission potential of the population. For endoparasites, such as *S. vortens*, current methods of determining parasite burden involve euthanasia of fish to examine intestinal contents (Whaley & Francis-Floyd 1991; Sangmaneedet 1999; Jørgensen & Sterud 2004).

In the current study, a non-invasive method of parasite quantification, based on a previous study by Tojo and Santamarina (1998), was developed using *S. vortens* faecal counts to estimate the degree of intestinal colonization. Species-level identification of *S. vortens* was confirmed using novel 16S rDNA PCR primers. To address the important issue of *S. vortens* aggregation within a host population, the parasite quantification method was successfully applied to test the 80/20 rule. Leading on from this, the role of the trophozoite in parasite transmission was examined using further faecal analysis (trophozoite survival), *in vitro* experiments (trophozoite tolerance to low pH) and an antibody-based technique (in the search for putative *S. vortens* cysts). Overall, the study aimed to provide novel information on the life cycle of *S. vortens*, specifically its mode of transmission to a new host.

3.3. MATERIALS AND METHODS

3.3.1. Fish origin and general maintenance

Juvenile angelfish (*Pterophyllum scalare*, N=168) were obtained from J&K Aquatics (Taunton, UK) and maintained as described in Chapter 2, section 2.1. All the experiments described below were conducted under these conditions.

3.3.2. Parasite origins

Spironucleus vortens (ATCC 50386). Trophozoite cultures were maintained in Keister's modified TYI-S-33 medium as described in Chapter 2, section 2.2.

Spironucleus vortens Sv1. An English-bred infected angelfish (identified by the presence of *Spironucleus* trophozoites in faeces, August 2011) was euthanized by overdose of MS-222 (Sigma-Aldrich). The entire intestinal tract was removed and transferred to 10 ml Keister's modified culture medium containing 0.5 mg/ml penicillin and streptomycin, 5 mg/ml gentamycin and 1 mg/ml collistin sulphate (all from Sigma-Aldrich), and incubated for 72 h at 24°C. The organism was then sub-cultured 5 times as described above to allow an increase in trophozoite number and remove bacterial/fungal contamination. Finally, a ciliate contaminant was removed at room temperature (20°C) by low speed centrifugation at 112 g_{av} for 3 min. The resulting pellet, containing the axenic

Spironucleus isolate, was aseptically transferred to fresh culture medium and maintained as described above, without antibiotics. Freezer stocks of the new isolate were prepared after a total of 6 subcultures by suspending *ca.* 10^6 cells/ ml in 10% DMSO (v/v, Sigma-Aldrich) and cooling to -80°C in an isopropanol bath at a controlled rate of 1°C per min. Vials of frozen cultures were then transferred to liquid N_2 for long term storage. Molecular identification of this new *Spironucleus* isolate (herein *Sv1*) was confirmed by PCR (see below).

Spironucleus barkhanus (ATCC 50467). Trophozoites from a liquid N_2 culture were thawed and incubated overnight in Keister's modified TYI-S-33 culture medium supplemented with 1 mg/L bile (sourced from local slaughter house) at 20°C, according to Sterud (1998).

3.3.3. Species-level identification of *S. vortens* using 16S rDNA PCR

A new primer pair, SV-1f 5'-TGTGGGAGACTGTGCTCTTG-3' and SV-1r: 5'-AGCATACTCCCCCAGGAACT-3', was designed to specifically amplify 158 bp of the 16S rRNA gene of *S. vortens* beginning at positions 704 (SV-1f) and 842 (SV-1r) of the GenBank Accession Number U93085 *S. vortens* gene sequence (Keeling & Doolittle 1997). These primers were designed using Primer3 (Rozen & Skaletsky 2000) and their suitability for PCR confirmed using OligoAnalyzer version 3.1 (PrimerQuest®). The Spiro-1f/1r primer pair from Jørgensen & Sterud (2004), which amplifies the 16S rRNA gene of most *Spironucleus* and *Hexamita* species, was employed as a positive control, producing an amplicon of 1431 bp. Total DNA was extracted from the *Sv1* intestinal isolate, *S. vortens* ATCC strain (positive control), *S. barkhanus* ATCC strain (negative control) and dH_2O (negative control) using the DNeasy Blood and Tissue Kit (Qiagen). Each 10 µl PCR reaction consisted of 2 µl of extracted DNA, 1 µl of each primer (10 pmol/µl, Eurofins), 0.1 µl dNTPs (0.25 mM, Thermo Scientific), 0.6 µl $MgCl_2$ (1.5 mM, Thermo Scientific), 1 µl of PCR buffer (ABgene), 0.1 µl of Taq Polymerase (0.05 U/µl, Thermo Scientific) and 4.2 µl of dH_2O. The PCR cycle was as follows: 95°C for 5 min, 95°C for 45 s, 56°C for 1 min, 72°C for 2 min, 72°C for 4 min and finally held at 4°C in a 96 well thermal cycler (Applied Biosystems). The denaturing, annealing and elongation steps were repeated for 35 cycles. Gel electrophoresis of the PCR products (2 µl each plus 1 µl loading dye, Applied Biosystems) and 100 kb DNA ladder was performed on 1.5% (w/v) agarose gels (Bioline) containing ethidium bromide (Invitrogen) with an

applied voltage of 120 V. Gels were then visualized and imaged using an UV transilluminator (GelDoc-It).

3.3.4. Detection and quantification of *S. vortens* trophozoites in angelfish faeces by light microscopy

Fresh faecal samples from angelfish were collected from the bottom of clean plastic tanks using a plastic pipette. Faecal samples were placed on a glass slide with a drop of fresh dechlorinated water and compressed using a 22 x 22 mm coverslip. These squash preparations were examined by light microscopy for the presence of *S. vortens* trophozoites, which were identified according to their length (10-20 μm), pyriform shape and characteristic torpedo-like cell motility. The number of trophozoites per sample was estimated by counting the number of parasites present for a 15 min period (X400 magnification) until the whole sample had been examined (*ca.* 50 fields of view). The PCR method described above, using the SV-1f/1r primer pair, was employed in order to confirm the presence of *S. vortens* in the faeces of angelfish. A total of 17 angelfish faecal samples, from fish with varying degrees of *Spironucleus* infection (as previously determined by faecal counts, see below), were analysed in order to test the sensitivity of the method for non-invasive *in vivo* diagnosis. Tank water (1 ml) from a highly infected and uninfected fish was also tested for the presence of *S. vortens*, with fresh dechlorinated water used as an additional negative control.

3.3.5. Comparison of infection prevalence and intensity via faecal and intestinal trophozoite counts

Two faecal samples (in order to account for variation in parasite shedding by the host over time) were collected from 20 fish for non-invasive quantification of the number of *S. vortens* trophozoites. Later the same day, the fish were euthanized with an overdose of MS-222 anaesthetic and dissected. The entire intestinal tract was removed and cut into four sections: anterior, anterior-middle, middle-posterior and posterior (according to Uldal & Buchmann 1996), and the total number of *S. vortens* trophozoites in each section quantified as for the faecal samples (squash preparation of intestinal sections under X400 magnification). Trophozoite counts derived from angelfish faeces and the four angelfish intestinal sections were first incorporated into a generalized linear mixed model (GLMM) to account for the repeated faecal sampling of one individual. Since animal ID and faecal sample number did not have a significant effect on the faecal trophozoite count, the

average of the two faecal samples were used as dependent variables in a negative binomial general linear model (GLM) with intestinal trophozoite counts in the four different gut locations as independent variables. Models were reduced using a step-wise deletion process with an α-level of 0.05 and evaluation of AIC values to assess significance of model terms and overall model fit. The only independent variable which significantly correlated with faecal counts was the posterior intestine. Hence, the final model utilized $\log_{10}$ transformed faecal (dependent variable) and posterior intestinal (independent variable) count data and the square root link function. The model assumptions were checked for normal distribution (visual examination of histograms and Q-Q plots), heteroscedasticity (Fligner-Killeen test, p<0.05), overdispersion (theta = ~1) and proportion of variability in the dataset that is accounted for by the model (pseudo R^2 ≥0.7). The final model was then used to predict the number of trophozoites in the posterior gut based on parasite counts in faeces.

3.3.6. Pareto Principle (80/20 rule)

The *S. vortens* trophozoite faecal quantification method described above was used to test the Pareto Principle that *ca.* 80% of the effects come from 20% of the causes. Hosts (N=168, including uninfected individuals) were ranked from most to least infected according to trophozoite faecal counts and the relative proportions of host (0-1, with 0.05 increments) plotted against the corresponding proportions of parasites. The expected proportion of parasites, or transmission potential, was extrapolated from the top 20% of most infected individuals.

3.3.7. Survival of *S. vortens* trophozoites in faeces

Fresh faecal samples were collected from angelfish, transferred into 1 L plastic pots and incubated at 24°C for specific time intervals (0, 1, 2, 3, 14 or 36 days) in dechlorinated water (N=28 faecal samples per time point). After incubation, samples were examined and the number of *S. vortens* trophozoites counted as described above.

3.3.8. Survival of *S. vortens* trophozoites at varying pH *in vitro*

Log-phase *S. vortens* trophozoites from *in vitro* cultures (ATCC and *Sv1* strains) were inoculated into the wells of a 12-well plate to a final cell density of 2-3 x 10^6 cells/well (counted by fixation of a 10 µl sample from a homogenous cell suspension in 1.5% (v/v) formaldehyde using an Improved Neubauer haemocytometer prior to well

inoculation). Each well contained 2 ml of culture medium at different pH levels: pH 3, 4, 5, 6, 7 or 2 ml of distilled water (2 replicates of each pH per parasite strain). Trophozoite motility was used to monitor cell vigour using light microscopy (X200 magnification). Cells were incubated on a shaker between observations (50 rpm) to mimic the motions of stomach peristalsis and observed every hour for 3 h. Cell motility was ranked as follows: (-) immotile cells, (+) twitching cells (++), semi-motile/slow-moving cells, and (+++) cells with normal/healthy motility.

3.3.9. Putative *S. vortens* cysts

Encystment of S. vortens in vitro. To investigate whether *S. vortens* encystment could be induced, several methods were tested that are based on successful encystment protocols for related diplomonads, such as *Giardia* and other *Spironucleus* spp. These were as follows; (1) starvation: post-stationary phase cultures (i.e. >72 h) incubated in PBS (pH 7.2) or distilled water (Uldal 1996); (2) *Giardia* encystment medium: *S. vortens* trophozoites were grown to late log phase in culture medium, before being transferred to encystation medium, consisting of culture medium supplemented with 1 M NaOH (Sigma-Aldrich), 0.25 mg/ml bile (obtained from local slaughter house) and 5 mM lactic acid (Sigma-Aldrich, Gillin et al. 1989); (3) bile salts: taurocholic acid and glycocholic acid (both from Sigma-Aldrich) in culture medium (1, 2, 4, 8, and 16 mM); (4) fatty acids: oleic acid and myristic acid (both from Sigma-Aldrich), in culture medium (2, 1, 0.5, 0.25 and 0.125 mM). Approximately 10^6 *S. vortens* trophozoites were incubated with all treatments for 72 h in 12 well plates and examined by light microscopy every 24 h for the presence of putative cysts using the trypan blue (0.4% w/v, Sigma-Aldrich) exclusion assay to identify viable cells.

Morphological identification of putative S. vortens cysts in vivo. There are currently no commercially available cyst-specific stains for the identification of *Spironucleus*. Januschka et al. (1988), however, showed that the cysts of *S. muris* and *Giardia microti* have similar cyst wall protein compositions. Therefore, the GiardiaCel kit (Cellabs) was used to examine angelfish faecal samples for the presence of *Spironucleus* cysts. A total of 10 fresh and 10 two week old faecal samples (the latter incubated in aquarium water in closed Eppendorfs) were collected from angelfish and fixed, permeabilized and stained according to the manufacturer's instructions. The kit contained a *Giardia*-specific cyst wall primary antibody, which binds to CWP1, a protein component of the *Giardia* cyst wall (Chatterjee et al. 2010). A fluorescent FTIC-tagged

anti-mouse secondary antibody was used to visualize the cyst (λ_{ex} 490 nm, λ_{em} 530 nm). Cells were imaged at X200 and X600 magnification using confocal microscopy (Leica TCS SP2 AOBS). A *Giardia*-positive slide, supplied by the kit, was used as a positive control. *S. vortens* trophozoites (ATCC strain) from 5 day and 2 week old *in vitro* cultures were also examined in the same way.

3.3.10. Statistical analysis

All statistical analyses described above were conducted using R (version 2.15.1; R Core Team 2012). Mean abundance was used to compare faecal and intestinal trophozoite counts and is defined as the mean number of parasites counted per sample with zero counts included.

3.4. RESULTS

Quantification of *Spironucleus vortens* trophozoites present in angelfish faeces allowed accurate estimation of the degree of intestinal colonization by the parasite. Trophozoites survived for extended periods in angelfish faeces and remained motile at acidic pH. No *S. vortens* cysts were observed *in vivo* or *in vitro*.

3.4.1. Identification of *S. vortens* trophozoites in fresh angelfish faeces

The SV-1f/1r primer pair specifically distinguished *S. vortens* from *S. barkhanus* (Fig. 3.1a) and confirmed the presence of *S. vortens* in angelfish faecal samples (Fig. 3.1b). The smaller DNA fragment generated from the new primer pair was easy to amplify, and therefore the test more sensitive, than the previously documented Spiro-1f/1r primer pair (see Jørgensen & Sterud, 2004; data not shown), which only identifies *Spironucleus* to the genus level. Single celled, pyriform-shaped, highly motile flagellates with torpedo-like motion were observed at X400 magnification towards the centre of angelfish faeces using light microscopy (Fig. 3.2). These organisms were *ca.* 10-20 μm in length, abundant and were found freely swimming amongst the faecal matter. Numerous intracellular inclusions, putative vacuoles and/or bacteria, were observed within these organisms, which have been characteristically observed in *Spironulceus* trophozoites (Poynton & Sterud 2002). These cytoplasmic inclusions are less numerous in laboratory cultured isolates. The mean abundance of *S. vortens* trophozoites in faecal samples of all fish employed in this study (N=168) was 68, with a range of 1-1,322. In some instances, differences were observed in the sensitivity of the molecular and microscopic approaches

employed to identify *S. vortens* trophozoites. This is illustrated in Figure 3.1b (see †) whereby no *S. vortens* DNA amplification was apparent in faecal samples of fish previously deemed to be highly infected with *S. vortens* (>100 trophozoites counted) by the microscopic method. It should be noted, however, that not enough replicates were performed in order to directly compare the accuracy of the microscopic and molecular methods.

3.4.2. Correlation between faecal and intestinal trophozoite counts

The variation between faecal counts taken from the same fish over time is illustrated in Figure 3.3. The largest difference between two faecal samples from the same host was 685 trophozoites, a range of 135-820 parasites counted. The prevalence of infection in the intestinal tract of angelfish (N=20) was 100%, with a mean abundance of 3,096, approx. 37x greater than that of faecal samples, with a range of 1-18,430 in the posterior section (the intestinal section which consistently had the highest parasite load). There was a significant positive correlation between average faecal trophozoite counts and posterior intestinal trophozoite counts (negative binomial GLM, $Z = 3.979$, $p<0.001$, AIC = 44.60, pseudo $R^2 = 0.7$; Fig.3.4). Although individual faecal counts, i.e. count 1 or count 2, when incorporated individually into the model, also significantly correlated with posterior intestinal counts, the overall fit of both these models was reduced with regards to proportion of variability in the dataset that was accounted for by the models (pseudo $R^2 = 0.58$ and 0.50 for count 1 and count 2, respectively). Hence, obtaining the average of at least 2 faecal counts greatly increases reliability when predicting posterior intestinal trophozoite numbers.

3.4.3. Aggregation of *S. vortens* infection in angelfish

Figure 3.5 shows that 20% of angelfish hosts harbour approximately 83% of parasites, and thus transmission potential of the population. Of the total host population, 85% harboured 100% of the parasites
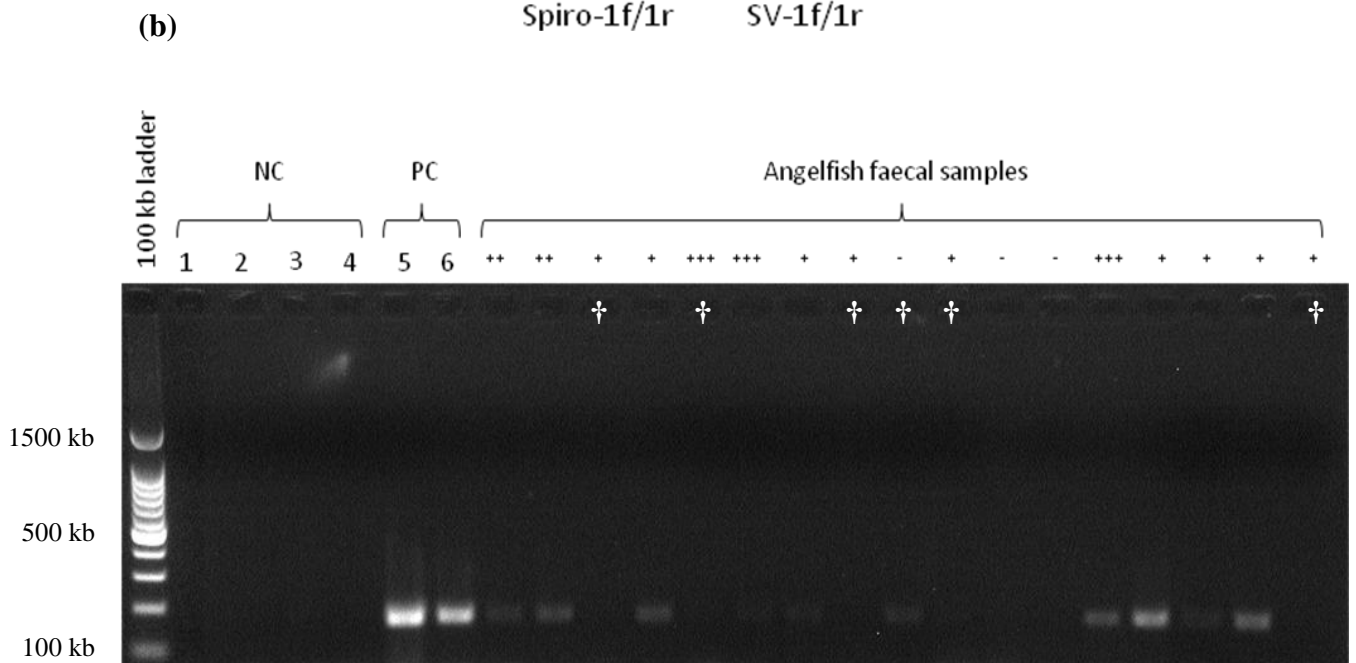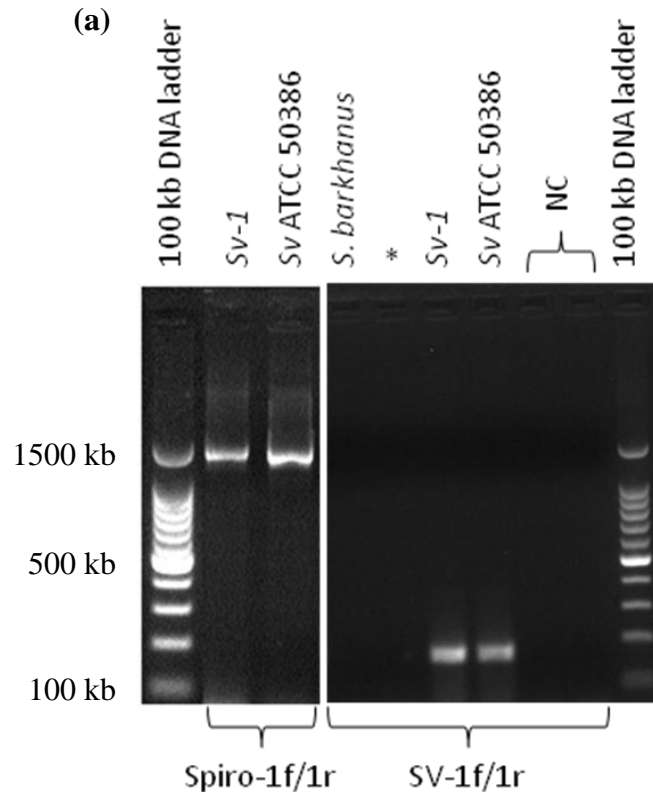
Fig. 3.1. Amplified *Spironucleus* DNA banding after 16S rDNA PCR. (a) The Spiro-1f/1r primer pair identified *Spironucleus vortens* ATCC and new intestinal isolate *Sv1* cultures to the genus level (1431 bp fragment), whilst the novel SV-1f/1r primer pair allowed species-specific identification of *S. vortens* (158 bp fragment)*,* indicated by lack of amplified DNA for *S. barkhanus* using this primer pair. NC = dH$_2$O negative controls, * = empty well. (b) Amplification of *S. vortens* DNA from angelfish faecal samples using the SV-1f/1r primer pair. (-) zero, (+) ≤ 50, (++) 51-100 and (+++) >100 trophozoites counted in previous faecal samples obtained from each fish, † indicates discrepancies between the PCR and microscopic counting method. NC = negative controls: (1) = fresh tank water, (2) tank water from a highly infected fish, (3) tank water from an uninfected fish and (4) dH$_2$O. PC = positive controls: (5) *S. vortens Sv1* strain and (6) *S. vortens* ATCC strain.
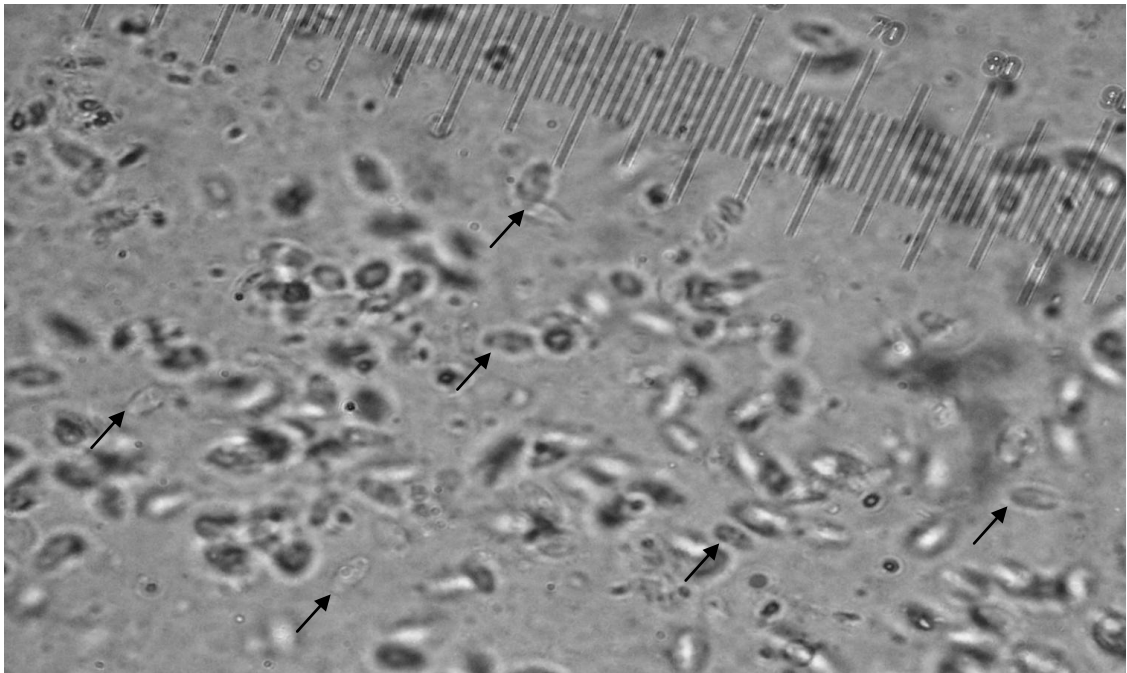
Fig. 3.2. *Spironucleus* trophozoites in angelfish faeces. Trophozoites were numerous (*ca.* 70) and highly motile. Note the characteristic length (*ca.* 10-20 µm) and pyriform shape of parasites, indicated by arrows (X400 magnification, 1 eye piece unit = 2.5 µm).

3.4.4. Survival of *S. vortens* trophozoites in faeces and varying pH

S. vortens trophozoites survived in the faeces of angelfish for a minimum of 36 days (the final time point examined during this experiment). Between 1-16 *S. vortens* trophozoites were observed in the 36 d old faecal samples, with a mean abundance of 2. This was a decline of 90% compared to the Day 0 samples (mean abundance 19.2, range 1-130). *S. vortens* trophozoites (both the *Sv1* and ATCC strains) survived for a minimum of 3 h in culture medium at pH 5 and 7 indicated by motility of the organisms. Parasite motility in dH$_2$O and at pH 6 was reduced to twitching (ATCC strain) or no motility (*Sv1* strain) after 3 h incubation in these conditions. Motility of the *Sv1* new intestinal isolate also diminished greatly following 3 h incubation in pH 5 and 7 culture media. However, for cells incubated in culture medium at pH ≤4 cell motility immediately ceased for both strains and trophozoites became irregular in morphology, eventually resulting in lysis of cells (Table 3.1).

Table 3.1. *Spironucleus vortens* survival under acidic pH. Survival of *S. vortens* (ATCC and *Sv1*) trophozoites over time in culture medium of varying pH and distilled water, indicated by (+++) healthy motility, (++) semi-motile, (+) twitching motility and (-) immotile cells. Cells were shaken between each observation.

Time (h)	pH 4	pH 5	pH 6	pH 7	dH$_2$O
S. vortens ATCC strain					
0	-	+++	+++	+++	+++
1	-	+++	+++	+++	+++
2	-	+++	++	+++	++
3	-	+++	+	+++	+
S. vortens Sv1 strain					
0	-	+++	+++	+++	+++
1	-	++	++	++	+++
2	-	+	+	++	++
3	-	+	-	+	+

3.4.5. Attempted induction and identification of *S. vortens* cysts

No viable cyst-like structures were observed after incubation in any of the cyst-induction media tested. After incubation, there was a marked increase in lysed cell debris (i.e. aggregations of organelles) and trypan blue was taken up by all remaining intact cellular structures, indicating dead or dying cells. Figure 3.6a shows the characteristic staining of the *Giardia* cyst wall, which was used as a positive control in the search for putative *S. vortens* cysts. Of all the angelfish faecal samples examined, no *Spironucleus* cyst-like structures were identified. There was a high degree of cross-reactivity of the *Giardia* cyst wall antibody with other matter found within the faecal samples, but no stained structures were observed that were similar in morphology to *Giardia* and *S. muris* cysts (see Januschka et al. 1988). Interestingly, however, *S. vortens* trophozoites from 5 day old and 2 week old cultures were positively labelled with this antibody (Fig. 3.6b-d). Unlike the *Giardia* cysts, intact trophozoites were labelled only around the periphery of the cell.
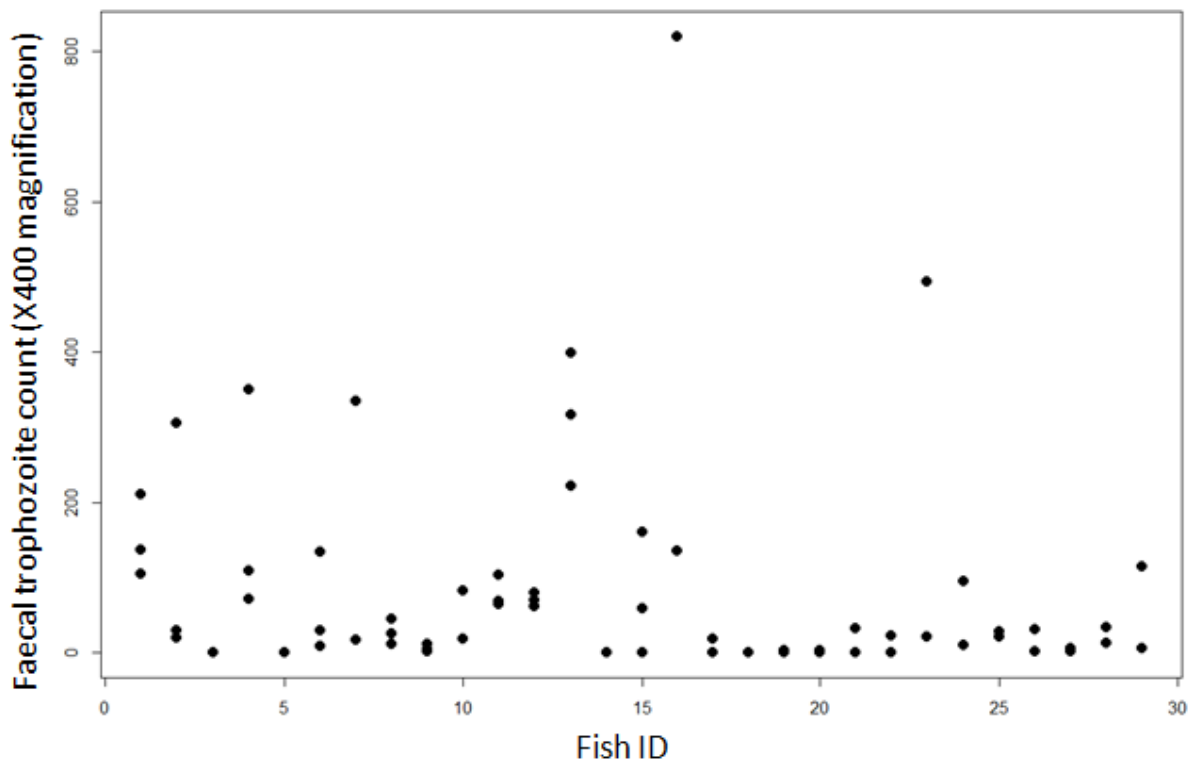
Fig. 3.3. Scatterplot of variability in the total number of *Spironucleus* trophozoites observed between faecal samples (n≥2) over time for each fish (29 in total).

3.5. DISCUSSION

The characteristic rapid, torpedo-like motility of *Spironucleus vortens*, as well as its pyriform shape and typical length of *ca.* 10-20 μm, allowed easy identification of *S. vortens* from squash preparations of angelfish intestinal sections and faecal pellets during this study. The presence of parasites in samples was confirmed using novel SV-1f/1r primers, which provided species level identification of *S. vortens*. Intestinal dissections revealed that all fish examined (N=20) were infected with *S. vortens*. Intensity of infection was greatest in the posterior intestine, which is comparable with previous observations by Poynton et al. (1995) and Sangmaneedet (1999).

As a non-invasive method of quantifying infection, faecal trophozoite counts were used as a tool to predict the degree of intestinal colonization by *S. vortens*. Faecal trophozoite counts have been used previously by Tojo and Santamarina (1998) as a means of estimating *S. salmonis* infections in salmonids. This study confirms the feasibility of employing faecal trophozoite counts to estimate the degree of intestinal colonization. Faecal counts correlated significantly with trophozoite counts observed in the posterior intestine of angelfish. Hence, the prediction curve (see Fig. 3.4) developed during this study may be used as a reliable means of estimating intestinal infection by *S. vortens* in angelfish. It is important to note, however, that the mean abundance of posterior intestinal trophozoite counts was 37x greater than the faecal trophozoite counts. Hence, care must be taken whilst interpreting faecal samples where no trophozoites are detected for both the microscopic and molecular identification methods as this may be due to human counting error, reduced parasite motility in the sample, or differential parasite shedding by the host over time. The latter is true of *Giardia*, where there is a periodicity in cyst excretion by the host (McGlade et al. 2003). It is therefore recommended that a minimum of two faecal samples are analysed from the same fish in order to estimate intestinal colonization.

The disease dynamics of *S. vortens* were investigated in terms of parasite aggregation in hosts using data from faecal trophozoite counts. In the current study, angelfish-*S. vortens* aggregation matched the 80/20 rule with 20% of the hosts harbouring 83% of parasites. These highly infected hosts, termed "supershedders", account for the bulk of the transmission potential (Lloyd-Smith et al. 2005). Woolhouse et al. (1997) observed a similar aggregation pattern for the protozoan parasites *Leishmania* and *Plasmodium*. The same authors suggested that control measures should focus on this 20% core of highly infected individuals. Hence, the non-invasive trophozoite quantification

method developed during this study may be applied in aquaculture to identify and treat the top 20% of infected individuals in order to efficiently control disease outbreaks. This would be especially useful for broodstock or other highly prized angelfish and discus.
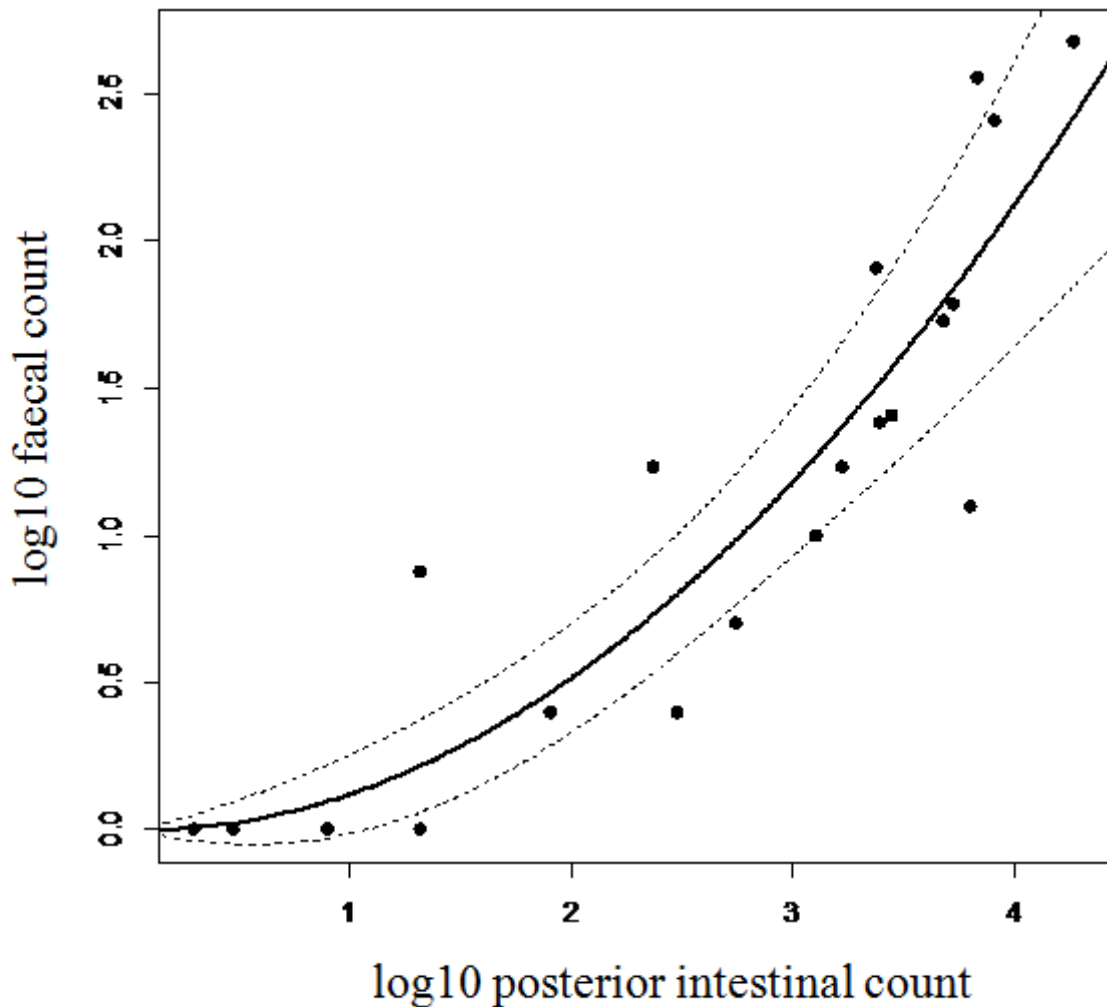
Fig. 3.4. Correlation between faecal and posterior intestinal trophozoite counts. A scatterplot of $\log_{10}$ transformed faecal trophozoite count vs. posterior intestinal trophozoite count. The continuous line represents predicted values of posterior counts for a given faecal count, derived from a negative binomial general linear model (Z = 3.979, p<0.001, theta = 0.308 and pseudo R^2 = 0.7). This prediction curve was overlaid on top of a scatterplot of the actual count data. Dashed lines represent upper and lower standard errors of the model.

A small proportion of expelled *S. vortens* trophozoites (*ca.* 10% of the number recovered from fresh faecal samples) survived for 36 days in angelfish faeces. This is the first observation of prolonged survival of diplomonad trophozoites in host faeces and suggests that *S. vortens* trophozoites are able to utilize substrates present in the faeces and withstand fluctuations in nutrients, temperature and O_2 tensions for long-term survival. Millet et al. (2010) found that *S. vortens* consumes O_2 at a rate of 62 nmol/min/10^7 cells in a closed reaction vessel, suggesting a highly effective O_2 scavenging mechanism. *S. vortens* and *S. salmonis* are only capable of surviving in water for a limited time (10 h and 5 min, respectively, Kent et al. 1992; Millet et al. 2011) a finding which was confirmed during the current study whereby *S. vortens* trophozoite motility was dramatically reduced after 3 h. Hence, faecal matter is likely to confer a substantial degree of protection for the trophozoite against the external environment. For example, the presence of O_2 consuming gut bacteria and saprophytic organisms will result in the removal of O_2 from faecal pellets generating a microaerobic habitat. Indeed, trophozoites were mainly found towards the centre of faecal samples where O_2 tensions would be at their lowest (pers. obs.). *S. salmonis* trophozoites have also been observed in the faeces of salmonids (Tojo & Santamarina 1998). The fact that *S. vortens* and *S. salmonis* cluster together in 16S rDNA phylogenies suggests that they are closely related, and may explain the similarities observed in trophozoite faecal shedding (Fard et al. 2007). Trophozoites of the marine parasites *S. salmonicida* and *S. barkhanus* have not yet been described in faecal pellets. If confirmed, a possible explanation for this could be due to the high salt composition of the surrounding marine environment, hence requiring a cyst form for survival outside the host.

As *S. vortens* trophozoites can survive for extended periods in angelfish faeces they potentially represent a transmission stage to new hosts, but if ingested they would have to withstand the acidic pH of the stomach. *S. vortens* trophozoites generally remained motile at pH 5-7, but motility instantly ceased at pH ≤4, eventually resulting in cell lysis. The stomach pH of freshwater angelfish has not been well characterised, however that of *Holacanthus passer*, a marine angelfish species, has been reported to range from 2-5 (Martínez-Díaz & Pérez-España 1999). In another cichlid, *Oreochromis niloticus*, stomach pH levels range from 0.9-7 (Getachew 1989), being more acidic after feeding due to the secretion of gastric fluids for digestion. Hence, at the more alkaline end of the scale it may be plausible that *S. vortens* trophozoites can survive passage through the stomach. Indeed, *Spironucleus* trophozoites have previously been

documented in the stomach of hosts, including mice (Fain et al. 2008), Siamese fighting fish (O'Brien et al. 1993) and angelfish (Sangmaneedet 1999), with that of mice being confirmed by molecular identification. As fish are coprophagic, it is highly likely that *S. vortens* trophozoites would be readily consumed and, given the appropriate conditions, may survive passage to the intestine. Indeed, Sangmaneedet (1999) showed that oral infection of angelfish with *S. vortens* trophozoites resulted in intestinal colonization by this parasite.
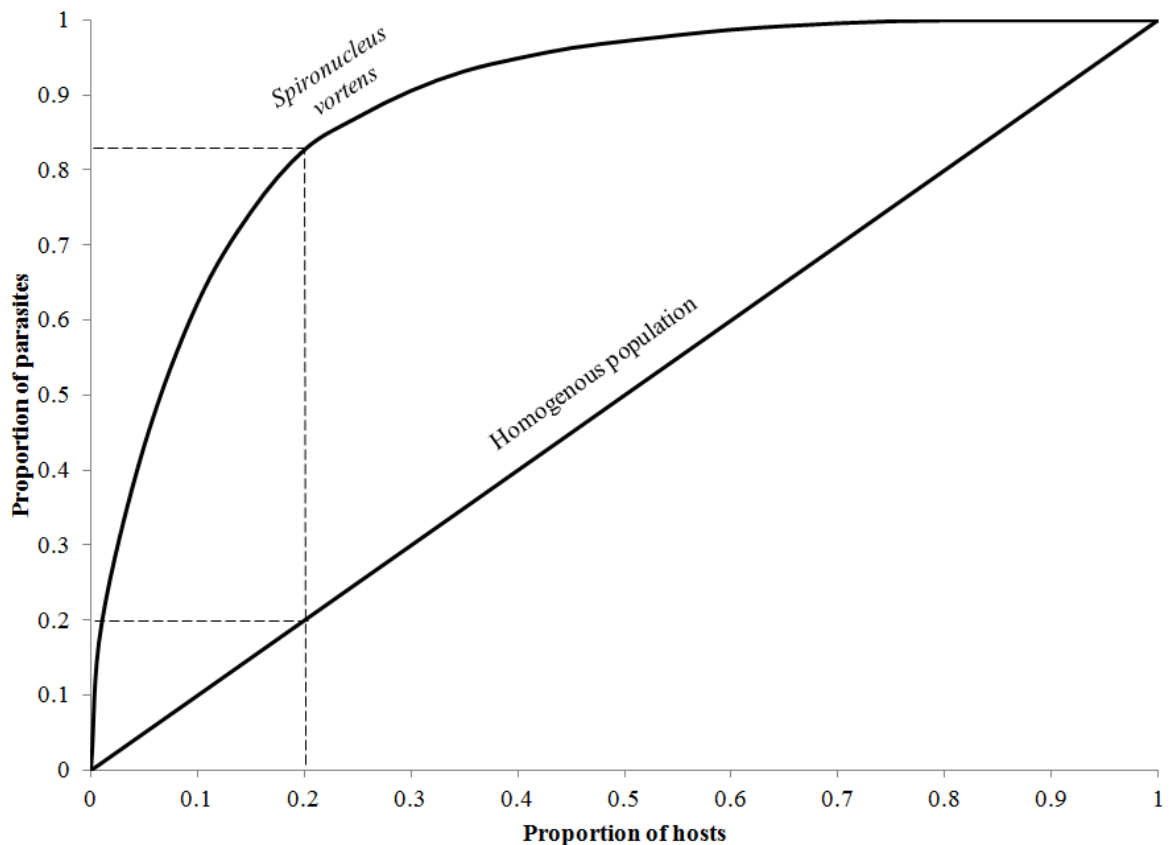
Fig. 3.5. Transmission potential of *Spironucleus vortens* according to the 80/20 rule. Fitted line plot (continuous line) of the proportion of hosts (N=168), ranked from most to least infected with *S. vortens*, against proportion of parasites in order to test the Pareto Principle (or 80/20 rule) of parasite aggregation in a host population. The distribution of a homogeneous population is also indicated. Dashed lines indicate the expected proportion of parasites present in 20% of the hosts.

It has been proposed that cyst-like structures confer long-term survival of *Spironucleus* species outside the host (Woo & Poynton 1995). However, despite various methods being employed during the current study to induce encystment in *S. vortens*, no

viable cyst-like structures were identified. Hence, under the conditions described, neither starvation (in spent culture medium and water) nor putative chemical triggers of encystment, e.g. bile and lactic acid, as documented for encystment of related diplomonads, *S. salmonis* and *G. intestinalis* (see Gillin et al. 1989; Uldal 1996), induced encystment of *S. vortens in vitro*. For some protists, e.g. *Entamoeba histolytica*, it has been notoriously difficult to induce encystment *in vitro*, despite the confirmed presence of cysts *in vivo*. For *E. histolytica*, reactive O_2 species from the host immune system or intestinal microbiota have been suggested as potential triggers of encystation, a stress factor that may not be present to the same degree *in vitro* (Aquilar-Díaz et al. 2010). As *S. vortens* occupies a similar niche to *E. histolytica* (i.e. posterior intestine), this may explain the failure to induce encystment *in vitro*. Hence, during this study angelfish faecal samples were also analysed for the presence of putative *S. vortens* cysts. Due to morphological similarities between the cyst walls of *Giardia muris* and *S. muris* (see Poppe et al. 1992) a cyst wall antibody from *G. intestinalis* was employed to identify *S. vortens* cysts in angelfish faeces. Again, no such structures were identified, either indicating a lack of cysts or non-specificity of the *Giardia* antibody with *S. vortens* cysts. Interestingly however, *S. vortens* trophozoites (ATCC strain) were found to be positively labelled with the antibody. The antibody has been previously shown not to react with *Giardia* trophozoites (WB strain, in culture since 1978, Chatterjee et al. 2010), which suggests that either the cell membrane of *S. vortens* trophozoites shares a similar epitope with the *Giardia* cyst wall, perhaps as a constituent of a protective pellicle, or that these trophozoites were in the process of encysting. Completion of the genome sequence of *S. vortens* will provide further insight into the presence or absence of encystment-specific genes in this organism.

In conclusion, this study sheds light on important aspects of *S. vortens* transmission and calls into question the existence of an encysted stage. This is especially relevant in aquaculture where host density, and therefore transmission potential via the faecal-oral route and/or skin lesions, is high. Prolonged survival of *S. vortens* trophozoites in faecal pellets outside the host is a novel discovery that requires further physiological elucidation in terms of the capacity of the organism to tolerate high fluctuations in O_2 tensions and nutrition status. The non-invasive methods (faecal counts and 16S rDNA PCR) employed in this study require further investigation to determine their applicability in aquaculture for reliable diagnosis of *S. vortens* infection and subsequent control of Spironucleosis.
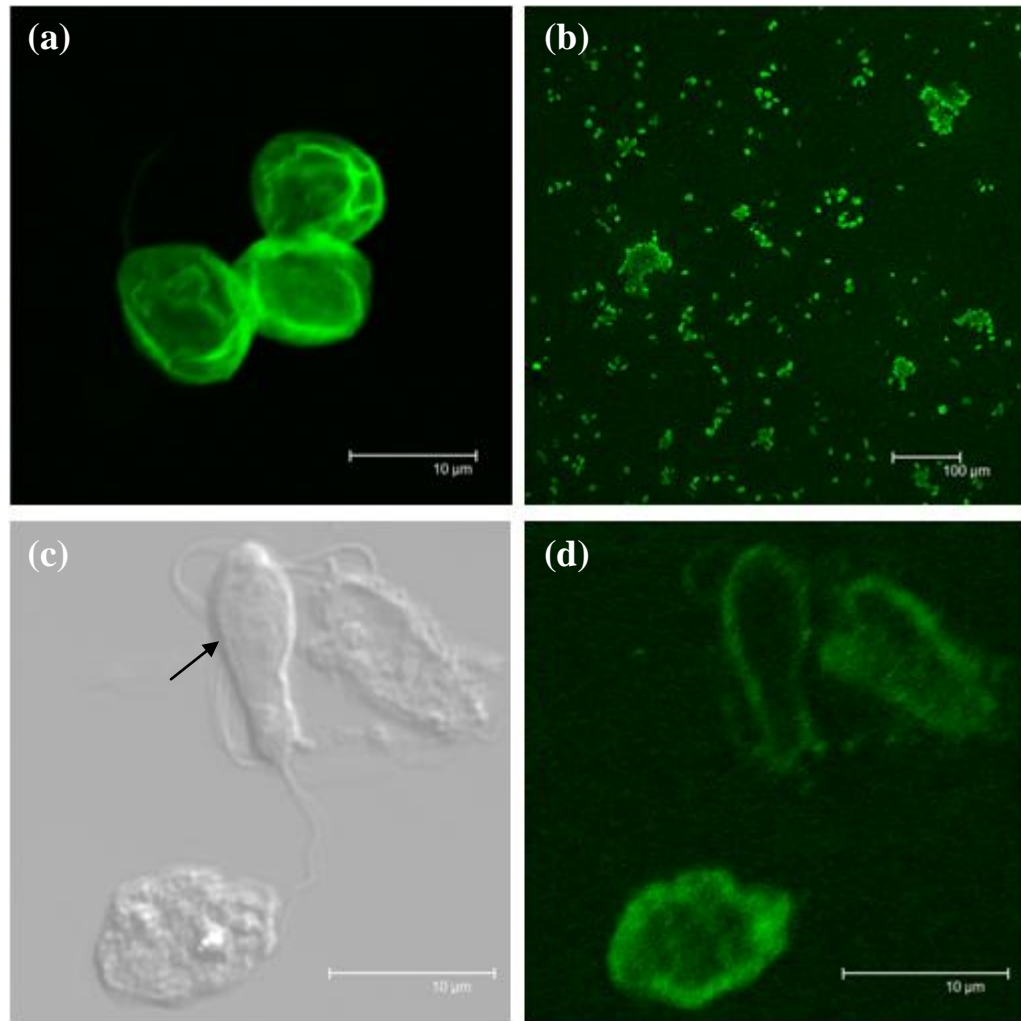
Fig. 3.6. Staining of diplomonads with the GiardiaCel antibody. (a) *Giardia* cysts (positive control, X600), (b) 2 week old *Spironucleus vortens* culture (X200), (c) DIC image of 5 day old *S. vortens* culture, the arrow indicates an intact trophozoite with visible flagella (X600), and (d) fluorescence FITC image of (c) (X600). The debris at the bottom left hand side of images (c) and (d) is an un-intact (dead) trophozoite from the culture.

3.6. REFERENCES

Andersson JO, Sjögren AM, Horner DS, Murphy CA, Dyal PL, Svärd SG, Logsdon Jr JM, Ragan MA, Hirt RP, Roger AJ (2007). A genomic survey of the fish parasite *Spironucleus salmonicida* indicates genomic plasticity among diplomonads and significant lateral gene transfer in eukaryote genome evolution. BMC Genomics 8: 51-76

Ankarklev J, Jerlström-Hultqvist J, Ringqvist E, Troell K, Svärd SG (2010). Behind the smile: cell biology and disease mechanisms of *Giardia* species. Nat Rev Microbiol 8: 413-422

Aquilar-Díaz H, Díaz-Gallardo M, Laclette JP, Carrero JC (2010). *In vitro* induction of *Entamoeba histolytica* cyst-like structures from trophozoites. PLoS Negl Trop Dis 16: e607

Bailey C, Kramer J, Mejia A, MacKay J, Mansfield KG, Miller AD (2010). Systemic Spironucleosis in two immunodeficient rhesus macaques (*Macaca mulatta*). Vet Pathol 47: 488-494

Biagini GA, McIntyre PS, Finlay BJ, Lloyd D (1998). Carbohydrate and amino acid fermentation in the free-living primitive protozoan *Hexamita* sp. Appl Environ Microbiol 64: 203-207

Breban R, Vardavas R, Blower S (2007). Theory versus data: how to calculate R_0? PLoS One 2: e282

Chatterjee A, Carpentieri A, Ratner DM, Bullitt E, Costello CE, Robbins PW, Samuelson J (2010). *Giardia* cyst wall protein 1 is a lectin that binds to curled fibrils of the GalNAc homopolymer. PLoS Pathogens 6: e1001059

Fain MA, Karjala Z, Perdue KA, Copeland MK, Cheng LI, Elkins WR (2008). Detection of *Spironucleus muris* in unpreserved mouse tissue and faecal samples by using a PCR assay. J Am Assoc Lab Anim Sci 47: 39-43

FAO (2005). Fisheries and aquaculture topics. Ornamental fish. Topics fact sheets. In: FAO Fisheries and Aquaculture Department [online]. Rome, Italy. Updated 27 May 2005 [Cited 8 January 2013] URL: http://www.fao.org/fishery/topic/13611/en

Fard MRS, Jørgensen A, Sterud E, Bleiss W, Poynton SL (2007). Ultrastructure and molecular diagnosis of *Spironucleus salmonis* (Diplomonadida) from rainbow trout *Oncorhynchus mykiss* in Germany. Dis Aquat Org 75: 37-50

FDA (2012). Safety & health. Antimicrobial resistance. Animal husbandry and disease control: aquaculture. In: FDA Animal & Veterinary [online]. Maryland, USA. Updated 5 September 2012 [Cited 8 January 2013], URL: http://www.fda.gov/AnimalVeterinary/SafetyHealth/AntimicrobialResistance/ucm082099.htm

Getachew T (1989). Stomach pH, feeding rhythm and ingestion rate in *Oreochromis niloticus* L. (Pisces: Cichlidae) in Lake Awasa, Ethiopia. Hydrobiologica 174: 43-48

Gillin FD, Boucher SE, Rossi SS, Reiner DS (1989). *Giardia lamblia*: the roles of bile, lactic acid, and pH in the completion of the life cycle *in vitro*. Exp Parasitol 69: 164-174

Januschka MM, Erlandsen SL, Bemrick WJ, Schupp DG, Feely DE (1988). Comparison of *Giardia microti* and *Spironucleus muris* cysts in the vole: an immunocytochemical, light and electron microscopic study. J Parasitol 74: 452-458

Jørgensen A, Sterud E (2004). SSU rRNA gene sequence reveals two genotypes of *Spironucleus barkhanus* (Diplomonadida) from farmed and wild Arctic charr *Salvelinus alpinus*. Dis Aquat Org 62: 93-96

65

Jørgensen A, Sterud E (2007). Phylogeny of *Spironucleus* (Eopharyngia: Diplomonadida: Hexamitinae). Protist 158: 247-254

Keeling PJ, Doolittle WF (1997). Widespread and ancient distribution of a noncanonical genetic code in diplomonads. Mol Biol Evol 14: 895-901

Kent ML, Ellis J, Fournie JW, Dawe SC, Bagshaw JW, Whitaker DJ (1992). Systemic hexamitid infection in seawater pen-reared chinook salmon. Dis Aquat Org 14: 81-89

Kolisko M, Silbermann JD, Cepicka I, Yubuki N, Takishita K, Yabuki A, Leander BS, Inouye I, Inagaki Y, Roger AJ, Simpson AGB (2010). A wide diversity of previously undetected free-living relatives of diplomonads isolated from marine/saline habitats. Environ Microbiol 12: 2700-2710

Lloyd D, Harris JC, Maroulis S, Wadley R, Ralphs JR, Hann AC, Turner MP, Edwards MR (2002). The 'primitive' microaerophile *Giardia intestinalis* (syn. *lamblia*, *duodenalis*) has specialized membranes with electron transport and membrane-potential-generating function. Microbiology 148: 1349-1354

Lloyd-Smith JO, Schreiber SJ, Kopp PE, Getz WM (2005). Superspreading and the effect of individual variation on disease emergence. Nature 438: 355-359

Martínez-Díaz SF, Pérez-España H (1999). Feasible mechanisms for algal digestion in the king angelfish. J Fish Biol 55: 692-703

McGlade TR, Robertson ID, Elliot AD, Thompson RCA (2003). High Prevalence of *Giardia* detected in cats by PCR. Vet Parasitol 110: 197-205

Millet CO, Cable J, Lloyd D (2010). The diplomonad fish parasite *Spironucleus vortens* produces hydrogen. J Eukaryot Microbiol 57: 400-404

Millet CO, Lloyd D, Coogan MP, Rumsey J, Cable J (2011). Carbohydrate and amino acid metabolism of *Spironucleus vortens*. Exp Parasitol 129: 17-26

Noga EJ (2010). Methods for diagnosing fish diseases. In: Noga EJ (ed.), Fish disease: diagnosis and treatment, Wiley-Blackwell, Iowa, USA, pp 4-81

O'Brien GM, Ostland VE, Ferguson HW (1993). *Spironucleus*-associated necrotic enteritis in angelfish (*Pterophyllum scalare*). Can Vet J 34: 301-303

Paull GC, Matthews RA (2001). *Spironucleus vortens*, a possible cause of hole-in-the-head disease in cichlids. Dis Aquat Org 45: 197-202

Philbey AW, Andrew PL, Gestier AW, Reece RL, Azey KE (2002). Spironucleosis in Australian king parrots (*Alisterus scapularis*). Aust Vet J 80: 154-160

Poppe T, Mo TA, Iversen L (1992). Disseminated hexamitosis in sea-caged Atlantic salmon. Dis Aquat Org 14: 91-97

Poynton SL, Fraser W, Francis-Floyd R, Rutledge P, Reed P, Nerad TA (1995). *Spironucleus vortens* n. sp. from the fresh-water Angelfish *Pterophyllum scalare*: morphology and culture. J Euk Microbiol 42: 731-742

Poynton SL, Sterud E (2002). Guidelines for species description of diplomonad flagellates in fish. J Fish Dis 25: 15-31

PrimerQuest® program, IDT, Coralville, USA [Cited 05 March, 2013] URL: http://eu.idtdna.com/pages/scitools

R Core Team (2012). R: A language and environment for statistical computing. R Foundation for Statistical Computing, Vienna, Austria. ISBN 3-900051-07-0 [Cited 24 March 2013] URL: http://www.r-project.org/

Rozen S, Skaletsky HJ (2000). Primer3 on the WWW for general users and for biologist programmers. In: Krawetz S, Misener S (eds.), Bioinformatics methods and protocols: methods in molecular biology, Humana Press, Totowa, NJ, pp 365-386

Sangmaneedet S (1999). *Spironucleus vortens* of the freshwater angelfish (*Pterophyllum scalare*): growth requirements, chemotherapeutants, pathogenesis and immunity. PhD Thesis, Virginia Polytechnic Institute and State University, pp 62-81

Sangmaneedet S, Smith SA (2000). *In vitro* studies on optimal requirements for the growth of *Spironucleus vortens*, an intestinal parasite of the freshwater angelfish. Dis Aquat Org 39: 135-141

Sterud E (1998). *In vitro* cultivation and temperature-dependent growth of two strains of *Spironucleus barkhanus* (Diplomonadida: Hexamitidae) from Atlantic salmon *Salmo salar* and grayling *Thymallus thymallus*. Dis Aquat Org 33: 57-61

Sterud E, Poynton SL (2002). *Spironucleus vortens* (Diplomonadida) in the ide, *Leuciscus idus* (L.) (Cyprinidae): a warm water hexamitid flagellate found in Northern Europe. J Eukaryot Microbiol 49: 137-145

Tojo JL, Santamarina MT (1998). Oral pharmacological treatments for parasitic diseases of rainbow trout *Oncorhynchus mykiss*. I: *Hexamita salmonis*. Dis Aquat Org 33: 51-56

Uldal A (1996). Life cycle observations on *Hexamita salmonis* from rainbow trout intestine. *In vitro* studies. Bull Eur Ass Fish Pathol 16: 112-114

Uldal A, Buchmann K (1996). Parasite-host relations: *Hexamita salmonis* in rainbow trout *Oncorrhynchus mykiss*. Dis Aquat Org 25: 229-231

Whaley J, Francis-Floyd R (1991). A comparison of metronidazole treatments for hexamitiasis in angelfish. Proc IAAAM, pp 110-114

Williams CF, Lloyd D, Kolarich D, Alagesan K, Duchene D, Cable J, Williams D, Leitsch D (2012). Disrupted intracellular redox balance of the diplomonad fish parasite *Spironucleus vortens* by 5-nitroimidazoles and garlic-derived compounds. Vet Parasitol 190: 62-73

Williams CF, Lloyd D, Poynton SL, Jørgensen A, Millet COM, Cable J (2011). *Spironucleus* species: economically important fish pathogens and enigmatic single-celled eukaryotes. J Aquac Res Development S2-002

Woolhouse MEJ, Dye C, Etard JF, Smith T, Charlwood JD, Garnett GP, Hagan P, Hii JLK, Ndhlovu PD, Quinnell RJ, Watts CH, Chandiwana SK, Anderson RM (1997). Heterogeneities in the transmission of infectious agents: implications for the design of control programs. Proc Natl Acad Sci USA 94: 338-342

Woo PTK, Poynton SL (1995). Diplomonadida, Kinetoplastida and Amoebida (Phylum Sarcomastigophora). In: Woo PTK (ed.), Fish Diseases and Disorders, Vol. 1, Protozoan and Metozoan Infections, CAB International, Wallingford, UK, pp 27-96

Chapter 4

Synergistic effect of garlic-derived ajoene oil and 5-nitroimidazole, metronidazole, against the ornamental fish parasite *Spironucleus vortens*

CHAPTER 4:

Synergistic effect of garlic-derived ajoene oil and 5-nitroimidazole, metronidazole, against the ornamental fish parasite *Spironucleus vortens*

4.1. ABSTRACT

Spironucleus vortens is a protozoan parasite associated with significant mortalities in angelfish and discus. Control of this parasite is especially problematic due to restrictions on the use of the drug of choice, metronidazole (MTZ), on outdoor fish farms. However, garlic (*Allium sativum*), employed for millennia in human and veterinary medicine, is undergoing a revival following experimental validations of its antimicrobial efficiency. Ajoene ((E,Z)-4,5,9-trithiadodeca-1,6,11-triene 9-oxide), is a stable transformation product of allicin, the primary biologically active component of garlic. In the current study, an ajoene oil crude extract had a minimum inhibitory concentration (MIC) of 40 µg/ml against *S. vortens*. Using GC-MS and NMR spectroscopy, this ajoene extract was found to contain a mixture of the (E) and (Z)-ajoene isomers along with diallyl disulphide (DADS) and diallyl trisulphide (DATS). The only component of the ajoene crude oil found to substantially inhibit *S. vortens* growth by optical density monitoring (Bioscreen C Reader) was (Z)-ajoene (MIC 16 µg/ml). Ajoene oil acted in synergy with metronidazole (MTZ) *in vitro*, reducing the individual MIC of this drug (4 µg/ml) by 16-fold, and that of ajoene oil by 200-fold with a fractional inhibitory concentration (FIC) index of 0.263. This synergistic interaction was confirmed *in vivo*. *S. vortens*-infected angelfish fed for 5 consecutive days with 0.5% (v/w) MTZ combined with 0.05% (v/w) ajoene experienced a significant reduction in faecal trophozoite count, whilst those fed on 0.5% MTZ flakes (half the recommended oral dose) alone did not. This study demonstrates for the first time the synergistic interaction between MTZ and ajoene oil both *in vitro* and *in vivo*. Future work should evaluate the potential synergy of ajoene and MTZ against MTZ-resistant bacteria and protists.

4.2. INTRODUCTION

Antibiotic discovery is arguably the greatest medical breakthrough of the Twentieth Century. Overuse of these "wonder drugs" has however led to an exponential incline in antibiotic resistance (>20,000 potential resistance genes documented to date, Liu & Pop 2009), coupled with a decline in development of new antibiotics by the pharmaceutical industry. Furthermore, there is a lack in our understanding of fundamental mechanisms of resistance as a result of this microbial arms race (see review by Davies & Davies 2010). In addition to resistance, some therapeutic agents (e.g. fluoroquinolones) can have serious adverse effects on the patient, whilst others (e.g. nitroimidazoles) have been classified as potential human carcinogens (IARC 1987; Lipsky & Baker 1999). Collectively, these factors have led some authors to warn of the return to the pre-antibiotic era in medicine. As a result, research into alternative herbal remedies, such as garlic, is undergoing a revival.

The antimicrobial properties of garlic (*Allium sativum*) have been exploited for millennia. Ancient civilizations, from the Egyptians to the Romans reaped the benefits of garlic's broad-ranging medicinal uses to treat a variety of common ailments such as gastrointestinal disorders, asthma and convulsions (Harris et al. 2001). To date the antifungal, antiprotozoal, antibacterial and antiviral effects of *Allium*-derived compounds have been extensively documented and validated *in vitro* (see review by Williams & Lloyd 2012). Despite this, little in the way of pharmacological development of *Allium*-based drugs has taken place (Martin & Ernst 2003). Of the few clinical trials that have been conducted, those involving allicin (diallyl thiosulphinate), the main biologically active component of the garlic clove, have resulted in poor outcomes for gastrointestinal infections. For example, despite the success of *in vitro* studies against the gastric pathogen *Helicobacter pylori*, clinical treatment trials failed to eradicate the infection (Graham et al. 1994; Aydin et al. 1997; Ernst 1999). These negative effects were attributed to the low allicin content of the treatments (McNulty et al. 2001). Indeed, many of the commercially available garlic supplements were found to contain undetectable levels of allicin (Freeman & Kodera 1995). Allicin itself is produced from its precursor alliin by the action of alliinase (Lawson et al. 1991). Alliinase is irreversibly inhibited at gastric pH, hence restricting allicin production in the lower gut (Lawson & Hughes 1992). Some studies have employed encapsulated garlic powders, designed to bypass the stomach, hence allowing the release of allicin in the intestinal tract. However, even

71

studies employing preparations with high allicin content failed to eradicate *H. pylori* infections (Martin & Ernst 2003).

On decomposition, allicin has been documented to yield hundreds of reaction products, many of which are antimicrobial (Block 2010). Of particular note is ajoene ((E, Z)-4, 5, 9-trithiadodeca-1, 6, 11-triene 9-oxide), which is extracted from allicin under heating or methanolic conditions (Block et al. 1984; Naznin et al. 2008). Ajoene has a comparable antimicrobial activity to that of allicin; however its stability is much greater under exposure to elevated temperature, UV light and long term storage (Naznin et al. 2008). Due to the unstable nature of allicin, it is likely that many of the antimicrobial effects of garlic can be attributed to the many reaction products of this highly reactive garlic component, and not directly to allicin itself. Interestingly, Freeman & Kodera (1995) showed that allicin does not decompose to its usual reaction products of diallyl disulphide (DADS), ajoene and dithiins under gastric (pH 1.2) and intestinal (pH 7.5) simulations. Hence, it is possible that previous clinical trials which employed high concentrations of allicin failed for this reason.

Disease control is a major limiting factor of fish production in aquaculture. Treatments such as malachite green, antibiotics and other drugs have been banned from use on food fish in Europe and North America due their toxicity and carcinogenicity in fish and humans (see reviews by Schelkle et al. 2009; Williams et al. 2011). Hence tonnes of fish are lost annually due to disease outbreaks and ineffective infection control (FAO 2012). This is especially true in the case of Spironucleosis, an intestinal disease caused by the protozoan parasite *Spironucleus*. Several outbreaks of Spironucleosis have been documented on fish farms (Mo et al. 1990; Poppe et al. 1992; Poppe & Mo, 1993; Sterud et al. 1998), with the only known effective treatment being the 5-nitroimidazole, metronidazole (MTZ), which has been banned from use on European and American food fish due to its carcinogenic properties in humans (Commission Regulation No. 613/98 1998; FARAD 2010). MTZ is still available for treatment of ornamental fish in contained aquaria, however this drug has been documented as cytotoxic and genotoxic in fish and requires veterinary prescription, meaning that it should only be used as a last resort (Cavas & Ergene-Gozukara 2005; Khalil et al. 2007).

Allium-derived compounds have previously been found to be effective against *Spironucleus vortens*, putative causative agent of hole-in-the-head disease in ornamental fish (Paull & Matthews 2001), *in vitro* (Millet et al. 2011a). A later study by Williams et al. (2012, see Chapter 5) investigated the mode of action of garlic-derived compounds

and MTZ, suggesting that ajoene and MTZ may have a synergistic antiparasitic effect due to their complementary modes of action. Indeed, garlic extracts are commonly used as fish food additives in the ornamental industry due to their role in folk-lore medicine (Millet et al. 2011). As a result, this study aimed to evaluate the combinatorial effect of MTZ with ajoene *in vitro* and *in vivo*, using *S. vortens*-infected angelfish.

4.3. MATERIALS AND METHODS

4.3.1. Fish origin and maintenance

Juvenile angelfish (*Pterophyllum scalare*, N=58) were obtained from J&K Aquatics (Taunton, UK) and maintained as described in Chapter 2, section 2.1. Fish were fed with specially prepared flake food, described below.

4.3.2. Organism and culture

Trophozoites of two *Spironucleus vortens* strains, ATCC 50386 and *Sv1* (freshly isolated from juvenile English-bred angelfish, described in Chapter 3), were maintained separately in Keister's modified TYI-S-33 medium as described in Chapter 2, section 2.2.

4.3.3. Inhibitors

The garlic-derived allicin (2% v/v), ajoene oil (18% v/v), (Z)-ajoene (98% v/v), (E)-ajoene (98% v/v) and dithiin (un-quantified dithiin-rich fraction) extracts were provided by NEEM Biotech Ltd. All other garlic-derived compounds, allyl alcohol (AA), allyl sulphide (AS), allyl disulphide (AD), diallyl disulphide (DADS), diallyl trisulphide (DATS), methyl disulphide (MD), allyl methyl sulphide (AMS), allyl methyl disulphide (AMD), propyl sulphide (PS) and propyl disulphide (PD) were obtained from Lancaster Synthesis Ltd. The 5-nitroimidazole, metronidazole (MTZ) was sourced in powder form (Sigma-Aldrich).

4.3.4. Gas chromatography mass spectrometry (GC-MS)

In order to assess the impurities present in the ajoene (18% (v/v)) preparation, samples were subjected to GC-MS analysis. GC-MS provides good resolution of volatile sample components, by modification of column temperature. The instrument used was an Agilent 6890 GC with a 5973N MS and a 7683 AS. Sample separation was achieved using an Agilent HP-5MS non-polar column with a 30 m x 0.25 mm internal diameter and a 0.25 µm phase thickness. An on-column injection method was employed with an

injection port temperature of 36°C, and an injection volume of 0.2 µl. The initial oven temperature was 35°C, with an initial ramp of 5°C/min to 240°C, where it was held for 3 min, and a second ramp of 10°C/min to a final temperature of 300°C, held for 2 min. The total run time was 55 min. The MS source temperature was 230°C, with scanning between 35-250 amu (EI$^+$ 70eV). Samples were analysed after a 10 min solvent delay and identified by the MS library software (Agilent ChemStation). A positive peak ID was only confirmed with >90% accuracy (R match) from the library.

4.3.5. Nuclear magnetic resonance (NMR) spectroscopy

The presence of (E) and/or (Z)-ajoene isomers in the ajoene oil extract was determined by ^{1}H NMR spectroscopy. Ajoene oil was diluted 1:100 in CDCl$_3$ (Sigma-Aldrich) and its ^{1}H NMR spectrum was recorded according to Millet et al. (2011b) using a Bruker Avance DPX400 spectrometer with a 5 mm ^{1}H probe at 400 MHz and 300 K. The acquisition time of spectra was 2.56 s using 90° pulses and a relaxation delay time of 1 s over a spectral width of 11 ppm over 16 scans. CDCl$_3$ solvent was used as an internal lock and chemical shifts are expressed as parts per million (ppm). Compounds were identified by comparison with spectra of standard solutions according to Naznin et al. (2008).

4.3.6. Automated optical cell density monitoring

A Bioscreen C optical density reader (Labsystems, Finland) was employed to monitor the growth of *S. vortens* as described in Chapter 2, section 2.3. The inhibitory effects of a number of *Allium*-derived compounds were quantified against *S. vortens* (ATCC strain) *in vitro*, these were: allicin, ajoene oil, (E)-ajoene, (Z)-ajoene, AA, AS, AD, DADS, DATS, MD, AMS, AMD, PS, PD and dithiins (concentration range: 100, 50, 25, 12.5, 6, 3 and 1, 0.5 and 0.25 µg/ml and 1:100, 1:200, 1:400, 1:800, 1:1600 for the dithiin-rich extract). MTZ was used as a positive control (concentration range: 160, 80, 40, 20, 10, 5, 2.5, 1, 0.5 and 0.25 µg/ml). Various combinations of ajoene oil and MTZ were also employed using the following concentration ranges: 8, 4, 2, 1, 0.5, 0.25 µg/ml ajoene oil and 4, 2, 1, 0.5 and 0.25 µg/ml MTZ. All concentrations of ajoene oil were combined with one of the MTZ concentrations in turn. The inhibitory effect of MTZ, ajoene oil, AA and DADS was also tested against the freshly isolated *S. vortens Sv1* strain, as described above. All compounds were diluted in DMSO apart from allicin and AA which were diluted in sterile distilled water. Each well of the honeycomb plate

contained 290 µl Keister's modified TYI-S-33 medium, 10 µl log-phase cell suspension, at a final density of 10^4 cells/ well, and 3 µl of the required inhibitor concentration (in the combination experiment, 1.5 µl of each compound was loaded). Positive (cells with no inhibitors), negative (no cells or inhibitors) and solvent (cells with 3 µl DMSO) controls were also prepared. Final growth yields were calculated from the resulting growth curves. These final yields were then plotted against inhibitor concentration in order to determine the MIC of compounds, with MIC defined as the minimum inhibitor concentration(s) to completely inhibit *S. vortens* growth. Finally, the fractional inhibitory concentration (FIC), or the lowest concentration of each ajoene + MTZ combination to completely inhibit growth, was derived for each component, as follows:

$$\text{FIC(component A)} = \frac{\text{MIC}_{(A)1}}{\text{MIC}_{(A)2}}$$

Where $\text{MIC}_{(A)1}$ corresponds to the MIC of component A when tested in the most efficient combination of A and B, and $\text{MIC}_{(A)2}$ is the MIC of component A when tested alone. An FIC index for each ajoene oil/MTZ combination was calculated to assess the synergistic, additive or antagonistic effects of the various combinations, as follows:

$$\text{FIC Index} = \Sigma \text{ FIC A} + \text{FIC B}$$

This study employs guidelines proposed by Odds (2003) to determine synergy, no interaction (indifference) and antagonism between inhibitor concentrations, as follows: synergy = FIC<0.5, indifference = FIC 0.5-4.0 and antagonism = FIC>4.0. Normally distributed FIC indexes of equal variance, derived from the combinatorial effect of ajoene oil and MTZ (N=3 for each combination), were analysed by one-sample T-test using Minitab software (Version 16). Each FIC index was analysed for significant difference from 0.5, the FIC index value which indicates synergistic interaction between inhibitors according to Odds (2003).

4.3.7. Preparation of fish food treatments

All treatments were firstly dissolved in 1 ml ethanol (Fisher Scientific) and then re-suspended in 100 ml dH_2O to the desired concentration. Fish flake food (TetraMin, 2 g for each treatment) were soaked in each treatment at the desired concentration overnight

at room temperature. Excess moisture was removed from the flake treatments by freeze drying. The resulting ajoene content of dried flakes was quantified by high performance liquid chromatography (HPLC). HPLC analysis was carried out on an Agilent 1100 series HPLC system using an ODS 4.6 x 250mm with ODS guard cartridge. All HPLC solvents were purchased from Rathburn Chemicals (Scotland). Samples were solvated in methanol and eluted with an aqueous acetonitrile mixture using a gradient method as follows: 45% acetonitrile up to 13 min, after which the concentration was increased up to 80% before decreasing again to 45% at 18 min. The flow rate was 1 ml/min with a pressure of 400 bar and detection at 254 nm. The recommended MTZ dose for treatment of Spironucleosis is 10 mg/g fish food (Francis-Floyd & Reed 1994). This concentration is approximately 1000-fold greater than the MIC of this drug *in vitro*. Hence a higher concentration of ajoene, compared to its *in vitro* MIC was prepared. Preliminary investigations were conducted to define the concentration of flake-soaked ajoene that was palatable to angelfish. Fish (N=2 for each concentration) were fed with 0, 5, 10 and 50 µl ajoene/g flakes (0, 0.5, 1 and 5% v/w, respectively) over the course of 1 d. The only ajoene concentration which fish readily consumed was the 0.5% preparation. Fish from the 0.5% ajoene flakes preliminary treatment group were then continuously fed on this preparation for 5 d without any behavioural changes (i.e. inappetite or erratic behaviour). Subsequently, the concentration of each treatment employed in the main experiment was as follows: 0.5% ajoene oil, 0.5% (v/w, 5 mg/g) MTZ, 0.05% (0.5 µl/g) ajoene oil and 0.5% MTZ combination. The chosen concentration of MTZ is half the recommended dose in ornamental fish (Francis-Floyd & Reed 1994) in order to assess possible synergistic interactions between lower concentrations of this drug and ajoene oil. Freeze-dried control flakes consisted of 2 ml ethanol in 100 ml dH$_2$O without inhibitors.

4.3.8. *In vivo* treatment

Naturally occurring *S. vortens* infections in angelfish (N=50) were quantified using faecal trophozoite counts (described in Chapter 3). The average trophozoite counts from two faecal samples were quantified in order to gain a more accurate estimation of the degree of infection due to differential host parasite shedding over time. *S. vortens* infections were quantified in this way at Day 0 (pre-treatment). Fish were then randomly separated into groups and treated as follows: Group 1 (N=10) = control flakes, Group 2 (N=9) = 0.5% ajoene flakes, Group 3 (N=8) = 0.5% MTZ flakes, Group 4 (N=10) = 0.05% ajoene and 0.5% MTZ combination flakes and, as an added control, Group 5

(N=10) = 0.0005% (w/v, 5 mg/L) MTZ bath. The concentration of MTZ employed in the bath treatments were as recommended by Tojo & Santamarina (1998) as a positive control. The concentration of ajoene employed was the highest concentration tested that was palatable to fish (as described above). The reduction in sample sizes from N=10 for the ajoene oil and MTZ treatment groups is due to difficulties in obtaining faecal samples from some fish during the experiment. Fish in each group were fed daily with the allocated flake treatment (approx. 3% body weight) for 5 d, with daily 25% water changes of aquaria in order to dilute the levels of accumulated ajoene and MTZ (Whaley & Francis-Floyd 1991). On Day 5 post-flake treatment, 100% water changes took place for all treatment groups and the infection intensity was quantified by trophozoite faecal counts, as described above. For the MTZ bath treatment, pre-treatment tropohozoite faecal counts were conducted on Day 0, after which fish were incubated for 1 h in a 1 L plastic pot containing 0.0005% MTZ on Day 1, Day 3 and Day 5. Post-treatment trophozoite faecal counts were conducted on Day 6.

A one-tailed Mann-Whitney non-parametric test was employed to identify potential significant difference between angelfish faecal trophozoite counts before and after treatment (Group 1 = control, Group 2 = ajoene oil, Group 3 = MTZ, Group 4 = ajoene oil + MTZ combination and Group 5 = MTZ bath treatment). The pre-treatment faecal counts were hypothesized to be significantly greater than the post-treatment faecal counts with an α value of 0.05. Efficacy of treatments (E_t) were calculated according to Schelkle et al. (2011) as follows:

$$\textbf{If } L_t < L_0, \textbf{ then } E_t = (L_0 - L_t) / L_0$$
$$\textbf{If } L_t \geq L_0, \textbf{ then } \Delta E_t = 0$$

Where L_0 = faecal trophozoite count before treatment and L_t = faecal trophozoite count after treatment.
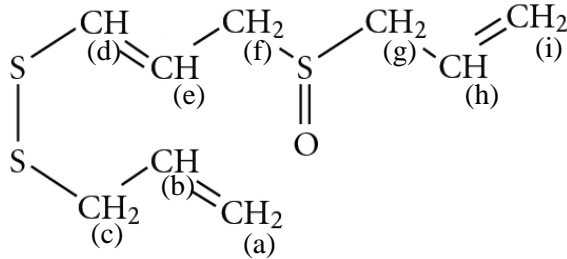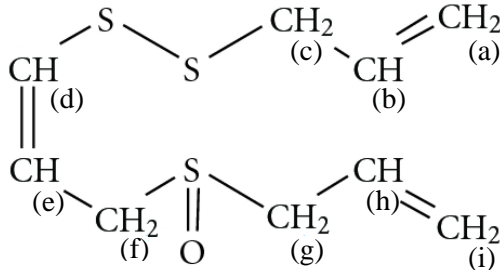
4.4. RESULTS

Ajoene oil and MTZ had a synergistic effect against *Spironucleus vortens* growth *in vitro* and *in vivo*. The only component of the ajoene oil found to have antiparasitic activity against *S. vortens* was (Z)-ajoene.

4.4.1. Analysis of garlic-derived compounds present in ajoene oil

GC-MS chromatogram revealed a number of garlic-derived components present in the crude ajoene oil extract. These were DADS (14.8 min), 3-vinyl-4H-1,3-dithiin (17.8 min), 2-vinyl-4H-1,2-dithiin (18.7 min) and DATS (21.2min), see Figure 4.1. No ajoene was detected by this method; however a mixture of (E) and (Z)-ajoene isomers were identified in NMR spectra of the ajoene oil (Table 4.1), which account for the 18% ajoene proportion of the crude oil extract.

Table 4.1. ^{1}H chemical shifts (δ) of ajoene isomers derived from NMR spectra of ajoene oil crude extract. (E) and (Z)-ajoene spectra were consistent with that described previously by Naznin et al. (2008).

Compound	H atom group	δ (ppm)
(E)-Ajoene	(a) $\underline{CH_2}$=CH-CH$_2$	5.20
	(b) CH$_2$=$\underline{CH}$-CH$_2$-S-, m	5.20
	(c) –S-S-CH$_2$-, d	3.36
	(d) =CH-S-S-, d	6.38
	(e) =$\underline{CH}$-CH$_2$-,m	5.90
	(f, g) -$\underline{CH_2}$-SO-$\underline{CH_2}$-, m	3.50
	(h) CH$_2$=$\underline{CH}$-CH$_2$-SO-, m	5.40
	(i) $\underline{CH_2}$=CH-CH$_2$-	5.40
(Z)-Ajoene	(a) $\underline{CH_2}$=CH-CH$_2$-	5.20
	(b) CH$_2$=$\underline{CH}$-CH$_2$-S-, m	5.20
	(c) –S-S-CH$_2$-, d	3.38
	(d) =CH-S-S-, d	6.56
	(e) =$\underline{CH}$-CH$_2$-,m	5.80
	(f, g) -$\underline{CH_2}$-SO-$\underline{CH_2}$-, m	3.50
	(h) CH$_2$=$\underline{CH}$-CH$_2$-SO-, m	5.40
	(i) $\underline{CH_2}$=CH-CH$_2$	5.40

Fig. 4.1. GC-MS chromatogram of sulphonated compounds present in ajoene oil crude extract. (a) diallyl disulphide (DADS), (b) 3-vinyl-4H-1,3-dithiin, (c) 2-vinyl-4H-1,2-dithiin and (d) diallyl trisuphide (DATS).

4.4.2. *In vitro* inhibitory effect of *Allium*-derived compounds and MTZ against *S. vortens*

The MIC and IC_{50} values of *Allium*-derived compounds against *S. vortens* (ATCC strain) were as follows: ajoene oil = 40 µg/ml, IC_{50} = 5 µg/ml (Fig 4.2a); (Z)-ajoene = 16 µg/ml, IC_{50} = 10 µg/ml (Fig 4.2b); AA = 10 µg/ml, IC_{50} = 0.33 µg/ml (Fig 4.2c); AMD = 20 µg/ml, IC_{50} = 6 µg/ml (Fig 4.2d); DADS IC_{50} = 7 µg/ml (Fig 4.2e); allicin = 1240 µg/ml, IC_{50} = 880 µg/ ml (Fig 4.2f). The MIC and IC_{50} for all other *Allium*-derived compounds tested ((E)-ajoene, AS, AD, DADS, DATS, MD, AMS, PS, PD and dithiins) were not determined as they were greater than the highest concentration tested (>160 µg/ml or >1:100 dilution of the dithiin-rich extract). The MICs of ajoene oil (50 µg/ml), AA (6 µg/ml) and DADS (>160 µg/ml) against the *S. vortens Sv1* strain was similar to that of the ATCC strain. Interestingly, however, the MTZ MIC values for the two strains

varied greatly, with the ATCC strain being more susceptible to MTZ (MIC = 4.5 µg/ml, IC_{50} = 1.6 µg/ml, Fig 4.2g) than the more recently isolated *Sv1* strain (MIC undetermined). The IC_{50} of MTZ against the *Sv1* strain was calculated as ~0.5 µg/ml, however none of the concentrations tested (≤160 µg/ml) completely inhibited the growth of this strain, demonstrated in Figure 4.3 by increased lag-phases. Growth curves for both strains are provided in Appendix 1 and 2.

Table 4.2. *In vitro* fractional inhibitory concentrations (FICs) of different combinations of metronidazole (MTZ) and ajoene against *Spironuleus vortens* (ATCC strain) growth. The FIC index, with ± standard deviation (N=3), represents the sum of the MTZ and ajoene FIC values for each combination. IND and SYN indicate indifferent and synergistic interactions, respectively. (*) Asterisks indicate significant difference from 0.5, the threshold value of synergy (T-test, $p < 0.05$ *, $p < 0.0001$ **).

MTZ + Ajoene combination (µg/ml)	FIC MTZ	FIC Ajoene	FIC Index (±SD)
4 + 0.1	1	0.204	1.204 (±0.261) IND
2 + 0.1	0.5	0.1	0.600 (±0) IND
1 + 0.025	0.25	0.083	0.333 (±0.101) IND
0.5 + 0.2	0.125	0.175	0.300 (±0.035) SYN*
0.25 + 0.2	0.0625	0.2	0.263 (±0) SYN**

4.4.3. *In vitro* synergistic activity of ajoene oil and MTZ against *S. vortens* growth

A combination of 0.25 µg/ml MTZ and 0.2 µg/ml ajoene oil had a significant synergistic effect against *S. vortens* growth. This combination had a calculated FIC index of 0.263 (±0 SD), which is significantly lower than Odds' (2003) threshold value of 0.5 (T-test, $p < 0.05$), indicating considerable synergistic activity between these combinations. The FIC index for all ajoene oil and MTZ combinations tested are summarized in Table 4.2. Growth curves are given in Appendix 1.

4.4.4. *In vivo* combinations of ajoene oil and MTZ significantly reduce *S. vortens* infections.

The effects of administration of flakes containing (1) 0.5% ajoene oil, (2) 0.5% MTZ, (3) 0.05% ajoene oil + 0.5% MTZ in combination as well as a 0.0005% MTZ bath

treatment on *S. vortens* faecal counts in angelfish are summarized in Figure 4.4. The only treatments that significantly reduced *S. vortens* faecal counts of angelfish were the flakes containing a combination of ajoene oil (0.05%) and MTZ (0.5%) and the MTZ bath treatment (0.0005%, MW, $p < 0.05$ for both). These treatments had relatively high E_t values of 64.5% and 68.2%, respectively, whilst E_t values for all other treatments was <50% (Table 4.3).

Table 4.3. Efficacy of different treatments (E_t) in reducing *Spironucleus vortens* faecal counts of infected angelfish. E_t is calculated as follows: (trophozoite faecal count (TFC) after treatment – TFC before treatment) / TFC after treatment. SD = standard deviation.

Treatment Group	N	Et (±SD)
Control flakes	10	0.395 (±0.471)
Ajoene flakes	9	0.305 (±0.359)
MTZ flakes	8	0.480 (±0.419)
Ajoene +MTZ flakes	10	0.645 (±0.397)
MTZ bath	10	0.682 (±0.388)

4.5. DISCUSSION

The antimicrobial effect of ajoene, a stable garlic derivative, against *Spironucleus vortens* was evaluated alone and in combination with the 5-nitroimidazole MTZ. The ajoene oil crude extract employed during this study contained 18% ajoene as a mixture of (E) and (Z)-ajoene isomers. Ajoene itself was not detected on the GC-MS chromatogram of the ajoene oil, however a mixture of polysulphides, DADS and DATS, as well as vinyl dithiins, 2-vinyl-4H-1,2-dithiin and 3-vinyl-4H-1,3-dithiin were detected. It is possible that the ajoene component of the oil may have decomposed as a result of conditions employed during the analysis, resulting in some of the polysulphides and/or vinyl dithiins observed. Pure (E/Z)-ajoene isomers, used as a control during the GC-MS analysis, were prepared using DMSO as a solvent, resulting in a large solvent peak which swamped the chromatogram, masking any sulphonated compounds which might have been present (data not shown). However, polysulphides and vinyl dithiins are common by-products in the extraction of ajoene from garlic and are produced under thermal degradation of allicin (Naznin et al. 2008). Hence, it is not certain at this stage whether the polysulphides and

vinyl dithiins observed on the ajoene oil chromatogram were already present in the ajoene oil, or whether they are the result of ajoene degradation.

The ajoene oil crude extract inhibited *S. vortens in vitro* growth with an MIC of 40 µg/ml. This MIC was 10-fold greater than that of MTZ (4 µg/ml), the drug of choice for treatment of *S. vortens* infections, and 2.5-fold less than that documented previously by Millet et al. (2011a, 107 µg/ml). This may be due to differences in ajoene oil extraction methods employed in the previous study, which may have resulted in less of the active component(s) being present, or as a result of prolonged *in vitro* cultivation of the organism which is known to affect parasite virulence (e.g. *Leishmania infantum*, Moreira et al. 2012). In order to assess whether the ajoene component of the crude oil extract was responsible for the observed growth inhibition of *S. vortens*, pure preparations of (E) and (Z)-ajoene as well as the potential polysulphide and dithiin contaminants of the oil: DADS, DATS and a dithiin-rich preparation, were also assayed. The only component of the ajoene oil that was found to have a significant inhibitory effect against *S. vortens in vitro* growth was (Z)-ajoene, MIC = 16 µg/ml. This individual MIC is approximately 2.5-fold less than that of the ajoene oil, which is reflected in the lower ajoene content found in this crude extract (18%). The antimicrobial activity of the (Z)-ajoene isomer has previously been documented to exceed that of the (E)-isomer (see review by Williams & Lloyd 2012). In contrast to previously published data by Millet et al. (2011a) the dithiin-rich preparation tested during this study did not have a quantifiable inhibitory effect against *S. vortens*. This may be due to differences in the extraction process leading to a lower yield of vinyl dithiins and/or polysulphide contaminants present in the current preparation. The MIC of DADS against *S. vortens* was unclear, with trophozoite growth increasing at higher concentrations of the compounds, but an IC$_{50}$ value of 7 µg/ml was derived. A number of other garlic-derives, allyl alcohol, sulphides and polysulphides, previously documented to be degradation products of allicin, as well as allicin itself, were also tested for their inhibitory effects against *S. vortens*. The MIC value for the majority of the compounds examined was greater than the highest concentration tested, however AA and AMD had substantially low MIC values of 10 and 20 µg/ml, respectively. The MIC of AA against *S. vortens* is comparable with that of *Giardia intestinalis* and *Trichomonas vaginalis* (see review by Williams & Lloyd 2012).

(a)

MIC = 40 µg/ml
IC$_{50}$ = 5 µg/ml

Ajoene conc. (µg/ml)

(b)

MIC = 16 µg/ml
IC$_{50}$ = 10 µg/ml

(Z)-Ajoene conc. (µg/ml)

(c)

MIC = 10 µg/ml
IC$_{50}$ = 0.33 µg/ml

AA conc. (µg/ml)

(d)

MIC = 20 µg/ml
IC$_{50}$ = 6 µg/ml

AMD conc. (µg/ml)

(e)

MIC = unclear
IC$_{50}$ = 7 µg/ml

DADS conc. (µg/ml)

(f)

MIC = 1240 µg/ml
IC$_{50}$ = 880 µg/ml

Allicin conc. (µg/ml)

(g)

MIC = 4.5 µg/ml
IC$_{50}$ = 1.6 µg/ml

MTZ conc. (µg/ml)

Final Growth Yield (OD 420-580 nm)
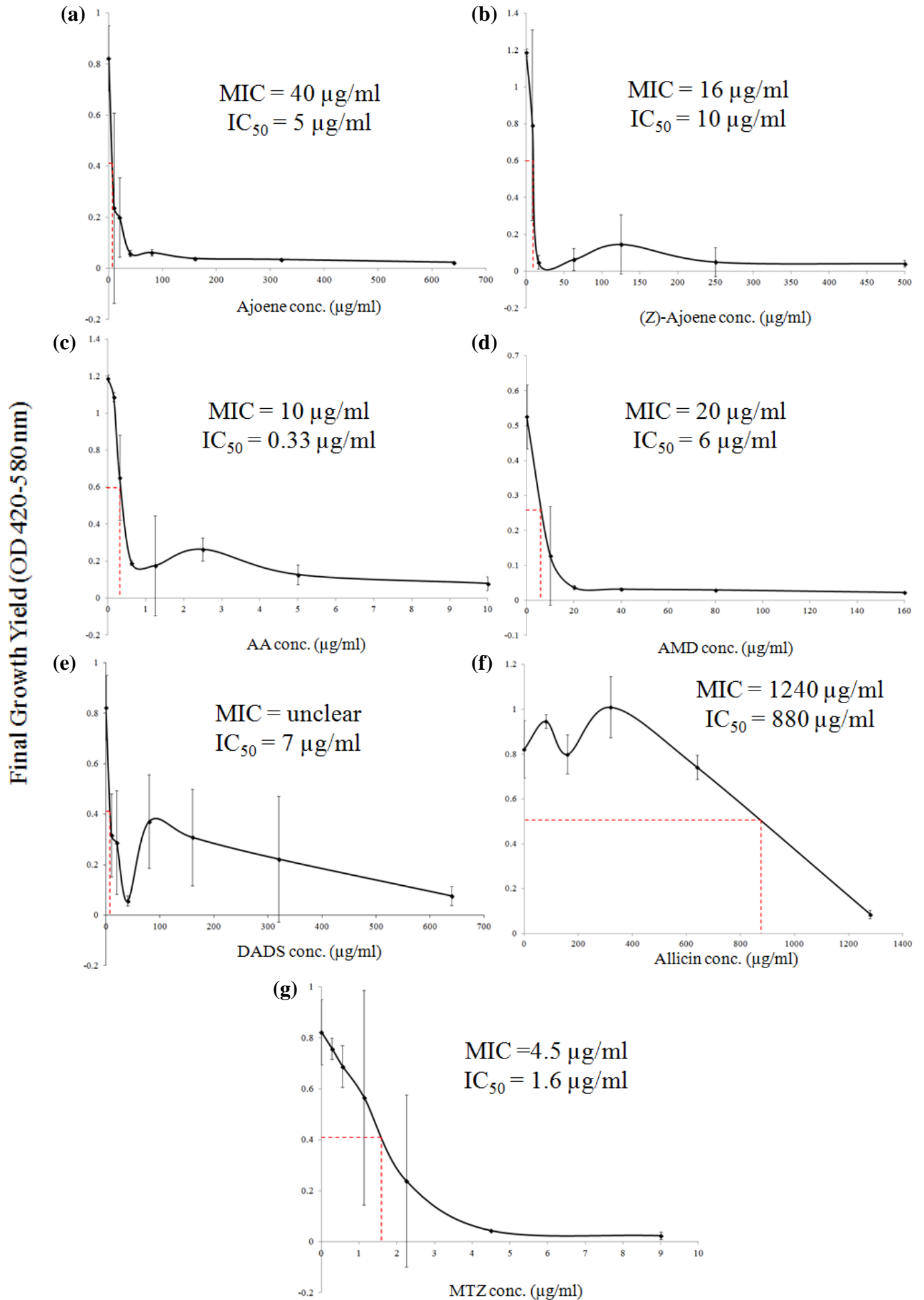
Fig. 4.2. Minimum inhibitory concentrations (MIC) of garlic derivatives against *Spironucleus vortens* (ATCC strain). (a) ajoene oil, (b) (z)-ajoene, (c) allyl alcohol (AA), (d) allyl methyl disulphide (AMD), (e) diallyl disulphide (DADS), (f) allicin and (g) metronidazole (MTZ) against *S. vortens* growth by optical density (OD) monitoring at 420-580 nm. Final yield was derived from the highest cell density (or OD) obtained from growth curves under incubation with various concentrations of ajoene oil. IC_{50} is defined as the ajoene oil concentration at which final yield was reduced by 50% (indicated by the red dashed line). Error bars represent ± standard deviation of 3 replicates.

The antimicrobial effect of AMD has not been well-documented; however it would seem that the presence of two S-atoms in this methylated compound greatly contributes to its biological activity, as AMS did not inhibit parasite growth at the concentrations tested. Allicin, the primary biologically active component of the garlic clove, was less potent than ajoene, AA and AMD, having a comparably high MIC value of 1240 µg/ml against *S. vortens* growth. This value is comparable to that documented previously by Millet et al. (2011a, >160 µg/ml).

The synergistic activity of garlic-derived compounds with drugs has been well-documented (see review by Sivam 2001). For example, garlic extracts have been shown to have synergistic activity with chloroquine, ampicillin and omeprazole against *Plasmodium berghei*, *Staphylococcus aureus* and *Helicobacter pylori*, respectively (Perez et al. 1994; Jonkers et al. 1999; Eja et al. 2011). In the current study, significant synergy between MTZ and ajoene oil was obtained using concentrations of 0.25 and 0.2 µg/ml, respectively. This results in a 16-fold reduction from the individual MIC of MTZ, using a 200-fold decrease in the *in vitro* MIC of ajoene oil. The efficiency of this ajoene-MTZ combination against *S. vortens* infections in angelfish was confirmed *in vivo*. Treated flake food containing 0.5% ajoene oil or 0.5% MTZ individually did not significantly reduce *S. vortens* infections in angelfish. For the MTZ food treatment, this was not surprising as the recommended dose for ornamental fish is higher than the concentration employed here (10 mg/g flakes or 1%, Francis-Floyd & Reed 1994). However, when this 0.5% MTZ dose was combined with just 0.05% ajoene oil in flake food, a significant reduction in *S. vortens* infection was observed. The observed synergy between ajoene and MTZ may be explained by the complimentary modes of action of these compounds. Williams et al. (2012) demonstrated that ajoene depletes intracellular thiols and inhibits the thioredoxin reductase (TrxR) of *S. vortens* at concentrations close to the *in vitro* MIC

and IC_{50}, respectively, as documented here. TrxR and other non-protein thiols are important cellular antioxidants, which play a key role in detoxification of reactive O_2 species within cells (see review by Müller et al. 2003). MTZ had a similar effect to ajoene, but was also shown to form covalent adducts with several redox-related proteins (Williams et al. 2012, Chapter 5). Hence, treatment of *S. vortens* with ajone and MTZ leads to redox imbalance, which results in severe oxidative stress and eventually cell death. The MTZ bath treatment, consisting of 0.0005% MTZ in 1 L water (the recommended dose in fish, Tojo & Santamarina 1998), also significantly reduced *S. vortens* infections, further validating this dose for successful treatment of ornamental fish.
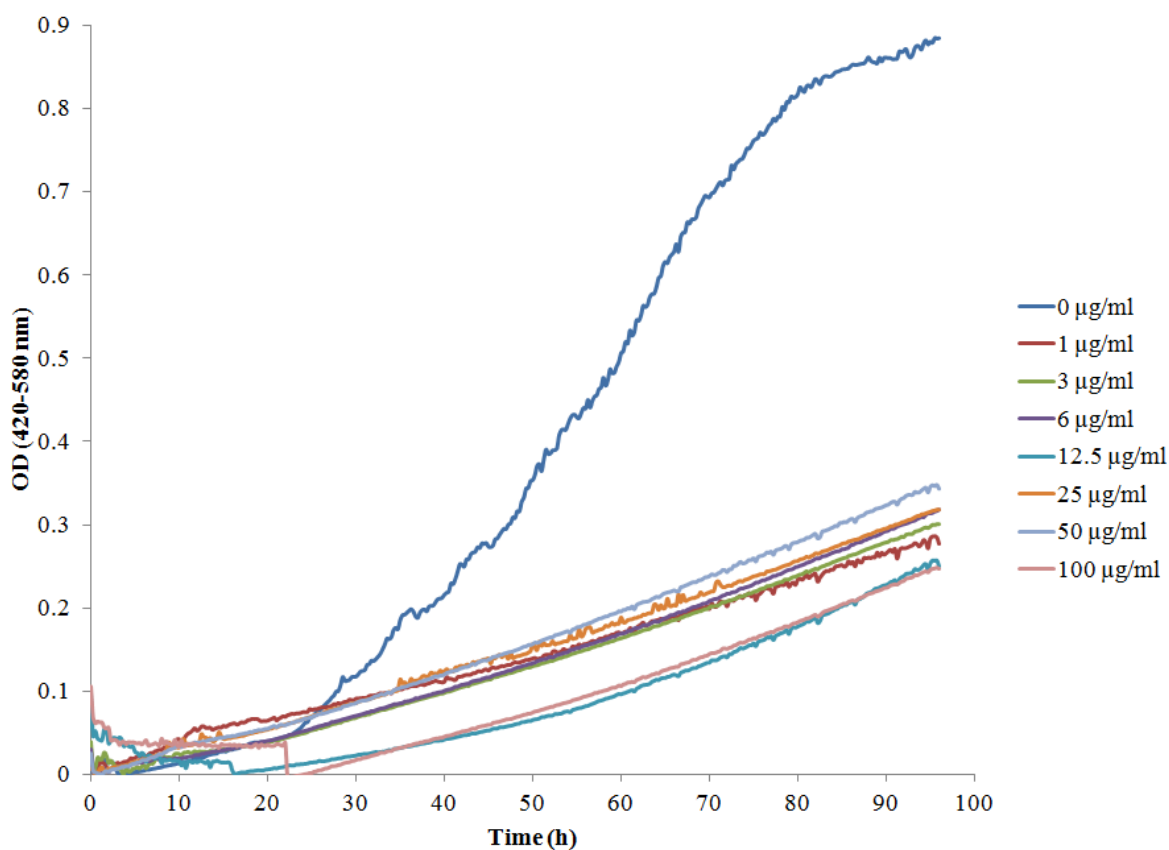
Fig. 4.3. *Spironucleus vortens Sv1* growth over time under incubation with various concentrations of metronidazole (MTZ) by optical cell density monitoring at 420-580 nm.
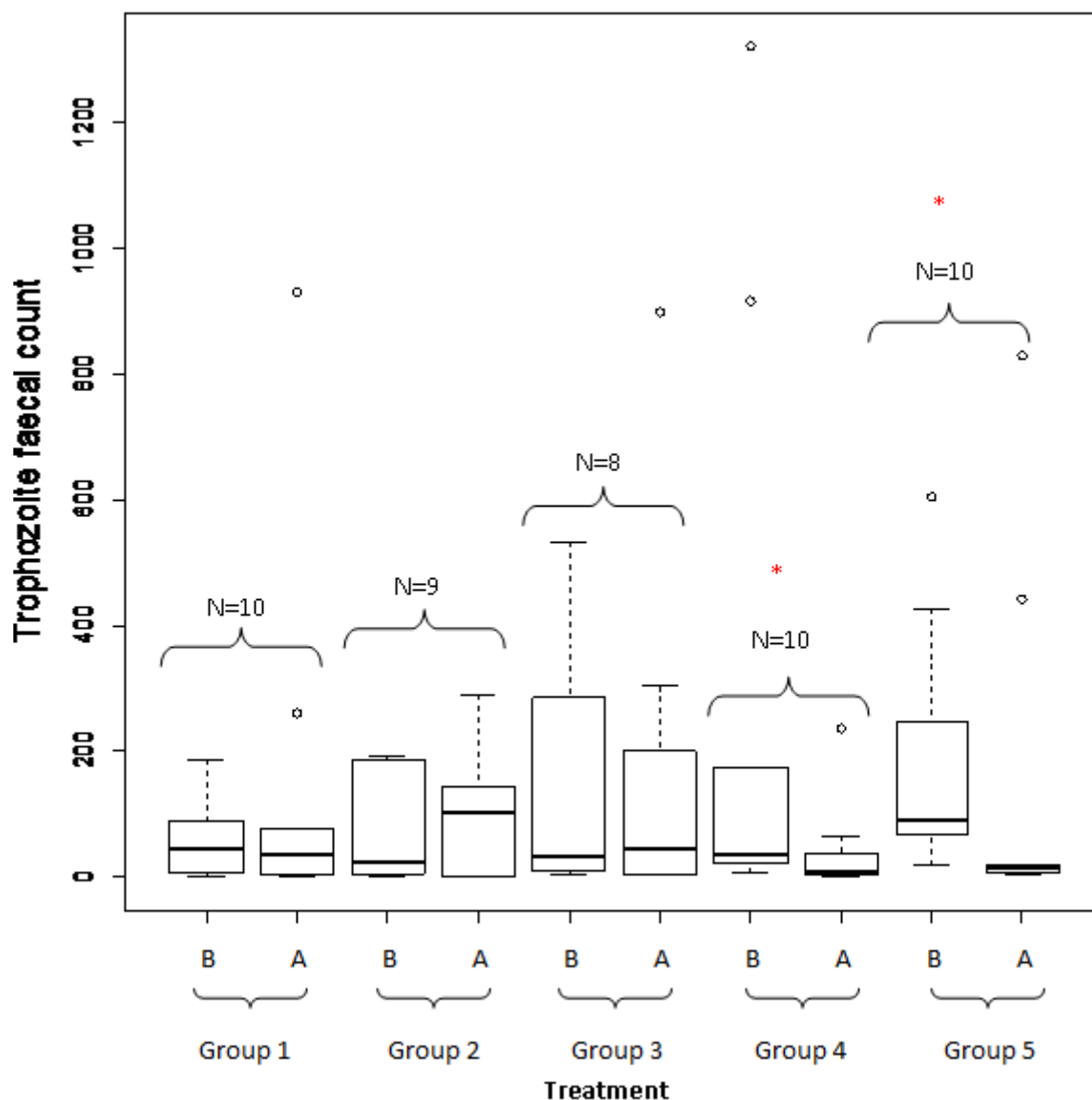
Fig. 4.4. Boxplots of *Spironucleus vortens* faecal trophozoite counts in angelfish before (B) and after (A) treatment with untreated flakes (Group 1) 0.5% (v/w) ajoene flakes (Group 2), 0.5% (v/w) metronidazole (MTZ) flakes (Group 3), a combination of 0.05% ajoene and 0.5% MTZ (v/w) flakes (Group 4) and a 0.0005% (w/v) MTZ bath treatment (Group 5). Circles indicate outliers in the data set. Red asterisks indicate treatments where trophozoite faecal counts were significantly lower after treatment as compared to before treatment.

The *in vitro* MIC values of ajoene oil, AA and DADS against the new *S. vortens Sv1* strain (*ca.* 3 months in culture) was similar to that of the ATCC strain (*ca.* 22 years in culture). Interestingly, however, the MIC of MTZ could not be determined against this new isolate. None of the MTZ concentrations tested (≤100 µg/ml) completely inhibited the growth of this strain, resulting in prolonged lag phases and an increase in cell density over time at all concentrations tested. This suggests that the *Sv1* strain is less susceptible to MTZ than the ATCC strain and may be the result of increased drug pressure in the ornamental aquaculture industry, or as an artefact of prolonged *in vitro* culture. This highlights the need for more in depth investigation into the prevalence and mechanism of MTZ resistance in aquaculture, and emphasizes the importance of identification and development of alternative treatments for effective parasite control.

The current study provides an in-depth account of the inhibitory effects of a wide range of garlic derivatives against *S. vortens* growth and demonstrates, for the first time, the synergistic activity of ajoene with MTZ. A more comprehensive study using a higher concentration of ajoene oil should be conducted in order to assess whether addition of this stable garlic derivative into fish food can be used to treat and/or prevent *S. vortens* infections in fish. If successful, incorporation of ajoene oil as an additive to fish food may be of great commercial interest and could be applied to control Spironucleosis in ornamental and food aquaculture alike.

4.6. REFERENCES

Aydin A, Ersoz G, Tekesin O, Akcicek E, Tuncyurek M, Batur Y (1997). Does garlic oil have a role in the treatment of *Helicobacter pylori* infection? Turk J Gastroenterol 8: 181-184

Block E (2010). Garlic and other Alliums: The Lore and the Science. The Royal Society of Chemistry, Cambridge, UK, 2010; pp 172-193

Block E, Ahman S, Jain MK, Crecely R, Apitz-Castro R, Cruz MR (1984). The chemistry of alkyl thiosulfate esters. 8. (E,Z)-Ajoene: a potent antithrombotic agent from garlic. J Am Chem Soc 106: 8295-8296

Cavas T, Ergene-Gozukara S (2005). Genotoxicity evaluation of metronidazole using the piscine micronucleus test by acridine orange staining. Environ Toxicol Phar 1: 107-111

Commission Regulation (EC) No. 613/98 (1998). Off J Eur Commun L82/14-17 [Cited 18 February 2013] URL: http://ec.europa.eu/health/files/mrl/regpdf/1998_03_18-0613_en.pdf

Davies J, Davies D (2010). Origins and evolution of antibiotic resistance. Am Soc Microbiol 74: 417-433

Eja MA, Arikpo GE, Enyi-Idoh KH, Ikpeme EM (2011). An evaluation of the antimicrobial synergy of garlic (*Allium sativum*) and utazi (*Gongronema latifolium*) on *Escherichia coli* and *Staphylococcus aureus*. Malays J Microbiol 7: 45-49

Ernst E (1999). Is garlic an effective treatment of *Helicobacter pylori* infection? Arch Intern Med 159: 2484-2485

FAO Fisheries and Aquaculutre Department (2012). The state of world fisheries and aquaculture 2012. Part 1: World review of fisheries and aquaculture. Food and Agriculture Organisation of the United Nations, Rome, 2012

FARAD (2010). Restricted and prohibited drugs in food animals. USA Food and Drug Administration [online]. Updated 2 August 2012 [Cited 18 February 2013] URL: http://www.farad.org/eldu/prohibit.asp

Francis-Floyd R, Reed P (1994). Management of *Hexamita* in ornamental cichlids. FAIRS, VM 67 [Cited 31 January 2013] URL: http://www.extension.org/sites/default/files/w/0/02/Management_of_hexamita_in_ornamental_cichlids.pdf.

Freeman F, Kodera Y (1995). Garlic chemistry: stability of S-(2-propenyl) 2-propene-1-sulfinothioate (allicin) in blood, solvents and simulated physiological fluids. J Agric Food Chem 43: 2332-2338

Graham DY, Anderson S-Y, Lang Y (1994). Garlic or jalapeno peppers for the treatment of *Helicobacter pylori* infection. Am J Gastroenterol 94: 1200-1202

Harris JC, Cottrell SL, Plummer S, Lloyd D (2001). Antimicrobial properties of *Allium sativum* (garlic). Appl Microbiol Biotechnol 57: 282-286

IARC (1987). Evaluation of carcinogenetic risk to humans. IARC 7: 250-251[Cited 25 March 2013] URL: http://monographs.iarc.fr/ENG/Monographs/suppl7/suppl7.pdf

Jonkers D, van den Broek E, van Dooren I, Dorant TE, Hageman G, Stobberingh E (1999). Antibacterial effect of garlic and omeprazole on *Helicobacteri pylori*. J Antimicrob Chemother 43: 837-839

Khalil WKB, Mahmoud MA, Zahran MM, Mahrous KF (2007). A sub-acute study of metronidazole toxicity assessed in Egyptian *Tilapia zillii*. J Appl Toxicol 27: 380-390

Lawson LD, Wang Z-Y J, Hughes BG (1991). Identification and HPLC quantification of the sulphides and dialk(en)yl thiodulfinates in commercial garlic products. Planta Med 57: 363-370

Lawson LD, Hughes BG (1992). Characterization of the formation of allicin and other thiosulfinates from garlic. Planta Med 58: 345-350

Lipsky BA, Baker CA (1999). Fluoroquinolone toxicity profiles: a review focusing on newer agents. Clin Infect Dis 28: 352-364

Liu B, Pop M (2009). ARDB-Antibiotic Resistance Genes Database. Nucleic Acids Res 37: D443–D447

Martin KW, Ernst E (2003). Herbal medicines for treatment of bacterial infections: a review of controlled clinical trials. J Antimicrob Chemother 51: 241-246

McNulty CAM, Wilson MP, Hayinga W, Johnston B, O'Gara EA, Maslin DJ (2001). A pilot study to determine the effectiveness of garlic oil capsules in the treatment of dyspeptic patients with *Helicobacter pylori*. Helicobacter 6: 249-253

Millet CO, Lloyd D, Williams C, Williams D, Evans G, Saunders RA, Cable J (2011a). Effect of garlic and *Allium*-derived products on the growth and metabolism of *Spironucleus vortens*. Exp Parasitol 127: 490-499

Millet COM, Lloyd D, Coogan MP, Rumsey J, Cable J (2011b). Carbohydrate and amino acid metabolism of *Spironucleus vortens*. Exp Parasitol 129: 17–26

Mo TA, Poppe T, Iversen L (1990). Systemic hexamitosis in salt-water reared Atlantic salmon. Bull Eur Assoc Fish Pathol 10: 69

Müller S, Liebau E, Walter RD, Krauth-Siegel RL (2003). Thiol-based redox metabolism of protozoan parasites. Trends Parasitol 19: 320-328

Naznin MT, Akagawa M, Okukawa K, Maeda T, Morita N (2008). Characterization of E- and Z-ajoene obtained from different varieties of garlics. Food Chem 106: 1113-1119

Odds FC (2003). Synergy, antagonism, and what the chequerboard puts between them. J Antimicrob Chemother 52: 1

Perez HA, Rosa MDL, Apitz R (1994). *In vivo* activity of ajoene against rodent malaria. Antimicrob Agents Chemother 38: 337-339

Poppe T, Mo TA, Iversen L (1992). Disseminated hexamitosis in sea-caged Atlantic salmon. Dis Aquat Org 14: 91-97

Poppe T, Mo TA (1993). Systemic, granulomatous hexamitosis of farmed Atlantic salmon: interactions with wild fish. Fish Res 17: 147-152

Schelkle B, Shinn AP, Peeler E, Cable J (2009). Treatment of gyrodactylid infections in fish. Dis Aquat Org 86: 65-75

Sivam GP (2001). Protection against *Helicobacter pylori* and other bacterial infections by garlic. J Nutr 131: 1106S-1108S

Sterud E, Mo TA, Poppe TT (1998). Systemic Spironucleosis in sea-farmed Atlantic salmon *Salmo salar*, caused by *Spironucleus barkhanus* transmitted from feral Arctic char *Salvelinus alpinus*? Dis Aquat Org 33: 63-66

Tojo JL, Santamarina MT (1998). Oral pharmacological treatments for parasitic diseases of rainbow trout *Oncorhynchus mykiss*. I: *Hexamita salmonis*. Dis Aquat Org 33: 51-56

Whaley J, Francis-Floyd R (1991). A comparison of metronidazole treatments for hexamitiasis in angelfish. Proc IAAAM, pp 110-114

Williams CF, Lloyd D, Poynton SL, Jørgensen A, Millet COM, Cable J (2011). *Spironucleus* species: economically-important fish pathogens and enigmatic single-celled eukaryotes. J Aquac Res Development S2-002

Williams CF, Lloyd D (2012). Composition and antimicrobial properties of sulphur-containing constituents of garlic (*Allium sativum*). In: Essential Oils as Natural Food Additives: Composition, Quality and Antimicrobial Activity. Valgimigli L (Ed), Nova Publishers, Inc. NY, USA, pp 287-304

Williams CF, Lloyd D, Kolarich D, Alagesan K, Duchene D, Cable J, Williams D, Leitsch D (2012). Disrupted intracellular redox balance of the diplomonad fish parasite *Spironucleus vortens* by 5-nitroimidazoles and garlic-derived compounds. Vet Parasitol 190: 62-73

Chapter 5

Disrupted intracellular redox balance of the diplomonad fish parasite *Spironucleus vortens* by 5-nitroimidazoles and garlic-derived compounds

CHAPTER 5:

Disrupted intracellular redox balance of the diplomonad fish parasite *Spironucleus vortens* by 5-nitroimidazoles and garlic-derived compounds

Adapted from:

Disrupted intracellular redox balance of the diplomonad fish parasite *Spironucleus vortens* by 5-nitroimidazoles and garlic-derived compounds

C.F. Williams [a,*], D. Lloyd [a], D. Kolarich [b], K. Alagesan [b], M. Duchêne [c], J. Cable [a], D. Williams [d], D. Leitsch [c]

[a] School of Biosciences, Cardiff University, Cardiff CF10 3AX, Wales, UK
[b] Max Planck Institute of Colloids and Interfaces, Department of Biomolecular Systems, Am Mühlenberg 1, 14476 Potsdam, Germany
[c] Institute of Specific Prophylaxis and Tropical Medicine, Center for Pathophysiology, Infectiology and Immunology, Medical University of Vienna, Vienna, Austria
[d] NEEM Biotech Limited, Unit 1, Willowbrook Technical Units, Llandogo Road, St. Mellons, Cardiff CF3 0EF, Wales, UK

5.1. ABSTRACT

The 5-nitroimidazole, metronidazole, has traditionally been employed in veterinary medicine to treat a range of infections including the diplomonad fish parasite *Spironucleus*. This study aims to determine the mode of action of metronidazole on *Spironucleus vortens*, including the specific mechanism of activation of the pro-drug and subsequent cellular targets of the drug metabolites. Due to the ban on use of metronidazole in the treatment of production animals in Europe and USA, garlic-derived compounds were also investigated as natural alternatives to metronidazole chemotherapy. Scanning electron microscopy (SEM) provided an overview of gross cellular damage caused by metronidazole and garlic derivatives. Proteomic analyses by 2D gel electrophoresis identified the proteins involved in specific covalent adduct formation with nitroimidazoles. Furthermore, thioredoxin reductase (TrxR) activity and non-protein thiol concentration were assayed in extracts of *S. vortens* before and after treatment with nitroimidazoles and garlic-derivatives. Metronidazole and

garlic-derived compounds caused severe damage of trophozoites indicated by membrane blebbing and lysed cell debris. Analysis of the *S. vortens* proteome identified several proteins capable of specific nitroimidazole binding, including; uridine phosphorylase, enolase, protein disulphide isomerase, aminoacyl-histidine dipeptidase and malic enzyme. Of the compounds tested, metronidazole and the garlic-derived compound ajoene were the most effective at inhibiting TrxR activity and depleting non-protein thiols. These data suggest TrxR-mediated activation of nitroimidazoles, leading to depletion of non-protein thiols. Redox imbalance due to antioxidant failure is implicated as the mode of action of nitroimidazoles and garlic-derived compounds, ultimately leading to cell death. Possible synergy between garlic derivatives and metronidazole should be further investigated *in vitro* in order to determine their theoretical implications.

5.2. INTRODUCTION

The protozoan parasite, *Spironucleus vortens* (Poynton et al. 1995), is a flagellated diplomonad which commonly infects the hindgut of ornamental fish. Its host range extends from tropical cichlids, such as angelfish, to the ide, a cold water cyprinid (see review by Williams et al. 2011). Onset of systemic infection is thought to be associated with 'stress' of the fish host, with Spironucleosis being linked to 'hole-in-the-head disease', a common manifestation causing high mortality in cichlids (Paull and Matthews 2001). The global trade in ornamental fish is a multi-million dollar industry, with imports and exports worth an estimated \$283 million and \$238 million respectively (European Commission 2008). Treatment of Spironucleosis is therefore of significant importance in aquaculture.

Metronidazole, a 5-nitroimidazole derivative, the "gold-standard" treatment for a range of microaerophilic and anaerobic pathogens, was the traditional drug of choice against Spironucleosis (Freeman & Klutman 1997; Sangmaneedet and Smith 1999). However, the drug has been banned from use in the treatment of food fish in Europe and USA, due to its potential carcinogenic properties, persistence in the environment and toxicity to aquatic organisms (Lanzky & Halting-Sørensen 1997; Commission Regulation No. 613/98 1998; Payne et al. 1999). Despite this, metronidazole is still available by veterinary prescription for the treatment of ornamental fish, and is widely used in some areas of South East Asia (Mohamed et al. 2000). However, it was recently shown that *Allium sativum* (garlic)-derived compounds have an inhibitory effect on the growth and gas metabolism of *S. vortens in vitro* (Millet et al. 2010). Garlic is a broad-spectrum antimicrobial agent, exhibiting antibacterial, antifungal, antiprotozoal and antiviral properties (Tsai et al. 1985; Singh et al. 1990; Lun et

al. 1994; Tsao et al. 2003). The inhibitory effect of garlic extract on other important fish parasites, including *Ichthyophthirius* and *Gyrodactylus* has also been documented (Buchmann et al. 2003; Abd El-Galil & Aboelhadid 2011). Furthermore, there have been no cases concerning the development of garlic resistance by pathogens documented to date. These attributes make it an attractive alternative in the treatment of Spironucleosis in fish. In addition, further characterisation of the mode of action of garlic compounds may lead to the development of a new class of drug based on the complex chemistry of the garlic clove, having potent broad-spectrum antimicrobial activity.

In its administered form, metronidazole does not exert antimicrobial activity. Reductive activation at the drug nitro group by the target organism is required in order to generate the biologically-active nitroradical anion and further reduced intermediates (Lloyd & Pedersen 1985). Recent studies have questioned the long-standing belief that activation of the metronidazole pro-drug is mediated by pyruvate:ferredoxin oxidoreductase (PFOR)-associated ferredoxin alone, with subsequent indiscriminate protein binding and DNA damage (Edwards 1993). Evidence is mounting for an alternative thioredoxin reductase (TrxR)-mediated nitroreductase activation pathway, as demonstrated in the protozoan parasites *Entamoeba histolytica*, *Trichomonas vaginalis* and *Giardia intestinalis* (see Leitsch et al. 2007, 2009, 2011). In both *E. histolytica* and *T. vaginalis*, subsequent binding of metronidazole metabolites to specific protein targets occurs, most of which are associated with Trx-mediated redox regulation (Leitsch et al. 2007, 2009). Metronidazole activation is also coupled with depletion of intracellular non-protein thiols, which are major components of the cellular antioxidant system, further implementing redox imbalance as the mode of action of metronidazole.

The chemistry of the garlic clove is complex, and the mode of action of garlic derivatives has not been fully elucidated. Allicin (diallyl thiosulphinate), the primary biologically active component of the garlic (Cavallito & Bailey 1944), undergoes rapid decomposition to form other active reaction products including allyl alcohol (AA), diallyl disulphide (DADS), higher polysulphides as well as ajoene (see review by Williams & Lloyd 2012). However, allicin itself has been documented to inhibit cysteine proteinases, alcohol dehydrogenases and, much like metronidazole, the TrxR of *E. histolytica* (see Ankri & Mirelman 1999). Both AA and DADS cause oxidation of NAD(P)H and depletion of glutathione, coupled with an increase in H_2O_2 production in the pathogenic yeast *Candida albicans*, causing severe oxidative stress and, in the case of DADS, apoptotic cell death (Lemar et al. 2005, 2007). Furthermore, ajoene is documented to change the phospholipid

composition of the protozoan parasite *Trypanosoma cruzi*, which contributes to create an anti-proliferative effect (Urbina et al. 1993). Thus, the mode of action of metronidazole and some garlic-derived compounds are similar in that they target important intracellular redox components.

In order to exploit antimicrobial agents to their full potential, it is critical to understand their mode of action in relation to specific target(s) in different hosts. In this study *S. vortens* was chosen to further investigate the nitroreductase activity of TrxR in protozoan parasites, specifically that of the diplomonads. Furthermore, the mode of action of garlic derivatives, AA, DADS, allicin and ajoene, was investigated as a potential alternative therapy to metronidazole in the treatment of Spironucleosis in fish. This was achieved using a novel combination of high resolution scanning electron microscopy (SEM), proteomic techniques and enzyme assays.

5.3. MATERIALS AND METHODS

5.3.1. Organism and culture

Spironucleus vortens, ATCC 50386, trophozoites were maintained in Keister's modified TYI-S-33 medium as previously detailed in Chapter 2, section 2.2. For some experiments, cells were incubated in 30 ml capacity culture flasks (Costar), with no head space where O_2 scavenging by cells generated an atmosphere of low O_2 tension. Parasite viability was monitored according to cell motility and visual estimation of cell density by phase contrast microscopy.

5.3.2. Inhibitors

Garlic derivatives allicin and ajoene were prepared by NEEM Biotech Ltd., with their purities assessed by high performance liquid chromatography (HPLC). Preparations of allicin and ajoene had purities of 2% (v/v) and 16-18.2% (v/v), respectively. Unless otherwise stated, all other antimicrobials and chemicals were sourced from Sigma-Aldrich. The purity of allyl alcohol (AA) and diallyl disulphide (DADS) was 99+% and 80%, respectively. The concentration range of all inhibitors employed during this study are within the range of the minimum inhibitory concentration (MIC) or IC_{50} (the concentration which inhibits parasite growth by 50%) as determined in Chapter 4 and provided in molar concentration in Table 5.1. This applies to all compounds apart from allicin, due to the already low allicin content present in the preparation provided.

Table 5.1. Final concentration in µM of garlic-derived components used in quantification of *Spironucleus vortens* non-protein thiols. The minimum inhibitory concentration (MIC) and IC_{50} (concentration which reduces growth by 50%) of these compounds against *S. vortens* growth is also provided for comparison (as determined in Chapter 4). ND = not determined.

Dilution factor	Concentration (µM)			
	Allicin	Ajoene oil	Allyl alcohol	Diallyl disulphide
1:6,250	20	100	2680	880
1:12,500	10	50	1340	440
1:25,000	5	25	670	220
1:50,000	2.5	12.5	340	110
1:100,000	1	6	170	55
MIC	8000	171	172	ND
IC_{50}	5400	21	6	48

5.3.3. Scanning electron microscopy (SEM)

S. vortens cultures were incubated for 1, 2, 4, 24 and 48 h with 50 µM metronidazole and 1:25000 dilution of AA, DADS, allicin and ajoene (corresponding to 0.7 mM, 0.2 mM, 5 µM and 30 µM of each component respectively) or left untreated. For metronidazole and ajoene, these concentrations are close to the *in vitro* MIC's of these compounds against *S. vortens* (see Millet et al. 2010). Samples were removed aseptically from each tube at the specified time intervals and fixed overnight (*ca.* 18 h) with 2% (v/v) glutaraldehyde in 0.5 M PIPES buffer (pH 7.2, containing 0.2 M sucrose and 2 mM CaCl$_2$). Samples were then washed in PIPES buffer (10 min, room temperature) and post-fixed in 1% (w/v) buffered osmium tetroxide (1 h, 4°C) in the same buffer. Following a second wash step in PIPES buffer, samples were dehydrated using a graded series of 50, 70, 90 and 100% ethanol (v/v, Fisher Scientific) (10 min each, room temperature). After being air dried in 100% ethanol on 13 mm diameter filter paper (0.2 µm pore size, Gelman Sciences), samples were coated with gold-palladium using a BioRad SC500 sputter coater and imaged under high vacuum using an FEI XL30 ESEM FEG fitted with

a secondary electron detector. Standard operating conditions were employed with an accelerating voltage of 10 kV, spot size 4 and a working distance of *ca.* 10 mm.

5.3.4. Sub-lethal incubation of *S. vortens* with inhibitors

S. vortens cells, grown under low O_2 tensions (as described above) were incubated for a sub-lethal incubation period with nitroimidazoles and garlic-derived compounds. This sub-lethal incubation period was determined by monitoring cell motility post-treatment at 30 min intervals. *S. vortens* trophozoites are capable of rapid swimming behaviour; however, under severe oxidative or chemotherapeutic challenge, cell motility is rapidly lost. Motility therefore provides a powerful tool for assessing *S. vortens* vigour. Incubation was terminated when cell motility had been reduced from rapid swimming to a twitching-motion, indicating severe chemotherapeutic stress. For nitroimidazoles and AA, an incubation period of 3 h was adequate to induce this effect (at concentrations of 50 µM and 0.7 mM, respectively). However, a 24 h incubation period was required to produce the same effect for DADS, allicin and ajoene treatment (0.2 mM, 5 µM and 30 µM, respectively). These incubation times were subsequently implemented in subsequent experiments.

5.3.5. Two-dimensional polyacrylamide gel electrophoresis (2DE)

S. vortens trophozoites were incubated with and without 50 µM of the 5-nitroimidazoles metronidazole, tinidazole and the 2-nitroimidazole azomycin (the latter two compounds were used as nitroimidazole controls), 0.7 mM AA and 30 µM ajoene for a sub-lethal period of incubation, at room temperature (as described above). Cells were then washed 4x in chilled PBS (pH7.2, containing, per L; 8 g NaCl, 0.2 g KCl, 1.44 g Na_2HPO_4 and 0.24 g KH_2PO_4) to remove serum components, harvested by centrifugation (1,250 *g*, 5 min) and the resultant pellets disrupted with 10% (w/v) trichloroacetic acid (TCA) in acetone at -20°C for 1 h. The resultant protein precipitates were then quantified, according to Bradford assay (see Chapter 2, section 2.4), processed and subject to 2DE according to Leitsch et al. (2005). Briefly, a minimum of 300 µg protein was diluted in rehydration buffer (8 M urea, 2 M thiourea, 0.5% Chaps, 15 mM dithiothreitol and 0.2% v/v ampholytes, pH 3-10) in a total volume of 400 µl. Bromophenol Blue (1 µl of a 0.4% w/v in 50% v/v glycerol solution) was then added to the protein extract and the entire sample transferred to an isoelectric focusing (IEF) rehydration tray. IEF was conducted with 18 cm immobilized pH gradient strips using the following program; rehydration for

12 h at 50 V, 1 h at 150 V, 1 h at 300 V, 1 h at 2000 V, 2 h at 5000 V and 7 h at 8000 V. IEF strips were then rinsed, equilibrated and transferred to vertical polyacrylamide (12.5% w/v) gels (30% T, 3% C) in 25% resolution buffer (1.5 M Tris/HCl, pH 8.8, 0.4% SDS and 5% v/v glycerol) overlaid with 0.8% agarose in resolution buffer. Gels were run overnight (*ca.* 18 h) at 4°C. Following 2DE, gels were stained using Coomassie brilliant blue R-250 (Bio-Rad). After de-staining in distilled H_2O, gels were imaged using an Epson 1680 Pro scanner with Melanie 2D gel analysis software (GeneBio, Geneva) for evidence of shifted protein spots between treated and untreated samples. Determination of shifted proteins was based on the following criteria: (1) the protein must be shifted by at least two different nitroimidazoles, and (2) the shifts should be differentially wide, depending on the nitroimidazole applied. The 5-nitroimidazole, tinidazole, produces shorter shifts than metronidazole, whereas the 2-nitroimidazole, azomycin, produces wider shift patterns with a smaller concentration of protein in the shifted position. Protein spots of interest were manually excised from the gel, and the resultant gel plugs (1.5 mm dia.) prepared for protein identification by mass spectrometry, as outlined below.

5.3.6.   Liquid chromatography mass spectrometry (LC-MS)

Tryptic digestion of Coomassie stained protein spots was performed as described previously by Kolarich et al. (2006) with minor modifications. In contrast to the published procedure, 1 µl trypsin (proteomics grade, Roche) containing 200 ng/µl was mixed with 2 µl of 25 mM ammonium bicarbonate in the re-swelling step. All the solvents used in the study were LC-MS grade (acetonitrile, formic acid (98%) and ammonium bicarbonate obtained from Fluka Analytical, Munich, Germany). Mass spectrometric analyses were performed on an AmaZon ETD ion trap (Bruker Daltoniks, Bremen, Germany) coupled to an Ultimate 3000 UHPLC system (Dionex). The instrument was set up to perform both collision-induced dissociation (CID) and electron-transfer dissociation (ETD) fragmentation on the selected precursors. A m/z range from 400-1500 Da was used for data dependent precursor scanning. The three most intense signals in every MS scan were selected for MS/MS experiments, and only signals with a charge state ≥ 2+ were selected for MS/MS. All data was recorded in the enhanced resolution mode. Tryptic peptides were online separated by reversed phase chromatography (ProteCol™ Capillary Column, SGE, Ringwood, Vic, Australia; 300 µm x 10 mm [trap column] and 300 µm x 150 mm [analytical column]). The samples were loaded onto the trap column in 100% solvent A (0.1% formic acid) and unbound

components were eluted by washing the trap column for 5 min in buffer A at a flow rate of 10 µl/min. The starting conditions for the analytical column were 2% solvent B (acetonitrile with 0.1% formic acid) and the flow rate on the analytical column was held at 5 µl/min throughout the experiment. After desalting the sample on the trap column, a gradient using an increasing solvent B concentration was applied. The gradient conditions were as follows: linear increase of buffer B from 2 to 30% (from 5 min to 61 min), further increase to 60% (61 to 76 min), followed by a steep increase to 90% (76 to 77 min). The column was held at 90% B for 5 min (77 to 82 min) before re-equilibrating the analytical column in 2% solvent B. Meanwhile, the trap column was re-equilibrated in 100% solvent A before injection of the next sample. Peptide trapping and reversed phase separation was performed at a column temperature of 45°C.

5.3.7. Mass spectrometric data analysis

Data analysis was performed using ProteinScape 3 (Bruker Daltonics) and MASCOT 2.3 (MatrixScience, UK) using the following search parameters: cysteine as carbamidomethyl was set as fixed modification, deamidation (Asn/Gln) and oxidation (Met) were set as variable modifications. Up to 2 missed cleavages were allowed. Peptide tolerance (both MS and MS/MS) was set at $\pm$ 0.2 Da. The data was searched against the NCBI protein database (no restriction in taxonomy), the SwissProt database (taxonomy restriction: mammalian; for identification of any trypsin and/or human contaminations) and against a publicly available *Spironucleus vortens* EST database (retrieved from http://genome.jgi-psf.org/Spivo0/Spivo0.info.html). The latter allowed identification of a number of entries in the database with high confidence, subsequently enabling the use of the identified sequences for BLAST searches against various databases, which in turn permitted assignment of potential functions based on protein sequence homology. The following bioinformatic tools were used to annotate the selected sequences: BLAST, FASTA, Homstrad Blast, ProDom, Pfam, Inter Proscan, Conserved Domain and HMMER. BLAST searches were performed in NCBI using the PSI-BLAST application at NCBI (www.ncbi.nih.gov/BLAST/). FASTA searches were executed in EMBL-EBI where the sequences were searched against all the available protein databases (http://www.ebi.ac.uk/Tools/services/web/toolform.ebi?tool=fasta&context=protein). Furthermore, the sequences were run through the conserved domain database (CDD) at NCBI to identify any existing domains that might be indicative for the function of the gene(s) identified. The conserved domains in the respective identified sequences were

taken from the output result (http://www.ncbi.nlm.nih.gov/Structure/cdd/cdd.shtml). The protein database of Clusters of Orthologous Groups (COGs) is a tool to phylogenetically classify the complete complement of proteins (both predicted and characterized) encoded by complete genomes (http://www.ncbi.nlm.nih.gov/COG/old/xognitor.html). The default parameters of the COGNITOR were applied in our study. PFAM (http://pfam.sanger.ac.uk/) was used to further analyse the domains identified with CDD and COGNITOR. There, too, default parameters were used. When PFAM-A did not provide a meaningful result, PFAM-B was used. The lowest e-value for the hits was taken. The ProDom web server (http://prodom.prabi.fr/prodom/current/html/home.php) provides the user with a set of tools to visualize multiple alignments, phylogenetic trees and domain architectures of proteins, as well as a BLAST-based server for analysing new sequences for homologous domains. This tool was used in addition to the above domain and motif search tools. Default parameters were used and results with lowest e-value were selected. Scanprosite (http://expasy.org/prosite/) and Interproscan (http://www.ebi.ac.uk/Tools/InterProScan) were used with default parameters as additional tools analysing domains and motifs present in the protein sequences identified. HMMER was applied for searching sequence databases for homologs of protein sequences, and for making protein sequence alignments (profile hidden Markov model for sequence, http://hmmer.janelia.org/). To exclude any false positives and background introduced during sample preparation the data generated was used to perform MASCOT searches against the SWISSPROT database (using same criteria as mentioned above, taxonomy limitation: *Mammalia*). This allowed establishing a sample background derived from keratin and trypsin peptides.

5.3.8. Determination of thioredoxin reductase activity

S. vortens trophozoites were grown under low O_2 tensions for 24 h, as described above. Cells were washed 3x and re-suspended in 1 ml PBS, before being subject to two cycles of rapid freeze-thawing in liquid N_2. A small sample of the resultant disrupted cell suspension was used to determine total protein concentration using Bradford assay (see Chapter 2, section 2.4). A Thioredoxin Reductase Assay Kit (Cayman Chemicals) was employed to measure the NADPH-dependent reduction of Ellman's reagent, 5,5'-dithiobis-(2-nitrobenzoic acid) or DTNB, by the disrupted cell suspension (20 µl per reaction), where 1 unit is defined as the production of 2 µmol of the 2-nitro-5-thiobenzoate (TNB) product per min at 22°C. The specific TrxR inhibitor sodium

aurothiomalate (ATM, 20 μM) was used to discriminate between TrxR and non-TrxR reduction of DTNB. The inhibitory effect of metronidazole, tinidazole, AA, DADS, ajoene and allicin against *S. vortens* TrxR was investigated at a concentration of 20 μM. Inhibitors were added directly to the reaction. A Bioscreen C automated optical density monitoring system (Labsystems, Finland) was employed to monitor changes in OD every min for 10 min, using a 405 nm filter. TrxR activity was calculated using the DTNB extinction coefficient of 6.35 mM^{-1} cm^{-1} at 405 nm.

5.3.9. Determination of total non-protein thiols

S. vortens cells were incubated under low O$_2$ tensions with 50 μM metronidazole and tinidazole, and 1:6,250, 1:12,500, 1:25,000, 1:50,000 and 1:100,000 dilution of allicin, ajoene, AA and DADS (component equivalents are given in Table 5.1) in triplicate at 24°C, for a sub-lethal incubation period, as described above. Cells were harvested, washed 3x in PBS (pH 7.2) and disrupted in 20 mM EDTA and 0.1% (v/v) Triton-X100 (500 μl total volume) for 5 min. Insoluble material was removed by centrifugation and protein content of the supernatant determined by Bradford assay (see Chapter 2, section 2.4). Proteins (400 μl supernatant) were then precipitated in 20 mM EDTA (200 μl) and 20% (w/v) TCA (200 μl) for 5 min. Precipitated proteins were removed by centrifugation and the resulting non-protein thiols in the supernatant quantified. A 340 μl sample volume was added to 660 μl neutralization buffer (0.4 M Tris, pH 8.9; 20 mM EDTA) and 170 μl DTNB, and the optical density measured at 412 nm spectrophotometrically (Leitsch et al. 2007). The non-protein thiol content of the sample was determined using the DTNB extinction coefficient of 13.1 mM^{-1} cm^{-1} per mg protein.

5.3.10. Statistical analysis.

T-tests were performed in Minitab 15 to assess whether nitroimidazoles and garlic derivatives had a significant effect on TrxR activity and non-protein thiols of *S. vortens*.

5.4. RESULTS

5.4.1. Effects of metronidazole and garlic-derivatives on gross cellular morphology

Normal (untreated) *Spironucleus vortens* trophozoites are pyriform in shape and possess a total of 8 flagella, of which 6 emerge anteriorly and 2 posteriorly (Fig 5.1a). It was not uncommon to see enlarged, rounded cells possessing >8 flagella, in untreated

samples, which are thought to be formed as a result of defective cytokinesis (Sangmaneedet and Smith 2000). Metronidazole, ajoene, allicin and diallyl disulphide (DADS) all caused extensive blebbing of the cell surface, indicating dead or dying cells (Figs 5.1b, d, e & f). These effects were most evident after ≥24 h incubation. However, allyl alcohol (AA) had the most pronounced effect, causing a noticeable reduction in cell number and a higher concentration of lysed cell debris after 24 h incubation (Fig 5.1c). A higher proportion of enlarged, irregular-shaped cells, having >8 flagella was also observed under metronidazole, DADS, allicin and ajoene treatment (visual estimation).
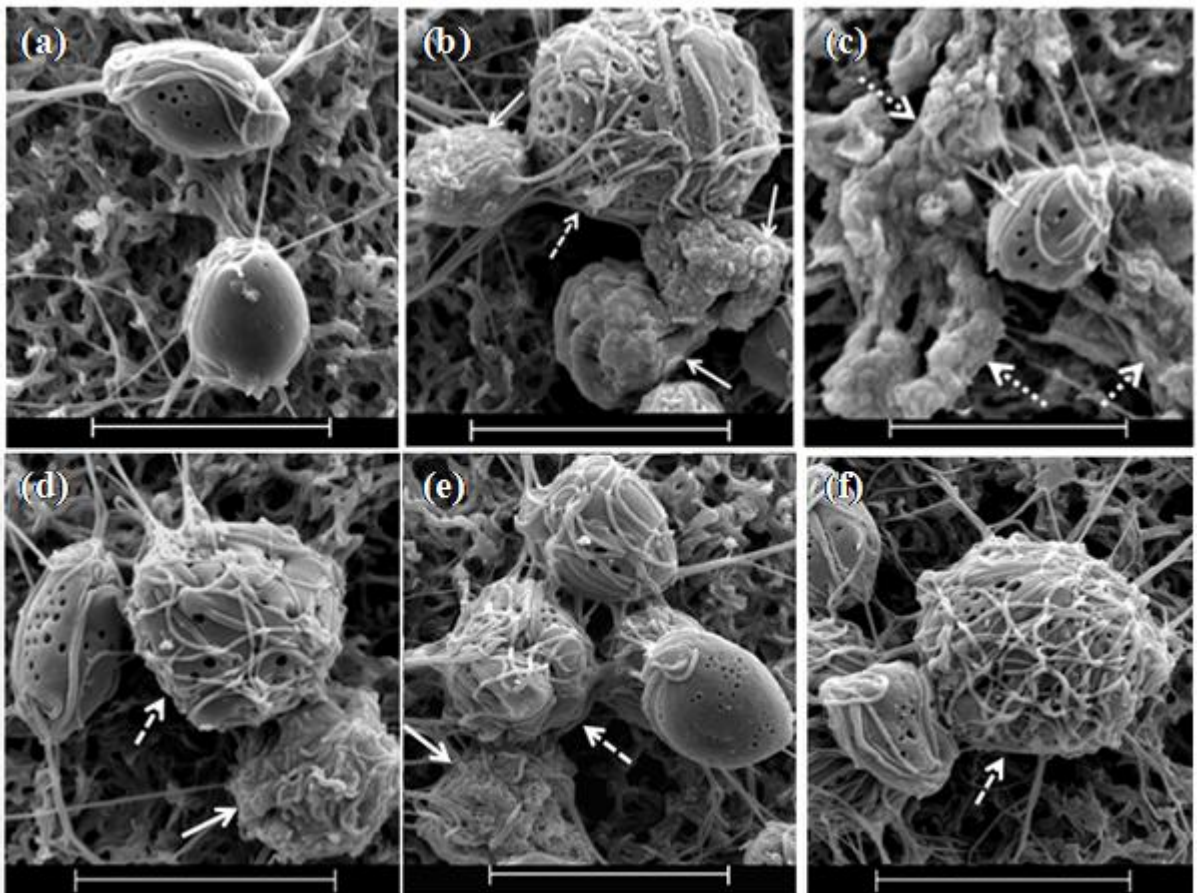
Fig 5.1. Scanning electron micrographs of *Spironucleus vortens*. Normal, untreated trophozoites are pyriform-shaped possessing 8 flagella (a). Trophozoites were incubated for 24 h with 50 µM metronidazole (b), 0.7 mM allyl alcohol (c), 0.2 mM diallyl disulphide (d), 5 µM allicin (e) and 31 µM ajoene (f). Full arrows indicate cells with blebbing of the outer membrane, broken arrows show irregular-shaped cells with abnormal flagellar number, dotted arrows highlight lysed cell debris. Scale bars = 10 µm.

5.4.2. Covalent adduct formation of 5-nitroimidazoles with discriminate *S. vortens* proteins

Two-dimensional gel electrophoresis of the total *S. vortens* proteome (Fig 5.2a) revealed specific nitroimidazole binding to 8 proteins (subsequently referred to as SvP1-8), indicated by a shift of the untreated native protein spot towards a more basic p*I* in the treated sample (Fig 5.2b). In order to verify that the protein shifts were attributed to binding of metronidazole rather than a physiological cellular response coinciding with the cytotoxic effect of drug treatment, *S. vortens* cells were also treated with another 5-nitroimidazole, tinidazole, and a 2-nitroimidazole, azomycin. Both tinidazole and azomycin have been shown previously to shift the same proteins as metronidazole in *E. histolytica* (see Leitsch et al., 2007). Thus, proteins were only deemed to have formed covalent adducts if shifts were produced by treatment with 2 or more nitroimidazoles (Fig 5.3). Differences in protein shift patterns produced by different nitroimidazoles are attributed to varying pKa's between nitroimidazoles due to the presence of different side chains at the N1 position (Leitsch et al. 2007). Tinidazole produced shorter protein shifts than metronidazole, whilst azomycin produced wider protein shifts. In some instances, SvP3 4, 5, 7 and 8, protein shifts by azomycin were not detected. In the case of SvP1, 4, 6 and 7, chains of adducts were formed as a result of nitroimidazole binding. Treatment of *S. vortens* with AA and ajoene did not result in reproducible shifts in specific proteins; therefore no further analysis was conducted for these treatments.

5.4.3. Assignation of protein function to 5-nitroimidazole bound proteins

Liquid chromatography mass spectra obtained from the 8 proteins of interest were searched against a publicly available EST database for *S. vortens*. This allowed identification of significant lengths of peptide stretches that in turn enabled BLAST homology searches using the obtained protein sequences. Useful sequence data could be acquired for all but one protein sample, SvP3, thus potential protein functions could be assigned to 7 of the 8 samples (see Table 5.2): SvP1, uridine phosphorylase and TrxR; SvP2, hypothetical protein; SvP4, enolase; SvP5, protein disulphide isomerase; SvP6, aminoacyl–histidine dipeptidase; SvP7, malic enzyme and SvP8, enolase. Protein spot Sv1 revealed significant amounts of two proteins, uridine phosphorylase and thioredoxin reductase (TrxR), however it should be noted that nitroimidazole induced shifting of this spot was not always reproducible (1/3 independent experiments). For SvP2, BLAST homology searching resulted in a high score for a hypothetical protein. It is also worth

noting that enolase was also identified by MALDI TOF MS/MS (matrix assisted laser desorption ionization time of flight tandem mass spectrometry) and subsequent MASCOT database search (data not shown).
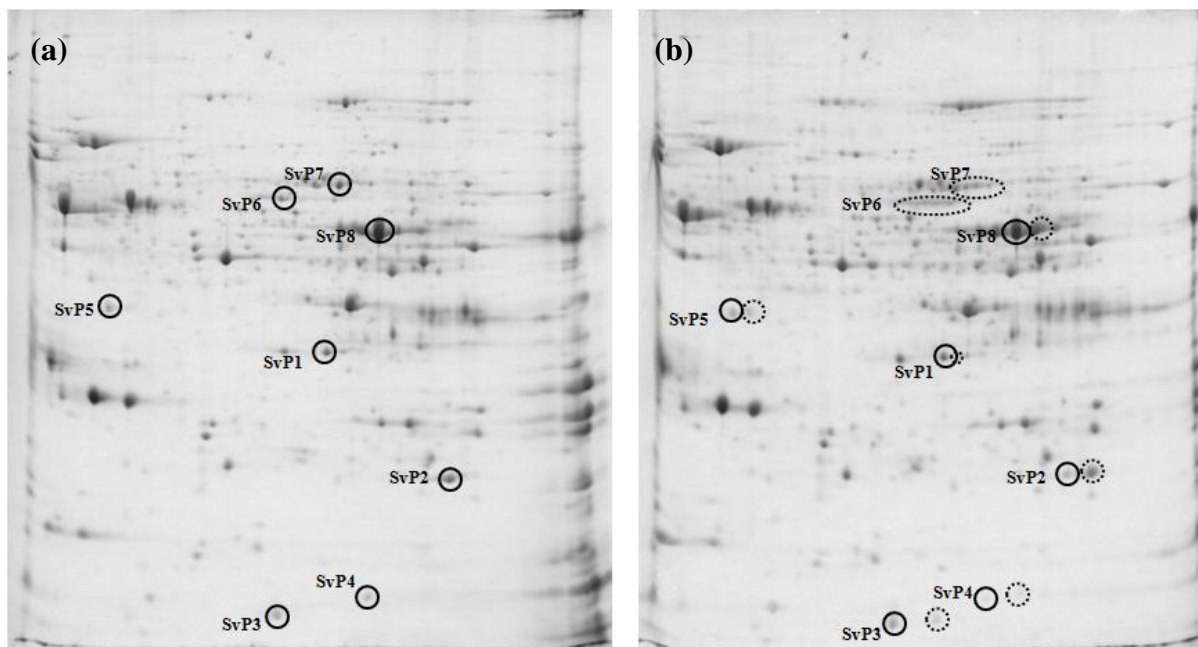
Fig 5.2. Complete two dimensional gel electrophoretogram of protein spots of interest, labelled SvP1-8, isolated from *Spironucleus vortens* (a) before and (b) after treatment with metronidazole. Proteins were manually excised from 2DE gels, trypsin digested and analysed by LC-MS. Full circles indicate native protein spots, broken elipses indicate shifted proteins caused by metronidazole binding.

5.4.4. TrxR inhibition by nitroimidazoles and garlic-derived compounds

The nitroimidazoles and garlic-derived compounds tested had varying degrees of inhibition against *S. vortens* NADPH-dependent TrxR activity. Results are based on percentage differences from the untreated sample, having maximal (100%) TrxR activity of 1.08 ± 0.032 μmol/min/mg protein. All compounds tested had a minimum TrxR inhibition rate of *ca.* 50% at 20 μM (Fig 5.4). Of the 5-nitroimidazoles, metronidazole was the most effective, decreasing TrxR activity by $78 \pm 27\%$ of the untreated sample. Tinidazole showed a lower degree of TrxR inhibition, diminishing activity by $29 \pm 16\%$. AA and DADS had similar activities to tinidazole, of $47 \pm 14\%$ and $55 \pm 12\%$, respectively. However, the most efficient TrxR inhibitors of the compounds tested were the garlic constituents ajoene and allicin, which both inhibited TrxR activity by 100%.
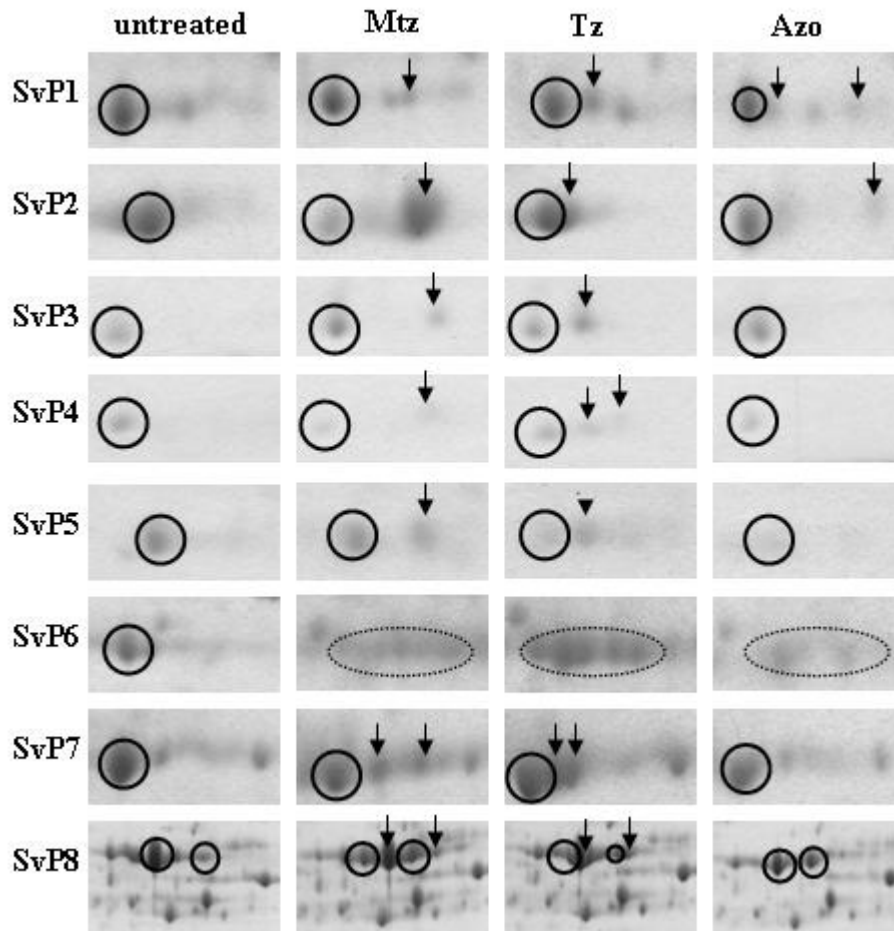
Fig 5.3. Comparison of shift patterns created by covalent adduct formation of *Spironucleus vortens* proteins (SvP1-8) with the 5-nitroimidazoles, metronidazole (Mtz) and tinidazole (Tz) and the 2-nitroimidazole, azomycain (Azo). Full circles indicate native proteins, arrows indicate shifted proteins. Broken circles indicate multiple shifts of the same protein caused by nitroimidazole treatment.

Table 5.2. *Spironucleus vortens* proteins (SvP1-8) identified from Capp database using MASCOT and ProteinScape.

Protein	No.[a]	Accession no.	MASCOT score	E-value	No. of shifts[b]
Uridine phosphorylase (UPL-1) [*Giardia lamblia* ATCC 50803]	SvP 1	CAPP4686.g1	701.3	2e-92	1
Thioredoxin reductase	SvP 1	CAPP4408.g1	560.6	[c]	1
Hypothetical protein FVAG_03003	SvP 2	CAPP409.G1	1474.6	0.16	1
Unidentified	SvP 3	CAPO2306.B1	40.2	0.79	1
Enolase [*Spironucleus vortens*]	SvP 4	CAPO2397.G1	753.6	2e-125	1
Protein disulfide isomerase PDI2 [*Giardia lamblia* P15]	SvP 5	CAPP6312.g1	1134.1	6e-31	1
Aminoacyl-histidine dipeptidase [*Giardia lamblia* ATCC 50803]	SvP 6	CAPP6585.B1	865.4	1e-53	5
Malic enzyme [*Giardia intestinalis* ATCC 50581]	SvP 7	CAPP4306.B1	550.5	4e-83	2
Enolase [*Spironucleus vortens*]	SvP 8	CAPO2052.B1	1076.5	0	2

[a] Numbering corresponds to protein spots in Fig 2 and 3
[b] No. of shifts after metronidazole treatment
[c] Not able to identify peptide fragment

5.4.5. Effects of nitroimidazoles and garlic-derivatives on total non-protein thiols

S. vortens total non-protein thiols were quantified according to the degree of DTNB reduction to TNB by thiol –SH groups. Percentage calculations are based on the concentration of thiols present in the untreated sample (21.17 ±4.35 nmol/mg protein), taken as 100% total thiols. The 5-nitroimidazoles metronidazole and tinidazole had different effects on the total non-protein thiol pool of *S. vortens* (Fig 5.5a). A concentration of 50 μM metronidazole caused a significant inhibition of thiol levels to 64 ±8% of the untreated sample. At concentrations >50 μM metronidazole, however, thiol levels returned to normal, a recovery which was significant (T-test, p =0.018). Tinidazole, on the other hand, caused a permanent decrease in thiol levels, significantly so at concentrations ≥25 μM (T-test, p≤0.005). The maximum degree of thiol depletion by

tinidazole was 65 ±2% of the untreated sample. AA caused a significant increase in the total thiol pool to 173 ±22% of the untreated sample, at a concentration of *ca.* 3 mM (Fig 5b, T-test, p=0.001). In contrast, DADS significantly depleted thiol levels by 74 ±11% of the untreated sample, at a concentration of 55 μM (Fig 5b, T-test, p=0.002). Ajoene and allicin both gave the same pattern of thiol depletion, whereby a burst in thiol levels was characteristic after treatment with low concentrations of the compounds (Fig 5c). In the case of allicin, for example, a significant increase in thiol levels by 154 ±58% of the untreated sample was evident (T-test, p=0.011) at 2.5 μM. However, at higher concentrations, ajoene produced a significant depletion of thiols to 71 ±8% (100 μM, T-test, p=0.04) of the untreated sample, whilst allicin again caused a significant increase in thiol levels to 184 ±36% (20 μM, T-test, p=0.019).

5.5. DISCUSSION

Treatment of *Spironucleus vortens* with allyl alcohol (AA) caused a visible reduction in cell number, which was most prominent ≥24 h post incubation. This was coupled with a marked increase in concentration of lysed cell debris, indicating ruptured cells. Extensive membrane blebbing of cells treated with metronidazole, allicin and diallyl disulphide (DADS) is characteristic of severe cell injury. Membrane blebbing has been described as an early feature of apoptosis (Barros et al. 2003). Programmed cell death has not yet been examined in *S. vortens*, however an apoptotic cell death pathway was recently documented in *G. intestinalis*, a diplomonad relative of *S. vortens* (see Corrêa et al. 2009). In addition, metronidazole, allicin and DADS have all previously been documented to induce apoptosis in the protozoan parasite *Blastocystis hominis* and the yeasts *Saccharomyces cerevisiae* and *Candida albicans*, respectively (Nasirudeen et al. 2004; Lemar et al. 2007; Gruhlke et al. 2010). However, it is also possible that the membrane blebs observed here are indicative of necrotic cell death. Necrotic blebs are associated with more intense stimuli such as hypoxia, metabolic poisoning and a high concentration of free radicals, and occur at the final stages of necrosis, prior to cell lysis (Barros et al. 2003). A high proportion of irregular-shaped cells possessing abnormal flagellar number were also observed for metronidazole, DADS, allicin and ajoene treatments. This may indicate inhibition of cytokinesis during cell division, which occurs by longitudinal binary fission (Woo & Poynton 1995). However, lower proportions of such cells are also commonly observed under normal culture conditions (Sangmaneedet

& Smith 2000), therefore at present, it is not clear whether this observation is drug-induced.

Analysis of the *S. vortens* proteome revealed 8 proteins which formed covalent adducts with the 5-nitroimidazoles, metronidazole and tinidazole. Protein functions could be assigned to 7 of the 8 nitroimidazole bound proteins, some of which have previously been identified as specific cellular targets of nitroimidazole metabolites. These include enolase and malic enzyme, which are specific metronidazole targets in *T. vaginalis* (see Leitsch et al. 2009) and uridine phosphorylase, a pyrimidine nucleoside phosphorylase, which bears similarities with previous observations in *E. histolytica* of nitroimidazole binding with a purine nucleoside phosphorylase (Leitsch et al. 2007). The other identified proteins, protein disulphide isomerase and aminoacyl-histidine dipeptidase, are novel nitroimidazole targets in *S. vortens*. Interestingly, in the case of the 2-nitroimidazole, azomycin, covalent adducts were not always formed. In *E. histolytica*, all proteins were found to be consistently shifted by 2- and 5-nitroimidazoles (Leitsch et al. 2007). This may indicate differences in the mode of action of 2- and 5-nitroimidazoles in *S. vortens*.

Unlike previous data obtained for *E. histolytica*, *G. intestinalis* and *T. vaginalis* (see Leitsch et al. 2007, 2009, 2011), *S. vortens* TrxR was not one of the proteins that gave a clear pI shift in response to nitroimidazole binding. TrxR was however identified as a secondary protein isolated from protein spot SvP1 along with uridine phosophorylase. The close proximity of TrxR to other proteins on the gel may account for the lack of obvious nitroimidazole binding to TrxR in *S. vortens*. Interestingly, as for *E. histolytica*, *T. vaginalis* and *G. intestinalis* (see Leitsch et al. 2007, 2009, 2011) nitroimidazole binding with pyruvate:ferredoxin oxidoreduxtase (PFOR) was not observed in *S. vortens*.

Despite the lack of obvious covalent adduct formation of nitroimidazoles with TrxR, enzymatic assay of this protein in *S. vortens* revealed significant inhibition by metronidazole. TrxR activity was reduced to 22% of its normal rate by metronidazole, which is more than double that reported for metronidazole-treated *E. histolytica* and *T. vaginalis* albeit using the recombinant enzyme expressed in *Escherichia coli* (see Leitch et al. 2007, 2009). This supports the Leitsch et al. (2007) hypothesis, thus implicating TrxR as a potential site of nitroimidazole activation in *S. vortens*. Inhibition of total non-protein thiols by metronidazole did not occur at similar concentrations to that of TrxR (20 µM), with significant thiol depletion only observed at 50 µM metronidazole. Interestingly, these thiol levels were significantly stimulated at elevated metronidazole

concentrations. This may indicate that *S. vortens* is capable of re-modelling its thiol antioxidant system, in response to inhibition of TrxR, which could be mediated by increased influx of cysteine from the culture medium. TrxR activity was inhibited to a lesser extent under tinidazole challenge to *ca.* 50% of normal function, with total non-protein thiol levels significantly decreased to the same degree. The *in vitro* MIC of tinidazole is reported to be higher than that of metronidazole for *T. vaginalis* treatment, which may account for differences in the degree of TrxR inhibition by these compounds (Sobel et al. 2001).
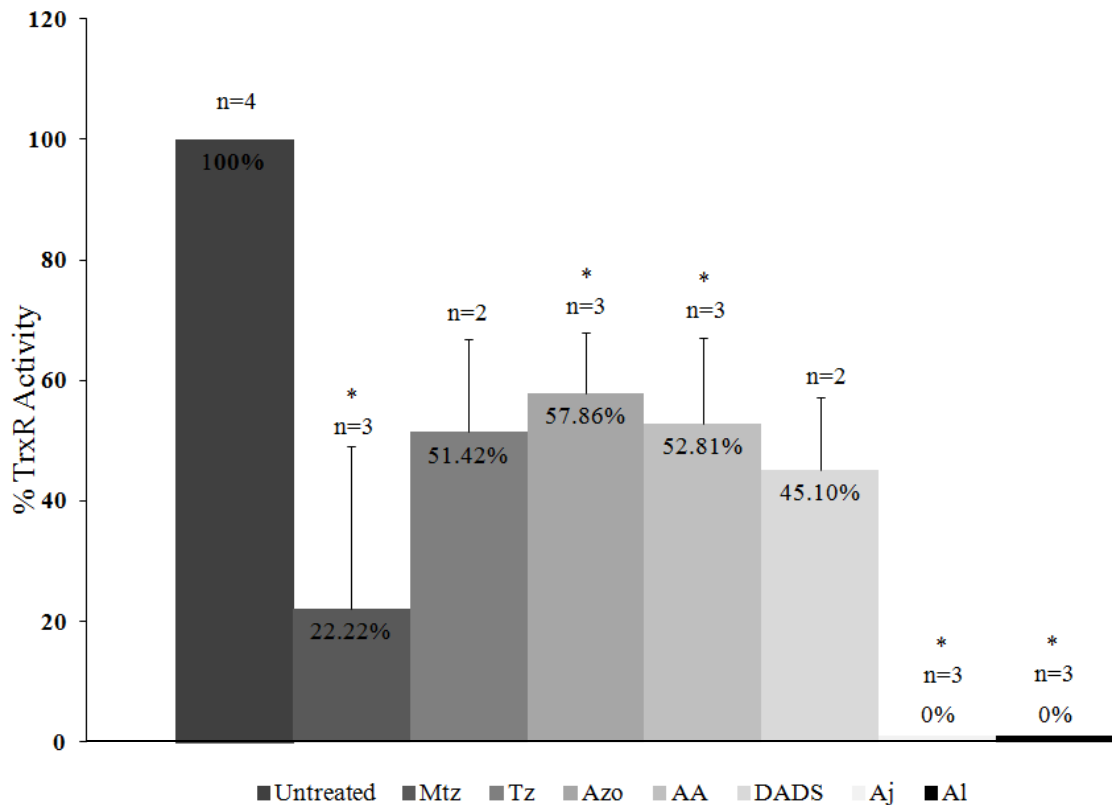
Fig. 5.4. The inhibitory effect of 5-nitroimidazoles, metronidazole (Mtz) and tinidazole, (Tz) and garlic-derived compounds, allyl alcohol (AA), diallyl disulphide (DADS), ajoene (Aj) and allicin (Al) on the NADPH-dependent activity of *Spironucleus vortens* thioredoxin reductase. Asterisks indicate points of significant difference from the untreated sample (T-test, $p \leq 0.05$). Error bars represent standard deviation of replicates (n=2-4).
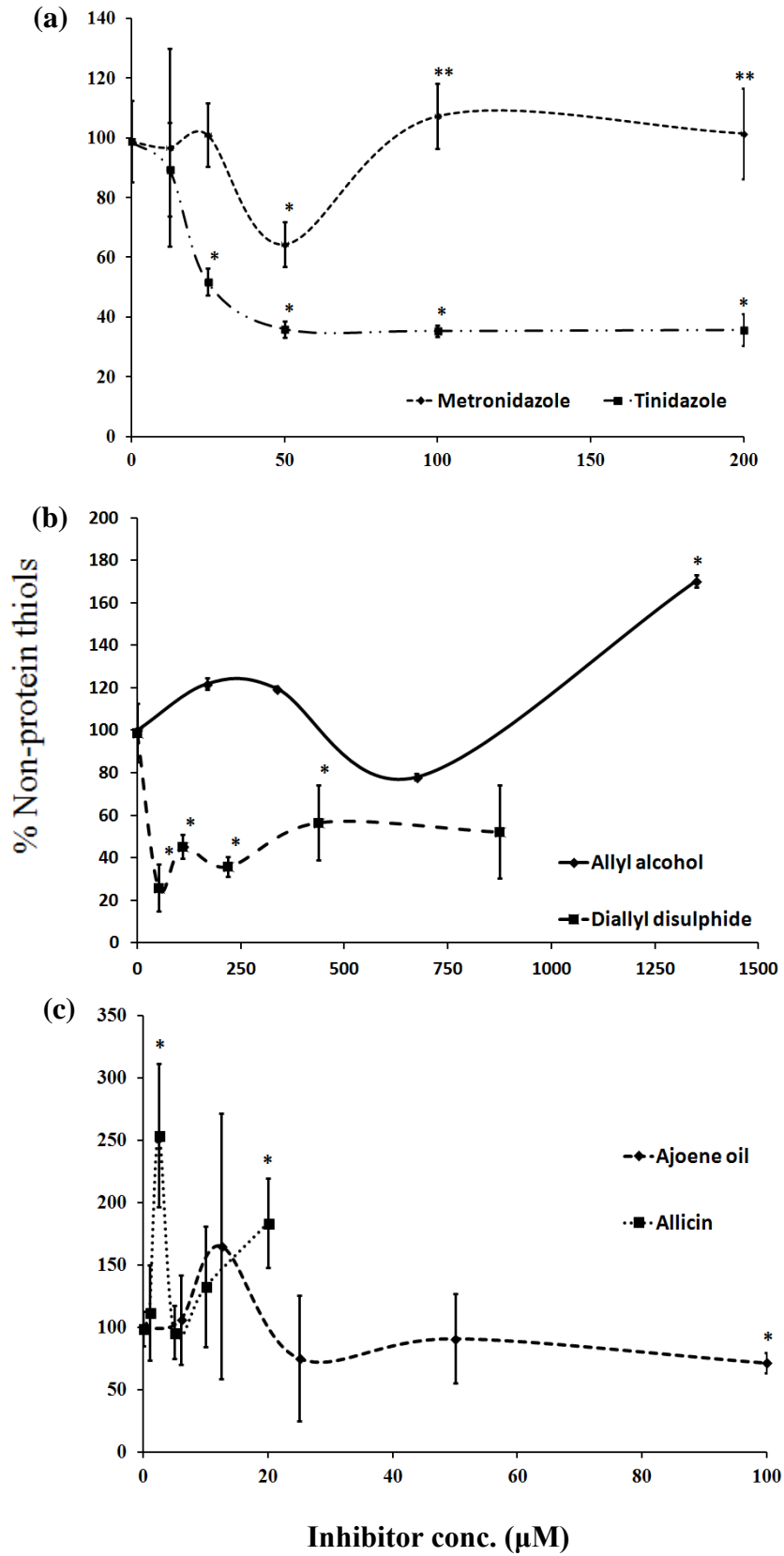
Fig 5.5. The effect of nitroimidazoles (a), metronidazole and tinidazole, and garlic-derived compounds allyl alcohol and diallyl disulphide (b), ajoene and allicin (c) on total non-protein thiol levels of *Spironucleus vortens*. Single asterisks indicate points of significant difference from the untreated value (100%), double asterisks indicate points of significant difference from adjacent data points (T-test, p≤0.05). Error bars represent standard deviation of replicates (n=3 in all cases except allyl alcohol treatment, where n=2).

Inhibition of TrxR, along with depletion of intracellular thiols may explain the discriminate binding of nitroimidazoles to specific protein targets, outlined above. Enolase and malic enzyme have previously been described as redox-controlled enzymes, specifically as interaction partners of Trx, in plants and yeast, respectively (Anderson et al. 1998; Wong et al. 2003; Hara et al. 2006). It was suggested that nitroimidazole binding to purine nucleotide phosphorylase in *E. histolytica* could be due to reductase activity of this enzyme along with the presence of an imidazole moiety in the purine substrate (Leitsch et al. 2007). The same, however, cannot be said of uridine phosphorylase, found here to form covalent adducts with nitroimidazoles in *S. vortens*. To the best of our knowledge, no reductase activity has been associated with this enzyme and its pyrimidine substrate lacks an imidazole moiety. However, it is plausible that interaction of nucleotide phosphorylases with TrxR is required *in vivo* in order to maintain these enzymes in a reduced state for normal activity. Interestingly, one of the novel nitroimidazole protein targets in *S. vortens*, protein disulphide isomerase (PDI), belongs to the Trx superfamily and itself has two Trx-like catalytic domains (Freedman et al. 1988). PDI is a multifunctional enzyme which catalyzes thiol-disulphide oxidation, reduction and isomerisation during protein folding, and is therefore important in maintaining cellular redox balance (Ellgaard & Ruddock 2005). Increased expression levels of PDI2 in a metronidazole-resistant *G. intestinalis* C5 strain have previously been described, with no significant inhibition of recombinant enzyme activity when subject to metronidazole challenge (Müller et al. 2007). Thus, it is feasible that nitroimidazole bindng to PDI does not interfere with the catalytic mechanism of this enzyme, and that increased expression in metronidazole-resistant isolates, which display minimal TrxR activity, may indicate the capacity of this enzyme to perform some of the roles of the thioredoxin system. Finally, the substrate of aminoacyl-histidine dipeptidase has been

described as an antioxidant in brain and muscle tissue, and also contains an imidazole ring (Kohen et al. 1988).

As for nitroimidazoles, the common characteristic of the garlic-derived compounds employed in the current study is that they have all previously been associated with inhibition of –SH containing enzymes (Ankri & Mirelman 1999; Gallwitz et al. 1999; Lemar et al. 2005, 2007). Indeed, allicin and ajoene had a clear inhibitory effect on *S. vortens* TrxR, with no detectible enzymatic activity being found at 20 µM of each compound. In the case of ajoene, this inhibitory effect was less pronounced on total non-protein thiol pools, only capable of significant thiol depletion at a much higher concentration of 100 µM, in a dose-dependent, hormetic effect. Conversely, allicin caused a significant increase in the non-protein thiol pool of *S. vortens*. However, the relatively low dose required to completely inhibit TrxR activity may again indicate a more complex antioxidant defence system present within the parasite, which may be able to compensate for inhibition of one system, e.g. Trx, by over-expression of another, as yet, uncharacterised system. AA produced a significant, albeit less pronounced, inhibition of TrxR activity, as compared to allicin, decreasing levels to *ca.* 50%. Total non-protein thiols, however, were mostly unaffected, and even increased at concentrations in excess of 1 mM. This is perhaps not surprising, as AA is readily oxidised to the toxic aldehyde acrolein by the action of alcohol dehydrogenase (Serafini-Cessi 1972). The mode of action of acrolein has previously been associated with inhibition of TrxR and depletion of Trx (Yang et al. 2004). DADS caused TrxR activity to drop to 45%, and significantly depleted *S. vortens* non-protein thiols, as previously described in *C. albicans* (see Lemar et al. 2007).

S. vortens is a parasite of great economic and veterinary importance in the aquaculture industry. Despite this, very few studies into the underlying biochemisty of the parasite have been conducted, making efficient chemotherapy challenging. This study is the first to investigate *S. vortens* proteomic interactions with novel and traditional chemotherapeutic agents. Results show that some parallels can be drawn between *S. vortens* and previously reported data on the medically important protozoan parasites *E. histolytica* and *T. vaginalis*. This is especially true in relation to the mode of action of nitroimidazoles, whereby TrxR activity is significantly reduced and specific redox-related proteins are targeted, thus supporting the theory of a novel pathway of nitroimidazole activation (Leitsch et al. 2007). The overall cellular consequences of activated nitroimidazoles and garlic-derived compounds are similar in that they result in severe

oxidative stress. Used in combination, these two classes of compounds might prove synergistic, thereby diminishing the metronidazole dosages required for effective parasite treatment. The extensive membrane blebbing observed after treatment with metronidazole, allicin and DADS is intriguing and may indicate the presence of a programmed cell death pathway in *S. vortens*, initiated by gross cellular redox and ionic imbalances. However, this needs further confirmation. Finally, the rapid doubling time, broad temperature range and aero-tolerant nature of *S. vortens* (see Millet et al. 2011a, b) make this parasite an ideal candidate to be a model organism for the discovery and development of new chemotherapeutic agents for protozoan parasites.

5.6. REFERENCES

Abd El-Galil MAA, Aboelhadid SM (2011). Trials for the control of trichodinosis and gyrodactylosis in hatchery reared *Oreochromis niloticus* fries by using garlic. Vet Parasitol 185: 57-63

Anderson LE, Li AD, Stevens FJ (1998). The enolases of ice plant and *Arabidopsis* contain a potential disulphide and are redox sensitive. Phytochemistry 47: 707-713

Ankri S, Mirelman D (1999). Antimicrobial properties of allicin from garlic. Microbes Infect 1: 125-129

Barros F, Kanaseki T, Sabirov R, Morishima S, Castro J, Bittner CX, Maeno E, Ando-Akatsuka Y, Okada Y (2003). Apoptotic and nectrotic blebs in epithelial cells display similar neck diameters but different kinase dependency. Cell Death Differ. 10: 687-697

Buchmann K, Jensen PB, Kruse KD (2003). Effects of sodium percarbonate and garlic extract on *Ichthyophthirius multifiliis* theronts and tomocysts: *in vitro* experiments. N Am J Aquacult 65: 21-24

Cavallito CJ, Bailey JH (1944). Allicin, the antibacterial principle of *Allium sativum*. I. Isolation, physical properties and antibacterial action. J Am Chem Soc 66: 1950-1951

Commission Regulation (EC) No. 613/98 (1998). Off J Eur Commun L82/14-17 [Cited 18 February 2013] URL:
http://ec.europa.eu/health/files/mrl/regpdf/1998_03_18-0613_en.pdf

Corrêa G, Vilela R, Menna-Barreto RFS, Midlej V, Benchimol M (2009). Cell death induction in *Giardia lamblia*: effect of beta-lapachone and starvation. Parasitol Int 58: 424-437

Edwards DI (1993). Nitroimidazole drugs - action and resistance mechanisms. II. Mechanism of resistance. J Antimicrob Chemother 31: 201-210

Ellgaard L, Ruddock LW (2005). The human protein disulphide isomerase family: substrate interactions and functional properties. EMBO Rep 6: 28-32

European Commission (2008) Background information on the consultation process on monitoring international trade in ornamental fish. [Cited 4 May 2011] URL: http://quin.unep-wcmc.Organ/species/OFT-PDF/Background%20information%20% 20monitoring%20ornamental%20fish%20trade.pdf

Freedman RB, Hawkins HC, Murant SJ, Reid L (1988). Protein disulphide-isomerase: a homologue of thioredoxin implicated in the biosynthesis of secretory proteins. Biochem Soc Trans 16: 96-99

Freeman CD, Klutman NE (1997). Lamp KC. Metronidazole. A therapeutic review and update. Drugs 54: 679-708

Gallwitz H, Bonse S, Martinez-Cruz A, Schlichting I, Schumacher K, Krauth-Siegel RS (1999). Ajoene is an inhibitor and subversive substrate of human glutathione reductase and *Trypanosoma cruzi* trypanothione reductase: crystallographic, kinetic and spectroscopic studies. Med Chem 42: 364-72

Gruhlke MCH, Portz D, Stitz M, Anwar A, Schneider T, Jacob C, Schlaich L, Slusarenko AJ (2010). Allicin disrupts the cell's electrochemical potential and induces apoptosis in yeast. Free Radical Bio Med 49: 1916-1924

Hara S, Motohashi K, Arisaka F, Romano PG, Hosoya-Matsuda N, Kikuchi N, Fusada N, Hisabori T (2006). Thioredoxin-*h*1 reduces and reactivates the oxidized cytosolic malate dehydrogenase dimmer in plants. J Biol Chem 281: 32065-32071

Kohen R, Yamamoto Y, Cundy KC, Amer BN (1988). Antioxidant activity of carnosine, homocarnosine, and anserine present in muscle and brain. Proc Natl Acad Sci USA 85: 3175-3179.

Kolarich D, Weber A, Turecek PL, Schwarz HP, Altmann F (2006). Comprehensive glyco-proteomic analysis of human α_1-antitrypsin and its charge isoforms. Proteomics 6: 3369-3380

Lanzky PF, Halting-Sørensen B (1997). The toxic effect of the antibiotic metronidazole on aquatic organisms. Chemosphere 1: 2553-2561

Leitsch D, Burgess AG, Dunn LA, Krauer KG, Tan K, Duchêne M, Upcroft P, Eckmann L, Upcroft JA (2011). Pyruvate:ferredoxin oxidoreductase and thioredoxin reductase are involved in 5-nitroimidazole activation while flavin metabolism is linked to 5-nitroimidazole resistance in *Giardia lamblia*. J Antimicrob Chemother DOI: 10.1093/jac/dkr192

Leitsch D, Radauer C, Paschinger K, Wilson IBH, Breiteneder H, Scheiner O, Duchêne M (2005). *Entamoeba histolytica*: analysis of the trophozoite proteome by two-dimensional polyacrylamide gel electrophoresis. Exp Parasitol 110: 191-195

Leitsch D, Kolarich D, Wilson IBH, Altmann F, Duchêne M (2007). Nitroimidazole action in *Entamoeba histolytica*: a central role for thioredoxin reductase. PLOS Biol 5: 1820-1834

Leitsch D, Kolarich D, Binder M, Stadlmann J, Altmann F, Duchêne M (2009). *Trichomonas vaginalis*: metronidazole and other nitroimidazole drugs are reduced by the flavin enzyme thioredoxin reductase and disrupt the cellular redox system. Implications for nitroimidazole toxicity and resistance. Mol Biol 72: 518-536

Lemar KM, Passa O, Aon MA, Cortassa S, Müller CT, Plummer S, O'Rourke B, Lloyd D (2005). Allyl alcohol and garlic (*Allium sativum*) extract produce oxidative stress in *Candida albicans*. Microbiology 151: 3257-3265

Lemar KM, Aon MA, Cortassa S, O'Rourke B, Müller CT, Lloyd D (2007). Diallyl disulphide depletes glutathione in *Candida albicans*: oxidative stress-mediated cell death studied by two-photon microscopy. Yeast 24 695-706

Lloyd D, Pedersen JZ (1985). Metronidazole radical anion generation *in vivo* in *Trichomonas vaginalis:* oxygen quenching is enhanced in a drug-resistant strain. J Gen Microbiol 131: 87-92

Lun ZR, Burri C, Menzinger M, Kaminsky R (1994). Antiparasitic activity of diallyl trisulfide (Dasuansu) on human and animal pathogenic protozoa (*Trypanosoma* sp., *Entamoeba histolytica* and *Giardia lamblia*) *in vitro*. Ann Soc Belg Med Trop 74: 51-59

Millet COM, Lloyd D, Williams CF, Williams D, Evans G, Saunders RA, Cable J (2010). Effect of garlic and *Allium*-derived products on the growth and metabolism of *Spironucleus vortens*. Exp Parasitol 127: 490-499

Millet COM, Lloyd D, Williams CF, Cable J (2011a). *In vitro* culture of the diplomonad fish parasite *Spironucleus vortens* reveals unusually fast doubling time and atypical biphasic growth. J Fish Dis 34: 71-73

Millet COM, Lloyd D, Coogan MP, Rumsey J, Cable J (2011b). Carbohydrate and amino acid metabolism of *Spironucleus vortens*. Exp Parasitol 129: 17-26

Mohamed S, Nagaraj G, Chua FHC, Wang YG (2000). The use of chemicals in aquaculture in Malaysia and Singapore. In: Use of Chemicals in Aquaculture in Asia: Proceedings of the Meeting on the Use of Chemicals in Aquaculture in Asia 20-22 May 1996, Tigbauan, Iloilo, Philippines. Arthur, J.R., Lavilla-Pitogo C.R., Subasinghe R.P. (Eds), Aquaculture Department, Southeast Asian Fisheries Development Center, pp 127-140

Müller J, Sterk M, Hemphill A, Müller N (2007). Characterization of *Giardia lamblia* WB C6 clones resistant to nitazoxanide and to metronidazole. J Antimicrob Chemother 60: 280-287

Nasirudeen AMA, Hian YE, Singh M, Tan KSW (2004). Metronidazole induces programmed cell death in the protozoan parasite *Blastocystis hominis*. Microbiology 150: 33-43

Paull GC, Matthews RA (2001). *Spironucleus vortens*, a possible cause of hole-in-the-head disease in cichlids. Dis Aquat Org 45: 197-202

Payne MA, Baynes RE, Sundlof SF, Craigmill A, Webb AI, Riviere JE (1999). Drugs prohibited from extralabel use in food animals. JAVMA 215: 28-32

Poynton SL, Fraser W, Francis-Floyd R, Rutledge P, Reed P, Nerad TA (1995). *Spironucleus vortens* n. sp. from the freshwater angelfish *Pterophyllum scalare:* morphology and culture. J Eukaryot Microbiol 42: 731-732

Sangmaneedet S, Smith SA (1999). Efficacy of various chemotherapeutic agents on the growth of *Spironucleus vortens*, an intestinal parasite of the freshwater angelfish. Dis Aquat Org 1: 47-52

Sangmaneedet S, Smith SA (2000). *In vitro* studies on optimal requirements for the growth of *Spironucleus vortens,* an intestinal parasite of the freshwater angelfish. Dis Aquat Org 39: 135-141

Serafini-Cessi F (1972). Conversion of allyl alcohol into acrolein by rat liver. Biochem J 128, 1103-1107

Singh UP, Pandey VN, Wagner KG, Singh KP (1990). Antifungal activity of ajoene, a constituent of garlic (*Allium sativum*). Can J Bot 68: 1354-1356

Sobel JD, Nyirjesy P, Brown W (2001). Tinidazole therapy for metronidazole-resistant vaginal trichomoniasis. Clin Infect Dis 33: 1341-1346

Tsao S, Yin M (2003). *In vitro* antimicrobial activity of four diallyl sulphides occurring naturally in garlic and Chinese leek oils. J Med Microbiol 50: 646-649

Tsai Y, Cole LL, Davis LE, Lockwood SJ, Simmons V, Wild GC (1985). Antiviral properties of garlic: *in vitro* effects on influenza B, herpes simplex and coxsackie viruses. Planta Med 5: 460-461

Urbina JA, Marchan E, Lazardi K, Visbal G, Apitz-Castro R, Gil F, Aquirre T, Piras MM, Piras R (1993). Inhibition of phosphatidylcholine biosynthesis and cell proliferation in *Trypanosoma cruzi* by ajoene, an antiplatelet compound isolated from garlic. Biochem Pharmacol 45: 381-387

Williams CF, Lloyd D, Poynton SL, Jørgensen A, Millet COM, Cable J (2011). *Spironucleus* species: economically-important fish pathogens and enigmatic single-celled eukaryotes. J Aquac Res Development S2-002

Williams CF, Lloyd D (2012). Composition and antimicrobial properties of sulphur-containing constituents of garlic (*Allium sativum*). In: Essential Oils as Natural Food Additives: Composition, Quality and Antimicrobial Activity. Valgimigli L (Ed), Nova Publishers, Inc. NY, USA, pp 287-304

Wong JH, Balmer Y, Cai N, Earley RL (2003). Unraveling thioredoxin-linked metabolic processes of cereal starchy endosperm using proteomics. FEBS Lett 547: 151-156

Woo PTK, Poynton SL (1995). Diplomonadida, Kinetoplastida and Amoebida (Phylum Sarcomastigophora). In: Fish Diseases and Disorders, Vol. 1. Protozoan and Metozoan Infections. Woo PTK (Ed), CAB International, Wallingford, UK, pp 27-96

Yang X, Wu X, Choi YE, Kern JC, Kehrer JP (2004). Effect of acrolein and glutathione depleting agents on thioredoxin. Toxicology 204: 209-218

Chapter 6

Glucose and glutamate: energy-yielding substrates of *Spironucleus vortens*

CHAPTER 6:

Glucose and glutamate: energy-yielding substrates of *Spironucleus vortens*

6.1. ABSTRACT

Unlike their mitochondriate ancestors, anaerobic/microaerophilic protists lack cytochrome-mediated oxidative pathways for energetic metabolism and instead employ substrate-level phosphorylation and fermentative pathways. For *Spironucleus vortens*, a diplomonad fish parasite, little research has been conducted into its fermentative metabolism. In the current study, glucose, the major carbohydrate component of TYI-S-33 culture medium, was confirmed as a secondary substrate of *S. vortens*. Instead, glutamate, a major amino acid taken up from the culture medium, was found to stimulate energy production by *S. vortens* in the form of NAD(P)H. Uptake of glutamate by *S. vortens* was also linked to stimulation of reduced glutathione, and concomitant uptake of malate had an additive effect. *S. vortens* cultures incubated with excess glutamate were able to reach the same yield as those maintained in normal glucose-containing culture medium, hence generating an equivalent energy yield. Glucose itself led to slight oxidation of *S. vortens* intracellular NAD(P)H, which oscillated in accordance with H_2O_2 production by the organism. Furthermore, the fact that glucose was the only substrate tested to significantly stimulate O_2 consumption by *S. vortens* links the process of O_2 scavenging to energy derived from glycolysis. Enzymatic assays revealed the presence of glutamate dehydrogenase, aspartate aminotransferase, malic enzyme, pyruvate:ferredoxin oxidoreductase and hydrogenase in *S. vortens*. These findings evoke new hypotheses regarding the antioxidant system and versatile energy-yielding metabolism of *S. vortens*.

6.2. INTRODUCTION

Spironucleus vortens is a protozoan parasite of great economic and veterinary importance in the ornamental aquaculture industry (see review by Williams et al. 2011). The opportunistic nature of this parasitic trophozoite means that, in stressed or immunocompromised hosts, the pathogen may leave the alimentary canal (its primary habitat), traverse the gut epithelial lining and form systemic infections by transmission

through the blood stream (Paull & Matthews 2001). Despite having been first isolated and described >20 years ago by Poynton et al. (1995), only recently have efforts focussed on characterizing the metabolic pathways of *S. vortens* (see Millet et al. 2010, 2011a).

Some protozoan parasites possess bacterial-like metabolic pathways, including the arginine dihydrolase pathway (*Giardia intestinalis*, see Schofield et al. 1990) and enzymes, e.g. pyruvate:ferredoxin oxidoreductase (PFOR) and hydrogenase (Horner et al. 1999, 2000). Previous research suggests that metabolic processes in *S. vortens* are likely to differ, even from its closest characterized diplomonad relatives, e.g. *G. intestinalis*. The growth rate of *S. vortens* (doubling time 1.79 h) greatly exceeds that of *G. intestinalis* (*ca.* 8 h) and rivals that of the fastest growing eukaryote, *Achlya bisexualis*, a water mould, with a biomass doubling time of 0.85 h (Millet et al. 2011b). H_2 production by *S. vortens* (77 nmol/min/10^7 cells, Millet et al. 2010) also exceeds that of *G. intestinalis* (2 nmol/min/10^7 cells, Lloyd et al. 2002) and more closely resembles that of *Trichomonas vaginalis* (20 nmol/min/10^7 cells, Ellis et al. 1992), a microaerophilic protozoan with well-defined hydrogenosomes (see review by Shiflett & Johnson 2010). Furthermore, *S. vortens* appears to lack the arginine dihydrolase pathway: it does however exhibit substantial proteolytic activity (Millet et al. 2011a). The latter is likely to play an important role in the ability of *S. vortens* to invade the intestinal epithelium and enter the bloodstream.

Another major difference between *Spironucleus* and *Giardia* is the apparent variation which exists in their mitochondrial-derived organelles (MDOs). *Giardia* has well-defined mitosomes, MDOs, which have lost almost all the canonical functions attributed to mitochondria (e.g. cytochrome-mediated oxidative phosphorylation) apart from iron sulphur cluster assembly, which has remained compartmentalised in *Giardia* mitosomes (Shiflett & Johnson 2010). *Spironucleus* spp., on the other hand, possess hydrogenosomes (Millet 2009; Millet et al. 2010; Jerlström-Hultqvist 2012; Williams et al. in press). These organelles have retained many more mitochondrial-derived functions than mitosomes, including substrate-level phosphorylation involving the fermentation of pyruvate to acetate, CO_2, H_2 and ATP (Chapman et al. 1985; 1986a; Steinbüchel & Müller 1986), in addition to components necessary for iron sulphur cluster assembly (reviewed by Lill 2009).

Millet et al. (2011b) discovered that growth of *S. vortens* displays an atypical biphasic pattern of logarithmic growth, whereby a slow preliminary phase increases sharply into a second rapid mode, referred to as µ1 and µ2, respectively. This was

explained by the fact that glucose (the principal carbohydrate component of the *S. vortens* culture medium) is a secondary substrate which is utilized only during the second stage of growth ($\mu 2$). Potential alternative substrates, including maltose (the main energy-yielding substrate of *T. vaginalis*, see Kuile 1994), arginine (alternative substrates for *G. intestinalis* and *T. vaginalis* see Schofield et al. 1990; Yarlett et al. 1996) and proline (the main energy-yielding substrate of trypanosomes, see Evans & Brown 1972), as well as pyruvate, serine and threonine were tested, but had no effect on the growth or gas metabolism of *S. vortens* (see Millet et al. 2011a). Hence, the primary energy-yielding substrate of *S. vortens* remains unknown; however it seemed likely to be an amino acid.

The main products of endogenous and glucose-supported metabolism of *S. vortens* were found to be identical, consisting of ethanol, lactate, acetate and alanine. The ratios of acetate and alanine differed, however, with more acetate than alanine being produced after the addition of glucose (Millet et al. 2011a). A similar scenario was observed in *G. intestinalis*, whereby a metabolic switch exists resulting in more acetate than alanine being produced under aerobic conditions (Paget et al. 1990). Alanine is a typical end-product of amino acid catabolism, when amino groups are transferred from glutamate to pyruvate (Lockwood & Coombs 1991). Hence, the amino acid pool derived from protein turnover could provide the primary substrates(s) of *S. vortens*.

In the current study, further potential candidates for the primary metabolic substrate of *S. vortens* were tested by spectrofluorimetry, O_2 electrode studies and optical density growth monitoring. Glutamate was one of the chosen substrates, which was previously found to be one of the major amino acids that were taken up by *S. vortens* from the culture medium (Millet et al. 2011a). Malate and pyruvate were also tested due to their roles in hydrogenosomal metabolism (Chapman et al. 1985, 1986a; Steinbüchel & Müller 1986; Hrdý & Mertens 1993). Enzymatic assays were conducted to investigate the presence and activity of metabolic enzymes in this organism.

6.3. MATERIALS AND METHODS

6.3.1. Organism and culture

Trophozoites of two *Spironucleus vortens* strains, ATCC 50386 and *Sv1* (isolated from juvenile English-bred angelfish, August 2011, described in Chapter 3), were maintained separately in Keister's modified TYI-S-33 medium as described in Chapter 2, section 2.2.

6.3.2. Spectrofluorometry

Log phase trophozoites (~10^7 cells/ml) were washed 2x in PBS (pH 7.2) and re-suspended in 1 ml PBS. A 100 µl volume of this cell suspension was then introduced into a stirred glass cuvette containing 1.5 ml PBS and 0.4 ml Amplex Red (kit from Invitrogen) in order to monitor H_2O_2 production by the organism. Glutathione (GSH) reduction was detected indirectly via glutathione S-bimane, GSB, a fluorescent adduct formed after the reversible reaction between GSH and monochlorobimane (MCB) (catalyzed by glutathione S-transferase, GST). Pre-incubation of cells for 30 min with 50 µM MCB was followed by washing 3x with PBS. A spectrofluorometer (Photon Technology International) was used to record simultaneously, at several wavelengths, fluorescence emission from each cell suspension, according to Aon et al. 2010: (1) H_2O_2 (λ_{ex} 530 nm, λ_{em} 590 nm), NAD(P)H autofluorescence (λ_{ex} 340 nm, λ_{em} 450 nm), oxidised flavin (FAD) autofluorescence (λ_{ex} 480 nm, λ_{em} 530 nm), GSH (λ_{ex} 390 nm, λ_{em} 480 nm); and cell size (90° side scatter, λ_{ex} 520 nm, λ_{em} 585 nm) was also measured. Background readings were established for each cuvette before addition of cells. Changes in the emission of each probe were monitored over time after addition of 5 mM of the following substrates: (1) glucose, (2) pyruvate, (3) glutamate, (4) malate, (5) glutamate and malate. All experiments were conducted under aerobic conditions using air-saturated buffer at room temperature (21±1°C) with 2-8 replicates for each substrate.

6.3.3. O₂ consumption by *S. vortens*

A Clark O_2 electrode was employed to monitor O_2 consumption by *S. vortens* in a 6 ml capacity closed system. The electrode was securely closed within the reaction vessel via an "O"-ring. O_2 was sensed by an Ag-Pt electrode covered by a gas-permeable Teflon membrane (4 M KCl electrolyte) and recorded using a chart recorder set at 5 mV FSD. All experiments were conducted at room temperature (20 ±1°C). Approximately 10^6 log-phase *S. vortens* trophozoites were washed 2x in PBS (pH 7.2) and suspended to a total volume of 3 ml in air-saturated PBS within the stirred reaction vessel. Glucose, glutamate, malate, a combination of glutamate and malate and pyruvate (5 mM each) were added to the cell suspension and subsequent changes in the rate of O_2 consumption calculated as a percentage of the endogenous rate. The changes in rates of O_2 consumption by both *S. vortens* strains at intervals over the range of 290 (air-saturated) to 0 µM O_2 were calculated from tangents taken from the decreasing gradients (n=2-12 for each substrate). The effect of different substrates on O_2 consumption by *S. vortens*

was compared statistically by ANOVA analyses in R (version 2.15.1; R Core Team 2012) using an α-level of 0.05. The overall model had an F-value of 6.622 on 5 and 16 degrees of freedom and a p-value of 0.002 with all model assumptions being normally distributed.

6.3.4. Optical density growth monitoring

Trophozoite growth was measured by optical density monitoring using a Bioscreen C Reader, as described in Chapter 2, section 2.3. Briefly, *ca.* 10^4 log phase trophozoites (in a 10 µl volume) were inoculated into 290 µl normal (control) or modified TYI-S-33 culture medium in the compartments of 100 well honeycomb plates. O_2 scavenging by *S. vortens* as well as the chemical reductants (i.e. cysteine and ascorbate) present in the culture medium produced anaerobic-microaerobic conditions within the wells. Modifications of the culture medium were as follows: (1) no glucose, (2) no ferric ammonium citrate (FAC), (3) no new born calf serum (NBCS), (4) no glucose, FAC and NBCS; or replacing glucose with the following substrates (concentration range: 1, 2, 3, 5, 7.5, 30 or 60 mM); (1) pyruvate, (2) glutamate, (3) malate, (4) glutamate and malate, and, (5) glucose (positive control). Log phase growth rates (µ1 and µ2) and final yield were calculated. The effect of different treatments on log-phase growth rates and yields of *S. vortens* were statistically compared to those of cells grown in normal culture medium using ANOVA analyses in R (version 2.15.1; R Core Team 2012) using an α-level of 0.05. Each model had F-values of 75.25 and 229.10 on 9 and 20 degrees of freedom for µ1 and final yield, and 78.17 on 8 and 19 degrees of freedom for µ2. The overall p-values for each model were <0.0001 with all model assumptions being normally distributed.

6.3.5. Enzyme assays

Log phase trophozoites were washed 2x in PBS (pH 7.2) and re-suspended in disruption buffer (20 mM EDTA + 0.1% Triton X-100) for 15 min at room temperature. This cell disruption method was employed for enzymatic assay of aspartate aminotransferase, glutamate dehydrogenase and malic enzyme. For O_2-sensitive enzyme assays, i.e. pyruvate:ferredoxin oxidoreductase and hydrogenase, cells were broken in a second disruption buffer (50 mM HEPES, 150 mM NaCl, 225 mM sucrose, 2 mM EDTA, pH 7.4) and shaken with acid-washed glass beads in a Braun MSK Cell Disintegrator (3x 30 s pulses at 4000 Hz) with all reagents and crude cell extracts kept anaerobic by sparging with N_2. Unbroken cells were pelleted at 800 g for 5 min and the supernatant retained for the assay (Ellis et al. 1993). Protein content was determined via

Bradford assay (Bradford 1976), as outlined in Chapter 2, section 2.4. A series of enzymatic assays were then conducted by adding 10 µl of a 1 mg/ml *S. vortens* protein extract (or purified enzyme, positive control) to the relevant reaction mixtures (after establishing a blank rate). All assays were conducted at room temperature ($21 \pm 1°C$) with a minimum of 2 replicates per assay. A spectrophotometer (Jenway 6300) was employed (path length 1 cm) to measure the change in absorbance over a 5 min period, with readings recorded at 30 s intervals, after addition of the enzyme to appropriate reaction mixtures as follows:

6.3.5.1. Aspartate aminotransferase (AST) activity (EC: 2.6.1.1): 134 mM L-aspartate, 6.64 mM α-ketoglutarate, 0.24 mM NADH, 5 U/ml lactate dehydrogenase, 1.25 U/ml malate dehydrogenase (MDH) in 50 mM sodium phosphate buffer (pH 7.4, Karmen 1955). The decrease in absorbance at 340 nm (oxidation of NADH) is directly proportional to AST activity. Specific enzyme activities were calculated using the NAD(P)H extinction co-efficient of 6.22×10^3 M^{-1} cm^{-1}.

$$\alpha\text{-ketoglutarate} + \text{L-aspartate} \xrightarrow{\text{AST}} \text{L-glutamate} + \text{Oxalacetate}$$

$$\text{Oxalacetate} + \text{NADH} + \text{H}^+ \xrightarrow{\text{MDH}} \text{Malate} + \text{NAD}^+$$
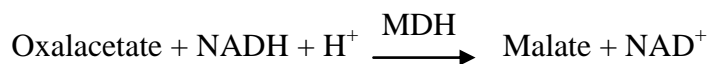
6.3.5.2. NADPH-specific glutamate dehydrogenase (GDH) activity (EC: 1.4.1.4): (1) forward reaction (reductive aminating activity); 100 mM Tris HCl (pH 8), 100 mM NH4Cl, 10 mM α-ketoglutarate and 0.1 mM NADPH; (2) reverse reaction (oxidative deaminating activity); 100 mM Tris-HCl (pH 9); 200 mM glutamate and 0.1 mM $NADP^+$ (Harper et al. 2010).

6.3.5.3. NADH-specific GDH activity (EC:1.4.1.2): (1) forward reaction; 100 mM phosphate buffer (HK_2PO_4/H_2NaPO_4; pH 7), 100 mM NH_4Cl, 10 mM α-ketoglutarate and 0.16 mM NADH; (2) reverse reaction; 100 mM phosphate buffer (pH 7), 100 mM L-glutamate and 2 mM NAD^+ (Harper et al. 2010).

The decrease in absorbance at 340 nm (NAD(P)H oxidation) was recorded for the forward reactions, and vice versa for the reverse ($NAD(P)^+$ reduction) reaction. Specific enzyme activities were calculated as above.

$$\alpha\text{-ketoglutarate} + NH_4Cl + NAD(P)H + H^+ \xleftrightarrow{\text{GDH}} \text{L-glutamate} + NAD(P)^+$$
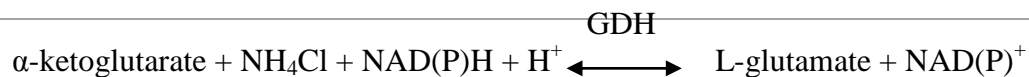
6.3.5.4. Malic enzyme (ME; decarboxylating) activity (EC: 1.1.1.39): 67 mM triethanolamine, 3.3 mM L-malic acid, 0.3 mM $NADP^+$ and 5 mM $MnCl_2$ (Geer et al. 1980). Specific enzyme activities were calculated as above.

$$\text{L-malate} + NADP^+ \xrightarrow{\text{ME}} \text{Pyruvate} + CO_2 + NADPH + H^+$$

6.3.5.5. Pyruvate:ferredoxin oxidoreductase activity (PFOR, EC: 1.2.7.1): 100 mM potassium phosphate buffer (pH 7.4), 20 mM dithiothreitol, 20 mM methyl viologen, 250 mM β-mercaptoethanol, 0.25 mM CoA and 0.1% (v/v) Triton X-100. A 2.5 mM Na-pyruvate solution was used to initiate the reaction after addition of the crude protein extract (100 μl). Methyl viologen replaced ferredoxin as the final electron acceptor. Reduction of this chromogen by PFOR was monitored at 600 nm, accompanied by a characteristic blue colour formation (Lindmark & Muller 1973). Specific enzyme activities were calculated using the methyl viologen extinction co-efficient of 6.3 x 10^3 M^{-1} cm^{-1}.

$$\text{Pyruvate} + CoA + \text{Methyl viologen}_{ox} \xrightarrow{\text{PFOR}} \text{Acetyl CoA} + CO_2 + \text{Methyl viologen}_{red}$$
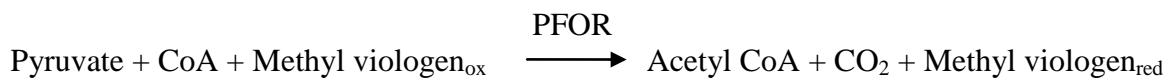
6.3.5.6. Hydrogenase activity (Hyd, EC: 1.18.99.1): 100 mM phosphate buffer (pH 7.4), 20 mM methyl viologen, 250 mM β-mercaptoethanol and 100 μl crude protein extract to initiate the reaction. Reduction of methyl viologen was monitored at 600 nm, and specific enzyme rates calculated as above (Lindmark & Muller 1973).

$$2 H^+ + 2 e^- + \text{Methyl viologen}_{ox} \xrightarrow{\text{Hyd}} H_2 + \text{Methyl viologen}_{red}$$
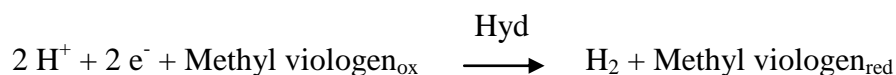
6.3.5.7. Calculation of enzymatic rates. Enzymatic rates were calculated according to Beer's Law:

$$\mathbf{\Delta A = e\ c\ l}$$

Where, ΔA is the measured absorbance change (Δabsorbance/min), e is the molar extinction coefficient, l is the path length (1 cm), and c is the molar concentration (moles/L).

6.4. RESULTS

6.4.1. Effects of metabolic substrates on redox dynamics of *Spironucleus vortens* by spectrofluorimetry

Administration of 5 mM glucose, pyruvate, glutamate or malate, or glutamate and malate in combination resulted in a decrease in 90° side light scatter from cells in a stirred suspension, thereby indicating substrate uptake. Under these aerobic conditions, glucose resulted overall in slight oxidation of the NAD(P)H pool but in an oscillatory manner accompanied by H_2O_2 production (indicated in Fig 6.1a). Pyruvate led to oxidation of the NAD(P)H pool to a greater extent than glucose, decreasing the fluorescence emission to 90% of endogenous levels (Fig. 6.1b). This was coupled with a decrease in the rate of H_2O_2 production down to *ca.* 28% of the endogenous rate. Glutamate produced a 10% increase in NAD(P)H levels, coupled with a slight decrease in the rate of H_2O_2 production (to 76% of the endogenous rate) and slight reduction of FAD pools to $FADH_2$ (Fig. 6.1c). There was no noticeable immediate change in H_2O_2, NAD(P)H or FAD pools on administration of malate (Fig. 6.1d). In addition, there was no change in 90° size scatter from cells, indicating that this substrate may not have been taken up. A combination of glutamate and malate, however, led to a 15% increase in NAD(P)H pools (Fig. 6.1e). As well as this, reduction of intracellular thiols was also evident on addition of glutamate plus malate, specifically in the glutathione (GSH) antioxidant system (*ca.* +4% of the endogenous level).

6.4.2. Effects of metabolic substrates on O_2 uptake by *S. vortens*

Of the substrates tested, glucose (5 mM) was the only compound to cause a significant increase in O_2 consumption by *S. vortens* (ANOVA, t = 4.362, p<0.0005; Fig. 6.2). Addition of glucose to stirred suspensions of *S. vortens* resulted in a *ca.* 80% increase in O_2 uptake by the organism. None of the other substrates tested were significantly different from the endogenous O_2 consumption rate of 39.3 nmol/min/10^7 cells (ANOVA, p<0.05).
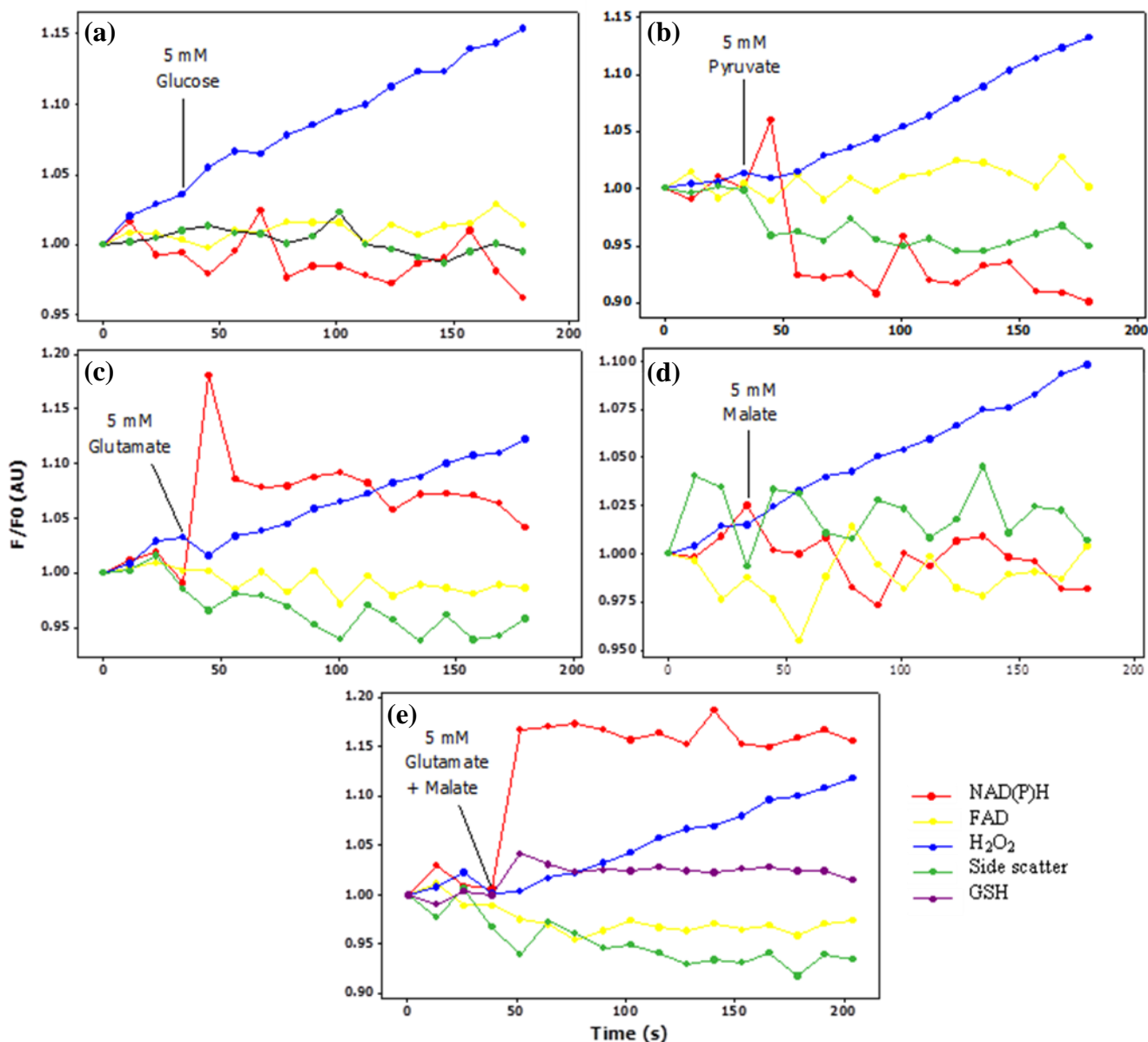
Fig. 6.1. Spectrofluorometric detection of changes in intracellular NAD(P)H, FAD and glutathione (GSH), extracellular production of H_2O_2 and cell size (90° side scatter) of *Spironucleus vortens* after addition of substrates (5 mM each): (a) glucose, (b) pyruvate, (c) glutamate, (d) malate and (e) a combination of glutamate and malate. Each trace is representative of 2-8 replicates.

6.4.3. Effects of metabolic substrates on the growth of *S. vortens*

Figure 6.3 summarizes the effect of different metabolic substrates on the growth of *S. vortens* under anaerobic-microaerobic conditions. All substrates were statistically compared to control growth rates ($\mu 1$ and $\mu 2$, Fig. 6.3a and 3b, respectively) and final yield (Fig. 6.3c) of cells grown in normal TYI-S-33 culture medium. Removing NBCS or

a combination of NBCS, FAC and glucose from the medium resulted in significant inhibition of logarithmic growth phases: $\mu1$ (t=2.84, p=0.01 and t=3.20, p=0.004, respectively) and $\mu2$ (no $\mu2$ for culture medium without NBCS, t=5.11, p<0.0001 for culture medium without NBCS, FAC and glucose), as well as a decrease in overall final yield of cells (t=15.41, p<0.0001). Eliminating FAC from culture medium resulted in an increase in the first logarithmic growth phase ($\mu1$; t=4.17, p=0.0005), decrease in the second logarithmic growth phase ($\mu2$; t=11.91, p<0.0001), but no significant difference in final yield (t>2.09, p>0.05). Removal of glucose from the medium led to a significant increase in $\mu1$ (t=7.77, p<0.0001) and a significant decrease in $\mu2$ and final yield (t=3.65, p=0.002 and t=9.59, p<0.0001, respectively). Addition of glutamate to the culture medium resulted in a significant decrease in the rates of $\mu1$ (t=6.05, p<0.0001) and $\mu2$ (t=7.02, p<0.0001), but no significant difference in final yield (t>2.09, p>0.05), whilst malate, pyruvate and a combination of glutamate and malate resulted in a significant decrease in $\mu1$ (t=13.89, 5.84 and 7.41, respectively and p<0.0001 for all), $\mu2$ (t=22.32, 8.31 and 8.44, respectively and p<0.0001 for all) and final yield (t=30.88, p<0.0001; t=6.51, p<0.0001 and t=3.25, p=0.004, respectively) of the organism. Addition of malate in concentrations in excess of 7.5 mM completely inhibited *S. vortens* growth.

Table 6.1. *Spironucleus vortens* metabolic enzymes. Enzymatic activity of aspartate aminotransferase (AST), malic enzyme (ME), $NAD(P)^+/NAD(P)H$-dependent glutamate dehydrogenase (GDH), pyruvate:ferredoxin oxidoreductase (PFOR) and hydrogenase (hyd) in *S. vortens*. ND = not detected.

Enzyme assayed	No. of replicates	Rate (nmol/ min/ mg protein)
AST	2	363 ±12
ME	3	2040 ±740
GDH: (i) NAD^+	3	92 ±8
(ii) NADH	3	ND
(iii) $NADP^+$	3	149 ±50
(iv) NADPH	3	ND
PFOR	2	285 ±4
Hyd	4	296 ±208

6.4.4. Rates of activity of metabolic enzymes present in *S. vortens*

Enzyme activities of AST, ME, PFOR and Hyd were detected in *S. vortens*. GDH oxidative (but not reductive) deaminating activity was also detected. All enzymatic rates are summarized in Table 6.1.

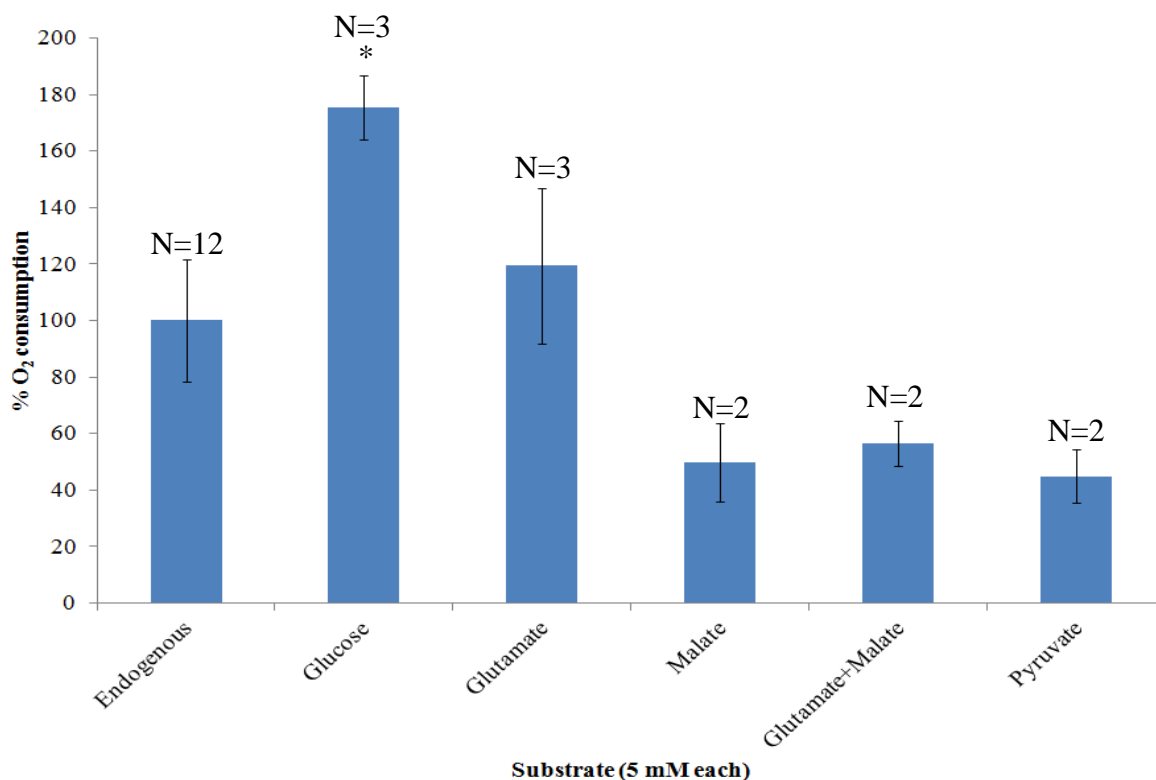**Fig. 6.2.** Percentage differences in O_2 consumption by *Spironucleus vortens*, as compared to endogenous rates, after addition of substrates (5 mM): glucose, glutamate, malate, a combination of glutamate and malate or pyruvate. Asterisks (*) indicate substrates which caused a significant difference in O_2 consumption from endogenous rates (ANOVA, p<0.0005). Error bars indicate standard deviation values.
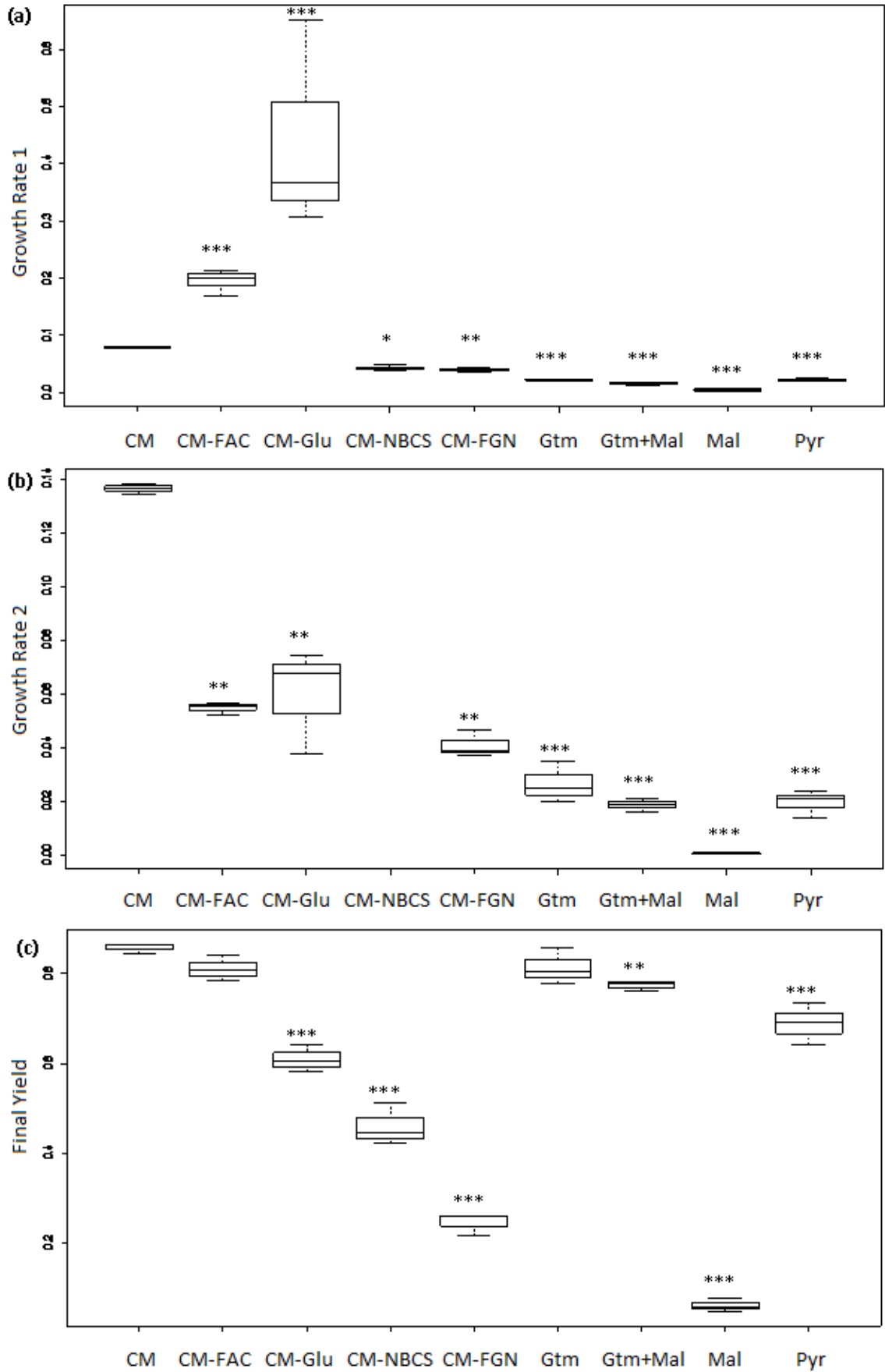
Fig. 6.3. Boxplots of *Spironucleus vortens* growth rates: log-phase 1 (a), log-phase 2 (b) and final yield (c) under different nutrient conditions. CM, normal culture medium; CM-FAC, culture medium - ferric ammonium citrate; CM-Glu, culture medium - glucose; CM-NBCS, culture medium - new born calf serum; CM-FGN, culture medium - FAC, Glu and NBCS; Gtm, glutamate; Gtm+Mal, glutamate + malate; Mal, malate; Pyr, pyruvate. Gtm, Gtm+Mal, Mal and Pyr replace glucose in the culture medium (60 mM each). Asterisks represent significant difference from the culture medium (CM) control (ANOVA; $p<0.05^*$, $p<0.005^{**}$, $p<0.0005^{***}$), n=3 for each treatment.

6.5. DISCUSSION

The three experimental methods employed in this study were conducted under different O_2 tensions, which must be taken into account whilst formulating hypotheses on potential metabolic pathways present within *Spironucleus vortens*. This is because presence of minute concentrations of O_2 (<0.25 µM) have been shown to have major consequences on the metabolic end products of *Giardia intestinalis*, a related diplomonad parasite (Paget et al. 1993).

6.5.1. Open system, air-saturated conditions: spectrofluorimetry

Glutamate was found to be taken up immediately by *S. vortens* in an air-saturated buffer suspension and led to an increase in the reduced NAD(P)H pool of the organism. Enzymatic assay of *S. vortens* glutamate dehydrogenase (GDH) revealed that the enzyme is only capable of oxidative deaminating activity. This reaction results in the production of α-ketoglutarate and NH_4Cl from glutamate with energy generated in the form of NAD(P)H. This explains the burst in NAD(P)H produced on addition of glutamate, confirming its role as an energy-yielding substrate in *S. vortens*. Addition of glutamate also resulted in a decrease in H_2O_2 production by the organism. This may be linked to the concomitant increase in the intracellular reduced glutathione (GSH) pool of *S. vortens*, as glutamate is a major component in glutathione synthesis (see review by Attick & Nathan 1984). Components of the glutathione system, including GSH peroxidase are usually associated with detoxification of H_2O_2 to H_2O, which may explain the observation seen here. This finding is intriguing as anaerobic protozoa, including *G. intestinalis* and *Trichomonas vaginalis*, lack GSH and instead utilize cysteine as their major intracellular

thiol (Brown et al. 1993; Ellis et al. 1994). Future studies are required to confirm the presence of a GSH antioxidant system and peroxidases in *S. vortens*.

Administration of malate alone did not affect the redox dynamics of *S. vortens*, with actual uptake of this substrate being questionable in this study when administered alone. Malate is known to be a substrate of hydrogenosomes (Hrdý & Mertens 1993) and *S. vortens* is reported here to have malic enzyme activity, which results in the formation of pyruvate and NAD(P)H. Intra-hydrogenosomal metabolic processes involve O_2-sensitive enzymes, including PFOR and hydrogenase (see review by Shiflett & Johnson 2010). Hence, if the presence of hydrogenosomes in *S. vortens* is confirmed, then the function of these organelles may be impaired under the aerobic conditions utilized in this experiment. Addition of malate with glutamate, however, had an additive effect on the reductive effect of glutamate. This finding is characteristic of mitochondria, whereby glutamate and malate are both substrates of complex I and are imported into these organelles via a malate-aspartate shuttle (Brand & Chappell 1974). There are no cytochromes present in *S. vortens* (see Williams et al. in press), however the organism may have retained a similar malate-aspartate antiporter from its mitochondriate ancestor.

Glucose, the main carbohydrate component of the culture medium produced oscillations in the intracellular NAD(P)H pool and H_2O_2 production by *S. vortens*, whereby bursts in NAD(P)H resulted in decreased production of H_2O_2. This suggests that energy derived from glucose is directly linked to O_2 consumption by the organism and may supply reducing power to a recently discovered flavodiiron protein (FDI), a terminal O_2 reductase found to be present in anaerobic protozoa, and which may be expressed in *Spironucleus barkhanus*, as it is represented in the genome (Di Matteo et al. 2008). The FDI protein of *G. intestinalis* and *T. vaginalis* converts O_2 to H_2O, explaining the decrease in H_2O_2 production observed after addition of glucose to the suspension. Indeed, energy generated from the oxidation of pyruvate is hypothesized to supply the FDI protein with reducing power via PFOR and ferredoxin (Chapman et al. 1986b; Smutná et al. 2009). This explains the observation of decreased H_2O_2 production as a result of the addition of pyruvate to *S. vortens*. PFOR activity in *S. vortens* was assayed under anaerobic conditions during this study. It therefore remains to be seen whether this O_2-sensitive enzyme could have remained active under the high O_2 tensions employed during the spectrophotometric assay employed here. Conversion of pyruvate to ethanol, lactate, acetate and alanine, the main products of endogenous/glucose-supported metabolism in *S.*

vortens (see Millet et al. 2011a) results in oxidation of the NAD(P)H pool, which also explains this observation seen during the current study.
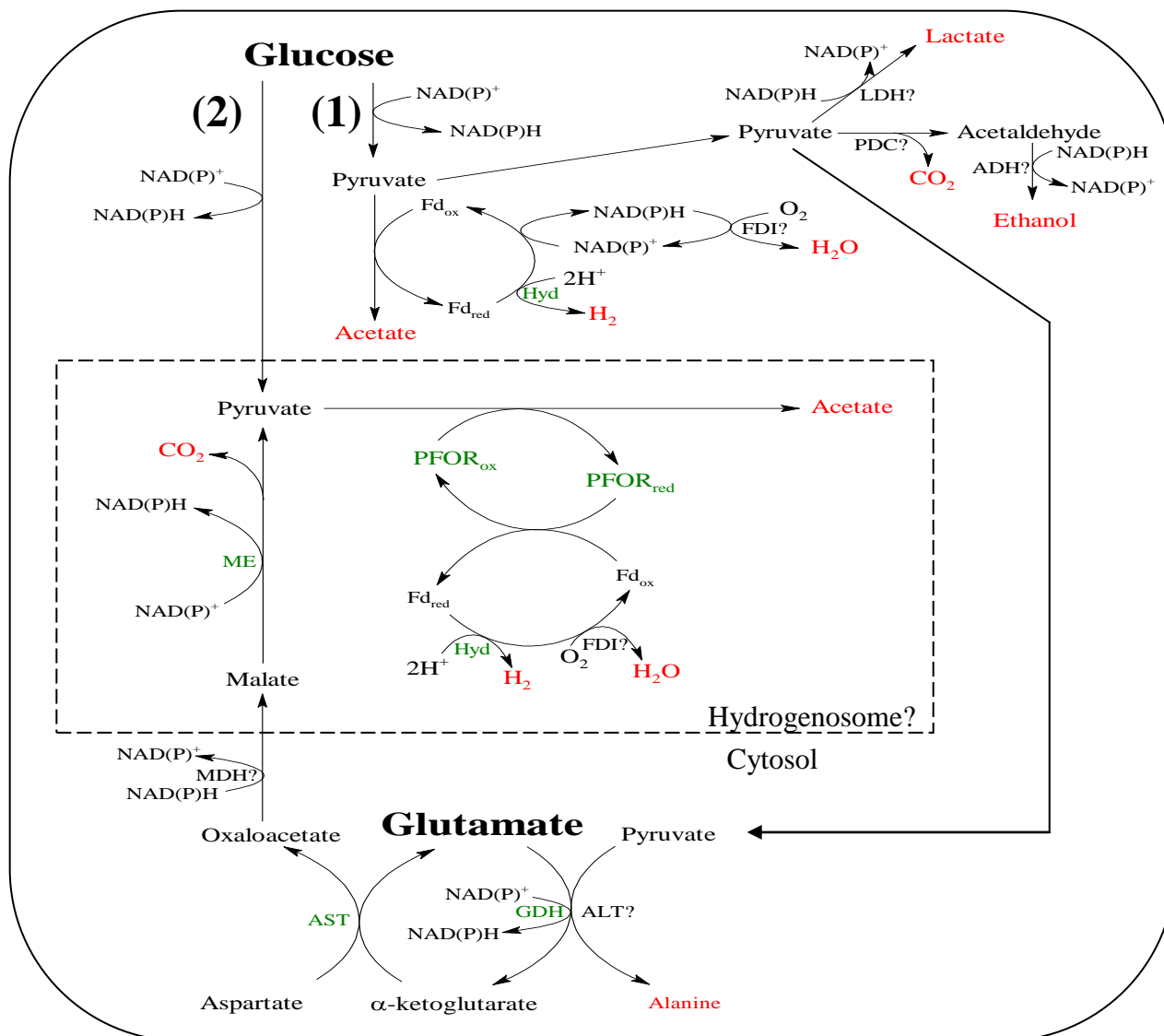
Fig. 6.4. Hypothesised pathways of glucose and glutamate metabolism and energy generation (in the form of NAD(P)H) by *Spironucleus vortens*. Two possible scenarios are given for glucose metabolism (1) cytosolic, or (2) hydrogenosomal. The latter has not yet been verified in *S. vortens*. Some enzymes included here have not yet been assayed in *S. vortens* and are indicated with a (?). Enzymes assayed during this study are highlighted in green. Metabolic end products are highlighted in red and are released from the cell (see Millet et al. 2011a). Fd, ferredoxin; Hyd, hydrogenase; FDI, flavodiiron protein; LDH, lactate dehydrogenase; PDC, pyruvate decarboxylase; ADH, alcohol dehydrogenase; ME, malic enzyme; MDH, malate dehydrogenase; PFOR, pyruvate:ferredoxin oxidoreductase; AST, aspartate aminotransferase; GDH, glutamate dehydrogenase; ALT, alanine aminotransferase.

6.5.2. Closed system, air-saturated conditions: O₂ consumption studies

The only substrate tested here to significantly stimulate O_2 consumption by *S. vortens* was glucose. This strengthens the hypothesis that energy derived from glucose-fueled metabolism enhances O_2 consumption by *S. vortens*. A similar observation was found previously, whereby glucose increased *S. vortens* O_2 uptake by 164% (Millet et al. 2011a). The fact that direct addition of pyruvate, the end product of glycolysis and a hydrogenosomal substrate, did not enhance O_2 consumption could suggest that the FDI protein of *S. vortens* is not entirely hydrogenosomal, but has a dual cytosolic location, as observed for the PFOR of *T. vaginalis* (see Meza-Cervantez et al. 2011).

6.5.3. Anaerobic-microaerobic conditions: growth monitoring

Removal of glucose from culture medium results in a significant increase in the first log phase (μ1) of *S. vortens* growth and significant reduction of the second log phase (μ2) and overall final yield. This confirms previous findings that glucose is a secondary substrate of *S. vortens*, which is only utilized during μ2 (Millet et al. 2011a). It appears that glucose is either inhibitory to growth during μ1, or, as suggested by Millet et al. (2011a), that it may be accumulated and stored during μ1 and only utilized as a metabolic substrate during μ2. Indeed, the latter is true of *G. intestinalis*, where glucose is accumulated and stored as glycogen during lag-phase and early logarithmic growth, before being utilized during late logarithmic growth (Pradhan et al. 2012). This finding was attributed to the biphasic activity of glycogen phosphorylase, which is minimal during the first 12 h of growth of newly established *G. intestinalis* cultures, before increasing in activity from 12-32 h (Pradhan et al. 2012). Hence, future work should focus on characterising the presence and subsequent activity of glycogen phosphorylase in *S. vortens*, which may explain glucose utilization as well as the biphasic growth pattern of this organism.

Replacement of glucose with an equivalent concentration of glutamate (60 mM) resulted in a significant decrease in both μ1 and μ2, but the final yield was not significantly different to that of glucose. This suggests near-equivalent energy yield from cells grown with glucose or glutamate additions to the culture medium (Bauchop & Elsden 1960; Lloyd & Callely 1965). However, glutamate is already present at a concentration of *ca.* 45 mM in the culture medium, with *S. vortens* having been shown previously only to utilize around 3.5 mM after 4 d (Millet et al. 2011a). Hence, glutamate is not limited within the culture medium. Nevertheless, final yields of cells grown with

the addition of 60 mM glutamate was significantly higher than those grown without glucose or glutamate, indicating that addition of excess glutamate does lead to enhanced growth. Addition of all other substrates tested (i.e. pyruvate, malate and a combination of glutamate and malate), up to a concentration of 60 mM each, resulted in significant inhibition of both growth rates and final yield. Malate was particularly inhibitory at concentrations in excess of 7.5 mM, resulting in zero growth. Hence, the identity of the primary substrate of choice for optimal *S. vortens* growth remains unknown. Future work should involve designing a well-defined culture medium in order to allow exclusion of potential substrates from the medium to better assess their effects on *S. vortens* growth.

New-born calf serum (NBCS) was found to be essential for *S. vortens* growth as its exclusion from the culture medium led to significantly reduced cell yields. Ferric ammonium citrate (FAC) is likely to be utilized by *S. vortens* during the second logarithmic phase of growth, however its removal from the culture medium did not significantly alter the final cell yield. FAC is an important source of iron for anaerobic/microaeophilic protozoans, which is employed in Fe-S clusters present in important metabolic enzymes, e.g. hydrogenase (Adams 1990). However, after *ca.* 3 subsequent subcultures excluding FAC from the medium, cell yield was found to be greatly decreased (data not shown). Hence, iron is confirmed as an important nutrient for long-term *S. vortens* growth.

Hydrogen is another metabolic end product of *S. vortens*, produced at a rate of 77 nmol/min/10^7 cells (Millet et al. 2010). This study confirms the presence of hydrogenase activity in *S. vortens*. In anaerobic protists H_2 production serves as a means of removing excess reducing power (as electrons and protons) from cells under anaerobic conditions (Lloyd et al. 2002). In *T. vaginalis*, O_2 sensitive enzymes, including hydrogenase and PFOR, are partially protected from O_2 by their compartmentalization in the hydrogenosomes (Shiflett & Johnson 2010). It remains to be confirmed whether *S. vortens* possesses hydrogenosomes, or like its distant relative, *Giardia*, all its energy-yielding metabolic pathways are cytosolic. Under highly oxidizing conditions these enzymes may be irreversibly inhibited, leading to knock on consequences on their metabolic pathways. In *G. intestinalis* and *Hexamita inflata*, alanine production was found to vary under different O_2 tensions, being highest under anaerobiosis (Paget et al. 1993; Biagini et al. 1998). Like *S. vortens*, *H. inflata* was able to grow without addition of the main carbohydrate substrate (glucose and maltose, respectively) to the medium, albeit with reduced growth rates and final yields (Biagini et al. 1998). Hence, amino acids

may play a substantial role in energy generation in these organisms. *Giardia* possesses a NAD(P)$^+$-depended GDH which is thought to cooperate with alanine aminotransferase (ALT) in the formation of alanine from pyruvate. Like *G. intestinalis*, *S. vortens* also incorporates glutamate from the medium and possesses GDH activity. Hence a similar pathway of energy generation from amino acids may be present in this organism. Malic enzyme activity was also detected in *S. vortens* and, unlike other aforementioned hydrogenosomal enzymes, was not O_2 sensitive. Taking information gained from the current study, as well as that of Millet et al. (2011a), into consideration, hypothesized energy-yielding metabolic processes of *S. vortens* are summarized in Figure 6.4.

Future work should involve in-depth immuno-electron microscopy to determine the type of MDOs that are present in *S. vortens*. Subsequently, isolation of these MDOs by subcellular fractionation should be employed to reveal the metabolic capacity of these organelles. Furthermore, growth of *S. vortens* under varying O_2 tensions in order to determine the growth and metabolic profile of this organism in aerobic and anaerobic environments will yield important information regarding the O_2 range of this pathogen. Collectively, these studies will provide great insight into the metabolic diversity which exists amongst the parasitic diplomonads.

6.6. REFERENCES

Adams MW (1990). The structure and mechanism of iron hydrogenases. Biochim Biophys Acta 1020: 115-145

Bauchop T, Elsden SR (1960). The growth of micro-organisms in relation to their energy supply. J Gen Microbiol 23: 457-469

Biagini GA, McIntyre PS, Finlay BJ, Lloyd D (1998). Carbohydrate and amino acid fermentation in the free-living primitive protozoon *Hexamita* sp. Appl Environ Microbiol 64: 203-207

Bradford MM (1976). A rapid and sensitive method for the quantification of microgram quantities of protein utilizing the principle of protein-dye binding. Anal Biochem 72: 248-254

Brand MD, Chappell JB (1974). Glutamate and aspartate transport in rat brain mitochondria. Biochem J 140: 205-210

Brown DM, Upcroft JA, Upcroft P (1993). Cysteine is the major low-molecular weight thiol in *Giardia duodenalis*. Mol Biochem Parasitol 61: 155-158

Chapman A, Linstead DJ, Lloyd D, Williams J (1985). ^{13}C NMR reveals glycerol as an unexpected major metabolite of the protozoan parasite *Trichomonas vaginalis*. FEBS Lett 191: 287-292

Chapman A, Linstead DJ, Lloyd D, Williams J (1986a). Pyruvate metabolism by trichomonads. Biochem Soc Trans 14: 1274

Chapman A, Cammack R, Linstead DJ, Lloyd D (1986b). Respiration of *Trichomonas vaginalis* components detected by electron paramagnetic resonance spectroscopy. Eur J Biochem 156: 193-198

Di Matteo A, Scandurra FM, Testa F, Forte E, Sarti P, Brunori M, Giuffrè A (2008). The O_2-scavenging flavodiiron protein in the human parasite *Giardia intestinalis*. J Biol Chem 283: 4061-4068

Ellis JE, Cole D, Lloyd D (1992). Influence of oxygen on the fermentative metabolism of metronidazole-sensitive and resistant strains of *Trichomonas vaginalis*. Mol Biochem Parasitol 56: 79-88

Ellis JE, Yarlett N, Cole D, Humphreys MJ, Lloyd D (1994). Antioxidant defences in the microaerophilic protozoan parasite *Trichomonas vaginalis*: comparison of metronidazole-resistant and sensitive strains. Microbiology 140: 2489-2494

Evans DA, Brown RC (1972). The utilization of glucose and proline by culture forms of *Trypanosoma brucei*. J Protozool 19: 686-690

Geer BW, Krochko D, Oliver MJ, Walker VK, Williamson JH (1980). A comparative study of the NADP-malic enzymes from Drosophila and chick liver. Comp Biochem Physiol 65B: 25-34

Harper CJ, Hayward D, Kidd M, Wiid I, can Helden P (2010). Glutamate dehydrogenase and glutamine synthetase are regulated in response to nitrogen availability in *Mycobacterium smegmatis*. BMC Microbiol 10: 138-150

Horner DS, Hirt RP, Embley TM (1999). A single eubacterial origin of eukaryotic pyruvate:ferredoxin oxidoreductase genes: implications for the evolution of anaerobic eukaryotes. Mol Biol Evol 16: 1280-1291

Horner DS, Foster PG, Embley TM (2000). Iron hydrogenases and the evolution of anaerobic eukaryotes. Mol Biol Evol 17: 1695-1709

Hrdý I, Mertens E (1993). Purification and partial characterization of malate dehydrogenase (decarboxylating) from *Tritrichomonas foetus* hydrogenosomes. Parasitol 107: 379-385

Jerlström-Hultqvist J (2012). Hidden diversity revealed. Genomic, transcriptomic and functional studies of diplomonads. Unpublished PhD Thesis, Uppsala University [Cited 26 February 2013] URL:
http://uu.diva-portal.org/smash/get/diva2:562514/FULLTEXT01

Karmen A (1955). A note on the spectrophotometric assay of glutamic-oxalacetic transaminase in human blood serum. J Clin Invest 34: 131

ter Kuile BH (1994). Adaptation of the carbon metabolism of *Trichomonas vaginalis* to the nature and availability of the carbon source. Microbiology 140: 2503-2510

Lill R (2009). Function and biogenesis of iron-sulphur proteins. Nature 460: 831-838

Lindmark DG, Müller M (1973). Hydrogenosome, a cytoplasmic organelle of the anaerobic flagellate *Tritrichomonas foetus*, and its role in pyruvate metabolism. J Biol Chem 248: 7724-7728

Lloyd D, Callely AG (1965). The assimilation of acetate and propionate by *Prototheca zopfii*. Biochem J 97: 176-180

Lloyd D, Ralphs JR, Harris JC (2002). *Giardia intestinalis*, a eukaryote without hydrogenosomes, produces hydrogen. Microbiology 148: 727-733

Lockwood BC, Coombs GH (1991). Amino acid catabolism in anaerobic protists. In: Coombs, GH, North M (Eds.), Biochemical Protozoology. Taylor and Francis, London, pp 113-122

Meza-Cervantez P, González-Robles A, Cárdenas-Guerra RE, Ortega-López J, Saaverda E, Pineda E, Arroyo R (2011). Pyruvate:ferredoxin oxidoreductase (PFO) is a surface-associated cell-binding protein in *Trichomonas vaginalis* and is involved in trichomonal adherence to host cells. Microbiology 157: 3469-3482

Millet COM (2009). Growth, metabolism, ultrastructure and chemotherapy of *Spironucleus vortens*. Unpublished PhD Thesis, Cardiff University

Millet COM, Cable J, Lloyd D (2010). The diplomonad fish parasite *Spironucleus vortens* produces hydrogen. J Euk Microbiol 57: 400-404

Millet COM, Lloyd D, Coogan MP, Rumsey J, Cable J (2011a). Carbohydrate and amino acid metabolism of *Spironucleus vortens*. Exp Parasitol 129: 17-26

Millet CO, Lloyd D, Williams C, Cable J (2011b). *In vitro* culture of the diplomonad fish parasite *Spironucleus vortens* reveals unusually fast doubling time and atypical biphasic growth. J Fish Dis 34: 71-73

Paget TA, Raynor MH, Shipp DWE, Lloyd D (1990). *Giardia lamblia* produces alanine anaerobically but not in the presence of oxygen. Mol Biochem Parasitol 42: 63-68

Paget TA, Kelly ML, Jarroll EL, Lindmark DG, Lloyd D (1993). The effects of oxygen on fermentation in *Giardia lamblia*. Mol Biochem Parasitol 57: 65-72

Paull GC, Matthews RA (2001). *Spironucleus vortens*, a possible cause of hole-in-the-head disease in cichlids. Dis Aquat Org 45: 197-202

Poynton SL, Fraser W, Francis-Floyd R, Rutledge P, Reed P, Nerad TA (1995). *Spironucleus vortens* n. sp. from the fresh-water Angelfish *Pterophyllum scalare*: morphology and culture. J Euk Microbiol 42: 731-742

Pradhan P, Lundgren SW, Wilson WA, Brittingham A (2012). Glycogen storage and degradation during *in vitro* growth and differentiation of *Giardia intestinalis*. J Parasitol 98: 442-444

R Core Team (2012) R: A language and environment for statistical computing. R Foundation for Statistical Computing, Vienna, Austria. ISBN 3-900051-07-0, URL http://www.R-project.org/

Schofield PJ, Costello M, Edwards MR, O'Sullivan WJ (1990). The arginine dihydrolase pathway is present in *Giardia intestinalis*. Int J Parasitol 20: 697-699

Smutná T, Gonçalves VL, Saraiva LM, Tachezy J, Teixeira M, Hrdý I (2009). Flavodiiron protein from *Trichomonas vaginalis* hydrogenosomes: the terminal oxygen reductase. Eukaryot Cell 8: 47-55

Steinbüchel A, Müller M (1986). Anaerobic pyruvate metabolism of *Tritrichomonas foetus* and *Trichomonas vaginalis* hydrogenosomes. Mol Biochem Parasitol 20: 57-65

Townson SM, Upcroft JA, Upcroft P (1996). Characterisation and purification of pyruvate:ferredoxin oxidoreductase from *Giardia duodenalis*. Mol Biochem Parasitol 79: 183-193

Williams CF, Lloyd D, Poynton SL, Jørgensen A, Millet COM, Cable J (2011). *Spironucleus* species: economically important fish pathogens and enigmatic single-celled eukaryotes. J Aquac Res Development S2-002

Williams CF, Millet COM, Hayes AJ, Cable J & Lloyd D (in press). Diversity in mitochondria-derived organelles of the parasitic diplomonads *Spironucleus* and *Giardia*. Trends Parasitol DOI: 10.1016/j.pt.2013.04.004

Yarlett N, Martinez MP, Moharrami MA, Tachezy J (1996). The contribution of the arginine dihydrolase pathway to energy metabolism by *Trichomonas vaginalis*. Mol Biochem Parasitol 78: 117-125

Chapter 7

Antioxidant defences of *Spironucleus vortens*: an aerotolerant anaerobic diplomonad parasite

CHAPTER 7:

Antioxidant defences of *Spironucleus vortens*: an aerotolerant anaerobic diplomonad parasite

Williams CF, Cable J, Yarlett N, Aon M & Lloyd D

Manuscript submitted for peer review

7.1. ABSTRACT

The aerotolerant anaerobic piscine diplomonad, *Spironucleus vortens*, is able to withstand high fluctuations in O_2 tensions during its lifecycle. From its primary microaerobic habitat, the intestinal tract of fish, the parasite is capable of causing extra-intestinal systemic infections. Trophozoites have been isolated from numerous organs as well as head lesions of the host, a highly aerobic environment. During transmission to a new host, *S. vortens* trophozoites have also been documented to survive for prolonged periods in the faeces of the fish host. In the current study, we further investigated the O_2 scavenging and antioxidant defence mechanisms which facilitate the survival of *S. vortens* under such oxidizing conditions. Closed O_2 electrode measurements revealed that the *S. vortens* ATCC 50386 strain was more O_2 tolerant than a freshly isolated *S. vortens* intestinal strain (*Sv1*). This may be explained by the effects of long-term *in vitro* culture, which may result in the loss of some parasite virulence factors. In contrast to the related human diplomonad, *Giardia intestinalis*, RP-HPLC revealed the major non-protein thiols of *S. vortens* to be glutathione (GSH, 776 nmol/ 10^7 cells) and H_2S. Furthermore, antioxidant proteins of *S. vortens* were assayed enzymatically and revealed that *S. vortens* possesses superoxide dismutase and NADH oxidase (883 and 37.5 nmol/min/mg protein, respectively) but like *G. intestinalis*, lacks catalase and peroxidase activity. Fluorimetry was also employed using fluorescent probes targeted to key intracellular redox components, which allowed visualization of redox dynamics in both untreated living cells and after treatment with inhibitors. H_2O_2 was produced by *S. vortens* at a rate of 2.85 pmol/min/10^6 cells. Metronidazole and the garlic-derived diallyl disulphide (DADS) led to depletion of *S. vortens* intracellular NAD(P)H pools and an increase in H_2O_2 production. Other garlic-derived compounds completely inhibited O_2 consumption by *S. vortens* (ajoene oil), or significantly depleted the intracellular GSH pool of the organism (allyl alcohol and DADS). Hence, antioxidant defence mechanisms of *S. vortens* may provide novel targets for parasite chemotherapy.

7.2. INTRODUCTION

Spironucleus vortens is a protozoan fish parasite capable of causing high mortalities in the ornamental aquaculture industry (see review by Williams et al. 2011). The organism primarily inhabits the middle to posterior intestinal tract of the host, a microaerobic environment which contains traces of O_2 at concentrations of 33-66 µM (JM Whittamore and RW Wilson pers. com.). *S. vortens* is regarded as an anaerobic organism, containing O_2-sensitive enzymes, e.g. pyruvate:ferredoxin oxidoreductase (PFOR) and hydrogenase (see Chapter 6), which play crucial roles in cellular metabolism and redox balance (Horner et al. 1999; Millet et al. 2010). As a result, *S. vortens* rapidly consumes O_2 from its immediate surroundings, thus creating its own optimal micro-environment (Millet et al. 2010). During its lifecycle, *S. vortens* trophozoites are able to tolerate high fluctuations in O_2 tensions, especially during an extra-intestinal systemic infection. Trophozoites have been isolated from head lesions of fish with hole-in-the-head disease, an environment which is likely to be quite aerobic in comparison to the intestinal tract (Paull & Matthews 2001). Trophozoites are also expelled into the faeces of the host, where a small proportion of parasites are able to survive for more than 36 d outside the host (see Chapter 3). O_2 consumption by *S. vortens* does not involve a phosphorylating respiratory chain, as the organism was previously shown to lack cytochromes (Williams et al. in press). The mechanisms employed by *Spironucleus* spp. to detoxify O_2 have not been elucidated and may provide novel pathways for chemotherapy.

Redox status plays a key role in cell survival (see review by Trachootham et al. 2008). Indeed, ultradian oscillatory redox mechanisms are conserved in evolutionary diverse cells, from yeasts to cardiomyocytes, and are essential for cellular coherence and survival (Lloyd et al. 2012). Redox cycling of intracellular thiols form the core of rhythmicity in yeast and heart cells (Lloyd et al. 2012). Similarly, thiol-based redox systems are crucial for the success and survival of protozoan parasites (see review by Müller 2004). Intracellular protein and non-protein thiols are the main cellular antioxidants present in protozoan parasites. These thiols play an important role in maintaining redox balance by detoxifying reactive oxygen species (ROS), produced as a result of parasite O_2 scavenging and/or the oxidative burst generated by the host immune system (see review by Müller 2004). During this process, thiol groups are cycled between their reduced and oxidised states. This cycling process is mediated by reductases which catalyse the NAD(P)H-dependent reduction of oxidised disulphides back to reduced di-

thiols (see review by Arrick & Nathan 1984). Thioredoxin (Trx) is one example of an almost ubiquitous small protein di-thiol, found in most prokaryotic and eukaryotic organisms, and plays a major role in cellular redox balance (Arnér & Holmgren 2000). Likewise, superoxide dismutase (SOD), catalase and peroxidase play important roles in superoxide anion ($\cdot O_2^-$) detoxification to O_2 and H_2O_2 (SOD) and further reduction of H_2O_2 to O_2 and H_2O (catalase and peroxidases) (Müller 2004). Non-protein thiols however differ between organisms. The microaerophilic protozoan parasites *Giardia intestinalis* and *Trichomonas vaginalis*, for instance, both utilize cysteine as their major non-protein thiol (Brown et al. 1993; Ellis et al. 1994). The aerobic malaria parasites *Plasmodium* spp. on the other hand possesses a complete glutathione (GSH) antioxidant system (Müller 2004) and trypanosomes employ the novel trypanothione (Fairlamb et al. 1985). Failure of antioxidant systems lead to accumulation of ROS, causing significant damage to proteins, lipids and DNA, and often triggers cell death (Circu & Aw 2010).

Garlic (*Allium sativum*) and garlic-derived compounds, are effective antimicrobial compounds, which have been employed in herbal medicine for millennia (see review by Harris et al. 2001). Active components of garlic extract, including ajoene and other sulphonated compounds, effectively inhibit *S. vortens* growth (Millet et al. 2011) and have been shown to work in synergy with metronidazole (MTZ), the conventional drug of choice (see Chapter 4). Williams et al. (2012, Chapter 5) demonstrated that administration of garlic-derived compounds inhibited the thioredoxin reductase (TrxR) of *S. vortens* and led to depletion of intracellular non-protein thiols. A similar finding was observed for MTZ (Williams et al. 2012). Hence, the mode of action of novel (i.e. garlic-derivatives) and existing (i.e. MTZ) chemotherapeutics is based on disrupting the intracellular redox balance of *S. vortens*, which eventually leads to cell death (Millet et al. 2011; Williams et al. 2012).

In the current study, the aerotolerant nature of *S. vortens* was examined by characterization of its O_2 scavenging and antioxidant defence mechanisms. The subsequent roles of the identified intracellular antioxidants were further investigated as novel chemotherapeutic targets. This is of direct relevance in the treatment of Spironucleosis, as MTZ has been banned from use on food fish in Europe and the US (Commission Regulation No. 613/98 1998; FARAD 2010); hence, alternative, non-harmful therapies are urgently needed.

7.3. MATERIALS & METHODS

7.3.1. Organism and culture

Trophozoites of two *Spironucleus vortens* strains, ATCC 50386 and *Sv1* (isolated from juvenile English-bred angelfish, August 2011, described in Chapter 3), were maintained separately in Keister's modified TYI-S-33 medium as described in Chapter 2, section 2.2. The trypanosomatid *Crithidia* sp. (obtained from Prof. Nigel Yarlett, Pace University, NY) was cultured in defined media as described by Bacchi et al. (1974) and used as a positive control from the HPLC analysis described below.

7.3.2. Inhibitors

The inhibitors metronidazole (MTZ, Sigma-Aldrich), auranofin (AF, Sigma-Aldrich), allyl alcohol (AA, Sigma-Aldrich), diallyl disulphide (DADS, Sigma-Aldrich) and ajoene (18%, Neem Biotech) were employed to investigate their effects on O_2 consumption and antioxidant defences of *S. vortens*. MTZ is the conventional drug of choice used to treat Spironucleosis, AF specifically inhibits thioredoxin reductase (TrxR) and garlic-derived compounds AA, DADS and ajoene have previously been shown to cause redox imbalance in *S. vortens* (see Williams et al. 2012, Chapter 5).

7.3.3. Oxygen measurements

A Clark O_2 electrode was employed to monitor O_2 consumption by *S. vortens* (ATCC and *Sv1* strains) in a 6 ml capacity closed system. The electrode was securely closed within the reaction vessel via an "O"-ring. O_2 was sensed by an Ag-Pt electrode covered by a gas-permeable Teflon membrane (4 M KCl electrolyte) and recorded by a chart recorder set at 5 mV FSD. All experiments were conducted at room temperature (21 $\pm 1°C$). Approximately 10^6 log-phase *S. vortens* trophzoites were washed 2x in PBS (pH 7.2) and suspended to a total volume of 3 ml in air-saturated PBS within the stirred reaction vessel. Glucose (5 mM) was provided as a respiratory substrate (as described in Chapter 6). The changes in rates of O_2 consumption by both *S. vortens* strains from 290 (air-saturated PBS) to 0 μM O_2 were calculated from linear parts of the slopes (n=3 for each strain). These rates were plotted against the O_2 tension at which the rate of O_2 consumption changed. The maximal rate of O_2 consumption (V_{max}), O_2 tension at which O_2 consumption ceased ($[O_2]_{V=0}$), and upper O_2 tension which was inhibitory to O_2 consumption ($[O_2]_{V=i}$) were also calculated for both strains. The effects of inhibitors,

MTZ (50 µM), AA, DADS and ajoene (1 mM each) on O_2 consumption by the ATCC strain were also analysed (n=2 for each treatment, n=4 for the untreated control).

7.3.4. Reverse-phase HPLC

Reduced thiols were analysed according to the methods of Ellis et al. (1994). Log phase *S. vortens* trophozoites (approx. 2 x 10^7 cells per sample) were washed 2x in PBS (pH 7.2), pelleted and re-suspended in 40 mM HEPPS/NaOH with 2 mM EDTA (pH 8). To assess the effects of inhibitors on the non-protein thiols of *S. vortens*, some samples (n=2 per treatment) were pre-treated with 50 µM metronidazole (MTZ), 50 µM auranofin (AF), 1 mM allyl alcohol (AA), 1 mM diallyl disulphide (DADS) or 1 mM ajoene (AJ) for 1 h at room temperature. To investigate the presence of trypanothione within *S. vortens*, some samples (n=2 per treatment) were pre-incubated for 24 h with 5 mM DFMO (difluromethylornithine) and/or [^{3}H]-spermidine (3.25 nmol, 50 µ Ci) in culture medium. Untreated control samples were conducted in triplicate. Thiols were then derivatized with 2 mM monobromobimane (MBB) in absolute ethanol and heated to 70°C for 30 min in a water bath. After cooling on ice, samples were deproteinized with 4 M methanesulphonic acid (pH 1.5, with LiOH) for 15 min on ice. Total protein concentration of each sample was determined at this point by Bradford assay (Bradford 1976) before removing derivatized proteins by centrifugation (10,000 g, 2 min). The supernatant was retained and passed through a 0.45 µm nylon-66 filter and separated by reverse-phase HPLC using a series LC 410 pump (Perkin–Elmer) coupled to a Beckman "Ultrasphere" column (5 µm particle size) with a 20 µl loop. A 30 µl volume of the derivatized thiol samples were injected into the injection port. The protocol consisted of an 84 min discontinuous gradient of solvents A = 0.25% (w/v) D-camphor sulphonate (pH 2.64), and B = 0.25% (w/v) D-camphor sulphonate containing 25% n-propanol. Thiols were eluted using a flow rate of 1 ml/min using: (1) isocratic step at 90% A, 10% B for 20 min, (2) linear gradient to 50% A and B for 40 min, and, (3) isocratic step at 50% A and B for 10 min. Starting conditions were regenerated after 5 min and maintained for 15 min prior to the next injection. The operating pressure was 1,300 psi. Fluorescently derivatized non-protein thiols were detected using an LS-1 fluorescence detector (Perkin-Elmer) fitted with a 1 µl flow cell, using λ_{ex} 375 nm and λ_{em} 480 nm. MBB derivatized standards, glutathione (GSH), propanethiol, methanethiol, trypanothione and H_2S, were prepared in the same way as the cell samples. Incorporation of [^{3}H]-spermidine by *S. vortens* was investigated by HPLC separation of thiols (as

described) and radiometric detection. Areas under the peaks were determined using b-RAM computer software (IN/US Systems), version 1.62. *Crithidia* sp. was used as a positive control for glutathione and trypanothione with samples prepared as described for *S. vortens*. For *Crithidia* sp., HPLC analysis was conducted using a modified method to that described above, according to Koledin et al. (2002). A Percosil column (Perkin-Elmer, 5 μm particle size) was employed along with solvents A = 0.25% acetic acid (v/v, pH 4.2) and B = 100% methanol (analytical grade). Thiols were eluted using the following gradient: 10 min isocratic 10% B, 15 min linear gradient 18% B, 15 min linear gradient 27% B, 10 min linear gradient 50% B, 10 min linear gradient 100% B, after which the column was returned to 10% B in 5 min, an equilibrated for a further 10 min.

7.3.5. Spectrofluorometry

Log phase trophozoites (~10^7 cells/ml) were washed 2x in PBS and re-suspended in 1 ml PBS. A 100 μl volume of this cell suspension was then introduced into a glass cuvette containing 1.5 ml PBS and 0.4 ml Amplex Red (kit from Invitrogen) in order to monitor H_2O_2 production by the organism. Oxidation of GSH pools were examined by pre-incubating cells for 30 min with 50 μM monochlorobimane (MCB) and washing 3x with PBS. Changes in levels of reduced GSH were monitored indirectly via glutathione S-bimane, GSB, a fluorescent adduct formed after the reversible reaction between GSH and MCB (catalyzed by glutathione S-transferase, GST; Cortassa et al. 2004). MCB treated cells (100 μl) were inoculated into another cuvette containing 1.8 ml PBS. A spectrofluorometer (Photon Technology International) was used to record the following emission wavelengths from each cell suspension simultaneously, according to Aon et al. (2012), NAD(P)H autofluorescence (λ_{ex} 340 nm, λ_{em} 450 nm), oxidised flavin (FAD) autofluorescence (λ_{ex} 480 nm, λ_{em} 530 nm), cell path length (1 cm, 90° side scatter, λ_{ex} 520 nm, λ_{em} 585 nm), H_2O_2 emission (λ_{ex} 530 nm, λ_{em} 590 nm) and GSH (λ_{ex} 390 nm, λ_{em} 480 nm). Background readings were established for each cuvette before addition of cells. Changes in the emission of each probe within the organism was monitored over time after addition of 5 mM glutamate and malate as a metabolic substrate (as described in Chapter 6) and inhibitors; 50 μM MTZ, 50 μM AF, 1 mM AA, 1 mM DADS or 1 mM ajoene.

7.3.6. Enzyme assays

Approx. 2 x 10^7 cells were washed 2x in PBS (pH 7.2), re-suspended in 20 mM EDTA and 0.1% (v/v) Triton X-100 (0.5 ml final volume) and left to stand for 5-10 min

at room temperature. Insoluble material was then removed by centrifugation (4°C). Protein content of the resulting supernatant was quantified by Bradford assay (Bradford 1976), as outlined in Chapter 2, section 2.4, and the same protein extract used for subsequent enzyme assays. All assays were conducted at room temperature (21±1°C) with a minimum of 2 replicates per assay. A spectrophotometer (Jedway 6300) was employed to measure the change in absorbance over a 5 min period, with readings recorded at 30 s intervals, after addition of the *S. vortens* protein extract (approx. 1 mg/ml stock) or purified enzyme to the following reaction mixtures:

7.3.6.1.NADH oxidase activity (EC: 1.6.3.1): 50 mM potassium phosphate, 0.07 mM NADH, 0.1 mM FAD and 100 μl *S. vortens* crude protein extract in a total reaction volume of 1.5 ml. The decrease in NADH absorbance was recorded at 340 nm and converted into the concentration rate of change using a molar extinction coefficient of 6.22×10^3 M^{-1} cm^{-1} (Reusch & Burger 1974).

7.3.6.2.Superoxide dismutase (SOD, EC: 1.15.1.1) activity: *S. vortens* SOD activity was measured indirectly via the SOD determination kit (Sigma-Aldrich) using a colorimetric method. Briefly, WST-1 (2-(4-iodophenyl)-3-(4-nitrophenyl)-5-(2, 4-disulphophenyl)-2H-tetrazolium, monosodium salt) produced a formazan product upon reduction with a superoxide anion ($2O_2^{\cdot -}$). This rate of reduction is linearly related to xanthine oxidase activity and is inhibited by SOD. Hence, the 50% inhibition of SOD was determined by following the decrease in WST-1 formazan at 440 nm (molar extinction coefficient = 37 $\times 10^3$ M^{-1} cm^{-1}). A 20 μl volume of *S. vortens* protein extract (or purified enzyme, positive control) was added to the reaction mixture, resulting in a 240 μl reaction volume.

7.3.6.3.Catalase activity (EC: 1.11.1.6): 50 mM potassium phosphate and 3% (v/v) hydrogen peroxide. The presence of catalase was confirmed by the appearance of O_2 bubbles immediately after addition of the enzyme (10 U/ml) or *S. vortens* crude protein extract (100 μl; McLeod & Gordon 1923). The total volume of the reaction was 650 μl.

7.3.6.4.Peroxidase activity (EC: 1.11.1.7): 100 mM K-phosphate buffer (pH 6 using KOH), 0.5% (w/v) H_2O_2 and 5% (w/v) pyrogallol. The reaction was initiated with 100 μl *S. vortens* crude protein extract in a total reaction volume of 1.5 ml (Chance & Maehly 1955).

7.3.6.5. Calculation of enzymatic rates. Enzymatic rates were calculated according to Beer's Law:

$$\Delta A = e\ c\ l$$

Where, ΔA is the measured absorbance change (Δabsorbance/min), e is the molar extinction coefficient, l is the path length (1 cm) and c is the molar concentration (moles/L).

7.3.7. Statistical analysis

Statistical differences between treatment groups were assessed using T-tests in Minitab (Version 16) using normally distributed data with equal variance.

7.4. RESULTS

Consumption of O_2 differs between two *Spironucleus vortens* strains (ATCC and *Sv1*) and is completely inhibited by the garlic-derived compound, ajoene. The major cellular antioxidants of *S. vortens* are GSH and H_2S; SOD and NADH oxidase are the predominant protective enzymes. Intracellular GSH levels are significantly depleted by AF and the garlic-derived AA and DADS.

7.4.1. Oxygen consumption by *S. vortens*

Changes in rates of O_2 consumption by *S. vortens* ATCC and *Sv1* strains introduced into air-saturated PBS (290 µM O_2) in a closed reaction vessel are illustrated in Fig. 7.1. Both strains consumed O_2 at similar maximal rates (V_{max}) of 27.3 and 24.2 nmol/min/10^7 cells, respectively. Tolerance to O_2, however, was different between the two strains. The O_2 tensions at which O_2 consumption ceased ($[O_2]_{V=0}$) was significantly different between strains (T-test, t=5.46, p=0.005), with V=0 occurring at higher $[O_2]$ for the ATCC strain (19 µM O_2) than the *Sv1* strain (5 µM O_2). Likewise, the upper O_2 tension which led to inhibition of O_2 consumption by the organisms ($[O_2]_{V=i}$) was significantly different between strains (T-test, t = 3.97, p=0.017). O_2 consumption by the *Sv1* strain was inhibited at 174.8 µM O_2, whilst no inhibition of O_2 consumption by the ATCC strain was observed up to the highest O_2 tension recorded. Hence, for the ATCC strain, $[O_2]_{V=i}$ lies above 237.8 µM O_2 (Table 7.1). Of the inhibitors tested, the garlic-derived ajoene oil (1 mM) had the greatest effect on O_2 consumption by *S. vortens* (ATCC strain only tested), reducing this rate by 100% of the control (uninhibited) value.

DADS (1 mM) also reduced the rate of O_2 consumption by *S. vortens* to 63.4% of the control value (Fig. 7.2).

Table 7.1. O_2 consumption by *Spironucleus vortens* (ATCC and *Sv1* strains). The maximal rate of O_2 consumption by *S. vortens* (V_{max}) strains are given as well as the O_2 tensions at which the rate of O_2 consumption by *S. vortens* strains is equal to zero ($[O_2]_{V=0}$) and is inhibited ($[O_2]_{V=i}$) at high $[O_2]$, with $\pm$ standard deviation (SD) values (n=3). Values for which significant difference between the two *S. vortens* strains was observed is indicated with an asterisk (T-test, $p<0.05$).

Spironucleus vortens strain	V_{max} (nmol/ min/ 10^7 cells)	$[O_2]_{V=0}$ (µM)*	$[O_2]_{V=i}$ (µM)*
S. vortens ATCC	27.3 ±9.8	19.0 ±1.6	>237.8 ±26.5
S. vortens Sv-1	24.2 ±14.1	5.1 ±4.0	174.8 ±7.2
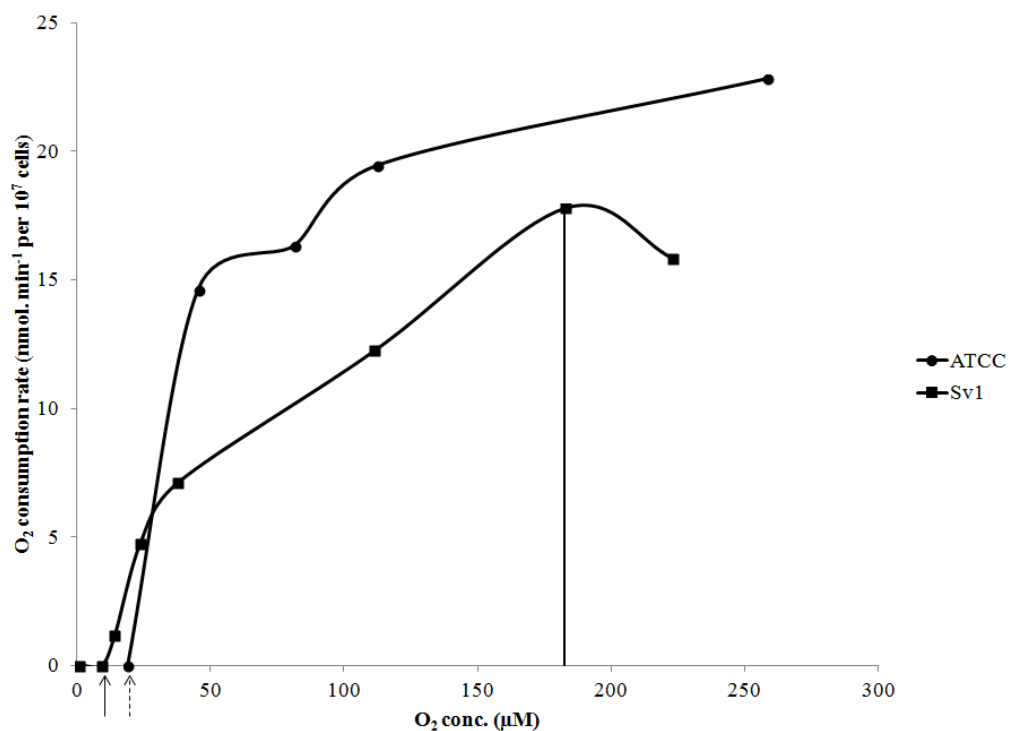
Fig. 7.1. Glucose (5 mM)-supported O_2 consumption rates by whole cell suspensions of *Spironucleus vortens* ATCC and *Sv1* strains in air-saturated PBS. The vertical line shows the upper O_2 tension at which the rate of O_2 consumption (V) by *S. vortens Sv1* is inhibited ($[O_2]_{V=i}$). The dotted and continuous arrows indicate the O_2 tensions at which V=0 ($[O_2]_{V=0}$) for *S. vortens* ATCC and *Sv1* strains, respectively. Rates are representative of 3 replicates for each strain.

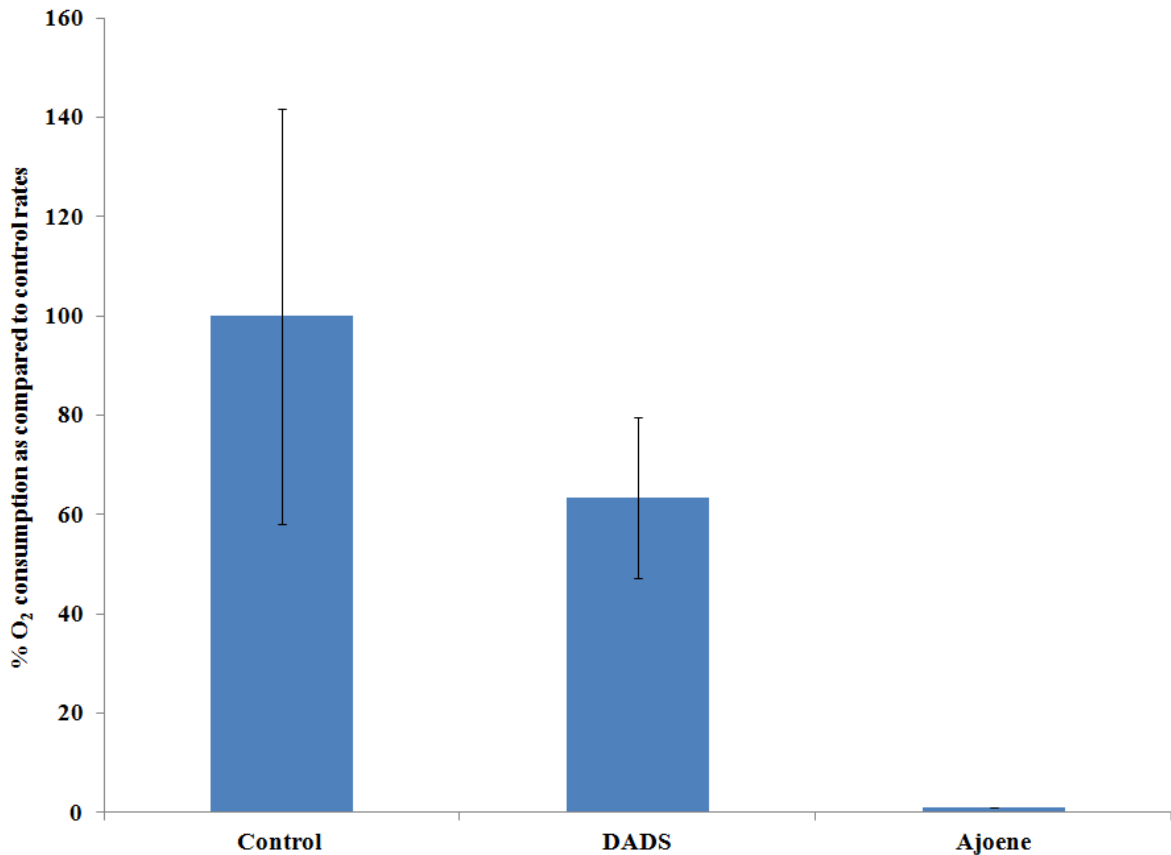**Fig. 7.2.** Percentage inhibition of O_2 consumption rate by *Spironucleus vortens* (ATCC strain) by diallyl disulphide (DADS, n=2) and ajoene oil (18%, n=2) as compared to the glucose (10 mM)-supported control O_2 consumption rate (n=4).

7.4.2. *S. vortens* non-protein thiol analysis

Reverse-phase HPLC analysis revealed that the major non-protein thiol of *S. vortens* was GSH (retention time = 40 min, Fig. 7.3a). *S. vortens* GSH content was calculated as 767 ($\pm$400 SD) nmol/10^7 cells. A small peak corresponding to H_2S was also identified on the *S. vortens* HPLC chromatogram (retention time = 54 min, Fig. 7.3a). The remaining peaks did not correspond to any of the other standards that were tested (i.e. methanethiol and propanethiol) and therefore remain unidentified. Unlike the positive control, *Crithidia* sp. (Fig. 7.3b), *S. vortens* did not incorporate [3H]-spermidine and growth was not inhibited by DFMO, hence *S. vortens* does not contain trypanothione. GSH production by *S. vortens* was significantly inhibited after 1 h incubation with AF, AA and DADS (T-test, t>2.77, p<0.05) to 23.8 ($\pm$14.33)%, 23.8 ($\pm$4.59)% and 39.7

($\pm$0.038)% of the control value, respectively (Fig. 7.4). MTZ and ajoene also reduced *S. vortens* GSH levels to 55.2 ($\pm$0.4)% and 39.2 ($\pm$26.4)% of the control value, respectively, however the degree of inhibition was not significantly different from the untreated control value (T-test, t<2.77, p>0.05).
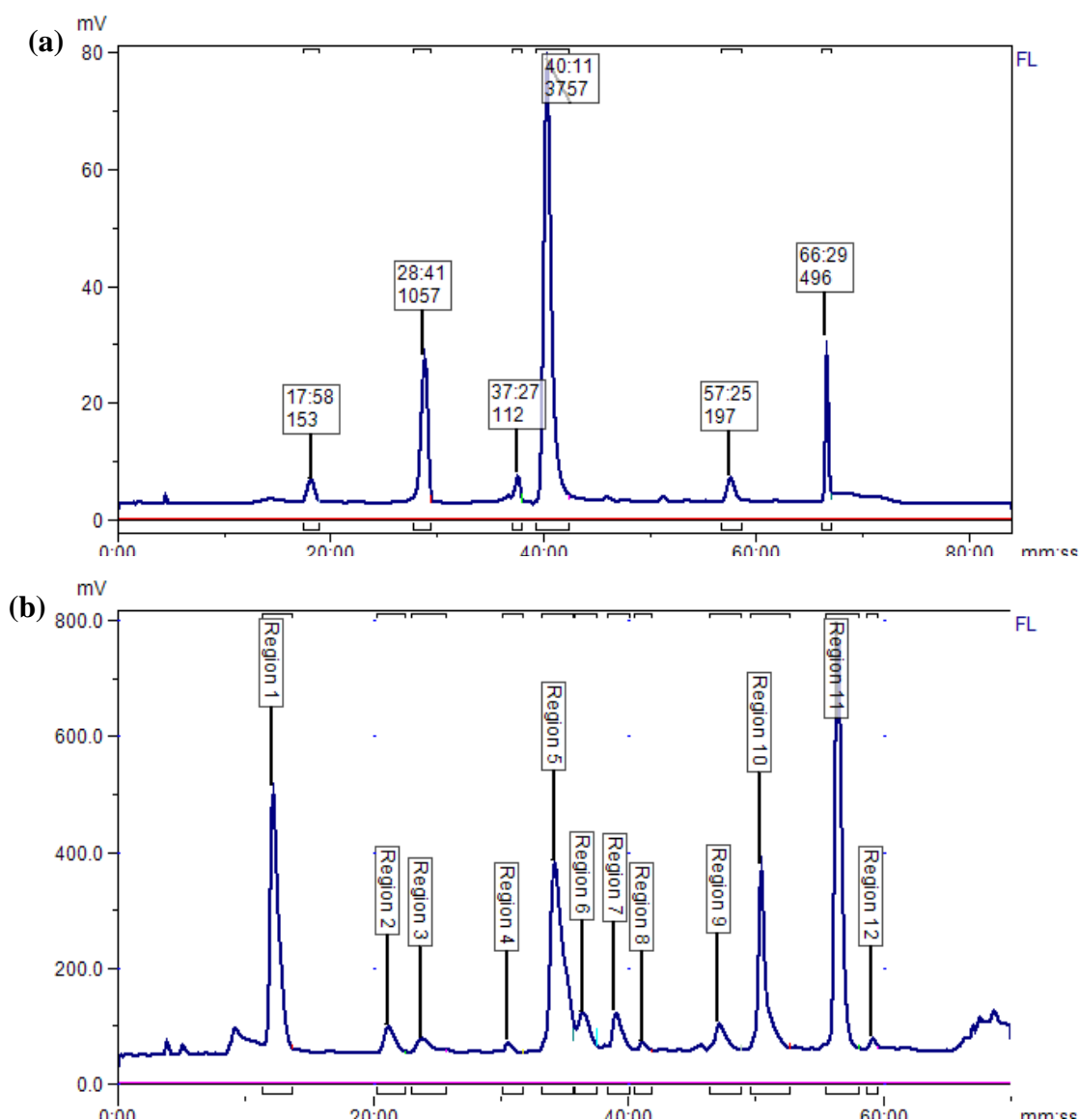
Fig. 7.3. Reverse-phase HPLC chromatograms of monobromobimane-derivatized non-protein thiols detected by fluorescence. Non-protein thiols of *Spironucleus vortens* ATCC strain (a). The major peak at 40 min and minor peak at 54 min correspond to glutathione (GSH) and H_2S, respectively. Non-protein thiols of *Crithidia* sp. (b). Region 3 (23.4 min) = GSH, region 10 (50.2 min) = glutathionylspermidine, region 11 (56.2 min) = trypanothione, region 9 (47.0 min) = H_2S. The remaining peaks in (a) and (b) are unidentified thiols.

7.4.3. Effects of inhibitors on *S. vortens* redox dynamics

Spectrofluorimetry was employed to investigate the immediate effects of inhibitors on the redox dynamics of *S. vortens*. Untreated cells produced H_2O_2 at a rate of 2.85 pmol/min/10^6 cells. MTZ led to immediate oxidation of the intracellular NAD(P)H pool (*ca.* -25%) and increase in H_2O_2 (*ca.* +31% of endogenous rates) released by the organism (Fig. 7.5a). AF decreased NAD(P)H and GSH levels (*ca.* -7% after 250 s, Fig. 7.5b). The only garlic-derived compound tested which had an immediate effect on the redox dynamics of *S. vortens* was DADS, causing an increase in H_2O_2 (*ca.* +125% of endogenous rates) production by the organism, coupled with slight oxidation of the NAD(P)H and GSH pools (*ca.* -2% after 250 s) and immediate contraction of cell size (increase in side scatter to 6%, Fig. 7.5c).

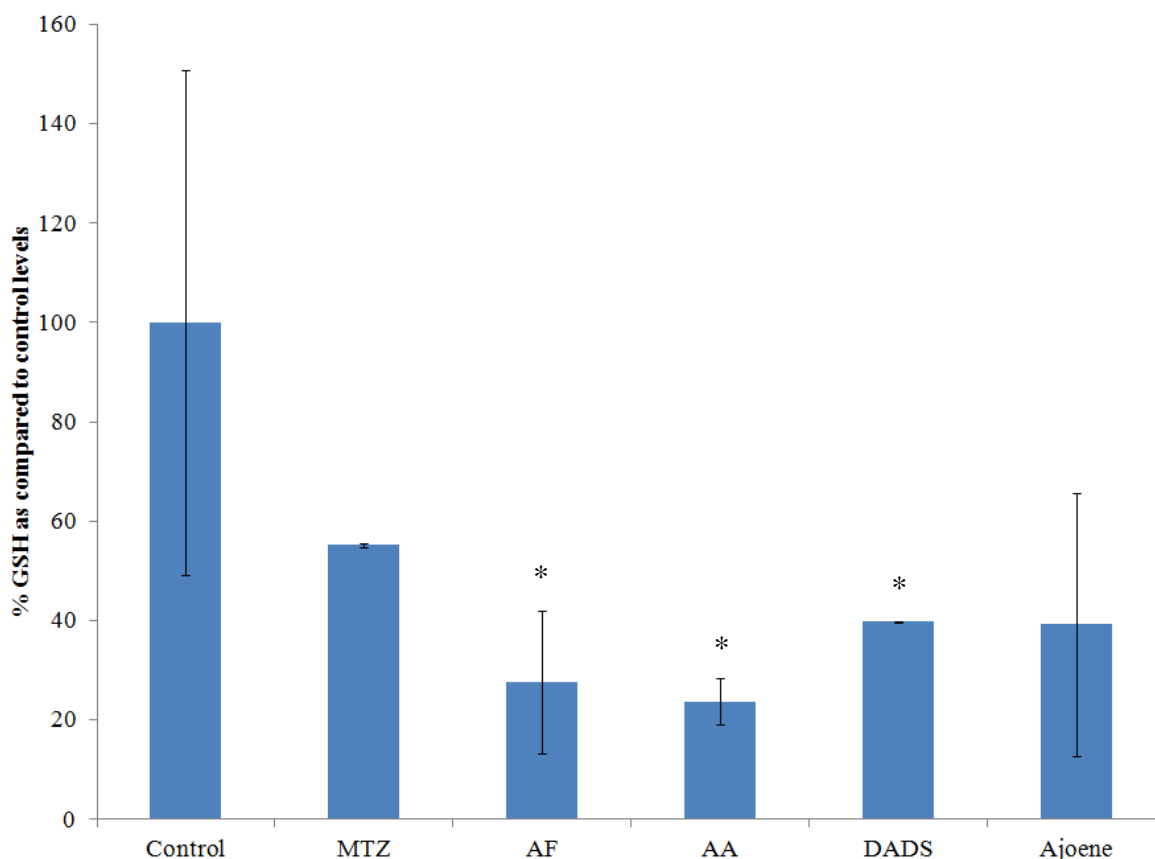**Fig.7.4.** Depletion of *S. vortens* glutathione (GSH) by 50 µM metronidazole (MTZ), 50 µM auranofin (AF), 1 mM allyl alcohol (AA), 1 mM diallyl disulphide (DADS) and 1 mM ajoene. Error bars show standard deviation of n=4 replicates for the control and n=2 replicates for the different treatments. Asterisks indicate significant reduction in GSH by AF, AA and DADS as compared to control levels (T-test, p<0.05).

7.4.4. Antioxidant enzymes of *S. vortens*

Both SOD and NADH oxidase activity were detected enzymatically in *S. vortens* cell-free extracts, at rates of 883 ($\pm$104) and 37.5 ($\pm$13) nmol/min/mg protein, respectively. No catalase or peroxidase activity was detected.

7.5. DISCUSSION

The aerotolerant nature of *Spironucleus vortens*, an "anaerobic" protozoan parasite, is reflected in its apparent high tolerance towards O_2. Consumption of O_2 by both the ATCC and *Sv1* strains was maximal at elevated O_2 tensions (*ca.* 150-250 μM O_2) and commenced at a rate of *ca.* 25 nmol/min/10^7 cells. This rate of O_2 consumption is comparable to that obtained previously for *S. vortens* by Millet et al. (2010; 62 nmol/min/10^7 cells). Interestingly, differences were observed between the $[O_2]_{V=0}$ and $[O_2]_{V=i}$ values of the ATCC and *Sv1* strains. The ATCC strain displayed elevated tolerance towards O_2, indicated by lack of inhibition to O_2 consumption at near air-saturated levels. Furthermore, the rate of detectable O_2 consumption reached zero at a higher O_2 tension for the ATCC strain than for the *Sv1* strain. These differences could be the result of prolonged *in vitro* cultivation of the ATCC strain (having been in culture for 22 years since 1991), resulting in decreased susceptibility to O_2. Loss of characteristic traits on prolonged laboratory culture has been documented previously, e.g. for *Leishmania* (see Moreira et al. 2012) and *Acanthamoeba* (see Köehsler et al. 2009) virulence. Long-term *in vitro* cultivation of *Acanthamoeba* results in reduced capacity for encystment (Köehsler et al. 2008), lowered peroxidase and protease activity (Mazur & Hadaś 1994) and increased susceptibility to drugs (Hughes et al. 2003).

Reproducible determination of K_m and K_t O_2 values for *S. vortens* have been hampered due to an apparent drift in O_2 consumption rates, which occurs during the open electrode experiments (CFW pers. obs.; Millet et al. 2009). Such experiments require cell suspensions to be stirred vigorously for prolonged periods (up to 4 h) with increasing O_2 tension. This undoubtedly leads to damage of cells and misleading K_m and K_t values. Based on the results presented here, it may be hypothesised that *S. vortens* is likely to have a higher threshold of inhibition by O_2 (K_t), and decreased affinity for O_2 (K_m) compared to other diplomonads, e.g. *Hexamita inflata* $K_m O_2 = 13$ μM, $K_t O_2 = 100$ μM; *Giardia intestinalis* $K_m O_2 = 6.4$ μM, $K_t O_2 = 80$ μM (Biagini et al. 1997).
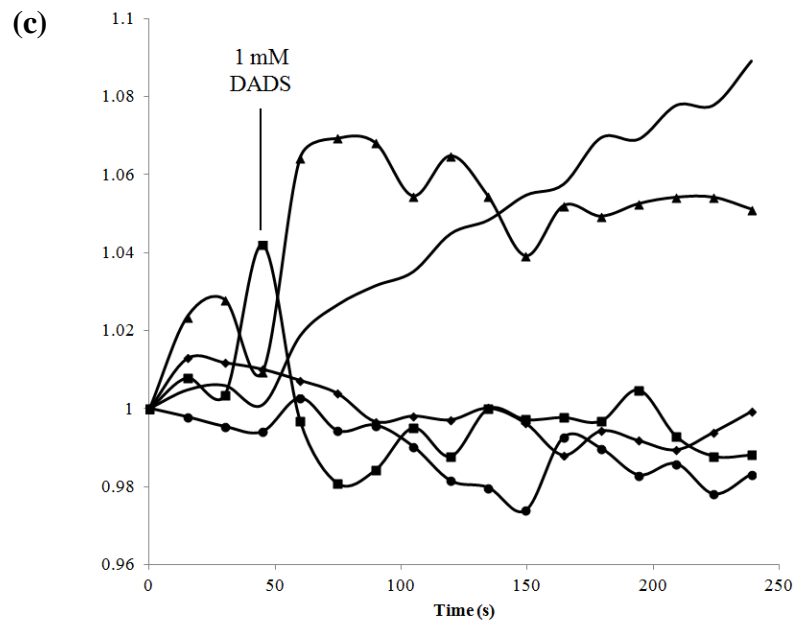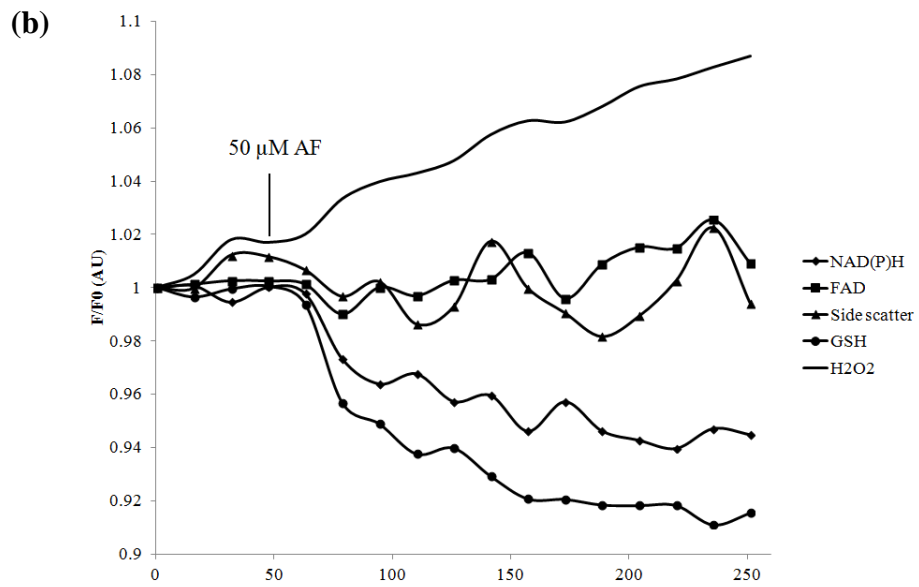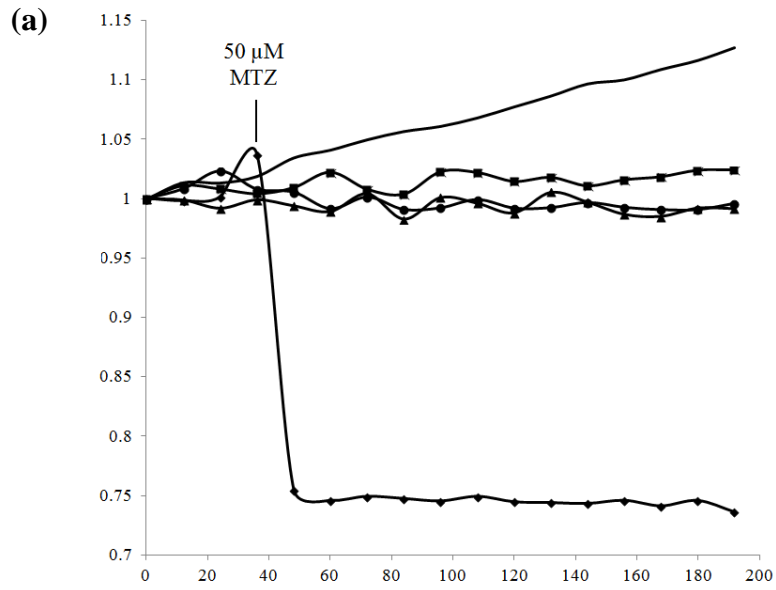
(a)

(b)

(c)

154

Fig. 7.5. The effect of (a) 50 µM metronidazole (MTZ), (b) 50 µM auranofin (AF) and (c) 1 mM diallyl disulphide (DADS) on the intracellular NAD(P)H, FAD, glutathione (GSH), H_2O_2 production and cell size (side scatter) of washed whole cell suspensions of *Spironucleus vortens* in PBS (n=2 per treatment).

The high tolerance of *S. vortens* towards O_2 can be explained by its surprisingly sophisticated antioxidant defence system. Glutathione (GSH) was found to be the major non-protein thiol of *S. vortens*. This is in contrast to other anaerobic/microaerophilic protozoan parasites, including *G. intestinalis* and *Trichomonas vaginalis*, which utilize cysteine, a low molecular weight thiol (Brown et al. 1993; Ellis et al. 1994). Hence, in terms of its non-protein thiols, *S. vortens* more closely resembles aerobic parasites, such as *Plasmodium* spp. and trypanosomes, which also utilize GSH (Arrick et al. 1981; Müller 2004). A small peak which corresponded to the retention time of H_2S was also observed in the HPLC chromatogram. This is consistent with the pungent H_2S smell which is present in 2-3 d old *S. vortens* cultures (CFW, pers. obs.). H_2S has been documented to play important roles in redox metabolism and cell signalling (Banerjee 2011); however a possible function in parasitic protozoa has not been characterized.

The diversity in utilization of different protein and non-protein thiols by protozoa is summarized in Table 7.2. Like *G. intestinalis* (see Brown et al. 1995, 1996a), *S. vortens* was also found to exhibit superoxide dismutase (SOD) and NADH oxidase activities, but lacked catalase and peroxidase. Hence, the mechanism by which *S. vortens* detoxifies H_2O_2 remains undetermined. It is likely to be mostly released from the cell, with extracellular H_2O_2 produced at a rate of 2.85 pmol/min/10^6 cells, which is comparable to that of *T. vaginalis* (33.5 pmol/min/mg protein, Chapman et al. 1999). A small proportion of the peroxide formed, however, is likely to be converted to the highly damaging hydroxyl radical, $OH^.$, via the Fenton reaction (Lloyd et al. 1997). At this point $OH^.$ may be detoxified by GSH resulting in its reduction to H_2O (Yadav & Mishra 2013). It has been documented that *S. barkhanus* also possesses a gene encoding peroxiredoxin (Coombs et al. 2004). Peroxiredoxins are an antioxidant family which, like peroxidases, decompose H_2O_2 to H_2O, using thioredoxin as a cofactor (see review by McGonigle et al. 1998; Stanley et al. 2011). In addition, a bacterial-derived gene encoding the iron protein, rubrerythrin, has been identified in *S. salmonicida* (see Andersson et al. 2007). The physiological role(s) of rubrerythrins have not yet been validated; however its function is again associated with peroxidase activity (Sztukowska et al. 2002).

Table 7.2. Documented intracellular antioxidants of *Spironucleus* (*Spi*), *Hexamita* (*Hex*), *Giardia* (*Gia*), *Trichomonas* (*Tri*), *Entamoeba* (*Ent*), *Trypanosomes* (*Try*) and *Plasmodium* (*Pla*). For specific species names, see reference list below.

Antioxidant	*Spi.*	*Hex.*	*Gia.*	*Tri.*	*Ent.*	*Try.*	*Pla.*
H₂S	+			+[13]	+[16]		
Cysteine	-	+[6]	+[8]	+[13]	+[17]		
Methanethiol	-			+[13]	+[16]		
Propanethiol	-			+[13]			
Glutathione	+	+[*7]	-[8]	-[13]	-[17]	+[24]	+[32]
Trypanothione	-				+[**18]	+[25]	-[32]
Thioredoxin	+[1]		+[9]	+[3]	+[19]	+[26]	+[32]
Flavodiiron protein	+[2]		+[2]	+[2]	+[2]		
NAD(P)H oxidase	+	+[7]	+[10]	+[14]	+[20]		
Superoxide dismutase	+	+[7]	-[11]	+[13]	+[17]	+[27]	+[33]
Catalase	-	-[7]	-[11]	-[13]	-[17]	-[28]	-[32]
Peroxidase	-	-[7]	-[11]	+[15]	+[21]	+[29]	+[32]
Peroxiredoxin	+[3]		+[3]	+[3]	+[22]	+[30]	+[34]
Glutaredoxin	-[4]		+[12]	-[12]	-[12]	+[31]	+[35]
Rubrerythrin†	+[5]			+[15]	+[23]		

[1]Williams et al. 2012; [2]Di Matteo et al. 2008; [3]Coombs et al. 2004; [4]Jelström-Hultqvist, 2012; [5]Andersson et al. 2007; [6]Biagini et al. 2001; [7]Biagini et al. 1997; [8]Brown et al. 1993; [9]Brown et al. 1996b; [10]Brown et al. 1996a; [11]Brown et al. 1995; [12]Rada et al. 2009; [13]Ellis et al. 1994; [14]Lindstead & Bradley, 1988; [15]Pütz et al. 2005; [16]Tokoro et al. 2003; [17]Fahey et al. 1984; [18]Ondarza et al. 1999; [19]Arias et al. 2007; [20]Bruchhaus et al. 1998; [21]Bruchhaus et al. 1997; [22]Choi et al. 2005; [23]Maralikova et al. 2010; [24]Arrick et al. 1981; [25]Fairlamb et al. 1985; [26]Reckenfelderbaumer et al. 2000; [27]Dufernez et al. 2006; [28]Baernstein, 1963; [29]Wilkinson et al. 2002; [30]Piacenza et al. 2008; [31]Comini et al. 2008; [32]Müller 2004; [33]Bécuwe et al. 1996; [34] Kawazu et al. 2008; [35]Rahlfs et al. 2001; *GSH reductase activity measured. **GSH derived from host/medium. †Function as an antioxidant not yet validated.

Interestingly, both peroxiredoxin and rubrerythrin localize to the hydrogenosomes of *T. vaginalis* (see Pütz et al. 2005). Hydrogenosomes are double-membraned mitochondrial-derived organelles (MDOs) which have undergone reductive evolution as a result of adaptation to parasitism (see review by Shiflett & Johnson 2010). They have lost cytochrome-mediated oxidative phosphorylation functions, but have retained some characteristics of mitochondria, e.g. ATP generation via substrate-level phosphorylation and iron-sulphur cluster assembly of proteins. These organelles also produce H_2 via an electron transport chain resulting from the donation of electrons from the bacterial-derived pyruvate:ferredoxin oxidoreductase (PFOR) to hydrogenase (see review by Shiflett & Johnson 2010). It has been proposed that in contrast to their diplomonad relatives, *Giardia* spp., *S. vortens* (see Millet et al. 2009) and *S. salmonicida* (see Jelström-Hultqvist 2012) also possess hydrogenosomes (Williams et al. in press). *Giardia* spp. contain further reduced MDOs called mitosomes (see review by Tachezy & Doležal 2011). The only known function of these organelles is Fe-S cluster assembly. One of the proteins present in the *Giardia* mitosome is glutaredoxin, an antioxidant enzyme which functions in a similar way to peroxiredoxins by converting H_2O_2 to H_2O, utilizing GSH as a cofactor (Rada et al. 2009). This contradicts previous studies (Brown et al. 1993) which claimed that *Giardia* does not contain GSH. However, it is likely that GSH is only present at low levels in *Giardia*, and hence be undetectable by HPLC (Rada et al. 2009). No MDO-targeted glutaredoxin genes have been found in the genome sequence of *S. salmonicida* (see Jelström-Hultqvist 2012). Hence, as in *T. vaginalis*, peroxiredoxins and rubrerythrins may play a role in detoxifying H_2O_2 in *S. vortens*, however their functionality and subcellular locations in this organism should be further investigated. Genes coding for another bacterial-derived antioxidant enzyme, a flavodiiron protein (FDI), have been documented in a number of anaerobic/microaerophilic protozoa, including *T. vaginalis*, *E. histolytica*, *G. intestinalis* and *S. barkhanus* (see DiMatteo et al. 2008). In *G. intestinalis* the FDI has high O_2 reductase activity (converting O_2 to H_2O), as well high affinity for O_2. Its primary purpose has been linked to O_2 scavenging, thus facilitating survival of the parasite in the microaerobic environment of the small intestine (*ca.* 60 μM O_2; DiMatteo et al. 2008). A hypothesized illustration of oxygen detoxification mechanisms in *S. vortens* is proposed in Figure 7.6.

As previously documented (Williams et al. 2012, Chapter 5), the inhibitors employed in the current study caused redox imbalance in *S. vortens*. The garlic-derived ajoene oil caused complete inhibition of O_2 scavenging by *S. vortens*, perhaps indicating

inhibition of the terminal O_2 reductase, FDI protein. Metronidazole (MTZ) gave immediate oxidation of the intracellular NAD(P)H pool of *S. vortens*. This is consistent with the previously documented mode of action of MTZ, whereby reductive activation of the MTZ pro-drug is facilitated by thioredoxin reductase (TrxR), which sources its reducing power from NADPH (Leitsch et al. 2007). NAD(P)H levels were also depleted as a result of auranofin (AF) and DADS treatment, albeit to a lesser extent than MTZ. This may be the result of the need for more reducing power within the cells to combat the oxidative stress caused by inhibition of TrxR (by AF: Aon et al. 2012) and depletion of non-protein thiols (by DADS: Williams et al. 2012). Indeed, DADS caused an immediate depletion of GSH which reached 40% of untreated levels after 1 h incubation. Similarly, MTZ and AF also caused depletion of GSH pools, significantly so in the case of AF after 1 h incubation. This is probably a consequence of the inhibition of the Trx antioxidant system, resulting in overwhelming reliance on the GSH system for detoxification of ROS. The GSH and Trx systems have been shown previously to work in concert in cardiomyocytes (Aon et al. 2012), hence it seems likely that a similar scenario is present in *S. vortens*. It is also known that treatment of *S. vortens* with MTZ, and especially DADS, resulted in an increase in H_2O_2 production by the organism, which implies inhibition of a peroxidase-like antioxidant, e.g. peroxiredoxin. A change in cellular morphology was observed as a result of this oxidative stress, with DADS-treated cells contracting in size.

In conclusion, the array of antioxidants documented here to be present within *S. vortens* explains the capacity of this anaerobe to thrive in environments of fluctuating O_2 tensions during its life cycle. Differences in susceptibility of the ATCC curated and freshly isolated *Sv1* strains to O_2 requires further biochemical elucidation, not least because this may reveal differences in strain pathogenicity. The assumed anaerobic nature of *S. vortens* should also be further investigated, with detectable O_2 consumption appearing to cease at microaerobic O_2 tensions. Like *G. intestinalis* (see Lloyd et al. 2000) and *T. vaginalis* (see Paget & Lloyd 1990), *S. vortens* may require low concentrations of O_2 for intra- and/or extra-cellular signalling processes. This, together with the fact that H_2 production in *S. vortens* has previously been documented to commence at 33 μM O_2 (Millet et al. 2010), hints at the potential microaerophilic nature of this parasite. Finally, it is important to further characterise the unusual bacterial-derived antioxidants previously documented to be encoded in the genomes of *Spironucleus* spp. For instance, rubrerythrin and FDI protein are suggested here to be

novel targets for chemotherapy by garlic-derived compounds. The current study provides further evidence that the mode of action of both garlic-derivatives and MTZ is based on disrupted intracellular redox balance, leading to oxidative stress in *S. vortens*, the result of which is lethal to the organism (Millet et al. 2011; Williams et al. 2012). Hence, maintaining intracellular redox balance is of paramount importance to the overall health of *S. vortens*, and provides novel chemotherapeutic targets, which require further investigation.
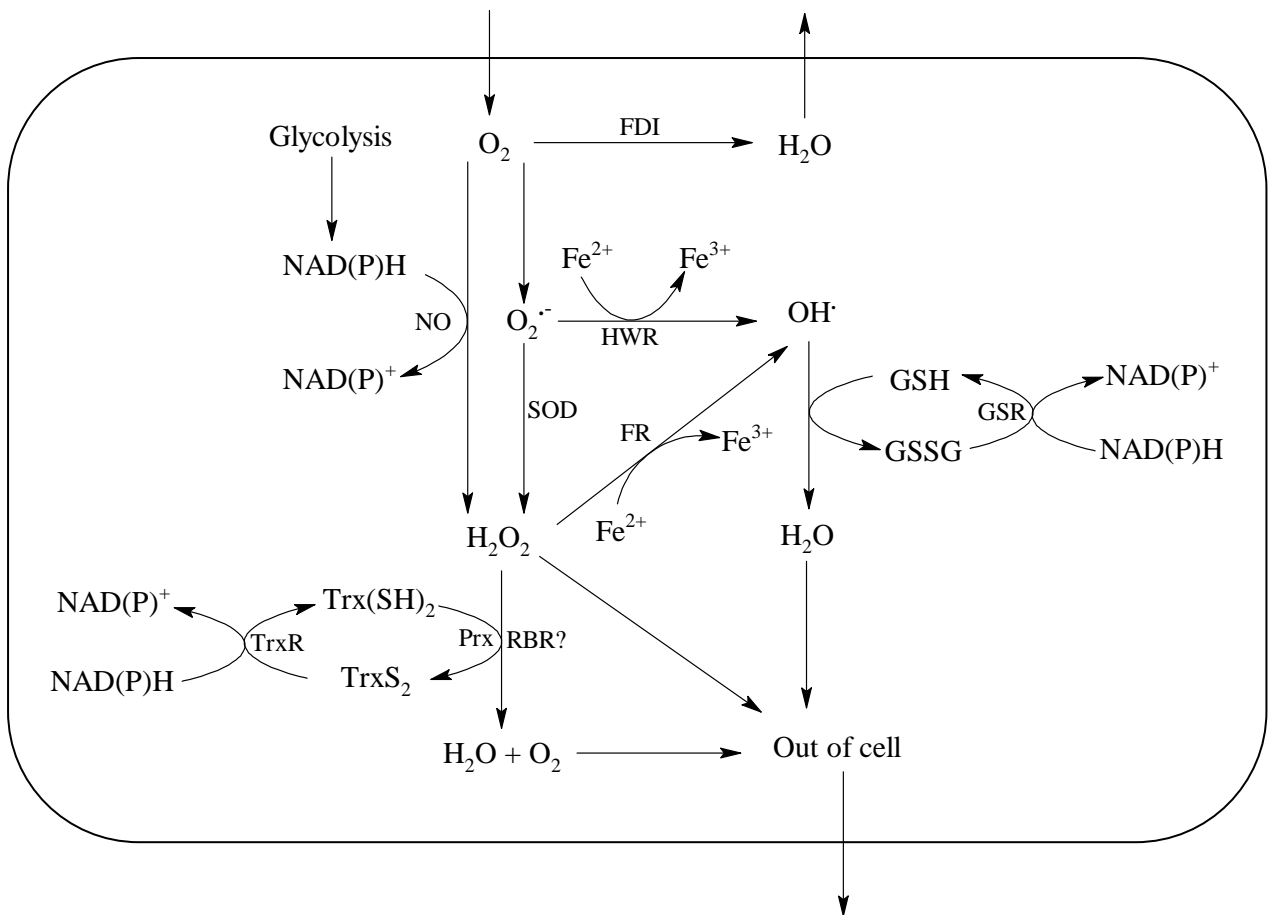

Fig. 7.6. Hypothesised antioxidant defence mechanisms of *Spironucleus vortens*, adapted from Biagini et al. (1997). FDI, flavodiiron protein; NO, NADH oxidase; SOD, superoxide dismutase; Trx(SH)$_2$, reduced thioredoxin; TrxS$_2$, oxidized thioredoxin; TrxR, thioredoxin reductase; Prx, peroxiredoxin; RBR, rubrerythrin (function undetermined); HWR, Haber-Weiss reaction; FR, Fenton reaction; GSH, reduced glutathione; GSSG, oxidized glutathione; GSR, glutathione reductase.

7.6. REFERENCES

Andersson JO, Sjögren ÅM, Horner DS, Murphy CA, Dyal PL, Svärd SG, Logsdon Jr JM, RaganMA, Hirt RP, Roger AJ (2007). A genomic survey of the fish parasite *Spironucleus salmonicida* indicates genomic plasticity among diplomonads and significant lateral gene transfer in eukaryote genome evolution. BMC Genomics 8: 51-76

Aon MA, Stanley BA, Sivakumaran V, Kembro JM, O'Rourke B, Paolocci N, Cortassa S (2012). Glutathione/thioredoxin systems modulate mitochondrial H_2O_2 emission: an experimental-computational study. JGP 139: 479-491

Arias DG, Gutierrez CE, Iglesias AA, Guerrero SA (2007). Thioredoxin-linked metabolism in *Entamoeba histolytica*. Free Radical Biol Med 42: 1496-1505

Arnér ES, Holmgren A (2000). Physiological functions of thioredoxin and thioredoxin reductase. Eur J Biochem 267: 6102-6109

Arrick BA, Griffith OW, Cerami A (1981). Inhibition of glutathione synthesis as a chemotherapeutic stratergy for trypanosomiasis. J Exp Med 153: 720-725

Arrick BA, Nathan CF (1984). Glutathione metabolism as a determinant of therapeutic efficacy: a review. Cancer Res 44: 4224-4232

Bacchi J, Lambros C, Goldberg B, Hutner SH, de Carvalho GD (1974). Susceptibility of an insect *Leptomonas* and *Crithidia fasciculata* to several established antitrypanosomatid agents. Antimicrob Agents Chemother 6:785-790

Banerjee B (2011). Hydrogen sulfide: redox metabolism and signaling. Redox Sign 15: 339-341

Bécuwe P, Gratepanche S, Fourmaux MN, van Beeumen J, Samyn B, Mercereau-Puijalon O, Touzel JP, Slomianny C, Camus D, Dive D (1996). Characterization of iron-dependent endogenous superoxide dismutase of *Plasmodium falciparum*. Mol Biochem Parasitol 76: 125-134

Biagini GA, Suller MTE, Finlay BJ, Lloyd D (1997). Oxygen uptake and antioxidant responses of the free-living diplomonad *Hexamita* sp. J Euk Microbiol 44: 447-453

Biagini GA, Park JH, Lloyd D, Edwards MR (2001). The antioxidant potential of pyruvate in the amitochondriate diplomonads *Giardia intestinalis* and *Hexamita inflata*. Microbiology 147: 3359-3365

Bradford MM (1976). A rapid and sensitive method for the quantification of microgram quantities of protein utilizing the principle of protein-dye binding. Anal Biochem 72: 248-254

Brown DM, Upcroft JA, Upcroft P (1993). Cysteine is the major low-molecular weight thiol in *Giardia duodenalis*. Mol Biochem Parasitol 61: 155-158

Brown DM, Upcroft JA, Upcroft P (1995). Free radical detoxification in *Giardia duodenalis*. Mol Biochem Parasitol 72: 47-56

Brown DM, Upcroft JA, Upcroft P (1996a). A H_2O-producing NADH oxidase from the protozoan parasite *Giardia duodenalis*. Eur J Biochem 241: 155-161

Brown DM, Upcroft JA, Upcroft P (1996b). A thioredoxin reductase-class of disulphide reductase in the protozoan parasite *Giardia duodenalis*. Mol Biochem Parasitol 83: 211-220

Bruchhaus I, Richter S, Tannich E (1997). Removal of hydrogen peroxide by the 29 kDa protein of *Entamoeba histolytica*. Biochem J 326: 785-789

Bruchhaus I, Richter S, Tannich E (1998). Recombinant expression and biochemical characterization of an NADPH flavin oxidoreductase from *Entamoeba histolytica*. Biochem J 330: 1217-1221

Chance B, Maehly AC (1955). Assay of catalase and peroxidises. In: Methods in Enzymology, II, pp 773-775

Choi M-H, Sajed D, Poole L, Hirata K, Herdman S, Toran BE, Reed SL (2005). An unusual surface peroxiredoxin protects invasive *Entamoeba histolytica* from oxidant attack. Mol Biochem Parasitol 143: 80-89

Chapman A, Linstead DJ, Lloyd D (1999). Hydrogen peroxide is a product of oxygen consumption by *Trichomonas vaginalis*. J Bioscience 24: 339-344

Circu ML, Aw TY (2010). Reactive oxygen species, cellular redox systems and apoptosis. Free Radic Biol Med 48: 749-762

Comini MA, Rettig J, Dirdjaja N, Hanschumann E-M, Berndt C, Krauth-Slegel RL (2008). Monothiol glutaredoxin-1 is an essential iron-sulphur protein in the mitochondrion of African trypanosomes. J Biol Chem 283: 27785-27798

Commission Regulation (EC) No. 613/98 (1998). Off J Eur Commun L82/14-17 [Cited 18 February 2013] URL: http://ec.europa.eu/health/files/mrl/regpdf/1998_03_18-0613_en.pdf

Coombs GH, Westrop GD, Suchan P, Puzova G, Hirt RP, Embley TM, Mottram JC, Müller S (2004). The amitochondriate eukaryote *Trichomonas vaginalis* contains a divergent thioredoxin-linked peroxiredoxin antioxidant system. J Biol Chem 279: 5249-5256

Cortassa S, Aon MA, Winslow RL, O'Rourke B (2004). A mitochondrial oscillator dependent on reactive oxygen species. Biophys J 87: 2060-2073

Di Matteo A, Scandurra FM, Testa F, Forte E, Sarti P, Brunori M, Giuffrè A (2008). The O_2-scavenging flavodiiron protein in the human parasite *Giardia intestinalis*. J Biol Chem 283: 4061-4068

Dufernez F, Yernaux C, Gerbod D, Noël C, Chauvenet M, Wintjens R, Edgcomb VP, Capron M, Opperdoes FR, Viscogliosi E (2006). The presence of four iron-containing

superoxide dismutase isozymes in trypanosomatidiae: characterization, subcellular localization, and phylogenetic origin in *Trypanosoma brucei*. Free Radic Biol Med 40: 210-225

Ellis JE, Yarlett N, Cole D, Humphreys MJ, Lloyd D (1994). Antioxidant defences in the microaerophilic protozoan parasite *Trichomonas vaginalis*: comparison of metronidazole-resistant and sensitive strains. Microbiology 140: 2489-2494

Fahey RC, Newton GL, Arrick B, Overdank-Bogart T, Aley SB (1984). *Entamoeba histolytica*: a eukaryote without glutathione metabolism. Science 224: 70-72

Fairlamb AH, Backburn P, Ulrich P, Chait BT, Cerami A (1985). Trypanothione: a novel bis(glutathionyl)spermidine cofactor for glutathione redictase in trypanosomatids. Science 227: 1485-1487

FARAD (2010). Restricted and prohibited drugs in food animals. USA Food and Drug Administration [online]. Updated 2 August 2012 [Cited 18 February 2013] URL: http://www.farad.org/eldu/prohibit.asp

Harris JC, Cottrell SL, Plummer S, Lloyd D (2001). Antimicrobial properties of *Allium sativum* (garlic). Appl Microbiol Biotechnol 57: 282-286

Horner DS, Hirt RP, Embley TM (1999). A single eubacterial origin of eukaryotic pyruvate:ferredoxin oxidoreductase genes: implications for the evolution of anaerobic eukaryotes. Mol Biol Evol 16: 1290-1291

Hughes R, Heaselgrave W, Kilvington S (2003). *Acanthamoeba polyphaga* strain age and method of cyst production influence the observed efficacy of therapeutic agents and contact lens disinfectants. Antimicrob Agents Chemother 47: 3080-3084

Jerlström-Hultqvist J (2012). Hidden diversity revealed. Genomic, transcriptomic and functional studies of diplomonads. Unpublished PhD Thesis, Uppsala University [Cited 26 February 2013] URL: http://uu.diva-portal.org/smash/get/diva2:562514/FULLTEXT01

Kawazu S-I, Komaki-Yasuda K, Oku H, Kano S (2008). Peroxiredoxins in malaria parasites: parasitologic aspects. Parasitol Int 57: 1-7

Köehsler M, Leitsch D, Füernkranz U, Duchêne M, Aspöeck H, Walochnik J (2008). *Acanthamoeba* strains lose their abilities to encyst synchronously upon prolonged axenic culture. Parasitol Res 102: 1069-1072

Köehsler M, Leitsch D, Duchêne M, Nagl M, Walochnik J (2009). *Acanthamoeba castellanii*: growth on human cell layers reactivates attenuated properties after prolonged axenic culture. FEMS Microbiol Lett 299: 121-127

Koledin T, Newton GL, Fahey RC (2002). Identification of the mycothiol synthase gene (*mshD*) encoding acetyltransferase producing mycothiol in actinomycetes. Arch Microbiol 178: 331-337

Leitsch D, Kolarich D, Wilson IB, Altmann F, Duchêne M (2007). Nitroimidazole action in *Entamoeba histolytica*: a central role for thioredoxin reductase. PLoS Biol 5: e211

Linstead DJ, Bradley S (1988). The purification and properties of two soluble reduced nicotinamide: acceptor oxidoreductases from *Trichomonas vaginalis*. Mol Biochem Parasitol 27: 125-134

Lloyd RV, Hanna PM, Mason RP (1997). The origin of the hydroxyl radical oxygen in the Fenton reaction. Free Radic Biol Med 22: 885-888

Lloyd D, Harris JC, Maroulis S, Biagini GA, Wadley RB, Turner MP, Edwards MR (2000). The microaerophilic flagellate *Giardia intestinalis*: oxygen and its reaction products collapse membrane potential and cause cytotoxicity. Microbiology 146: 3109-3118

Lloyd D, Cortassa S, O'Rourke B, Aon MA (2012). What yeast and cardiomyocytes share: ultradian oscillatory redox mechanisms of cellular coherence and survival. Integr Biol 4: 65-74

Maralikova B, Ali V, Nakada-Tsukui K, Nozaki T, van der Giezen M, Henze K, Tovar J (2010). Bacterial-type oxygen detoxification and iron-sulfur cluster assembly in amoebal relict mitochondria. Cell Microbiol 12: 331-342

Mazur T, Hadaś E (1994). The effect of the passages of *Acanthamoeba* strains through mice tissue on their virulence and its biochemical markers. Parasitol Res 80: 431-434

McGonigle S, Dalton JP, James ER (1998). Peroxiredoxins: a new antioxidant family. Parasitol Today 14:139-145

McLeod JW, Gordon J (1923). Catalase production and sensitiveness to hydrogen peroxide amongst bacteria: with a scheme for classification based on these properties. J Pathol Bacteriol 26: 326-331

Millet COM (2009). Growth, metabolism, ultrastructure and chemotherapy of *Spironucleus vortens*. Unpublished PhD Thesis, Cardiff University

Millet COM, Cable J, Lloyd D (2010). The diplomonad fish parasite *Spironucleus vortens* produces hydrogen. J Euk Microbiol 57: 400-404

Millet CO, Lloyd D, Williams C, Williams D, Evans G, Saunders RA, Cable J (2011). Effect of garlic and *Allium*-derived products on the growth and metabolism of *Spironucleus vortens*. Exp Parasitol 127: 490-499

Moreira D, Santarem N, Loureiro I, Tavares J, Silva AM, Amorim AM, Ouaissi A, Cordeiro-da-Silva A, Silvestre R (2012). Impact of continuous axenic cultivation in *Leishmania infantum* virulence. PLoS Negl Trop Dis 6: e1469

Müller S, Liebau E, Walter RD, Krauth-Siegel RL (2003). Thiol-based redox metabolism of protozoan parasites. Trends Parasitol 19: 320-328

Müller S (2004). Redox and antioxidant systems of the malaria parasite *Plasmodium falciparum.* Mol Microbiol 53: 1291-1305

Ondarza RN, Iturbe A, Hurtado G, Tamayo E, Ondarza M, Hernandez E (1999). *Entamoeba histolytica:* a eukaryote with trypanothione metabolism instead of glutathione metabolism. Biotechnol Appl Biochem 30: 47-52

Paget TA, Lloyd D (1990). *Trichomonas vaginalis* requires traces of oxygen and high concentrations of carbon dioxide for optimal growth. Mol Biochem Parasitol 41: 65-72

Paull GC, Matthews RA (2001). *Spironucleus vortens*, a possible cause of hole-in-the-head disease in cichlids. Dis Aquat Org 45: 197-202

Piacenza L, Peluffo G, Alvarez MN, Kelly JM, Wilkinson SR, Radi R (2008). Peroxiredoxins play a major role in protecting *Trypanosoma cruzi* against macrophage- and endogenously-derived peroxynitrite. Biochem J 410: 359-368

Pütz S, Gelius-Dietrich G, Piotrowski M, Henze K (2005). Rubrerythrin and peroxiredoxin: two novel putative peroxidases in the hydrogenosomes of the microaerophilic protozoon *Trichomonas vaginalis*. Mol Biochem Parasitol 42: 212-223

Rada P, Šmíd O, Sutak R, Doležal P, Pyrih J, Žárský V, Montagne J-J, Hrdý I, Camadro J-M, Tachezy J (2009). The monothiol single-domain glutaredoxin is conserved in the highly reduced mitochondria of *Giardia intestinalis*. Eukaryot Cell 8: 1584-1591

Rahlfs S, Fischer M, Becker K (2001). *Plasmodium falciparum* possesses a classical glutaredoxin and a second, glutaredoxin-like protein with a PICOT homology. J Biol Chem 276: 37133-37140

Reckenfelderbäumer N, Lüdemann H, Schmidt H, Steverding D, Krauth-Siegel RL (2000). Identification and functional characterization of thioredoxin from *Trypanosoma brucei brucei*. J Biol Chem 275: 7547-7552

Reusch, V.M., Burger, M.M. (1974). Distribution of marker enzymes between mesosomal and protoplast membranes. J Biol Chem 249, 5337-5345

Shiflett A, Johnson PJ (2010). Mitochondrion-related organelles in parasitic eukaryotes. Annu Rev Microbiol 64: 409-429

Stukowska M, Bugno M, Potempa J, Travis J, Kurtz Jr DM (2002). Role of rubrerythrin in the oxidative stress response of *Porphyromonas gingivalis*. Mol Microbiol 44: 479-488

Stanley BA, Sivakumaran V, Shi S, McDonald I, Lloyd D, Watson WH, Aon MA, Paolocci N (2011). Thioredoxin reductase-2 is essential for keeping low levels of H_2O_2 emission from isolated heart mitochondria. J Biol Chem 23: 33669-33677

Tachezy J, Doležal P (2011). The *Giardia* mitosomes. In: Luján HD, Svärd S (eds.), *Giardia* a model organism. Springer, Vienna, Austria, pp 185-200

Tokoro M, Asai T, Kobayashi S, Takeuchi T, Nozaki T (2003). Identification and characetization of two isoenzymes of methionine γ-lyase from *Entamoeba histolytica*. J Biol Chem 278: 42717-42727

Trachootham D, Lu W, Ogasawara MA, Valle NR-D, Huang P (2008). Redox regulation of cell survival. Antioxid Redox Sign 10: 1343-1374

Wilkinson SR, Meyer DJ, Taylor MC, Bromley EV, Miles MA, Kelly JM (2002). The *Trypanosoma cruzi* enzyme TcGPXI is a glycosomal peroxidase and can be linked to trypanothione reduction by glutathione or tryparedoxin. J Biol Chem 277: 17062-17071

Williams CF, Lloyd D, Poynton SL, Jorgensen A, Millet COM, Cable J (2011). *Spironucleus* species: economically important fish pathogens and enigmatic single-celled eukaryotes. J Aquac Res Development S2-002

Williams CF, Lloyd D, Kolarich D, Alagesan K, Duchene D, Cable J, Williams D, Leitsch D (2012). Disrupted intracellular redox balance of the diplomonad fish parasite *Spironucleus vortens* by 5-nitroimidazoles and garlic-derived compounds. Vet Parasitol 190: 62-73

Williams CF, Millet COM, Hayes AJ, Cable J, Lloyd D (in press). Diversity in mitochondria-derived organelles of the parasitic diplomonads *Spironucleus* and *Giardia*. Trends Parasitol DOI: 10.1016/j.pt.2013.04.004

Yadav A, Mishra PC (2013). Modeling the activity of glutathione as a hydroxyl radical scavenger considering its neutral non-zwitterionic form. J Mol Model 19: 767-777

Chapter 8

General discussion

CHAPTER 8: GENERAL DISCUSSION

This study has improved our understanding of the biology of *Spironucleus vortens* in relation to its lifecycle, biochemistry and chemotherapy. The fact that no *S. vortens* cysts were observed *in vitro* or *in vivo* along with the prolonged survival of *S. vortens* trophozoites in angelfish faeces, suggests that transmission of this parasite is facilitated by a trophozoite rather than a cyst stage (Chapter 3). Of course, this does not completely rule out the possibility of an encysted *S. vortens* stage, which may be required for survival in water following fragmentation of the faecal matter. Indeed, faecal matter is likely to confer physical protection to trophozoites, being densely populated with microbial fauna which contribute to O_2 scavenging and maintenance of an anaerobic-microaerobic environment (Piedecausa et al. 2012). Faecal matter also provides a rich supply of growth factors as well as major carbon and nitrogen sources (carbohydrates and amino acids). These latter biomolecules are further demonstrated here to be carbon and energy-yielding substrates for *S. vortens* (Chapter 6). Collectively, this information may be applied directly to fish farms to more efficiently control *S. vortens* outbreaks. The rarity, or perhaps complete absence, of an encysted stage in *S. vortens* implies that basic prevention methods, such as the use of disinfectants and an efficient filtration system to remove faecal debris from aquaria, should greatly reduce the incidence of parasite transmission.

During its life cycle, *S. vortens* is likely to experience fluctuations in both O_2 tensions and nutrient availability. Previously Millet et al. (2011a) commented on the high proteolytic capacity of *S. vortens* as well as the ability of this parasite to utilize amino acid substrates as well as carbohydrates. Monosaccharides, including glucose, and free amino acids are likely to be plentiful in the intestinal tract, however, during a systemic infection the parasite may have to rely heavily on its proteolytic activity in order to obtain its energy-yielding amino acid substrates. One such substrate was demonstrated here to be glutamate, which produces potential energy in the form of NAD(P)H in *S. vortens* (Chapter 6). Glucose is also a major substrate of this organism. The energy generated from its putative fermentative pathways, documented here, is likely to contribute to O_2 consumption and detoxification. Glutamate is also directly involved in the antioxidant defences of *S. vortens*, being a major component of glutathione, the major non-protein thiol of this organism. It was also observed that *S. vortens* can grow in the absence of

supplemental glucose; hence under periods of glucose-deficiency, the organism is able to depend on amino acid substrates, such as glutamate, alone.

O_2 levels in the intestinal tract, the primary habitat of *S. vortens*, range from 33-66 µM (JM Whittamore and RW Wilson pers. com.). During a systemic infection, however, *S. vortens* trophozoites have been recovered from open head lesions of infected fish (Paull & Matthews 2001), an environment which is likely to approach air-saturated levels (290 µM O_2). O_2 scavenging by a recently isolated strain of *S. vortens* (*Sv1*) is inhibited at concentrations in excess of 170 µM O_2, whereas that of the ATCC strain remains active at air-saturated levels, thus exhibiting a high degree of tolerance for O_2 (Chapter 7). Differences in the susceptibility of the new *Sv1* and ATCC strains to metronidazole were also observed (Chapter 4). Metronidazole-resistant *Giardia intestinalis* strains have been observed to have decreased affinity for O_2, which results in elevated intracellular O_2 tensions (Ellis et al. 1992). As a result, futile cycling of metronidazole ensues, whereby the metronidazole nitroradical metabolites are re-oxidized to the inactive parent compound (Lloyd & Pedersen 1985). A similar scenario may also be present in the new *Sv1* isolate which is less susceptible than the ATCC strain to metronidazole, as observed during this study. Although the *Sv1* isolate is more susceptible to O_2 at elevated tensions, the rates of O_2 consumption by this strain are generally lower as compared to the ATCC strain as O_2 tensions decrease from air saturated levels. This hints towards the possibility of there being differences in intracellular O_2 tensions between the two strains, however, this claim requires further investigation.

The high tolerance of *S. vortens* towards O_2 is reflected in its unusually sophisticated antioxidant defence system, whereby glutathione is the major non-protein thiol (Chapter 7). Microaerophilic protozoa, such as *Giardia* and *Trichomonas*, usually utilize cysteine as their major non-protein antioxidant. Hence, *S. vortens* more closely resembles aerobic protists such as *Plasmodium* and trypanosomes. The glutathione and thioredoxin antioxidant systems of *S. vortens* are shown here to be paramount for normal cellular function and viability. Disruption of intracellular redox balance by depletion of glutathione (Chapter 7) and inhibition of thioredoxin reductase (TrxR) by metronidazole and garlic-derivatives leads to oxidative stress (Chapter 5). This in turn results in irreversible damage to the cell, leading to changes in cellular morphology, growth inhibition, reduced motility and eventually cell death. Hence, maintaining a healthy redox balance is vital in *S. vortens*, and its disruption can lead to disastrous consequences.

Oxygen is also likely to play a key role in the antimicrobial activity of garlic-derived compounds. The eventual fate of garlic-derivatives is to be oxidized to inert forms. The different experiments employed in Chapters 5, 6 and 7 were conducted under different O_2 tensions. Ajoene was found to be the most effective of the garlic compounds tested against *S. vortens*. This may be because ajoene is already partially oxidized, and thus would be slower to react with air than a compound which possesses no S-O bonds (e.g. diallyl disulphide). This is directly related to the mode of action of garlic derivatives, whereby most of the chemistry involves a reaction between a protein cysteine sulphur and an un-oxidized sulphur of the garlic compound, thereby forming a new S-S bond (Block 2010). For example, in the case of the reaction between glutathione (GSH) and ajoene (A-S-(O)-S-A[1]):

$$GSH + A\text{-}S\text{-}(O)\text{-}S\text{-}A^1 \longrightarrow GS\text{-}S\text{-}A^1 + A\text{-}SOH$$
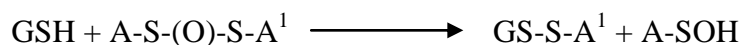
Hence, these mechanisms go some way to explain the depletion of intracellular thiols and inhibition of other antioxidant enzymes which possess a disulphide at their active site, including TrxR (Arnér & Holmgren 2000; Jacob et al. 2006).

Due to restrictions on the use of metronidazole on fish farms, garlic-derived compounds are shown here to be viable alternatives in the treatment and/or prevention of *Spironucleus* in fish. In particular, ajoene is a possible candidate to replace metronidazole in the treatment of Spironucleosis by incorporation into fish feed as a nutritional supplement as demonstrated in Chapter 4. Indeed, garlic extracts are already incorporated into some fish feeds, at a concentration of 1-2% (Millet et al. 2011b). The concentration of active garlic compounds, such as allicin, parent compound of ajoene, was undetectable in these commercially available preparations (Freeman & Kodera 1995). Hence, the antimicrobial efficacy of current commercially available garlic-supplemented fish food is questionable. Addition of ajoene to fish feed at an equivalent concentration would exert significantly greater antiparasitic activity and have an extended nutritional and antimicrobial shelf life, as compared to allicin, due to its increased stability (Naznin et al. 2008). Indeed, global fish feed demands reached 3.45 million tonnes in 2010, with a revenue of 1,331 million Euros (Huntington 2004); therefore an ajoene-supplemented fish food product with demonstrated antimicrobial efficacy is likely to be of great commercial interest. This would be favoured over a combination of ajoene and metronidazole, demonstrated in Chapter 4 to have synergistic activity, due to restrictions on the

administration of metronidazole to food fish (Commission Regulation No. 613/98 1998; FARAD 2010); hence any supplement containing metronidazole would be limited to ornamental fish alone. Further work should be conducted to assess the inhibitory effect of ajoene against other *Spironucleus* spp., such as *S. salmonicida*, which causes significant mortalities in salmon and trout (Williams et al. 2011), and also *S. meleagridis*, which is the major disease affecting farm-reared game birds (Cooper et al. 2004). If effective, administration of ajoene could be extended to supplement other animal feed, thus increasing its commercial potential. Future work should also focus on the potential application of ajoene as a complementary therapy in a clinical setting to treat cases of metronidazole-resistant parasites such as *Giardia* and *Trichomonas*. Garlic extracts have already proved promising for eliminating these pathogens *in vitro* with a commercial preparation of diallyl trisulphide (Dasuansu) also being administered as a herbal remedy to treat trichomoniasis in infected individuals (see review by Harris et al. 2001).

Unfortunately, the maximum concentration of ajoene which could be orally administered to angelfish during this study was 0.5% (v/w), which was not by itself enough to significantly reduce *S. vortens* infection in angelfish (Chapter 4). A higher concentration of this ajoene oil was not palatable to the fish. This may be because of the presence of polysulphides and vinyl dithiins, found to be contaminants in the ajoene oil, which are likely to produce a pungent flavour. Future work should focus on formulating a more pure ajoene extract to enhance the palatability of the oral treatment. The robust non-invasive model developed during this study for estimation of intestinal colonization by *S. vortens* (Chapter 3) is ideally suited for determining the efficacy of other chemotherapeutics.

The success of *S. vortens* as a parasite is reflected in its sophisticated antioxidant defence mechanisms and versatile metabolism which facilitates its survival during extra-intestinal systemic infection and transmission to a new host. Biological insights into the mechanism of action of new and existing chemotherapeutics against *S. vortens* highlights the importance of cellular redox balance in *S. vortens* provides a key route of parasite chemotherapy. Identification of other non-protein thiols present in *S. vortens* may reveal other novel antioxidants and thereby chemotherapeutic avenues. Completion of the genome sequence of *S. vortens* will allow further bioinformatic investigation into these novel targets for chemotherapy and provide greater insights into the biology of this pathogen.

REFERENCES

Arnér ES, Holmgren A (2000). Physiological functions of thioredoxin and thioredoxin reductase. Eur J Biochem 267: 6102-6109

Block E (2010). Garlic and other Alliums the lore and the science. The Royal Society of Chemistry, Cambridge, UK, pp 193-195

Commission Regulation (EC) No. 613/98 (1998). Off J Eur Commun L82/14-17 [Cited 18 February 2013] URL: http://ec.europa.eu/health/files/mrl/regpdf/1998_03_18-0613_en.pdf

Cooper GL, Charlton BR, Bickford AA, Nordhausen R (2004). *Hexamita meleagridis (Spironucleus meleagridis)* infection in chukar partridges associated with high mortality and intracellular trophozoites. Avian Dis 3: 706-710

Ellis JE, Wingfield JM, Cole D, Boreham PFL, Lloyd D (1992). Oxygen affinities of metronidazole-resistant and -sensitive stocks of *Giardia intestinalis.* Int J Parasitol 23: 35-39

FARAD (2010). Restricted and prohibited drugs in food animals. USA Food and Drug Administration [online]. Updated 2 August 2012 [Cited 18 February 2013] URL: http://www.farad.org/eldu/prohibit.asp

Freeman F, Kodera Y (1995). Garlic chemistry: stability of S-(2-propenyl) 2-propene-1-sulfinothioate (allicin) in blood, solvents and simulated physiological fluids. J Agric Food Chem 43: 2332-2338

Harris JC, Cottrell S, Plummer S, Lloyd D (2001). Antimicrobial properties of *Allium sativum* (garlic). Appl Micorbiol Biotechnol 57: 282-286

Huntington TC (2004). Feeding the fish: sustainable fish feed and Scottish aquaculture. Report to the Joint Marine Programme (Scottish Wildlife Trust and WWF Scotland) and RSPB Scotland. [Cited 19 March 2013]
URL: http://www.wwf.org.uk/filelibrary/pdf/feedingthefish.pdf

Jacob C, Knight I, Winyard PG (2006). Aspects of the biological redox chemistry of cysteine: from simple redox responses to sophisticated signaling pathways. Biol Chem 387: 1385-1397

Lloyd D, Pedersen J (1985). Metronidazole radical anion generation *in vivo* in *Trichomonas vaginalis*. J Gen Mic 131: 87-92

Millet COM, Lloyd D, Coogan MP, Rumsey J, Cable J (2011a). Carbohydrate and amino acid metabolism of *Spironucleus vortens*. Exp Parasitol 129: 17-26

Millet CO, Lloyd D, Williams C, Williams D, Evans G, Saunders RA, Cable J (2011b). Effect of garlic and *Allium*-derived products on the growth and metabolism of *Spironucleus vortens*. Exp Parasitol 127: 490-499

Naznin MT, Akagawa M, Okukawa K, Maeda T, Morita N (2008). Characterization of E- and Z-ajoene obtained from different varieties of garlics. Food Chem 106: 1113-1119

Paull GC, Matthews RA (2001). *Spironucleus vortens*, a possible cause of hole-in-the-head disease in cichlids. Dis Aquat Org 45: 197-202

Piedecausa MA, Aguado-Giménez F, Valverde JC, Llorente MDH, García- García B (2012). Influence of fish food and faecal pellets on short-term oxygen uptake, ammonium flux and acid volatile sulphide accumulation in sediments impacted by fish farming and non-impacted sediments. Aquacult Res 43: 66-74

APPENDIX

APPENDIX I

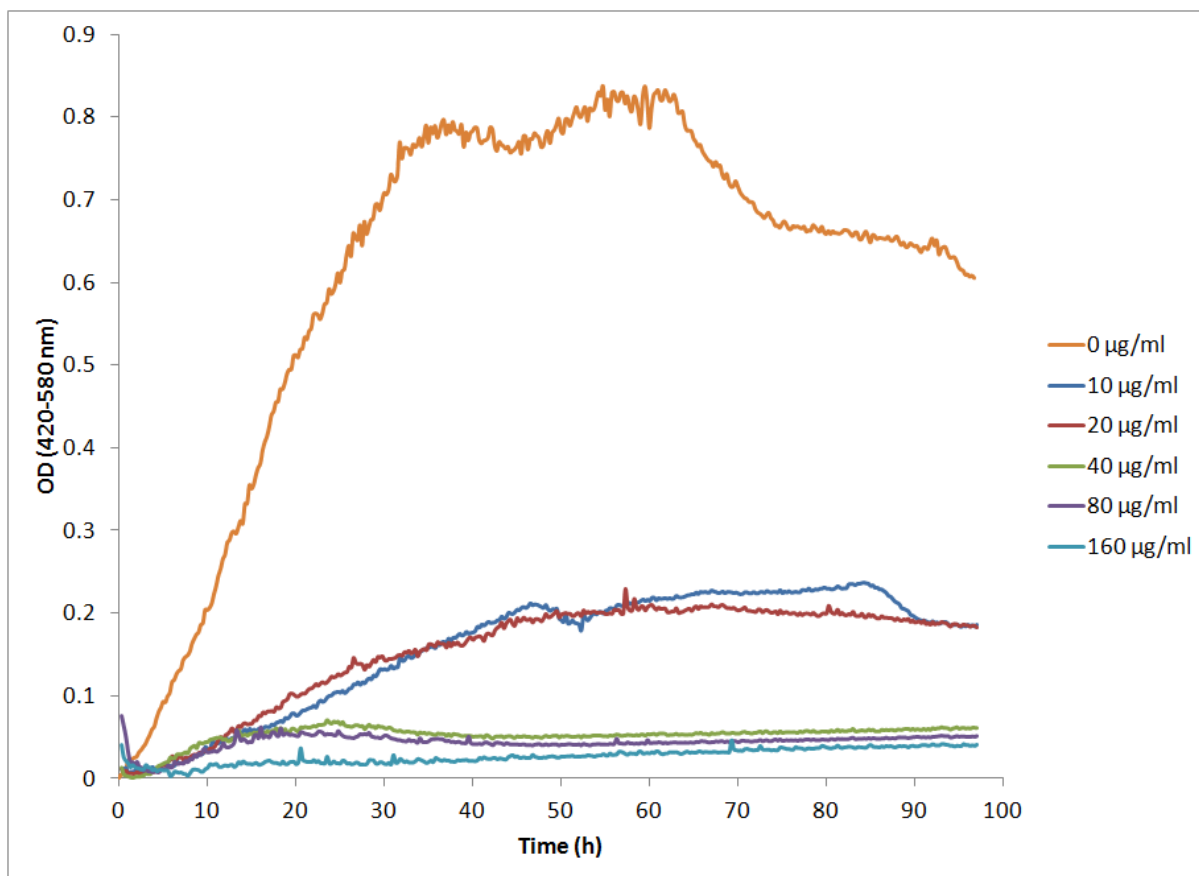*Spironucleus vortens* (ATCC strain) growth curves (raw data from Chapter 4).
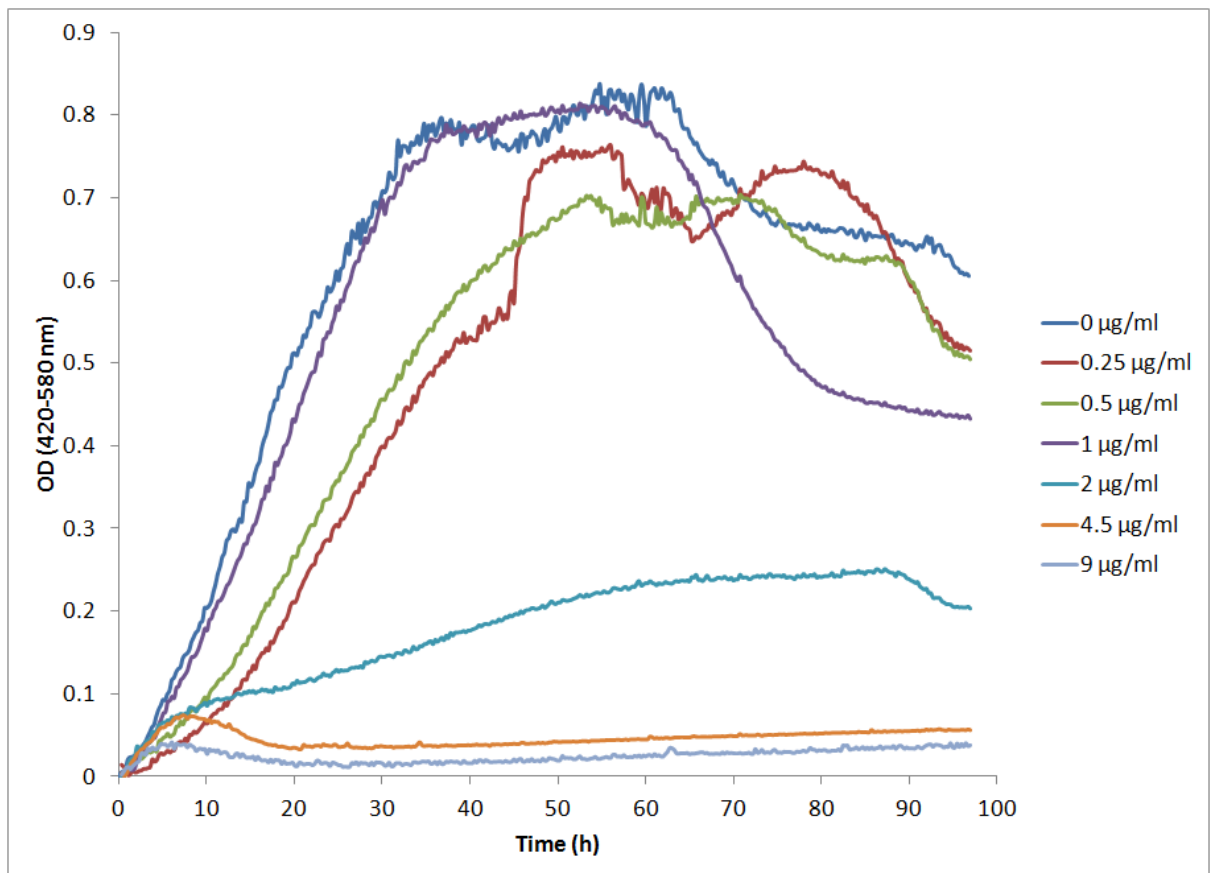
Fig. I. Inhibition of *Spironucleus vortens* (ATCC strain) growth with various concentrations of metronidazole (0-9 µg/ml) by automated optical cell density monitoring (420-580 nm, Bioscreen C Reader). Final yields were extrapolated at 72 h for 0 µg/ml (DMSO control) and at 55 h for all metronidazole concentrations, in order to calculate minimum inhibitory concentrations (see Chapter 4).

Fig. II. Inhibition of *Spironucleus vortens* (ATCC strain) growth with various concentrations of ajoene (0-640 µg/ml) by automated optical cell density monitoring (420-580 nm, Bioscreen C Reader). Final yields were extrapolated at 72 h for 0 µg/ml (DMSO control) and at 84 h for all ajoene concentrations, in order to calculate minimum inhibitory concentrations (see Chapter 4).
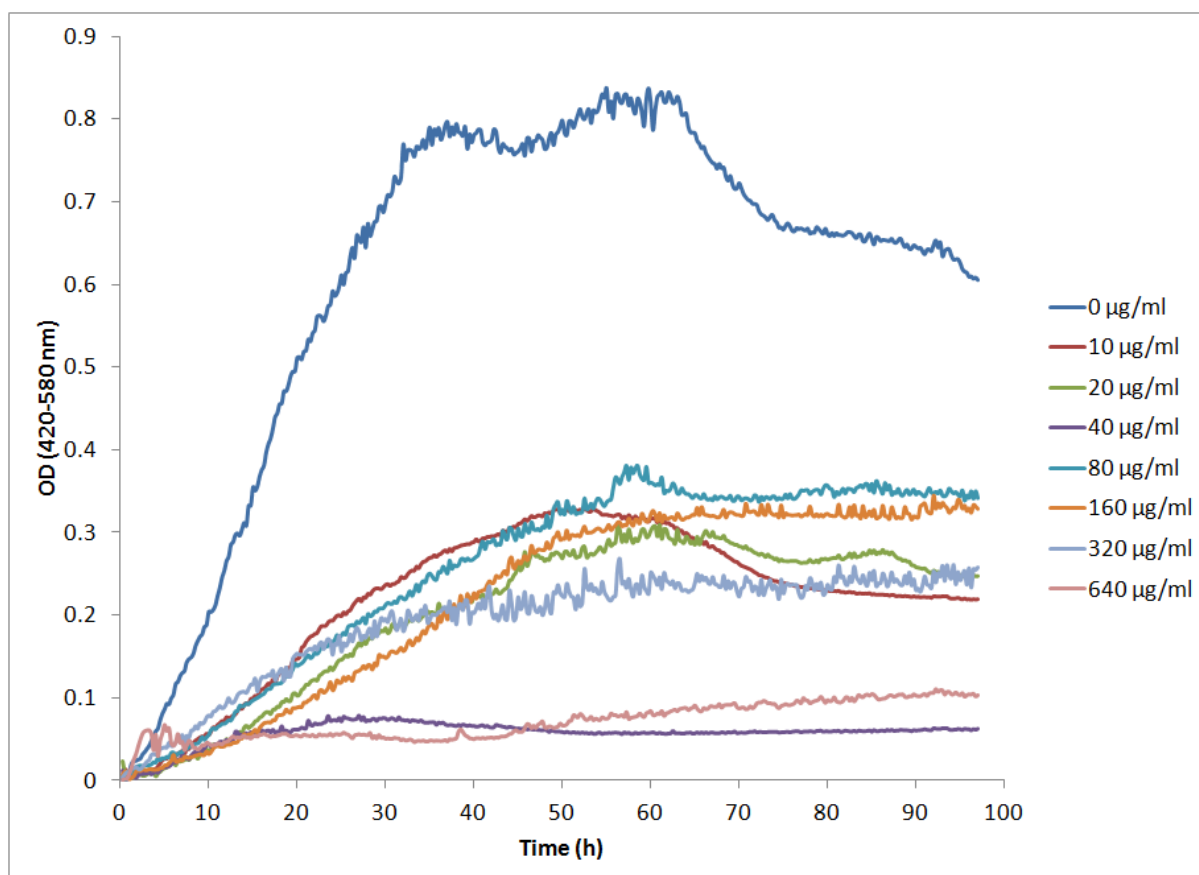
Fig. III. Inhibition of *Spironucleus vortens* (ATCC strain) growth with various concentrations of diallyl disulphide (DADS, 0-640 µg/ml) by automated optical cell density monitoring (420-580 nm, Bioscreen C Reader). Final yields were extrapolated at 72 h for 0 µg/ml (DMSO control) and at 58 h for all DADS concentrations, in order to calculate minimum inhibitory concentrations (see Chapter 4).
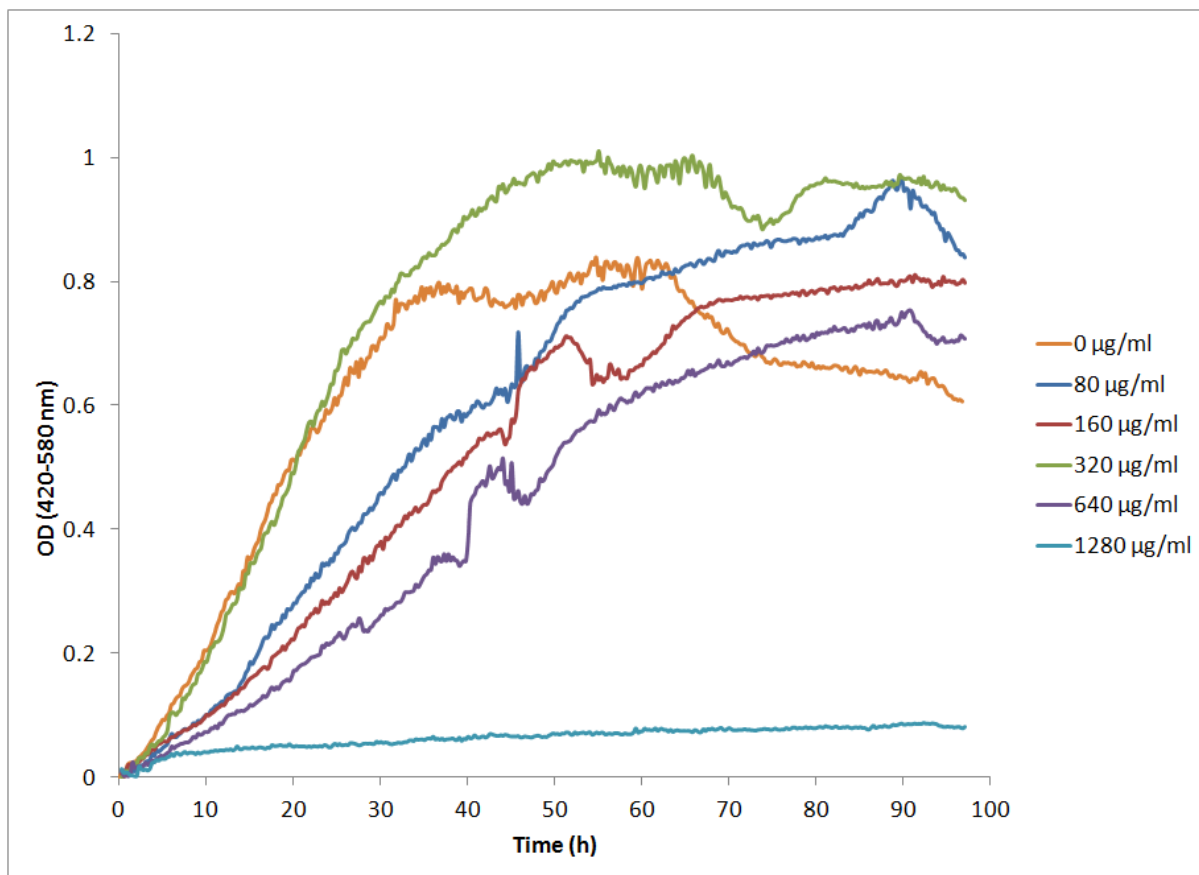
Fig. IV. Inhibition of *Spironucleus vortens* (ATCC strain) growth with various concentrations of allicin (0-640 µg/ml) by automated optical cell density monitoring (420-580 nm, Bioscreen C Reader). Final yields were extrapolated at 72 h for 0 µg/ml (DMSO control), 55 h for 320 µg/ml allicin and 90 h for all other allicin concentrations, in order to calculate minimum inhibitory concentrations (see Chapter 4).
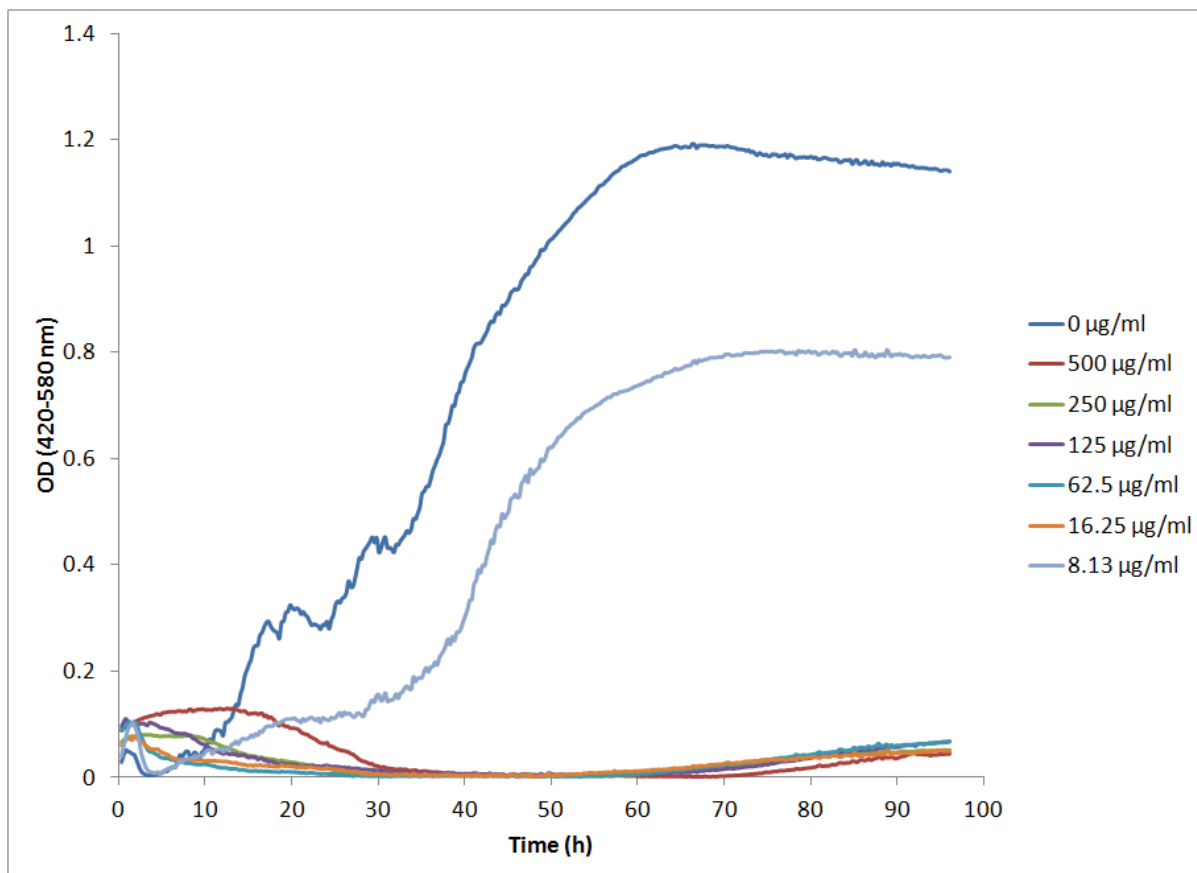
Fig. V. Inhibition of *Spironucleus vortens* (ATCC strain) growth with various concentrations of Z-ajoene (0-640 µg/ml) by automated optical cell density monitoring (420-580 nm, Bioscreen C Reader). Final yields were extrapolated at 64 h for 0 µg/ml (DMSO control) and 94 h for all Z-ajoene concentrations, in order to calculate minimum inhibitory concentrations (see Chapter 4).
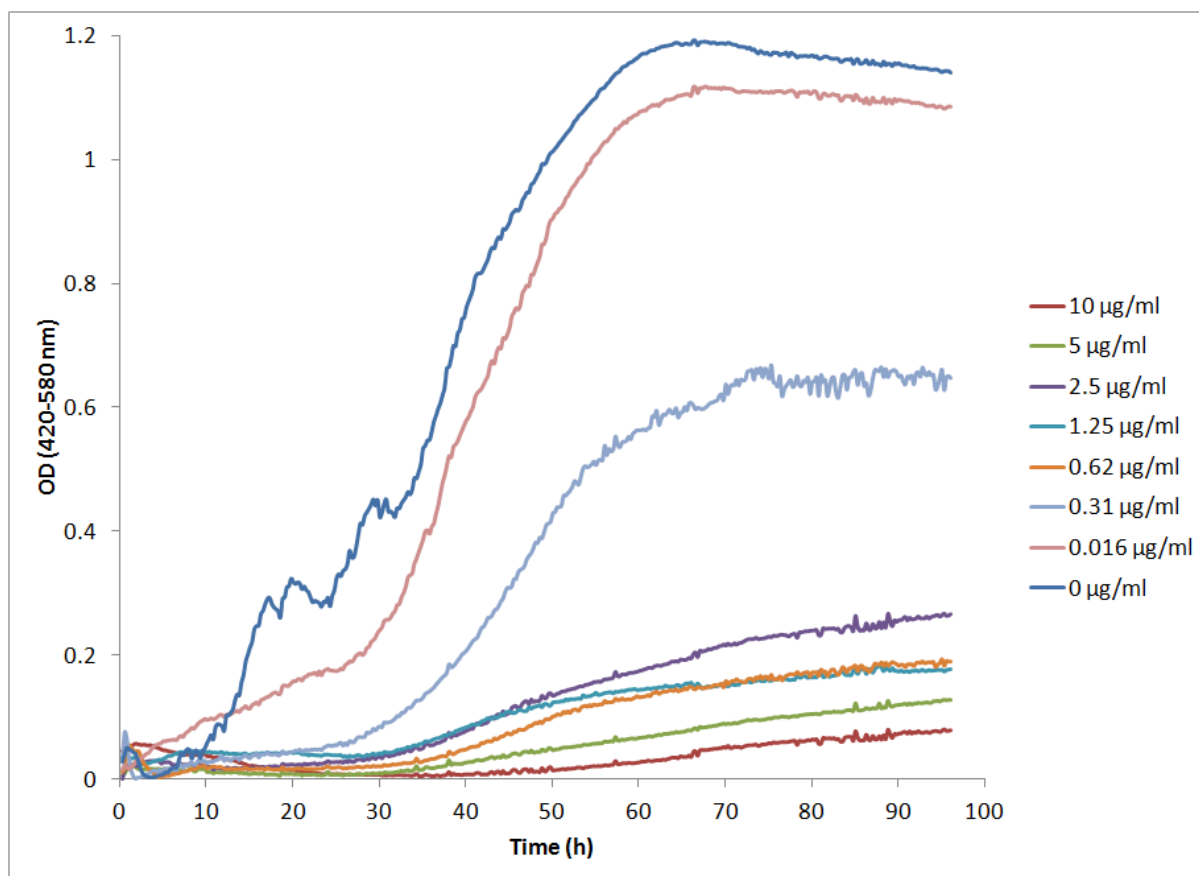
Fig. VI. Inhibition of *Spironucleus vortens* (ATCC strain) growth with various concentrations of allyl alcohol (AA, 0-640 µg/ml) by automated optical cell density monitoring (420-580 nm, Bioscreen C Reader). Final yields were extrapolated at 64 h for 0 µg/ml (DMSO control) and 94 h for all AA concentrations, in order to calculate minimum inhibitory concentrations (see Chapter 4).
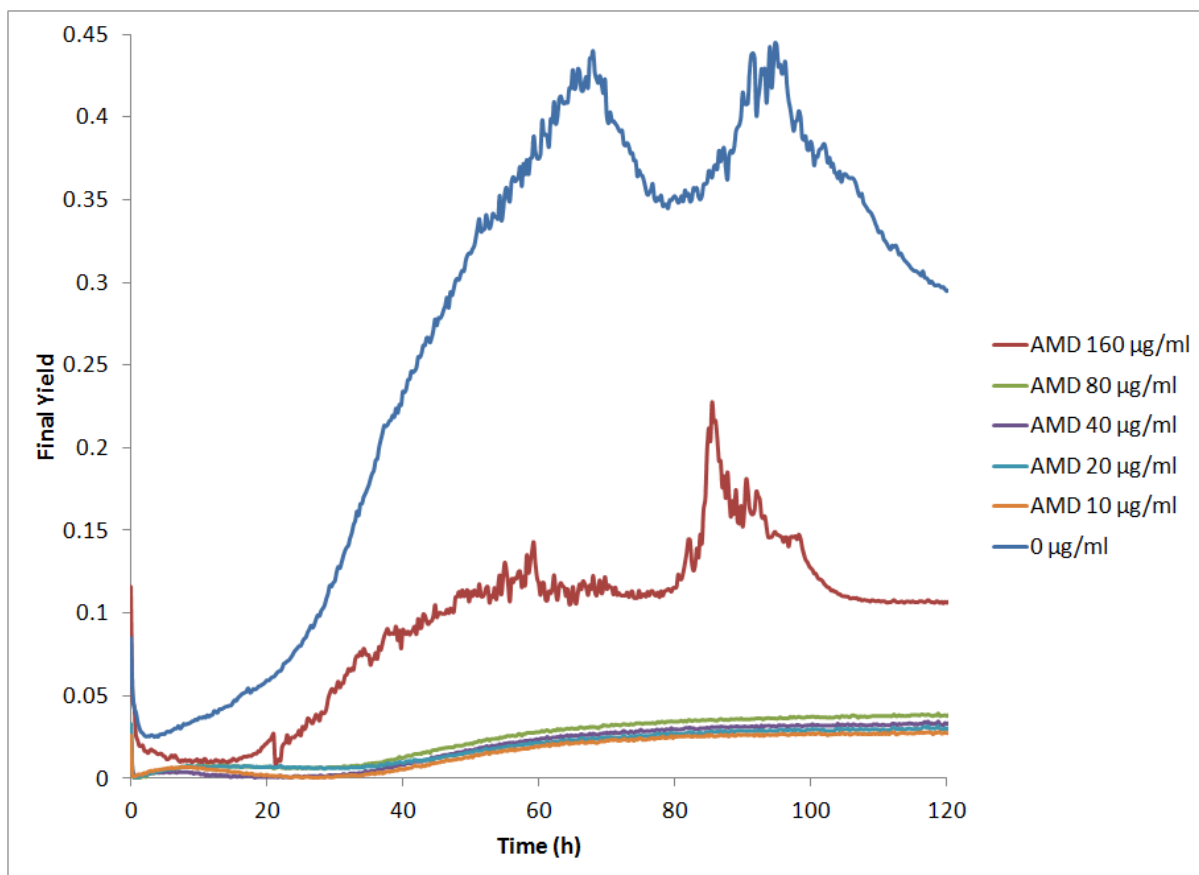
Fig. VII. Inhibition of *Spironucleus vortens* (ATCC strain) growth with various concentrations allyl methyl disulphide (AMD, 0-640 µg/ml) by automated optical cell density monitoring (420-580 nm, Bioscreen C Reader). Final yields were extrapolated at 68 h for 0 (DMSO control) and 160 µ/ ml AMD and 100 h for all other AMD concentrations, in order to calculate minimum inhibitory concentrations (see Chapter 4).
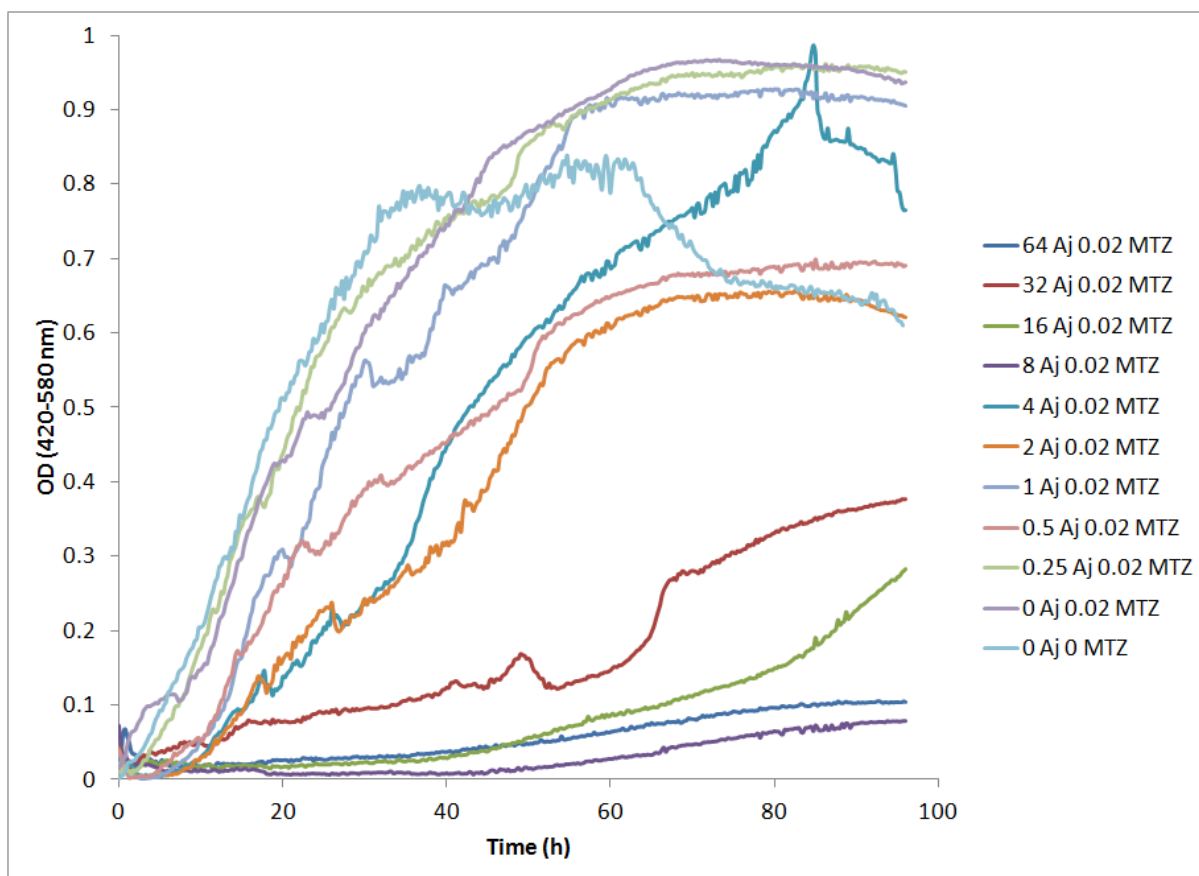
Fig. VIII. Inhibition of *Spironucleus vortens* (ATCC strain) growth with various combinations of ajoene (Aj, 0-64 µg/ml) and 0.02 µg/ml metronidazole (MTZ) by automated optical cell density monitoring (420-580 nm, Bioscreen C Reader). Final yields were extrapolated at 72 h for 0 µg/ml (DMSO control) and 82 h for all inhibitor concentrations, in order to calculate minimum inhibitory concentrations (see Chapter 4).

Fig. IX. Inhibition of *Spironucleus vortens* (ATCC strain) growth with various combinations of ajoene (Aj, 0-64 µg/ml) and 1 µg/ml metronidazole (MTZ) by automated optical cell density monitoring (420-580 nm, Bioscreen C Reader). Final yields were extrapolated at 72 h for 0 µg/ml (DMSO control) and 82 h for all inhibitor concentrations, in order to calculate minimum inhibitory concentrations (see Chapter 4).
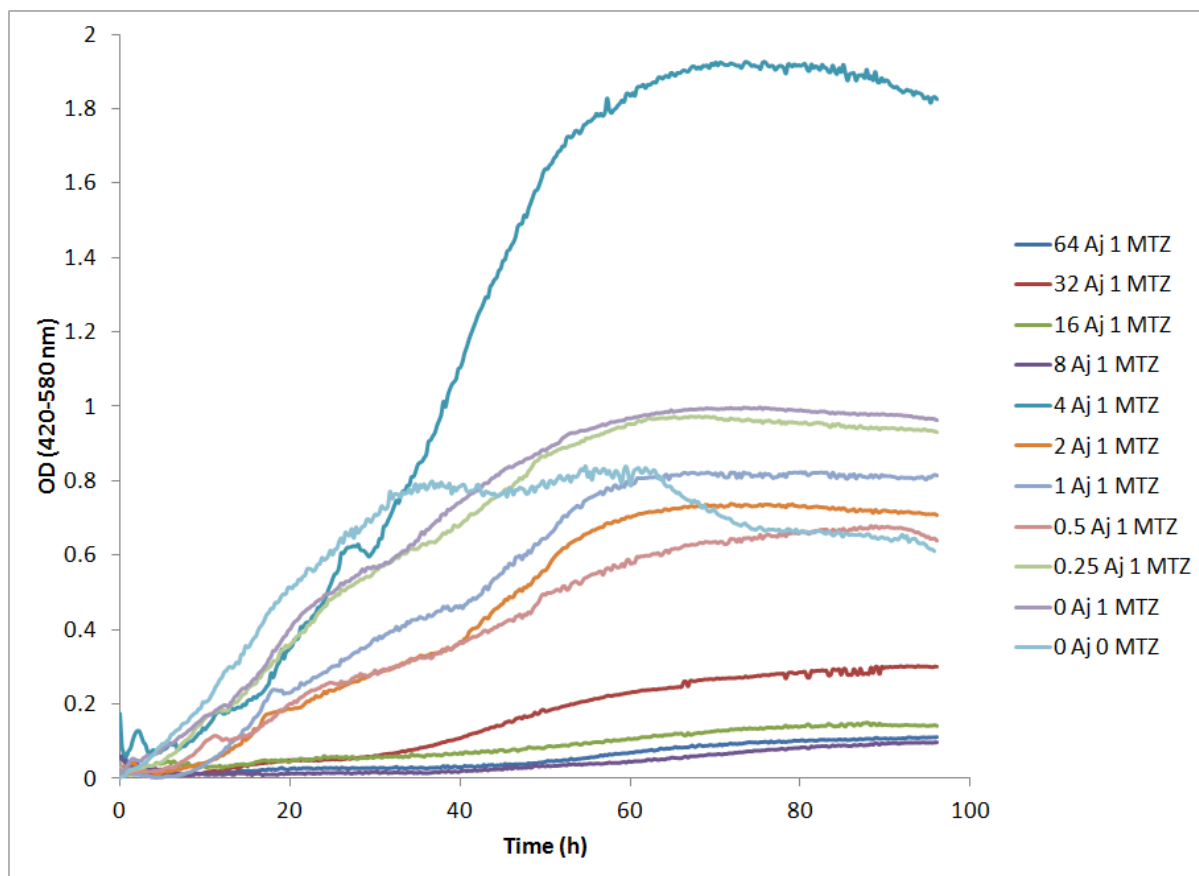
Fig. X. Inhibition of *Spironucleus vortens* (ATCC strain) growth with various combinations of ajoene (Aj, 0-64 µg/ml) and 2 µg/ml metronidazole (MTZ) by automated optical cell density monitoring (420-580 nm, Bioscreen C Reader). Final yields were extrapolated at 72 h for 0 µg/ml (DMSO control) and 82 h for all inhibitor concentrations, in order to calculate minimum inhibitory concentrations (see Chapter 4).

Fig. XI. Inhibition of *Spironucleus vortens* (ATCC strain) growth with various combinations of ajoene (Aj, 0-64 µg/ml) and 2.5 µg/ml metronidazole (MTZ) by automated optical cell density monitoring (420-580 nm, Bioscreen C Reader). Final yields were extrapolated at 72 h for 0 µg/ml (DMSO control) and 82 h for all inhibitor concentrations, in order to calculate minimum inhibitory concentrations (see Chapter 4).
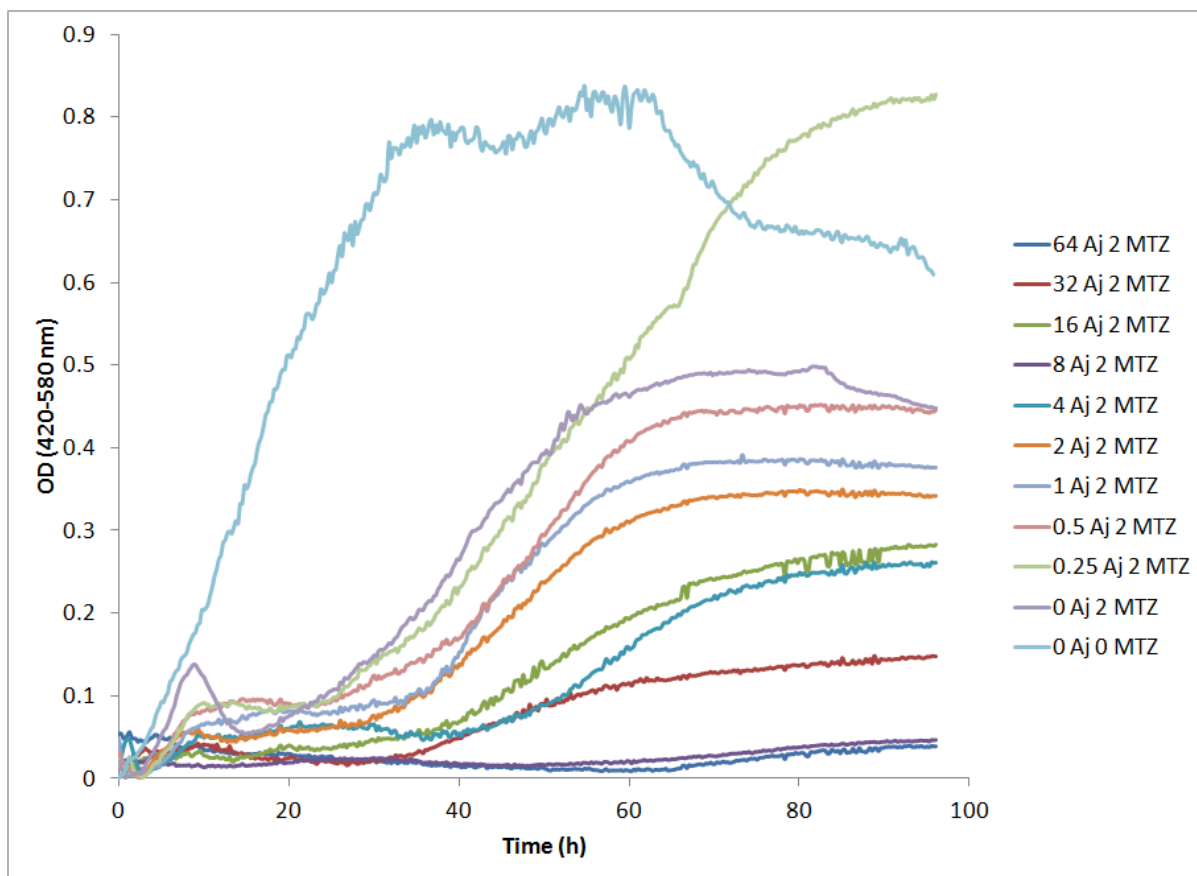
Fig. XII. Inhibition of *Spironucleus vortens* (ATCC strain) growth with various combinations of ajoene (Aj, 0-64 µg/ml) and 3 µg/ml metronidazole (MTZ) by automated optical cell density monitoring (420-580 nm, Bioscreen C Reader). Final yields were extrapolated at 72 h for 0 µg/ml (DMSO control) and 82 h for all inhibitor concentrations, in order to calculate minimum inhibitory concentrations (see Chapter 4).
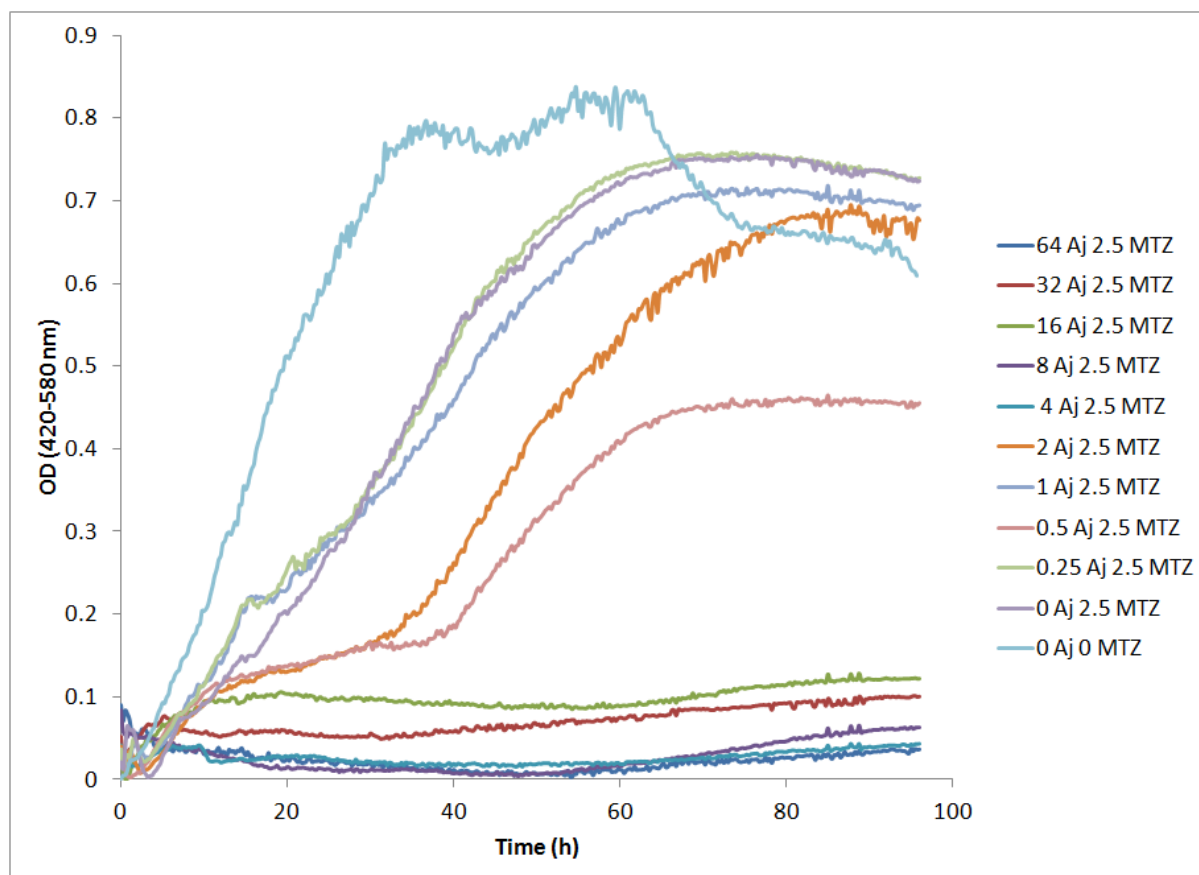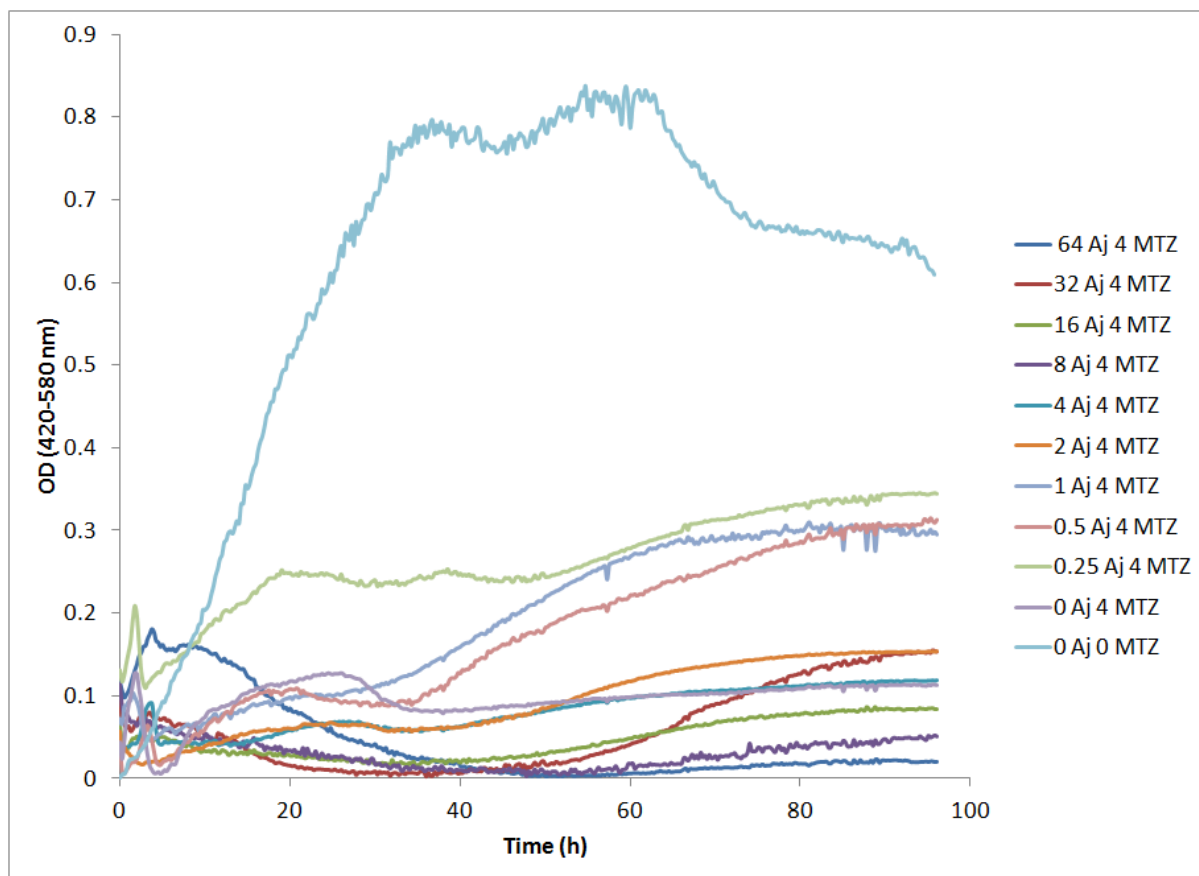
Fig. XIII. Inhibition of *Spironucleus vortens* (ATCC strain) growth with various combinations of ajoene (Aj, 0-64 µg/ml) and 4 µg/ml metronidazole (MTZ) by automated optical cell density monitoring (420-580 nm, Bioscreen C Reader). Final yields were extrapolated at 72 h for 0 µg/ml (DMSO control) and 82 h for all inhibitor concentrations, in order to calculate minimum inhibitory concentrations (see Chapter 4).
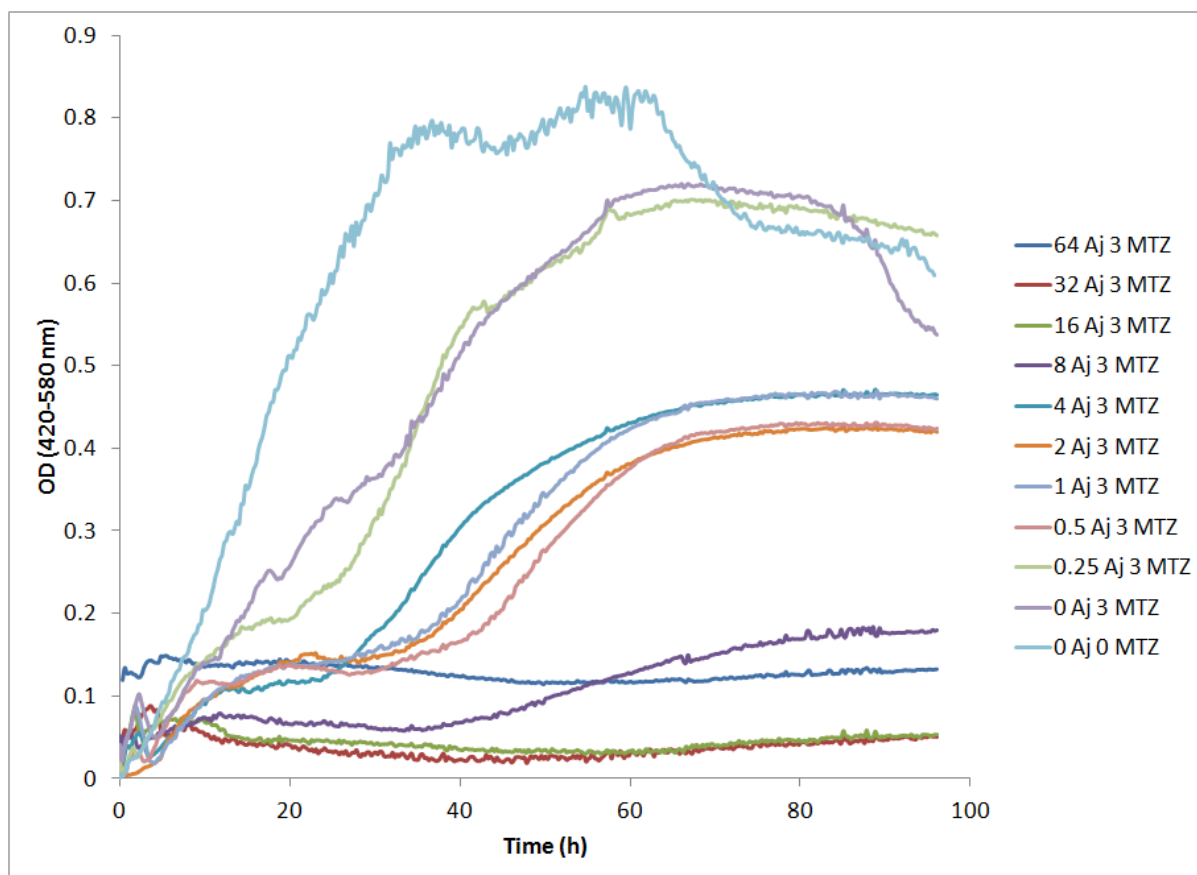
APPENDIX II

Spironucleus vortens (*Sv1* strain) growth curves (raw data from Chapter 4).

Fig. XIV. Inhibition of *Spironucleus vortens* (*Sv1* strain) growth with various concentrations of ajoene (0-100 µg/ml) by automated optical cell density monitoring (420-580 nm, Bioscreen C Reader) (see Chapter 4).

Fig. XV. Inhibition of *Spironucleus vortens* (*Sv1* strain) growth with various concentrations of diallyl disulphide (DADS, 0-100 µg.ml) by automated optical cell density monitoring (420-580 nm, Bioscreen C Reader) (see Chapter 4).
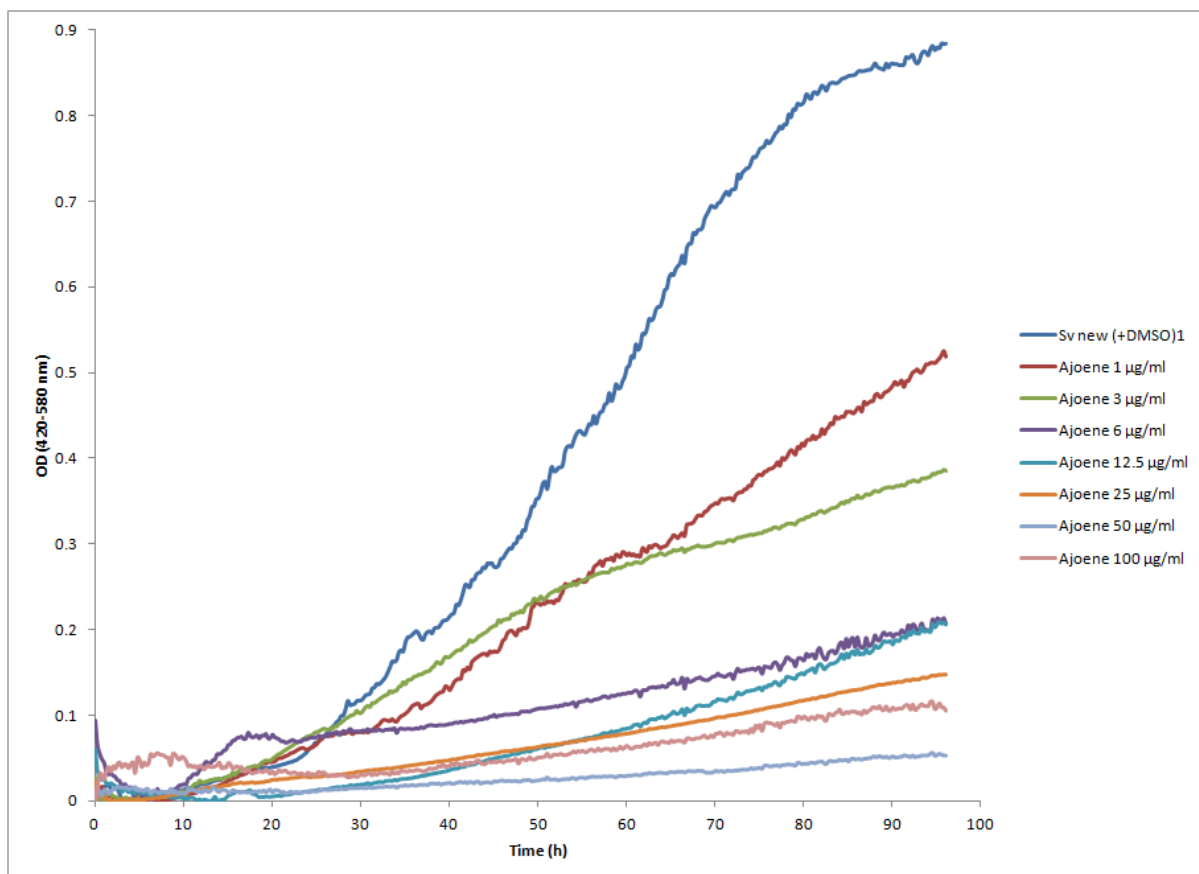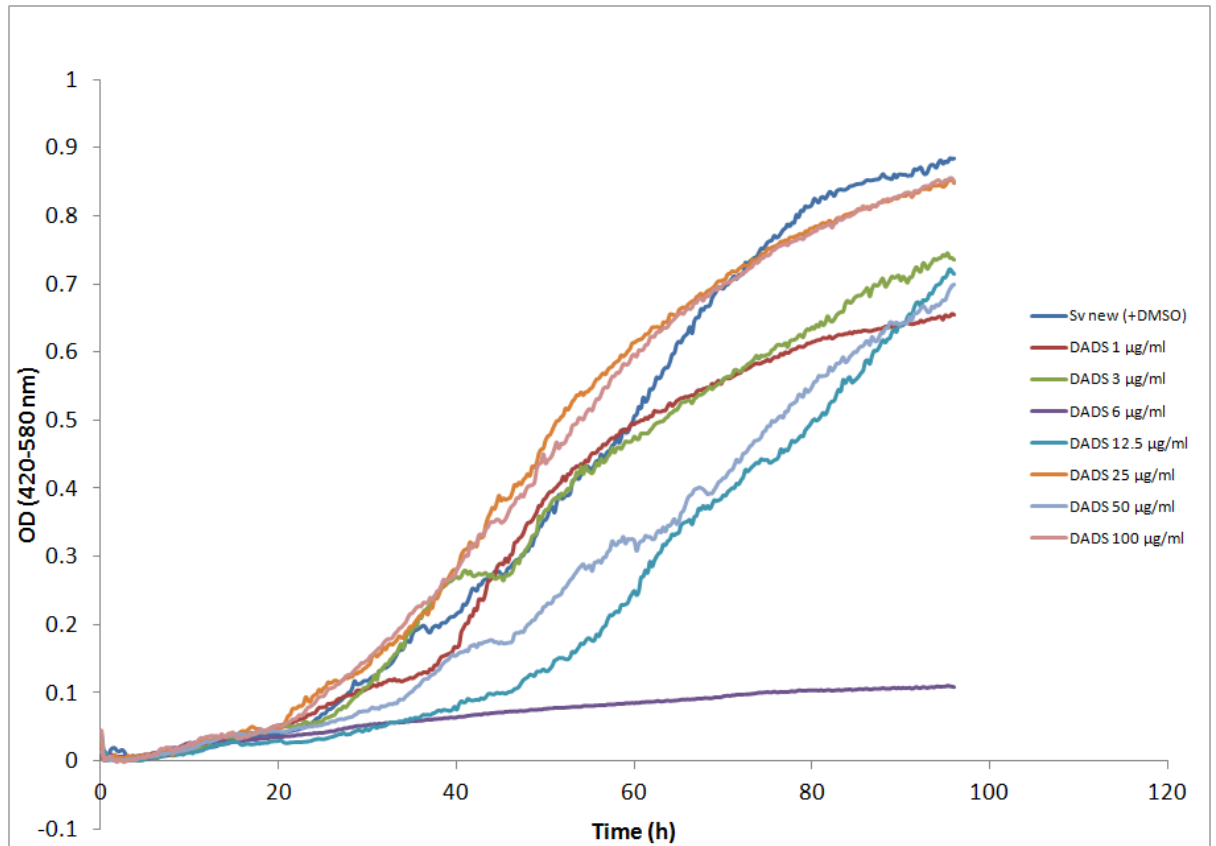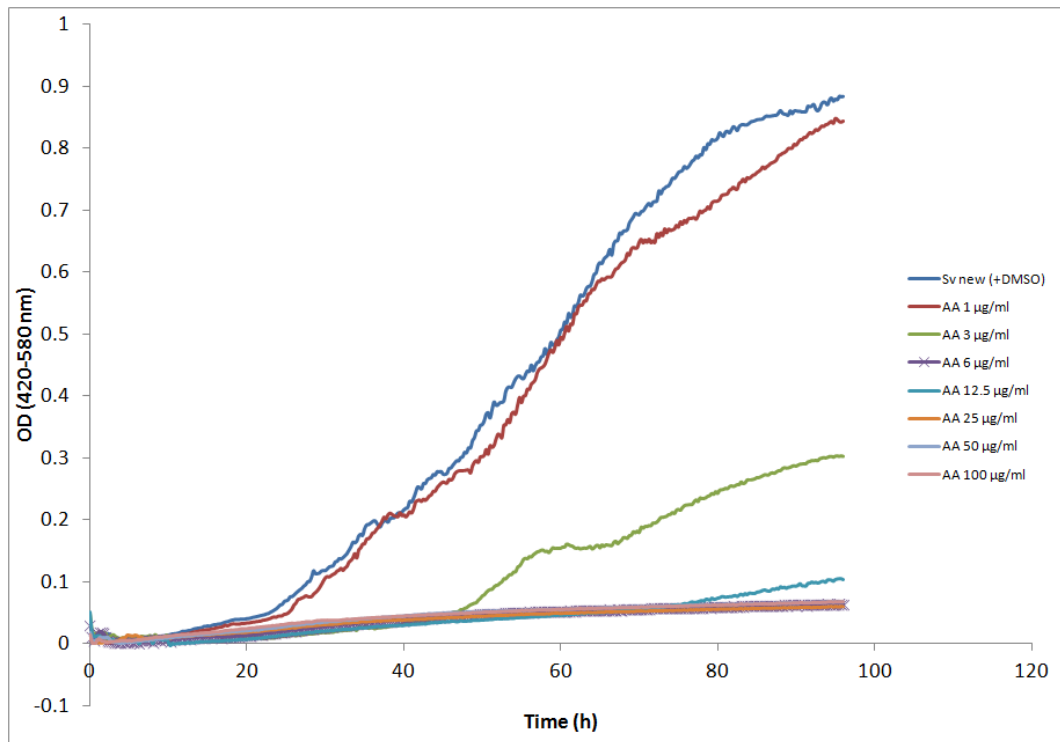
Fig. XVI. Inhibition of *Spironucleus vortens* (*Sv1* strain) growth with various concentrations of allyl alcohol (AA, 0-100 µg/ml) by automated optical cell density monitoring (420-580 nm, Bioscreen C Reader) (see Chapter 4).

APPENDIX III

Composition and Antimicrobial Properties of Sulphur-containing Constituents of Garlic (*Allium sativum*)

Catrin F. Williams and David Lloyd

Abstract

Active components of commercially available garlic preparations include; allicin, ajoene, allyl alcohol, diallyl disulphide and higher polysulphides. However as a natural mixture the antimicrobial effects may be synergistic and the most effective treatments obtained from fresh garlic extracts. Here, we summarise recent advances in the molecular mechanisms of action of these compounds and suggest future developments whereby chemical modification might be effective at improving the natural properties. Despite more than 6000 years of use, garlic appears not to have induced microbial resistance, a factor which is attributed both to its chemical complexity and to dynamics of degradation of the primary active component allicin.

Introduction

The antimicrobial properties of *Allium sativum* (garlic) have been exploited for thousands of years. Knowledge regarding its cultivation was first documented by the ancient Sumerians, *ca.* 2600-2100 BC, with the origin of garlic being assigned to the Tien Shan

Mountains of Kyrgyzstan and Kazakhstan. From here, garlic is thought to have been transported along ancient trading routes between China and the Mediterranean [1, 2]. Since then, the medicinal properties of garlic have been widely documented by the ancient Egyptians, Romans and Grecians. Historically, garlic was frequently employed by the fore-fathers of modern day medicine, including Hippocrates and Pliny the Elder, to treat a variety of common human medical complaints such as gastrointestinal disorders, pneumonia and wounds. The popularity of garlic soared during the middle ages when it was found that garlic could be used as a preventative agent of the plague [1]. In 1858, Louis Pasteur was the first to scientifically document the antibacterial effect of garlic [3].

Today garlic is described as a broad-spectrum antimicrobial agent [4] exhibiting antibacterial, antifungal, antiviral and antiprotozoal properties (Table 1). Its antimicrobial effects are believed to be attributed to a constituent of an ethyl alcohol-extractable constituent, diallyl thiosulphinate, or allicin as assigned by [5]. This study was the first to uncover the underlying chemistry of garlic by different extraction methods. In the garlic clove, the precursor of allicin, alliin, is physically separated from the enzyme alliinase by intracellular membranes, and resides in micro-compartments within the clove. Mechanical disruption of the clove destroys these separating membranes bringing allinase into contact with alliin, thereby rapidly producing allicin through condensation of two 2-propenesulfenic acid molecules (Figure 1). This contributes to the defence mechanism of the plant, with subsequent production of thiosulphinates and other repellent, sulphur-containing compounds [2].

Table 1. IC_{50}, MIC, and MLC values for microbial inhibition by garlic constituents and by freeze-dried garlic extract

A. Yeast [38, 40, 50]

	IC_{50} values (mg ml^{-1}) *Candida albicans*
Diallyl disulphide	0.073 (0.5mM)
Allyl alcohol	0.058 (1mM)
Whole garlic (freeze dried)	5

B. Protists [1, 19]

	IC$_{50}$ values (mg ml^{-1})			
Constituent	*Trichomonas vaginalis*	*Tritrichomonas foetus*	*Giardia intestinalis*	*Spironucleus vortens*
Allyl methyl sulphide	1.15	0.73	0.55	
Allyl sulphide (Diallyl sulphide)	0.7	0.8	1	
Methyl propyl sulphide	0.4	1.08	0.25	
Methyl sulphide	0.5	0.45	1.15	
Diallyl disulphide	0.3	0.08	0.08	
Dimethyl disulphide	0.33	0.3	0.2	
Dipropyl disulphide	0.15	0.18	0.45	
Methyl propyl disulphide	0.5	0.08	0.28	
Allyl mercapton	0.2	0.08	0.037	
Allyl alcohol	0.007	0.06	0.007	
Whole garlic (freeze-dried)	0.28	0.32	0.27	7.9

Definitions: IC$_{50}$ values, concentration required to inhibit growth by 50% using an optical density assay method.

MIC values, minimal inhibitory concentrations to maintain the viable population (using plate counts) at its initial number.

MLC values, minimal lethal concentrations to reduce viable population of to 0.1% of the starting inoculum count [97].

C. Bacteria [76]

Strain	Strain No.	MIC at 6h (mg ml^{-1})	MIC at 24h (mg ml^{-1})	MIC range at 24h (mg ml^{-1})	MLC at 6h (mg ml^{-1})	MLC at 24h (mg ml^{-1})	MLC range at 24h (mg ml^{-1})
Staphylococcus aureus	NCIMB 11857	0.35	0.8	0.6 to 1.3	>10	1.1	0.6 to 1.3
Staphylococcus aureus	INT 21	2.8	1	0.6 to 1.3	>10	2	1.3 to 2.5
Escherichia coli	INT M11	1.1	1	0.6 to 1.3	2	2	1.3 to 2.5
Candida albicans	INT C6	1.3	1.4	1.3 to 2.5	7.3	2.1	1.3 to 2.5
Escherichia coli	INT M18	1.3	1.7	1.3 to 2.5	2.3	2.2	1.3 to 2.5
Bacillus cereus	NCTC 2599	0.4	1.8	1.3 to 2.5	4.8	2.2	1.3 to 2.5
Bacillus subtilis	NCIMB 8993	1.9	1.8	1.3 to 2.5	6.9	2.4	1.3 to 2.5
Saccharomyces cerevisiae	INT M29	1.7	1.9	1.3 to 2.5	5.8	2.6	2.5 to 5.0
Proteus mirabilis	R3.68	1.8	1.9	1.3 to 2.5	>10	3	2.5 to 5.0
Escherichia coli	INT M40	1.9	2.2	1.3 to 2.5	>10	3.4	2.5 to 5.0
Escherichia coli	NCTC 10418	1.9	2.3	1.3 to 2.5	>10	3.5	2.5 to 5.0
Listeria monocytogenes	NCTC 11994	2.2	2.3	1.3 to 2.5	>10	3.7	2.5 to 5.0
Salmonella dublinii	INT M41	1.1	2.3	1.3 to 2.5	6.8	4.2	2.5 to 5.0
Salmonella enteriditis	P227165	1.1	2.4	1.3 to 2.5	>10	4.6	2.5 to 5.0

|						
Salmonella typhimurium	P227221	1.1	2.8	2.5 to 5.0	>10	4.8	2.5 to 5.0
Klebsiella areogenes	NCTC 8172	2	3.3	2.5 to 5.0	>10	8.8	5.0 to 10.0
Pseudomonas aeruginosa	NCTC 8626	3.5	9.1	5.0 to 10.0	7.7	>10	>10
Lactobacillus plantarum	INT L11	15.9	12.5	10.0 to 15.0	>100	29.5 – 49.6	25.0 to 75.0
Lactobacillus acidophilus	NCTC 1748	18.1	16.1	10.0 to 25.0	>100	31.2 – 51.5	25.0 to 75.0
Lactobacillus acidophilus	INT L9	18.5	16.7	10.0 to 25.0	>100	36 – 54.3	25.0 to 75.0
Lactobacillus casei	NCIMB 11970	21.5	17.5	15.0 to 20.0	>100	37.5 – 57.7	25.0 to 75.0
Enterococcus faecium	INT AP7	>100	18.5	10.0 to 25.0	>100	>100	100+
Pediococcus pentosaceus	INT AP8	33.5	34.5	25.0 to 37.5	>100	>100	100+
Pediococcus pentosaceus	INT AP6	37.5	39.7	37.5 to 50.0	>100	>100	100+

After Block, 1985 [1, 10].
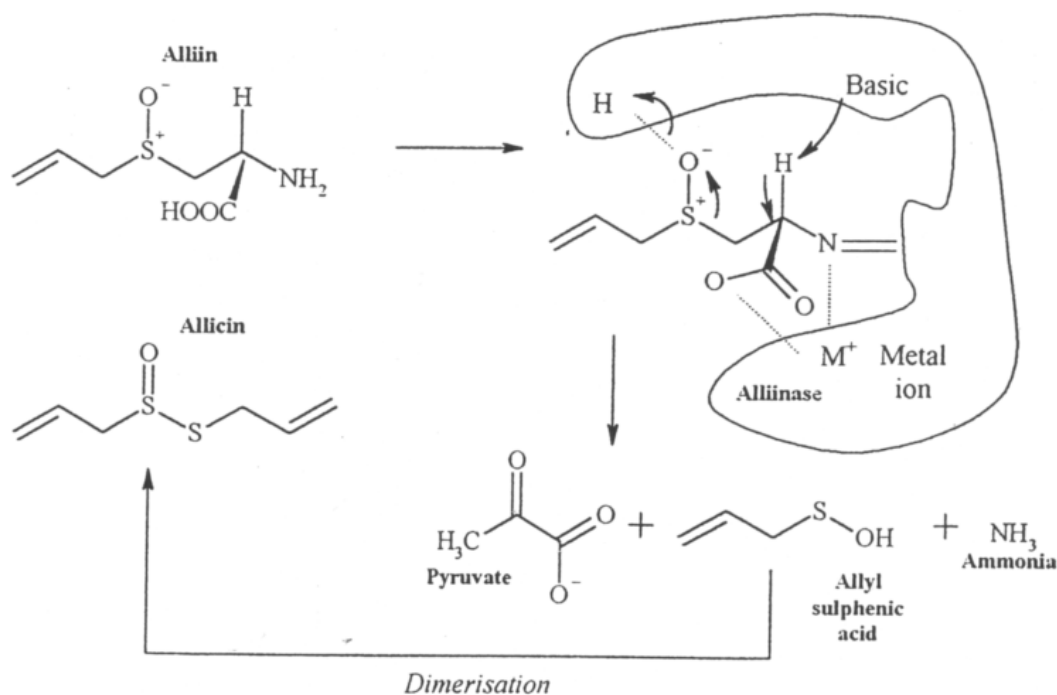
Fig 1. Formation of allicin (diallyl thiosulphinate) from alliin by the action of allinase.

Since experimental research into the antimicrobial properties of garlic began, two key aspects of its action have yet to be solved: (i) what is the mechanism of garlic's broad antimicrobial activity, and (ii) how it is that there are no reports of organisms with acquired resistance against garlic extracts or their constituents?

Garlic Chemistry

In 1844 Wertheim [6], first obtained pungent smelling oil from garlic using steam distillation and used the term allyl for the hydrocarbon it contained. It was not until 1944 that Cavallito and Bailey explored different methods of extraction [5], to produce diallyl disulphide, a diallyl thiosulphinate (allicin), and *S*-allylcysteine sulphoxide (alliin) (Figure 2 a,b). A cysteine sulphoxide and the enzyme alliinase were isolated four years later [7]. Lawson in 1996 separated several other cysteine sulphoxides and their corresponding thiosulphinates [8]. The pathways by which allicin decomposes [9], were elucidated using its analogue, *S*-methyl methane thiosulphinate (Figure 3) [10]. Various other degradative pathways yield ajoene and vinyldithiiins, both of which have potent antimicrobial properties.
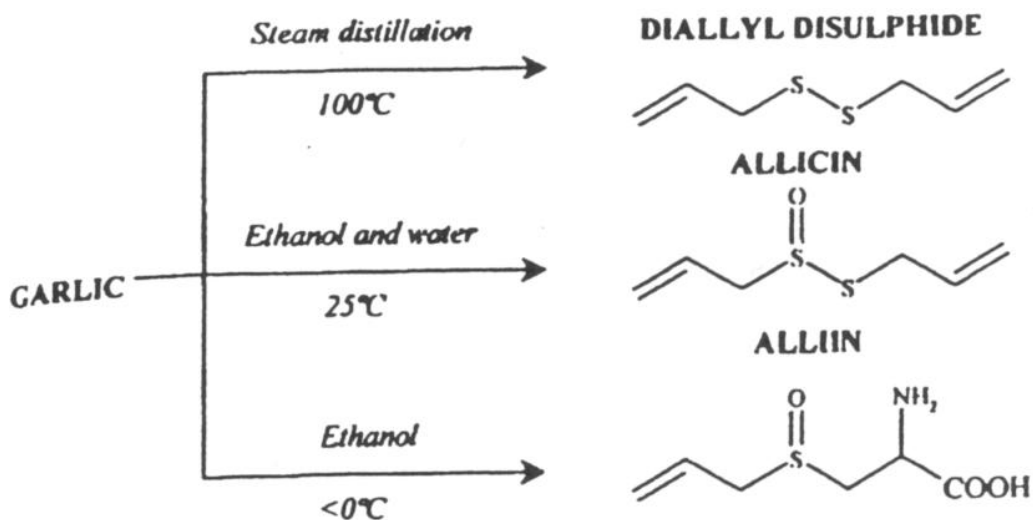
(A)
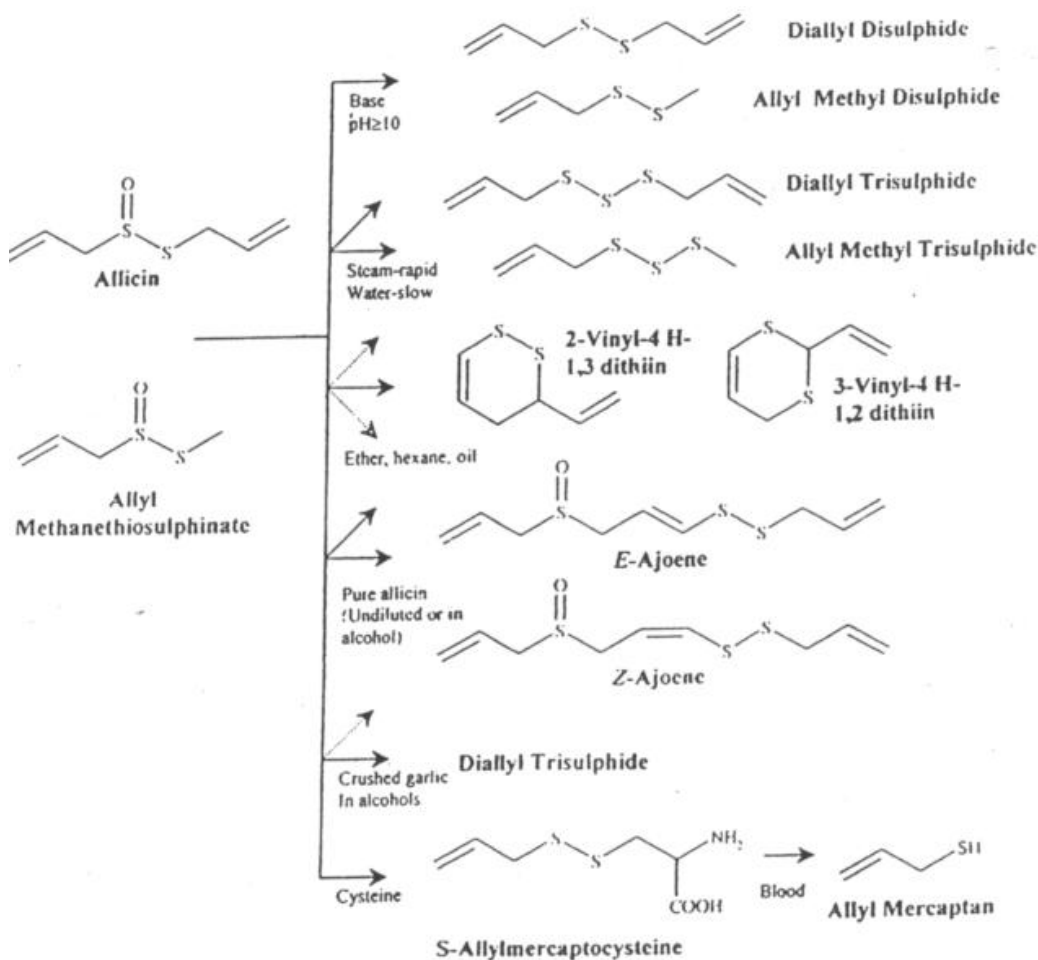
(B)

Fig. 2. (a) Sulphur compounds extracted from garlic. (b) Transformations of thiosulphinates. [1, 8].

195

A:-.Decomposition
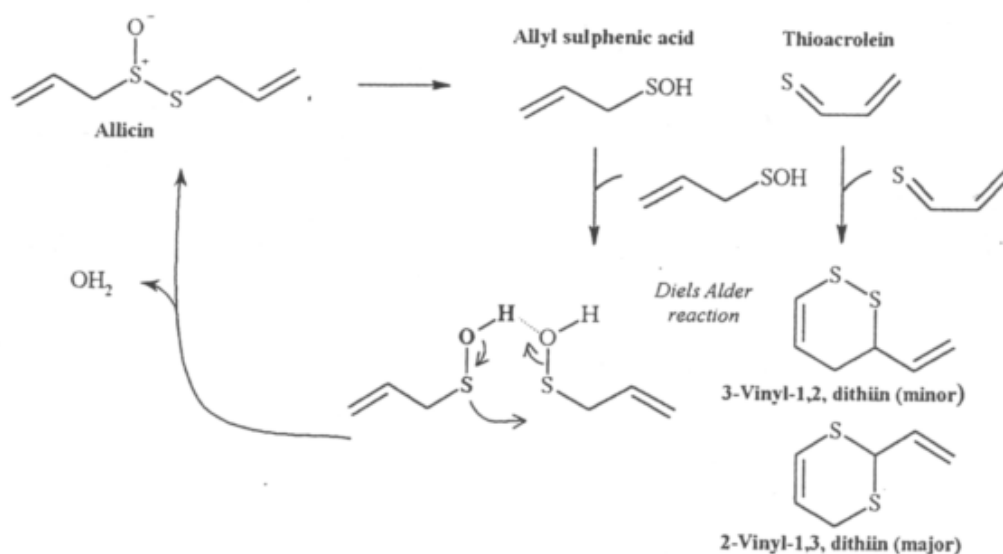
B:-Self-condensation
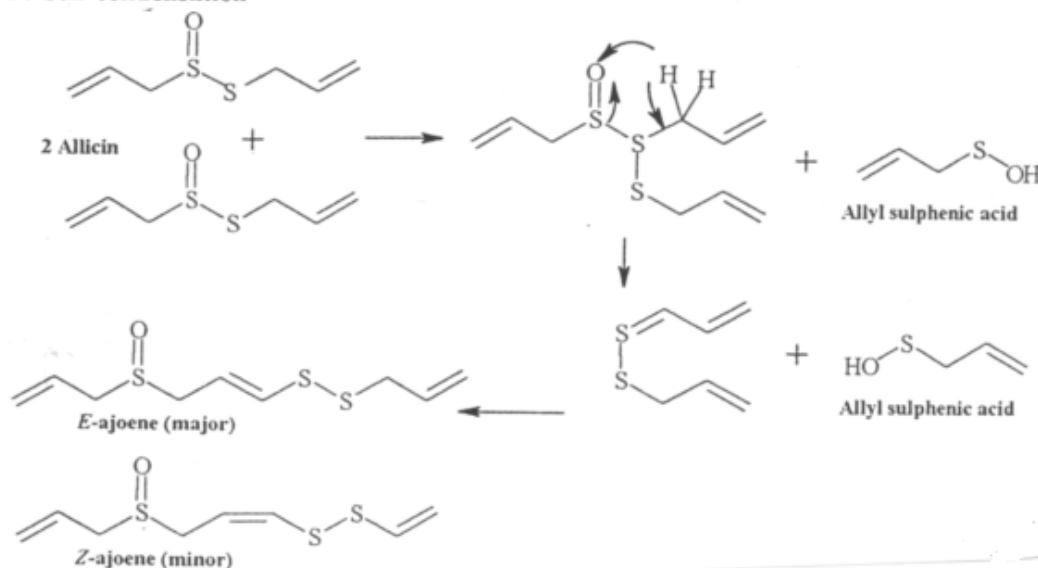
Fig, 3. Degradation pathways of allicin. After Lawson, 1996 [1, 8].

Allicin

Since the antimicrobial potential of allicin was first revealed in the 1940's, interest in the compound has burgeoned with respect to its possible application as a new antimicrobial agent. As the primary biologically active component of the garlic clove, the inhibitory effect of allicin has been quantified against a broad range of pathogenic organisms (Table 1). In addition, it out-performs commonly prescribed antibiotics in that it is effective against not only against Gram positive and Gram negative bacteria, but also against protists, fungi and viruses [11].

The lipophilic nature of allicin is implicated in its mode of action, conferring its ability to cross membrane barriers with relative ease [12]. Once inside the cell, allicin can powerfully inhibit thiol-dependent enzymes which are important in maintaining redox balance within the organism. These include cysteine proteinases, alcohol dehydrogenases and thioredoxin reductases, demonstrated in *Entamoeba histolytica*, a protozoan parasite which causes dysentery in humans [13]. The cysteine proteinases of the malaria parasite, *Plasmodium falciparum* (falcipain 2), and of the African sleeping sickness parasite, *Trypansosoma brucei* (rhodesain), are also inhibited by allicin, both of which are important factors in the pathogenicity of these protists [14]. Interestingly, mammalian cysteine proteinases are not as sensitive as the pathogens described above to allicin, with 10-fold higher concentration required to cause cytotoxoicity [13]. The differing sensitivities of the host and pathogen to allicin may be due to the fact that microbial cells possess little or no glutathione, an important thiol involved in cellular redox cycling. Therefore, once allicin thiolates the essential thiol-dependent enzymes described above, the pathogen has no means to successfully establish their reactivation.

Studies into the biological activity of allicin have been highly problematic due to the instability of this compound. Indeed, allicin is not only unstable but so reactive with O_2 upon formation, that storage can only be short term and under anaerobic conditions at low temperatures. At ambient temperature, or upon heating, allicin molecules undergo partial decomposition by one of two processes. The first results in the formation of allyl alcohol, diallyl disulphide, and diallyl trishulphide as well as higher polysulphides, and the second leads to the formation of ajoene. In addition, self-decomposition of allicin to thioacrolein produces vinyl dithiins by dimerization [10]. *In vitro* experiments involving human pathogens require at least ambient temperature for skin microbes such as *Staphylococcus aureus*, or with gut microbes, such as *Escherichia coli,* a temperature of 37°C to grow optimally. This means that in such experiments there is only a short window of opportunity for testing allicin before the compound begins to decompose (within 16 h at 23°C) [15]. Temperature is also likely to be a significant factor during *in vivo* experiments using animal models or in clinical trials involving allicin. In addition, oral administration of allicin results in loss of the compound during passage through the stomach, where the harsh acidic conditions (pH *ca.* 2) aids degradation to its breakdown products. However, these breakdown products of allicin some of which are far more

stable than allicin, also possess broad-ranging antimicrobial activities, so that efficacy of action is enhanced rather than lost after acid hydrolysis.

Ajoene

First characterised by Block et al. [16], ajoene is produced by the decomposition of allicin during methanolic extraction. Interest in this biologically active garlic constituent began when, in an earlier study, an unidentified component of garlic was capable of antithrombotic activity [17]. Although most of the research involving ajoene has focussed on its role as an effective antithrombotic and anticancer agent [18], its potential as an antibiotic has also recently come to light (see table). Ajoene is primarily composed of two vinyl dithiins, which have also recently been shown to have an antiparasitic effect against the protozoan fish parasite *Spironucleus vortens* [19], and can exist in the *E* or *Z* forms, with the *Z* form having slightly higher biological activity. Its stability is much higher than that of allicin, with the *E* form being more stable than the *Z* form to UV light, temperature and long term storage [20].

Ajoene has a particularly potent effect against HIV, and is thought to be an inhibitor of viral replication [14]. It is also reported to have high antifungal activity, with an MIC value of <20 µg/ml against *Candida albicans*, causative agent of thrush, and *Aspergillus niger*, associated with fungal ear infections, and is hypothesised to cause damage to the fungal cell wall [20a]. Naganawa et al. also quantified the inhibitory effect of ajoene against a range of fungi and bacteria [21], with Gram positives (e.g. *Bacillus cereus*) being more susceptible to ajoene than Gram negatives (e.g. *Escherichia coli*), having MIC's of 5 and 152 µg/ml respectively on solid agar tests. Ajoene is also documented to have an antiparasitic effect against *Trypanosoma cruzei*, causative agent of Chagas disease, with 40 µM ajoene capable of eradicating the parasite from African green monkey VERO cells within 96 h [22]. Here, treatment with ajoene resulted in a significant change in the phospholipid composition of *T. cruzei*, thus having an antiproliferative effect against the parasite. Furthermore, a single dose of ajoene (50 mg/kg) combined with the anti-malarial compound, chloroquine (4.5 mg/kg), completely inhibited further development *of Plasmodium berghei* in mice, with no obvious acute toxic effects on the mice themselves [23].

Allyl Alcohol

Allyl alcohol, one of the simplest constituents of garlic and many of its commercial preparations, is both pharmacologically active and antimicrobial [2]. It is produced from more complex constituents by two routes; the self-condensation reactions of allicin, and also by the reaction of alliin (the direct precursor of allicin) with water [8]. Ingestion of garlic is followed by rapid release of allyl alcohol [24], and it has been detected in exhaled air after oral administration of all preparations tested, especially freeze-dried garlic powders in tablets [25]. In addition to the chemical hydrolyses of its two major garlic precursors, further transformations of the thiosulphinates, diallyl trisulphide and diallyl disulphide lead to the production of allyl alcohol *in vivo* [10, 26]; up to one-third of all the allyl groups present can be accounted for by these processes [8]. Similar metabolic transformations have been demonstrated in experiments with rats [27]. Its heat stability is greater than other anti-yeast garlic constituents [28]. Allyl alcohol is an inhibitor of alcohol dehydrogenase, largely due to the formation of its aldehyde oxidation product, acrolein [29, 30]. As a hepato-toxicant, allyl alcohol dosage has to be controlled; even so up to 100ul per kg body weight in rats administered by gastric tube gave no measurable toxicity as indicated in subsequent investigations on hepatocytes [31]. Valuable insights into mechanisms of inhibition have come from studies of yeasts. Functionally significant of the 20 or so different alcohol dehydrogenases in *Saccharomyces cerevisiae* (baker's yeast) [32], and involved in allyl alcohol toxicity include the cytoplasmically-located ADH1 and 2 isoforms and the mitochondrial ADH3. The former enzymes are involved in ethanol formation and cellular growth [33], whereas the latter is not so well characterised, but may well be functional as a redox shuttle for the translocation of mitochondrial reducing equivalents (as NADH) from the mitochondrial matrix to the cytosol [34].

In the methylotrophic yeast, *Pichia pastoris,* allyl alcohol itself exerts little toxicity [35], but again acrolein, its oxidation product does. For both *Candida albicans* [36-38], and the important protozoal pathogen infecting the human upper intestine, *Giardia intestinalisi* [39], allyl alcohol is one of the most potent of the garlic components. A detailed two-photon laser scanning microscopy study of the redox changes in *C. albicans* revealed oxidation of NADH, depletion of glutathione and increased levels of reactive oxygen species [40]. Flow cytometry confirmed that cytotoxicity of allyl alcohol is mediated by oxidative stress. This results from disturbed intracellular redox status and

the accumulation of hydrogen peroxide and/or superoxide radical anions. Mitochondrial trans-membrane electrochemical potential was increased in the presence of 1mM allyl alcohol, and even with 200 times the MIC for this compound, glucose -supported respiration by intact organisms was unaffected. Thus the primary effects are not on mitochondria; it may well be that the major deleterious consequences of oxidative stress are on the physiology of transport *eg.* that involving the plasma-membrane membrane potential [41] as demonstrated in some other lower eukaryotes [42]. Synergistic action of combinations of diallyl disulphide or diallyl trisulphide with allyl alcohol against *Candida utilis* have been demonstrated [43]. Allyl alcohol also shows antiviral properties, for instance against HIV-infected cells [44].

Diallyl disulphide

Diallyl disulphide (DADS), another breakdown product in allium extracts is, like allyl alcohol, one of the most potent antimicrobials of the garlic constituents. Furthermore, it has been reported to inhibit cellular proliferation in human colon, liver and skin tumours [45]. Elevation of reactive oxygen species following DADS administration leads to apoptotic cell death in neuroblastomas [46]; in leukaemic cells, activation of the caspase-3 pathway is implicated in this process [47]. Since the 1980's the number of reports of anti-tumour cell activity of DADS have burgeoned and now can be counted in their hundreds. Two recent reports [48, 49], stress that the modulation of cellular redox networks are implicated. Similarly the range of its antimicrobial applications continues to be extended. In a detailed examination of the metabolic effects of DADS on the important pathogenic yeast, *Candida albicans*, showed that at least three of its primary target sites reside at the inner membrane of the mitochondria [50]. The glucose-stimulated respiration of whole organisms was 80% inhibited by 1mM DADS, as was the succinate-driven O_2 consumption of isolated mitochondria. Both an oligomycin-like inhibition of mitochondrial ATP synthase and a direct action at the level of the electron transport chain was demonstrated. The observed effects on the respiratory chain itself indicated that two different sites (at complexes 11 and 1V) were implicated; moreover, this garlic constituent was more effective at preventing oxidative phosphorylation than oligomycin (the most commonly-used and highly effective inhibitor of mitochondrial ATP synthesis by the F_1-F_0 ATP synthase). These events resulted in the

partial collapse of the trans-membrane electrochemical potential across the inner mitochondrial membrane of this highly aerobic yeast.

Intensities of NAD(P)H fluorescence both in the mitochondrial and cytosolic compartments were diminished more than three-fold, the cellular glutathione content was similarly decreased, and a five-fold higher fluorogenic detection of reactive O_2 species was almost immediately observed after DADS administration.

Mitochondrial dysfunction is well-known to be a critical condition that generally presages a life-death decision for cells. This is so in model organisms (eg. in yeasts) [51] and in mammalian tissues, eg. *in vivo* in the mammalian heart as well as in isolated cardiomyocytes [52]. An early indicator is the collapsing mitochondrial membrane potential that accompanies a cascade of events leading to apoptosis or necrosis. The time course of cell death in *C. albicons* follows a brief exposure (30min) to 0.5 mM DADS as assessed using the AlexaFluor 488 annexinV/propidium iodide (apoptotic/necrotic) method. In the two-photon laser scanning microscope it was possible to differentially count organisms in which plasma-membrane phosphatidyl-serine had been externalized (green fluorescence) alongside those in which plasma membranes had become permeabilized, allowing entry of propidium iodide (red fluorescence). Even within the transient exposure time, an increase of 11% of the population became necrotic as compared with a control untreated suspension of organisms. Apoptosis became evident within 2h of removal of DADS, affecting 20% of the organisms; at this time 50% of the cells had become necrotic. Further loss of viability to 80% was indicated by 4h.

We have suggested [50, 53] that the pivotal initiating event in the complex downstream sequence that leads to cell death in general, as well as in DADS-treated *C. albicans*, is thiol-depletion. In yeasts, as in mammals, the predominant thiol is glutathione: oxidation within the cells of the intra-mitochondrial redox state is a major consequence. Accordingly we confirmed that glutathione-S-transferase purified from equine liver (G6511, Sigma Aldrich) was inhibited by DADS; 40% inhibition was observed with this garlic component at 0.5mM.[50] Control experiments indicated that chemical oxidation of glutathione by DADS (i.e. that in the absence of the enzyme) did not occur. In *C. albicans in vivo* glutathione depletion after DADS treatment was observed by decreased fluorescence of its mono-chlorobimane derivative. Within 5 min, relocation of the glutathione adduct to the yeast vacuole was observed. The importance of glutathione antioxidant defence systems in the maintenance of yeast viability has been

repeatedly stressed [54]. Mutants for glutamyl-cysteine synthetase (GCS1), a key enzyme of the pathway of biosynthesis of this tri-peptide are highly sensitive to induction of apoptosis [55].

Higher Polysulphides

The higher polysulphide diallyl trisulphide has an $LC_{50\%}$ of $0.8 - 5.5$ μg. ml^{-1} against *Trypanosoma brucei*, the causative agent of sleeping sickness. This $LC_{50\%}$ value is far below the recommended threshold for human administration of the compound (this being 25 μg/ml). In fact, diallyl trisulphide is already commercially available in China as Dasuansu, commonly prescribed in the treatment of *Entamoeba histolytica* and *Trichomonas vaginalis* infections in humans.[1] Both DADS and diallyl trisulphide (20-500uM) affect the fluidity of the phospholipid hydrocarbon cores of lipid bilayers in model membranes [56]. Whereas tumour cell and platelet model membranes containing unsaturated fatty acids and cholesterol, and Candida model membranes containing ergosterol became partially rigidified by these allyl compounds, bacterial model membranes were not. These results indicate a plasma- membrane based site of action for the garlic constituents.

In an extensive study by, 40 clinical isolates of *Staphylococcus aureus*, 60 clinical isolates of MRSA and a total of 176 clinical isolates of *Candida* and *Aspergillus* spp. were tested for their susceptibility to four diallyl sulphides [57]. The MICs of these sulphur-containing compounds increased with an increasing number of S atoms as follows; diallyl tetrasulphide > diallyl trisulphide > diallyl disulphide > diallyl monosulphide. This effect was also seen against *Helicobacter pylori*, which causes chronic gastritis in humans [58], and also in the nosocomial pathogens *Pseudomonas aeruginosa* and *Klebsiella pneumoniae*.[57] Block speculates that this effect is probably due to the weakening of the S-S bonds with increasing number of S atoms, making the compound more reactive to –SH groups in the pathogen [2].

Whole Garlic Extract

It would seem evident that in order to preserve the complex chemistry of the garlic clove, it would be necessary to maintain, as much as possible, the reaction products generated the first moments after a clove is crushed. Numerous studies have thus investigated the antimicrobial activity of fresh or freeze-dried garlic powder. Freeze-dried

garlic powder is often packaged into capsules which are commercially available in health food shops as herbal supplements. However, the biological activity of such products is much reduced, as compared to that of fresh garlic, due to the huge reduction in biologically active constituents [38] (Figure 4). The antimicrobial activity of whole garlic extract is limited due to the high dose required to exert an effect. For example, in the case of the human vaginal parasite *Trichomonas vaginalis*, the $IC_{50\%}$ of whole garlic extract (0.28 mg/ml) is 40x greater than that of the garlic constituent allyl alcohol (0.007 mg/ml).[1] Despite this, clinical trials conducted by Soffar involving whole garlic as an antigiardial agent proved promising, deeming it safe for patient administration and shortening the treatment duration time as compared to the traditional drug of choice, metronidazole (Flagyl) [59]. In third world countries such as Cameroon in West Africa traditionally employ garlic juice to treat African eye worm infections caused by the nematode *Loa loa*, with no adverse effects observed to the cornea [60].
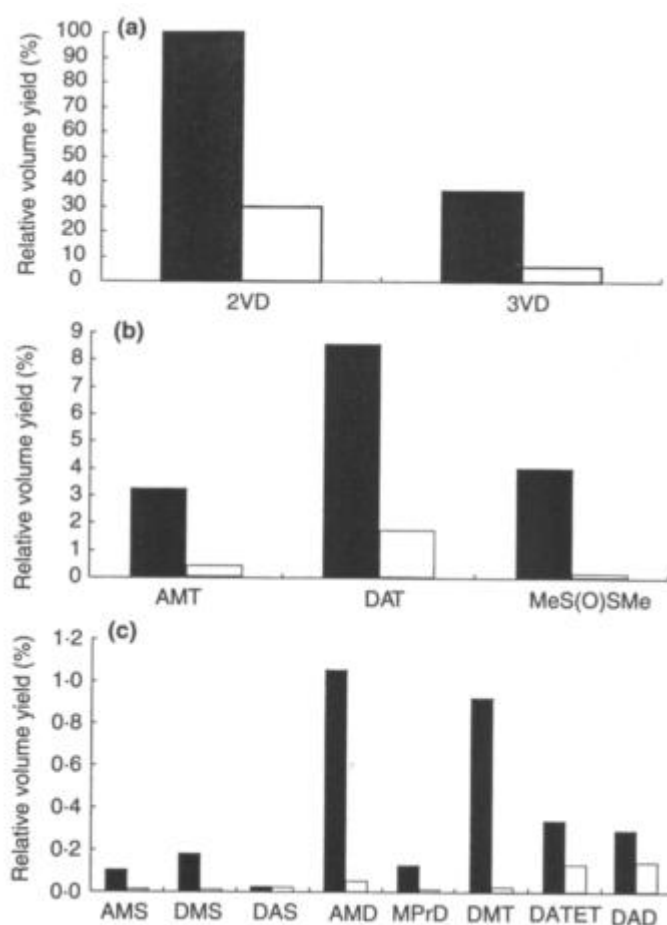

Fig 4. Comparison of yields of sulphur compounds from gas chromatography-mass spectrometry analysis of ■, fresh garlic extract (FGE) and □, garlic powder extract with

respect to production of 2-vinyldithiin from FGE taken as 100% yield. Graphs separated due to large variation in scale, 2VD, 2-vinyldithiin; 3VD, 3-vinyldithiin; AMT, allyl methyl trisulphide; DAT, diallyltrisulphide; MeS(O)SMe, methane methyl thiosulphinate; AMS, allyl methyl sulphide; DMS, dimethyl sulphide; DAS, diallyl sulphide; AMD, allyl methyl disulphide; MPrD, methyl propyl disulphide; DMT dimethyl trisulphide; DATET, dimethyl tetrasulphide; DAD, diallyl disulphide [38].

An interesting property of garlic is its ability it selectively inhibit pathogenic organisms but not harmless commensals. This is especially true in the case of a non-pathogenic genus of bacteria, the Lactobacilli. These "probiotic" microbes reside in the human intestinal, vaginal and urinary tract and are themselves able to inhibit the growth and colonisation of invading pathogenic organisms [61]. Rees et al. [62] found that the MIC of freeze-dried garlic extract was 10-fold higher for the Lactic acid bacteria (e.g. *Lactobacillus casei* MIC range 15-20 mg/ml) than that of pathogenic bacteria (e.g. *Bacillus cereus* MIC range 1.3-2.5 mg/ml). Thus the pactise of administration of garlic constituents holds a great advantage over the use of currently prescribed antibiotics which do not differentiate between pathogenic and non-pathogenic microbes. Thus a course of antibiotics can wipe-out the natural microflora of the gut, and sometimes lead to secondary infection; this is especially true in the case of *Clostridium difficile* which cases pseudo-membranous colitis [63]. Evidently, any reduction in the current antibiotic dosage would be very welcome. Indeed, garlic is also capable of working in synergy with antibiotics such as ampicillin, as demonstrated against *Staphylococcus aureus* [64]. The same study also revealed that ajoene had an additive effect with ampicillin against *Escherichia coli*. Furthermore, Cottrell showed that a garlic extract had a synergistic effect with methicillin against MRSA, thus re-establishing the susceptibility of this "superbug" to methicillin treatment [65].

Conclusion

At the beginning of the 20th century the discovery of antibiotics revolutionised modern medicine. However, soon after their introduction, the development of widespread resistance to these antimicrobials soon became apparent. Today, microbial resistance pathways have been characterised for all antibiotics introduced under clinical and agricultural settings [66]. In the case of garlic, however, there have been no documented

cases of resistance during its long history as an antimicrobial agent. Indeed, it has been estimated that resistance to beta-lactams is 1000-fold more likely than resistance to allicin [13]. This is attributed to the ability of this garlic constituent to target a wide range of cysteine-containing enzymes, along with the plethora of biologically active breakdown products that are formed on the decomposition of this evanescent compound. Furthermore, the evident selective and differential toxicity of garlic towards human pathogenic cells (*eg* tumour cell lines) means that *in vivo* administration is not a problem. As a result, some studies have already begun taking appropriate measures to design new drugs based on the complex chemistry of garlic. It is also possible to mimic the defence mechanism of the garlic clove using treatments containing the alliinase enzyme and its substrate, alliin, to produce allicin *in situ*. The treatments, which included other sulphoxide substrates of alliinase to produce more stable active products, all produced an antifungal effect against the cysteine-proteases of the rice blast fungus *Magnaporthe grisea* [67]. Synthetic construction of a stable S-(4-methoxyphenyl) propyl thiosulphinate derivative of allicin [68], and later an S-*p*-tolyl *t*-butyl thiosulphinate allicin analogue [69], have been described: both of these compounds require further assessment of their probable antimicrobial effects and possible toxicity to humans. However, these simple, synthetically produced representatives of allicin are the first steps along a brand new avenue of chemotherapy, which has the potential to revolutionize the way we treat microbial infections in a more rational manner.

Recent advances in our understanding of biochemical mechanisms of action of garlic constituents focus on the redox reactions at the core of the energy supply of the growing cell [70]. A delicate balance in redox reactions, driven by ultradian clocks, maintains the vitality and viability of the yeast organism [71]. The important central components (NAD(P)H, glutathione, thioredoxins, glutaredoxins) are pivotal in the production and elimination of reactive O_2 species. Oscillatory changes in redox state are observed in the mitochondrial and cytosolic compartments [72]. It is in the vicinity of these reactions that *Allium sativum* constituents interfere by making the redox potential more oxidized and hence depleting thiol pools. Glutathione reduction is of key significance in preservation of vitality and hence survival, not only of yeast, but also of mammalian cardiomyocytes [73]. The future challenge is to determine how it is that the sensitivities of this central mechanism is so much more in many microbial systems [1, 11,

19, 38, 39, 74-76], than in those of their higher animal hosts, *eg* fish [74, 75], and humans.

Acknowledgements

References

[1] Harris, J.C. *Giardia intestinalis, Trichomonas vaginalis* and *Tritrichomonas foetus*: suseptibility to antiprotozoal activity in *Allium sativum.* PhD Thesis, University of Wales, Cardiff, UK. 2001.

[2] Block, E. Garlic and other Alliums: The Lore and the Science. The Royal Society of Chemistry, 2010. Cambridge, UK; pp. 454

[3] Pasteur, L. *Ann. Chemie. Phys*. 1858, *52,* 404-418.

[4] Rios, J.L.; Reico, M.C. *J. Entopharm.* 2005, *100*, 80-84.

[5] Cavallito, C.J.; Bailey, J.H. *J. Am. Chem. Soc.* 1944, *61,* 1050-1951.

[6] Wertheim, T. *Ann. Chem. Pharm*. 1844, *51*, 289-315.

[7] Stoll, V.; Seebeck, E.; *Helv*. *Chem. Acta* 1948, *31,* 189.

[8] Lawson, L.D.; In *Garlic The Science and Therapeutic Application of Allium sativum and related species.* Koch H.P.; Lawson, L.D.; Eds. Williams & Wilkins, Baltimore, MD, 1996, pp. 37-107.

[9] Brodnitz, M.H.; Pascale, J.V.; Derslice *J. Agric. Food Chem.* 1971, *19*, 273-275.

[10] Block, E. *Sci. Am.* 1985, *252*, 114-119.

[11] Harris, J.C.; Cottrell, S.L.; Plummer, S.; Lloyd, D. *Appl. Microbiol. Biotech*. 2001, *57,* 282-286.

[12] Miron, T.; Rabinkov, A.; Mirelman, D. Wilchek, M.; Weiner, L. *Biochim. Biophys. Acta* 2000, *1463*, 20-30.

[13] Ankri, S.; Mirelman, D. *Microb. Infect.* 1999, *1*, 125-129.

[14] Waag, T.; Gelhaus, C.; Rath, J.; Stich, A.; Leippe, M.; Schirmeister, T. *Bioorg. Med. Chem. Lett*. 2010, *20,* 5541-5543.

[15] Cutler, R.R.; Wilson, P. *Brit. J. Med. Sci.* 2004, *61,* 1-4

[16] Block, E.; Ahman, S.; Jain, M.K.' Crecely, R.; Apitz-Castro, R.; Cruz, M.R. *J. Am. Chem. Soc.* 1984, *106,* 8295-8296.

[17] Apitz_Castro, R.; Cabrera, S.; Cruz, M.R., Ledezma, E.; Jain, M.K. *Thromb. Res*. 1983, *32*, 155-169.

[18] Kaschula, C.H.; Hunter, R.; Parker, M.I. *Biofactors* 2010, *36,* 78-85.

[19] Millet, C.O.M.; Lloyd, D.; Williams, C.F.; Williams, D.; Evans, G.; Saunders, R.A.; Cable, J. *Expt. Parasitol.* 2010, *127,* 490-499.

[20] Naznin, M.T.; Akagawa, M.; Okukawa, K.; Maeda, T.; Morita, N. *Food Chem.* 2008, *106,* 1113-1119. 20a Yoshida, S.; Kasuga, S.; Hayashi, N.; Ushiroguchi, T.; Matsuura, H.; Nakagawa, S. *Appl. Environ. Microbiol.* 1987, *53*, 615-617.

[21] Naganawa, R.; Iwata, N.; Ishikawa, K.; Fukuda, H.; Fujino, T.; Suzuki, A. *Appl. Environ. Microbiol.* 1996, *62*, 4238-4242.

[22] Urbina, J.A.; Marchan, E.; Lazardi, K.; Visbal, G.; Apitz-Castro, R.; Gil. F.; Aguirre, T.; Piras, M.M.; Piras, R. *Biochem. Pharmacol.* 1993, *45*, 2381-2387.

[23] Perez, H.A.; De la Rosa, M.; Apitz, R. *Antimicrob. Agents Chemother.* 1994*, 38,* 337-339.

[24] Egin-Schwind, C.; Eckard, R.; Jekat, F.W.; Winterhoff, H. *Planta Med.* 1992, *50*, 8-13.

[25] Laasko, L.; Seppanen-Laasko, T.; Hiltunen, R.; Muller, B.; Jansen, H.; Knoblock, K. *Planta Med.* 1989, *55,* 257-261.

[26] Block, E.; Putnam, D.; Zhao, S.H. *J. Agric. Food Chem.* 1992. *40,* 2431-2438.

[27] Germain, E.; Auger, J.; gines, C.; Siess, M.H.; Teyssier, C. *Xenobiotic,* 2002, *32,* 1127-1138.

[28] Choi, J.H.; Kyung, K.H. *J. Food Sci.* 2005, *70,* M305-M309.

[29] Rando, R.R. *Biochem. Pharmacol.* 1974, *23,* 2328-2331.

[30] Mapoles, J.E.; Iwahashi, M.; Lucas, D.; Zimmerman, B.T.; Simon, F.R. *Alcohol Clin. Exp. Res.* 1994, *18*, 632-639

[31] Tygstrup, N.; Jensen, S.A.; Krog, B.; Dalhofi, K. *J. Hepatol.* 1997, *27,* 158-162.

[32] Wills, G.; Phelps, J. *Biochem. Genet.* 1978, *16,* 415-432.

[33] Kruckerberg, A.L.; Dickinson, J.R. In *Physiology of Saccharomyces cerevisiae;* Schweitzer, J.R.D.M.; Ed. CRC Press, Boca Raton, FL 2004, pp. 107-155.

[34] Bakker, B.M.; Bro. C.; Kotter, P.; Luttik, M.A.; van Dijken, J.P.; Pronk, J.T. *J. Bacteriol.* 2000, *182*, 4730-4737.

[35] Johnson, M.A.; Waterham, H.R.; Ksheminska, G.P. et al., *Genetics* 1999, *151*, 1379-1391.

[36] Barone, F.E.; Tansley, M.R. *Mycologia* 1977, *69*, 793-825.

[37] Moore, G.S.; Atkins, R.D. *Mycologia* 1977, *69*, 341-348.

[38] Lemar, K.M.; Turner, M.P., Lloyd, D. *J. Appl. Microbiol.* 2002, *93*, 398-405.

[39] Harris, J.C.; Plummer, S.; Turner, M.P.; Lloyd, D. *Microbiology* 2000, *146*, 3119-3127.

[40] Lemar, K.M. ; Aon, M.A.; Cortassa, S.; O'Rourke, B.; Lloyd, D.. *Yeast* 2007, *24,* 695-706.

[41] Biagini, G.A.; Lloyd, D.; Kirk, K.; Edwards, M.R. *FEMS Microbiol. Lett.* 2001, *192*, 153-157.

[42] Lloyd, D.; Harris, J.C.; Biagini, G.A.; Hughes, m.; Maroulis, S.; Bernard, C.; Wadley, R.B.; Edwards, M.R. *Microbiology*, 2004, *150*, 1183-1190

[43] Chung, I.; Kwon, S.H.; Shim, S.T.; Kyung, K.H. *J. Food Sci.* 2007, *72*, M437-440.

[44] Shoji, S.; Furuishi, K.; Yanase, R.; Miyazaka, R.; Kino, M. *Biochem. Biophys. Res. Commun.* 1993, *194*, 610-621.

[45] Sundaram, S.G.; Milner, J.A. *Carcinogenesis* 1996, *17,* 669-673.

[46] Filomeni, G.; Aquilano, K.; Rotilio, G.; Ciriolo,; M.R. *Cancer Res.* 2003, *63*, 5940-5949.

[47] Park, E.K.; Kwon, K.B.; Park, K.I.; Park, B.H.; Jhee, E.C. Exp. Mol. Med. 2002, 34, 250-257.

[48] Hu, Y.; Urig, S.; Konkarevic, S.; Fischer, M.; Rahlfs, S.; Mersch-Sundermann, V.; Becker, K. J. *Biol. Chem.* 2007, *388*, 1069-1081.

[49] Iciek, M.; Marcinek, J.; Mleczko, U.; Wlodek, L. *Eur. J. Pharmacol*. 2007, *569*, 1 – 5697.

[50] Lemar, K.M.; Passa, O.; Aon, M.A.; Cortassa, S.; O'Rourke, B.; Muller, C.; Lloyd, D. *Microbiology* 2005, *151*, 3257-3265.

[51] Pereira, C.; Silva, R.D.; Saraiva, L.; Johansson, B.; Sousa, M.J., Corte-Real, M. *Biochim. Biophys. Acta*. 2008, *1783*, 1286-1302.

[52] Aon, M.A.; Cortassa, S.; Marban, E.; O'Rourke, B. J. Biol. Chem. 2003, *278*, 44735-44744.

[53] Lemar ,K.L.; Aon,M.A,; Cortassa,S.; O'Rourke,B.; Muller,C.; Lloyd,D. *Yeast* 2007, *24*, 695-706.

[54] Collinson,E.J.; Wheeler,G.L.; Garrido,E.O.; Avery, A.M.; Avery, S; Grant,C.M. *J. Biol. Chem.* 2002, *277*, 16712-16717.

[55] Baek, Y.U.; Kim, Y.R.; Yim, H.S.; Kang, S.O. *FEBS Lett.* 2004, *556*, 47-52.

[56] Tsuchiya, H.; Nagayama, M.J. *Biomed. Sci.* 2008, *15*, 653-660

[57] Tsao, S.; Yin, M. *Antimicrob. Chemother*. 2001, *47*, 665-670.

[58] O'Gara, E.A.; Hill, D.J.; Maslin, D.J. *Appl. Envir. Microbiol*. 2000, *66,* 2269-2273.

[59] Soffar, S.A.; Mokhtar, G.M.; *J. Egypt Soc. Parasitol.* 1991, *21,* 497-502.

[60] Takougang, I.; Meli, J.; Lamlenn, S.; Tatah, P.N.; Ntep, N. *Ann. Trop. Med. Parasitol*. 2007, *101*, 151-160.

[61] Reid, G.; Burton, *J. Microbes Infect.* 2002, *4*, 319-324.

[62] Rees, L.P., Minnis, S.F.; Plummer, N.T.; Slater, J.H.; Skyrme, D.A. *World J. Microb. Biotech*. 1993, *9*, 303-307.

[63] Reid, G.; Burton, J. Microbes Infect. 2002, 4, 319-324.

[64] Kelly, C.P.; Pothoulakis, C.; LaMont, M.T., *N. Engl. J. Med*. 1994, *330*, 257-262.

[65] Eja, M.E.; Arikpo, G.E.; Enyi-Idoh, K.H.; Ikpeme, E.M. *Malay. J. Microbiol*. 2011, *7*, 45-49.

[66] Cottrell, S. An investigation into the antibacterial effects of *Allium sativum* (garlic) Ph.D Thesis Cardiff University, 2003.

[67] Davies, J.; Davies, E. *Microbiol. Mol. Biol. Rev*. 2010, *74*, 417-434.

[68] Fry, F.H.; Okarter, N., Baynton-Smith, C.; Kershaw, M.J., Talbot, N.J.; Jacob, C. J. *Agric. Food. Chem.* 2005, *53*, 574-580.

[69] Hunter, R.; Caira, M.; Stellenboom, N. *Ann. N.Y. Acad. Sci.* 2005, *1056*, 234-241.

[70] Stellenboom, N.; Hunter, R.; Caira, M.R.; Bourne, S.A.; Barbieri, M. *Supramol. Chem.* 2009, *21*, 611-617.

[71] Lloyd, D; Murray, D.B. In *The Redox State and Circadian Rhythms* Vanden Driessche, T. *et al*., Eds. Kluver Academic Publishers,The Netherlands,2002, pp.85-94.

[72] Lloyd, D.; Lemar, K.L.; Salgado, L.E.J.; Gould,T.M.; Murray, D.B. *FEMS Yeast Res*.2003 , *3*, 333-33.

[73] Aon, M.A.; Cortassa, S.; Lemar, K.L.; Hayes, A.J.; Lloyd, D. *FEBS Lett.* 2007, *581*, 8-14.

[74] Aon, M.A.; Cortassa, S.; Maack, C.H.; O'Rourke, B. *J.Biol. Chem.* 2007, *282*, 21889-21900.

[75] Nya, E.J.; Austin, B. *J. Fish Dis.* 2009 *32*, 963-970.

[76] Nya, E.J.; Dawood, Z.; Austin, B. *J. Fish Dis.* 2010, *33*, 293-300.

[77] Skyrme, A. An investigation into the anti-bacterial effects of *Allium sativum.* PhD Thesis, University of Wales, Cardiff, UK, 1996.

[78] Stokes, E.J.; Ridgeway, G.L.; Wren, W.D.D. Clinical Microbiology, 6th. Edn. 1987 Edward Arnold Publishing C. Ltd., London.

APPENDIX IV
TECHNICAL DESIGN NOTE

Evaluation of two novel methods for assessing intracellular oxygen

Catrin F Williams[1]**, M Kombrabail**[2]**, K Vijayalakshmi**[2]**, Nick White**[3]**, G Krishnamoorthy**[2,4] **and David Lloyd**[1,4]

[1] School of Biosciences, Cardiff University, Cathays Park, Cardiff CF10 3AT, UK
[2] Department of Chemical Sciences, Tata Institute of Fundamental Research, Homi Bhabha Road, Mumbai, 400 005, India
[3] Vision Science Bioimaging Labs, School of Optometry and Vision Sciences, Cardiff University, Maindy Road, Cardiff CF24 4LU, UK

E-mail: gk@tifr.res.in and Lloydd@cardiff.ac.uk

Abstract

The ability to resolve the spatio-temporal complexity of intracellular O_2 distribution is the 'Holy Grail' of cellular physiology. In an effort to obtain a non-invasive approach of mapping intracellular O_2 tensions, two methods of phosphorescent lifetime imaging microscopy were examined in the current study. These were picosecond time-resolved epiphosphorescence microscopy (single 0.5 μm focused spot) and two-photon confocal laser scanning microscopy with pinhole shifting. Both methods utilized nanoparticle-embedded Ru complex (45 nm diameter) as the phosphorescent probe, excited using pulsed outputs of Ti-sapphire Tsunami lasers (710-1050 nm). The former method used a 1 ps pulse width excitation beam with vertical polarization via a dichroic mirror (610 nm, XF43) and a 20 $\times$ objective (NA 0.55, Nikon). Transmitted luminescence (1-2 $\times$ 10^4 counts s^{-1}) was collected and time-correlated single photon counted decay times measured. Alternatively, an unmodified Zeiss LSM510 Confocal NLO microscope with 40 $\times$ objective (NA 1.3) used successively shifted pinhole positions to collect image data from the lagging trail of the raster scan. Images obtained from two-photon excitation of a yeast (*Schizosaccharomyces pombe*) and a flagellate fish parasite (*Spironucleus vortens*), electroporated with Ru complex, indicated the intracellular location and magnitude of O_2 gradients, thus confirming the feasibility of optical mapping under different external O_2 concentrations. Both methods gave similar lifetimes for Ru complex phosphorescence under aerobic and anaerobic gas phases. Estimation of O_2 tensions within individual fibroblasts (human dermal fibroblast (HDF)) and mammary adenocarcinoma (MCF-7) cells was possible using epiphosphorescence microscopy. MCF-7 cells showed lower intracellular O_2 concentrations than HDF cells, possibly due to higher metabolic rates in the former. Future work should involve construction of higher resolution 3D maps of Ru coordinate complex lifetime distribution in cultured cell lines.

Keywords: intracellular O_2, two-photon excitation microscopy, pinhole shifting, time-correlated single photon counting, phosphorescence quenching, Ru complex, nanoparticles

(Some figures may appear in colour only in the online journal)

[4] Author to whom any correspondence should be addressed.

1. Introduction

The determination of oxygen tensions within living cells *in vivo* and *in vitro* is of the utmost importance for a deeper understanding of function of their biochemical and physiological functions. O_2 and its reduced products are essential not only for energy production (Chance and Williams 1955), but also for the maintenance of appropriate redox balance (Aon *et al* 2010) and cell signalling (Gitler and Danon 2003). Despite 50 years of research, uncertainties and controversies revolve around published values for tissue and intracellular pO_2. Many diverse methods have been employed; all are subject to problematic aspects and a truly non-invasive approach is still awaited.

Living organisms may be regarded as machines that harness the chemistry of O_2 in a highly controlled and precise series of free-energy conserving reactions. Thus a potentially catastrophically powerful oxidant is delivered to its sites of use with astonishing efficiency and minimal side reactions. Consequently the air we breathe (20.9%; 21.2 kPa O_2; 158 mmHg; equivalent to 278 μM in water at 37 °C) (Wilhelm *et al* 1977) represents for biological systems a huge excess of O_2. When studied *in vitro*, O_2-reactive systems of biological origin have highly avid binding characteristics and these become O_2-saturated at much lower partial pressures than ambient. The human O_2-delivery system (Vanderkooi *et al* 1991) displays a series of step-wise decreasing O_2 levels from alveolar air in equilibrium with arterial blood (containing the equivalent of 100 μM O_2) to the discharge of blood oxyhaemoglobin (depending on CO_2 tension) occurring with the range 80-20 mmHg = 60-30 μM O_2. The oxymyoglobin store of red muscle begins to unload at below 10 μM O_2 and the working pO_2 in active muscle is only about 3 mmHg (Wittenberg and Wittenberg 1989). The mean O_2 levels within the cells of some other human tissues are also unexpectedly low, e.g. 6-16 mmHg in white brain cortex (Cater *et al* 1961) and 7 mmHg in kidney medulla (Brezis *et al* 1984). Sites of O_2 utilization within cells include the mitochondria, peroxisomes and the membranes of the endoplasmic reticulum. Cytochrome *c* oxidase, the binuclear Cu-Fe haemoprotein, reacts by way of a multistage cyclic mechanism whereby a concerted and highly efficient four-electron reduction of O_2 on the inner surface of the inner mitochondrial membrane (Km $O_2 <$ 0.1 μM, Schindler 1964) leads to a residual steady-state level of O_2 that has not yet been accurately assessed. This can, however, be estimated indirectly by *in situ* non-invasive observations of the redox states of respiratory chain components using fluorimetric measurements for NAD(P)H (Chance *et al* 2005), and spectrophotometric measurements for flavoproteins and cytochromes (Jones and Mason 1978, Lloyd *et al* 1983).

Arguments that experimental conditions (e.g. use of anaesthetics) contribute to very low pO_2 values (Whalen and Nair 1967) in mammalian tissues do not apply in experiments with cultured cell lines and microorganisms. In many microorganisms, and especially in bacteria inhabiting low-oxygen environments, affinities for O_2 are very high (Lloyd 2002). Thus in *Escherichia coli* the cytochrome *bd* has a Km O_2 of 5 nM O_2 (D'Mello *et al* 1996).

The heterogeneous intracellular distribution of these sites of biological oxidation between individual classes of organelles and membranes results in a highly dynamic pattern of O_2 gradients on a sub-micrometre scale. The 'Holy Grail' of cellular physiology is to resolve the spatio-temporal complexity of intracellular O_2 distribution by constructing four-dimensional maps. Although two-photon excitation enables their dynamic imaging (Lemar *et al* 2007), quantification of the various species of reactive O_2 (OH^-, O_2^{--}, H_2O_2 and singlet O_2) in the past has largely relied on indirect data and has been often overestimated (Murphy 2009). On a larger scale, the dynamic distribution of O_2 *in vivo* in body fluids, tissues and organs is an important research aim, and a number of fluorophores and luminophores have been used for this purpose (Vanderkooi *et al* 1991, Vinogradov *et al* 1996, Devor *et al* 2011). Important features of delivery of O_2 to tissues thereby emerge.

Fluorescence lifetimes of organic fluorophores are mostly of the order of 10-20 ns and the diffusion path of a small molecule is very short (Suhling *et al* 2004). Extra time during which diffusion may occur greatly increases the volume of solution that influences the excited state of each fluorophore molecule (Vaughan and Weber 1970). Thus for some exceptionally long-lived cases, e.g. pyrenebutyric acid (100 ns in air-saturated water), the O_2-sensing sphere of influence of the probe is increased from 100 to 1000 times over that volume affecting the shorter lived excited molecules. This exceptionally long-lived fluorescent state has been employed for O_2-mapping in living cells, e.g. in cultured cells of mouse liver by the use of quantitative fluorescence microscopy (Benson *et al* 1980) and in *Amoeba proteus* (Podgorski *et al* 1981). The even longer lifetimes provided by O_2-quenchable phosphorescent luminophores (Vanderkooi *et al* 1987, Elson *et al* 2004, DeGraaf and Demas 2005), together with their other desirable photophysical properties (Amoroso *et al* 2007, 2008, Coogan *et al* 2010, Fernandez-Moreira *et al* 2010, Thorp-Greenwood *et al* 2011, Lloyd *et al* 2011) make them substances of choice for a burgeoning body of research.

For O_2 sensing, Ru(II) complexes show many advantages (Watts and Crosby 1971, Bacon and Demas 1987, Castellano and Lakowicz 1998). Lifetime measurements (Draaijer *et al* 1995, Periasamy *et al* 1996, Morris *et al* 2007) obviate or minimize some of the deficiencies of intensity determinations especially with respect to environmental influences (concentration of fluorophore, variation in excitation intensity, collection efficiency, propinquity to hydrophobic proteins or membranes, gradients of pH or ionic strength, etc (Zhong *et al* 2003, Botchway *et al* 2008)). Encapsulation in porous nanoparticles goes a further stage to making reliable intracellular assessments (Clark *et al* 1999, Buck *et al* 2004, Poulsen *et al* 2007, 2008a, 2008b).

In this paper we show that two independent approaches, namely pinhole shifting in a two-photon excitation beam and epiphosphorescence time-correlated single photon counting (TCSPC), give similar estimates of local O_2 concentrations within several different single-celled organisms and in suspension.
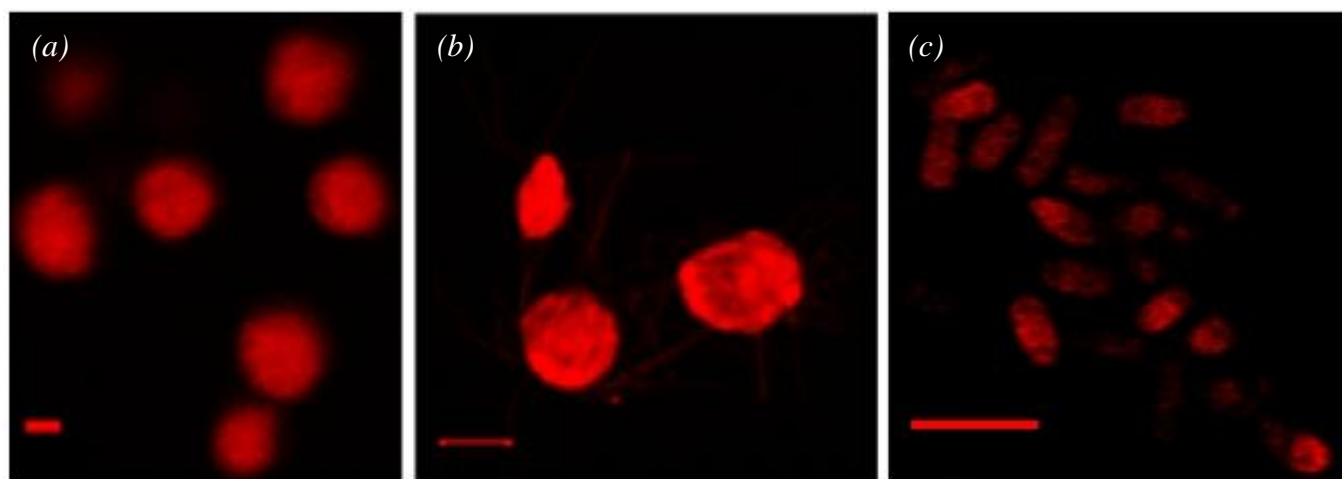
211

Figure 1. Two-photon confocal images of Ru coordinate complex electroporated into: (*a*) human adenocarcinoma (MCF-7) cells, (*b*) the flagellated protist, *Sp. vortens*, and (*c*) the fission yeast, *S. pombe*. Scale bars = 10 μm.

2. Materials and methods

2.1. Yeast and spironucleus cultures

The fission yeast *Schizosaccharomyces pombe* 972h- was maintained and grown on Petri dishes containing Sabouraud Maltose Agar (Difco). Organisms were transferred to unbaffled Ehrlenmayer flasks (50 ml) containing 10 ml YEPD liquid medium (0.3% yeast extract, 1% peptone and 1% glucose) and grown at 30 °C for 2 days on a rotary shaker at 150 rpm. Before electroporation, repeated centrifugation for 3 min at 2000 rpm (3000 g min) and re-suspension in 1.0 M sorbitol solution removed all nutrients. *Spironucleus vortens* was cultured as described by Millet *et al* (2010).

2.2. Human cells

Cultured cell lines, human mammary adenocarcinoma, MCF-7, were from the European Collection of Cell Cultures, Porton Down, Wiltshire, UK. Human fibroblasts (human dermal fibroblast (HDF) cells) were from TIFR Biology stocks. Cancer cells and HDF were maintained in Eagles Minimal Essential Medium supplemented with 10% foetal bovine serum, penicillin and streptomycin. Detachment from the plastic culture flasks was carried out using trypsin/EDTA, and was followed by re-suspension in growth medium.

2.3. Nanoparticle preparation

The Ru coordinate complex employed as a phosphorescent probe here has been extensively used and has proven a highly efficient O_2 sensor. Reagents (from Sigma-Aldrich) were $RuCl_3$ (57 mg, 0.0276 mmol) and 4,7-diphenyl-1, 10-phenanthroline disulfonic acid disodium salt (518 mg, 0.0965 mmol) in 20 ml distilled water refluxed with stirring for 2 days. After filtration and rotary evaporation, the product, $Ru([dpp(SO_3Na)_2]_3)Cl_2.6H_2O$, was passed down a Sephadex G25 size exclusion column and eluted with water. The first brown and purple fractions were discarded and the red fraction dried.

The product is $Ru([dpp(SO_3Na)_2]_3)Cl_2.6H_2O$ and it contains several isomers with the -SO_3Na substituents randomly positioned on the phenyl rings. However, previous reports indicate that the mixture of isomers gives no evidence of heterogeneous fluorescent lifetimes. Characterization of the
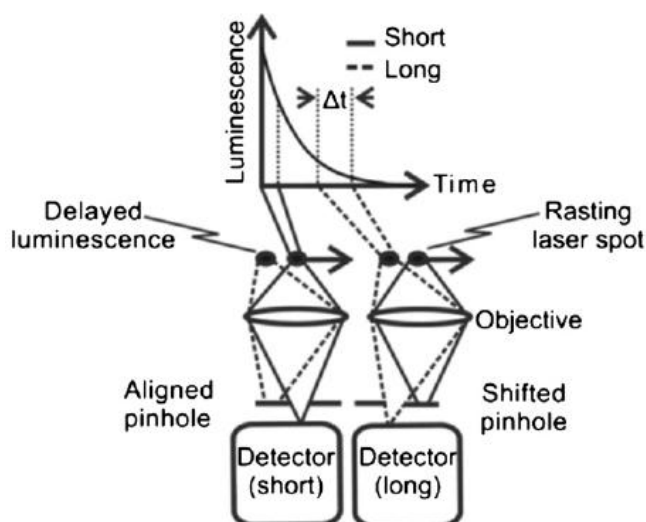

Figure 2. Schematic diagram of time-delayed image collection in the lagging direction of the raster scanned two-photon excitation beam (Ramshesh and Lemasters 2008).

compound by standard methods was performed as described (Castellano and Lakowicz 1998). The nanosensors were prepared by incorporation of $Ru([dpp(SO_3Na)_2]_3Cl_2.6H_2O$ by encapsulation using radical polymerization added drop-wise into a solution of 43 ml hexane, 3.08 g AOT and 1.59 g Brij30 in a round bottom flask. The solution contained 2.7 g acrylamide and 0.8 g N,N -methylenebis(acrylamide), and 9 ml of 10 mM sodium phosphate buffer, pH 7.2, were added to the microemulsion. The solution was stirred under argon throughout the preparation and deoxygenated by three freeze- vacuum-thaw cycles using liquid nitrogen as freezing medium.

To initiate the polymerization, 50 μl of a 10% (w/w) sodium bisulfite solution was added. The solution was kept under argon and stirred at room temperature for 2 h to ensure complete polymerization. Hexane was removed by rotary evaporation and the remaining solution was re-suspended in 96% ethanol and transferred to an Amicon ultra-filtration cell model 8200 (Millipore Corp., Bedford, MA, USA). The solution was washed with 600 ml 96% ethanol in order to separate surfactants, unreacted monomers and excess proteins from the
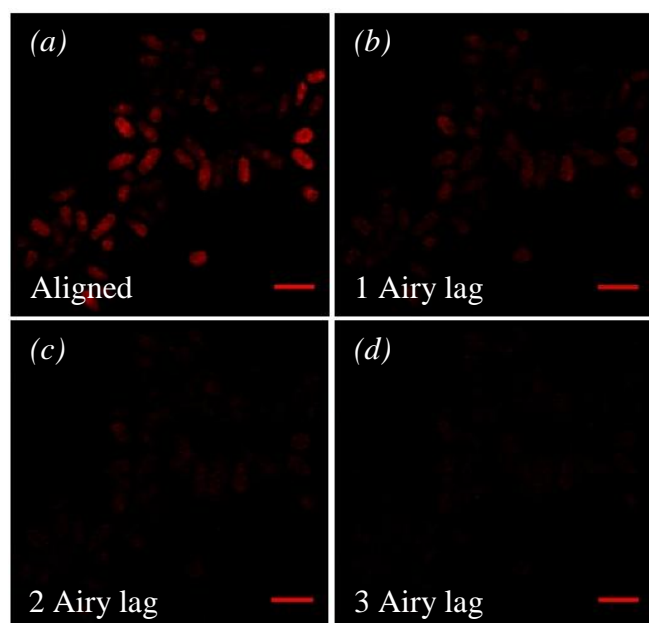
Figure 3. Two-photon laser scanning confocal images of Ru nanoparticle-electroporated *S. pombe* acquired by using (*a*) the optically-aligned excitation beam, (*b*), (*c*), (*d*) the pinhole shift giving displacement by 1, 2 or 3 Airy units, respectively. Scale bars = 10 μm.

Table 1. Lifetime of Ru nanoparticles in suspension or electroporated into MCF-7, Fixed yeast or HDF cells under aerobic (air) or anaerobic (nitrogen[b] or argon[c]) conditions, assayed by spectrometry, pinhole-shifting and epiphosphorescence-TCSPC methods. Different gas phases are expressed as equivalent dissolved [O$_2$] (mM).

Method Employed	[O$_2$] mM	Ru lifetime (μs)
Spectrometry* (Ru nanoparticles in suspension or in MCF-7 cells (in parentheses))	0	3.88 (4.06)[a]
	0.26	1.81 (2.29)
Pinhole shifting Fixed yeast	0	3.19[b]
	0.26	1.65
Epiphosphorescence TCSPC in buffer	0	3.28[a]
	0.26	0.95

[a]Values taken from Coogan *et al* (2010).

sensors using a 100 kDa filter under 2 bar pressure. The polymer particles containing Ru complex were then re-suspended in ethanol and passed through a suction filtration system (Millipore Corp., Bedford, MA) with a 0.025 μm nitrocellulose filter membrane and rinsed with 100 cm^3 ethanol. Hydrodynamic particle diameter (45 nm) was determined by right-angle light scatter of 632.8 nm laser light (HeNe) using a BI-200SM Goniometer (Brookhaven Inst., New York). Nanoparticles were stored at –18 °C. Re- suspension (18 mg ml^{-1}) was in 1.0 M sorbitol and dispersion was by treatment with 20 kHz ultrasound for 30 s at 4 °C at an amplitude providing the maximum cavitation intensity.

Table 2. Estimation of oxygen concentration in MCF-7 and HDF cells by the epiphosphorescence-TCSPC method. Each measurement corresponds to a different cell. Measurements made at regions either close to the centre or close to plasma membrane were made in the same cell. Cells were equilibrated with air ([O$_2$] = 0.26 mM).

Cell type	Cell no.	[O$_2$] mM Close to centre	Close to plasma membrane
MCF-7	1	0.13	0.25
	2	0.12	0.18
	3	0.12	0.15
	4	0.13	0.20
	5	0.16	0.26
HDF	1	0.24	0.25
	2	0.21	0.27
	3	0.23	0.28
	4	0.19	0.27
	5	0.22	0.25

2.4. Electroporation of nanoparticles into yeast, Sp. vortens, or human cells

The Biorad Labs Gene Pulser Transfection Apparatus (Bio-Rad Laboratories, CA) was fitted with a Capacitor Extender set at 450 V for yeasts and 340 V for human cells (capacitance 900 μF, resistance 200). Electroporation vessels were of 400 μl working volume; three high voltage pulses were employed.

2.5. Pinhole shifting with two-photon excitation confocal microscopy

Ramshesh (2007) and Ramshesh and Lemasters (2008) have described time-resolved imaging of long-lifetime luminescence of europium (Eu^{3+}) microspheres, and explored some aspects of the potential usefulness of the method for biological applications (e.g. O$_2$ sensing in feline myocytes). As in the original method used by these authors, we employed a Zeiss LSM510META NLO confocal

microscope with a Coherent Chameleon 140 fs pulsed Ti-sapphire laser system (with integral pump lasers) for two-photon excitation at 900 nm. This excitation avoids much of the autofluorescence expected from shorter wavelengths and also the longer wavelengths reduce the level of detection of any unblocked (reflected) IR since the PMTs are less sensitive. The single- photon excitation peak is at 450 nm. While this is not definitely predictive of a two-photon peak at 900 nm (i.e. 2 $\times$) this was a natural wavelength to choose in the absence of other information. An analysis of excitation efficiency at all available wavelengths is quite difficult, given the many variables involved, and because of this we have yet to seek a better wavelength to use. We used about 20% of the maximum laser intensity at the specimen plane. The ruthenium nanoparticles were imaged through a 685 nm shortpass emission filter after beam separation by a 545 nm longpass dichroic mirror using a 40 $\times$ 1.3NA Plan-Neofluar (Zeiss) oil immersion. The 685 nm shortpass filter is an IR blocking filter specifically designed for multiphoton imaging, i.e. to block the reflection of the TiS laser.
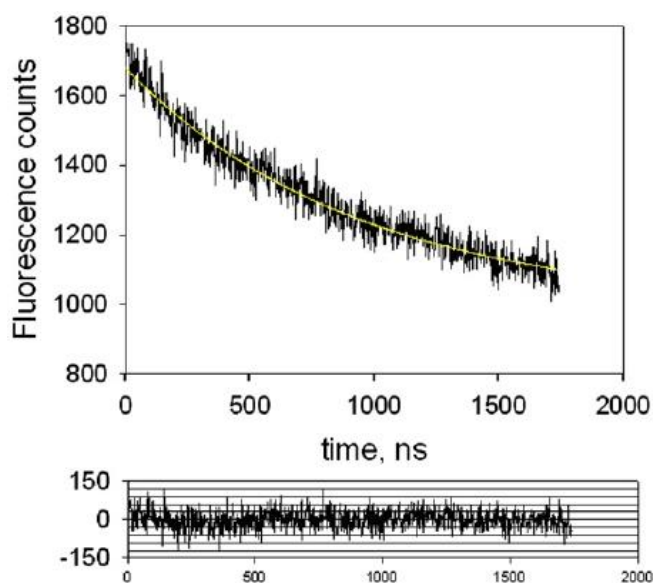
213

Figure 4. Typical phosphorescence trace (fitted line plot) of Ru complex-loaded nanoparticles taken up by HDF cells by epiphosphorescence. The estimated lifetime value is 0.93 μs. Residuals are given in the bottom panel. Residual intensity was due to residual levels of dark counts.

By collecting successive images from shifted confocal pinhole positions to image data from the lagging trail of the raster scan, a series of images was collected. Image intensities were determined using the standard Zeiss LSM software and plotted as a function of decay times (calculated from scan speed, pinhole offset and consequent image displacement from the optical axis).

2.6. Epiphosphorescence TCSPC

The ime-resolved fluorescence microscope was a combination of picosecond time-resolved fluorescence spectromenter and an inverted epiphosphorescence microscope (Paila *et al* 2011). The ime-resolved epiphosphorescence measurements were carried out with a TCSPC setup coupled with a picoseconds laser. A titanioum-sapphire picoseconds laser beam (Tsunami, Spectra Physics) pumped by a diode pumped CWNd-vanadate laser (532 nm) (Millenia X, Spectra Physics), and frequency doubled by a doubler, was used to excite a single cell at 495 nm. The pulse width of the excitation laser beam was typically ~1 ps. A pulse repetition rate of 80 MHz was reduced to a repetition rate of 0.5 MHz by a pulse picker. The ps pulses obtainedafter frequency doubling were guided to the objective lens by a dichroic mirror and focussed onto a single cell. The diameter of the focused beam was ~0.5 μm in the *xy* plane. The measurements typically require ~100 luminophore molecules in the observation volume. The instrument response function was estimated by the use of oxonol VI whose fluorescence lifetime is <50 ps. The full width at half maximum height of the instrument response function estimated in this way was ~160 ps. Phosphorescnece decays were analyzed fir a single exponential function by using the nonlinear fitting. Since the repetition rate (0.5 MHz) of the excitation pulse was shorter than the measured lifetimes we ensured that our analysis took care of the incomplete decay coming from the previous

excitation pulse. However, for single exponential decays this overlap does not cause any problem in the analysis even if the incomplete decays from the previous pulses are not taken into account.

3. Results, discussion and future work

Figure 1 shows that electroporation is an effective method for loading cells and organisms with polyacrylamide nanoparticles containing the Ru coordinate complex. For all three populations of organisms, nanoparticles have entered all cells. The images indicate that intracellular distributions are not confined to any specific subcellular organelles, although the distribution within a cell is heterogeneous and some organelles (e.g. nuclei) show lower intensity of emission. The method of laser scanning microscopy to acquire sequential images with delayed lifetimes (Ramshesh 2007, Ramshesh and Lemasters 2008) is shown in figure 2. This confocal pinhole-shifting method was employed in the current study, and allowed adequate resolution of the extent of phosphorescence quenching inside cells (figure 3).

In an alternative approach, time-resolved single photon counting of epiphosphorescence provides traces of decay kinetics: a typical trace (figure 4) indicates that both approaches to the determination of Ru nanoparticle phosphorescence lifetimes give similar values. For ethanol fixed dead *S. pombe* pinhole shifting under an anaerobic atmosphere gave a lifetime of 3.19 μs. This compared favourably to a corresponding value of 3.28 μs using the epiphosphorescence-TCSPC method, as well as a previously publishedvalue of 3.88 μs obtained using spectroscopy by Coogan *et al* (2010) (table 1). Slight differences in lifetime values obtained frim the latter method may be due to more efficient N_2 saturation of the cell/particle suspension, whereby three cycles of O_2 evacuation were employed prior ro generation of an anaerobic environment. Similar values were also obtained under air.

For living organisms or cultured cells, shorter phosphorescence lifetimes indicated quenching of Ru coordinate complex by intracellular O_2. Lifetime values obtained by epiphosphorescence TCSPC differed amongst the varying biological specimens, for example MCF-& cells showed lower O_2 concentrations than fibroblasts (table 2), possibly due to the higher metabolic rates in the former. These data also suggested slight differences between micro sites within an individual cell, with higher O_2 concentrations near the periphery of the cytosol (table 2). As yet, we have no values for intra-mitochondrial pO_2 where at the point of O_2 consumption values would be much lower. Higher resolution of the subcellular structure would provide detailed maps of O_2 distribution in 3D using *xy* scans at successive *z* coordinates. For this higher power objectives and appropriately adjusted paramenters will be employed. Figure 5 shows a typical standard curve obtained frim the epiphosphorescence-TCSPC method. This curve was used in estimations of O_2 concentrations inside a single HDF cell (figure 6). Time-dependent variations in intracellular O_2 concentration, if confirmed in a more systematic study, would be useful in revealing metabolic oscillations.

Major considerations of choice between the two methods employed in this study include biological information required and cost. While raster scanning two-photon excitation potentially provides 3D rendered images, epiphosphorescence photon quenching gives single point determinations. However, the cost implications of the former method are considerably greater.

Images obtained from two-photon excitation of a yeast (*S. pombe*) and a flagellate fish parasite (*Sp. vortens*) indicated the intracellular location and magnitude of O_2 gradients and confirmed the feasibility of optical mapping of cells and organisms under different external conditions. As well as obtaining measurements from single cells, Ru coordinatecomplex may prove useful to measure O_2 gradients *in situ* not only from intracellular sites, but also in interstitial extracellular locales (e.g. matrix elements in connective tissues) and in body fluids. However, further work is necessary to make reliable measurements of physiological significance.

Acknowledgments

References

Amoroso A J *et al* 2007 Rhenium fac-tricarbonyl bisimine complexes: biologically useful flurochromes for cell imaging application *Chem. Commun.* **29** 3066-8

Amoroso A J *et al* 2008 3-chloromethyl pyridyl bipyridine fac-tricarbonyl rhenium: a thiol-reactive luminophore for fluorescence microscopy accumulates in mitochondria *New J. Chem.* **32** 1097-102

Aon M A, Cortassa S and O'Rourke B 2010 Redox-optimized ROS balance: a unifying hypothesis *Biochim. Biophys. Acta* **1797** 865-77

Bacon J R and Demas J N 1987 Determination of oxygen concentrations by luminescence quenching of a polymer immobilized transition-metal complex *Anal. Chem.* **59** 2780-5

Benson D H, Knopp J A and Longmuir T S 1980 Intracellular oxygen measurements of mouse liver cells using quantitative fluorescence microscopy *Biochim. Biophys. Acta* **591** 187-97

Botchway S W *et al* 2008 Time-resolved and two-photon emission imaging microscopy of live cells with inert platinum complexes *Proc. Natl Acad. Sci. USA* **105** 16071-6

Brezis M, Rosen S, Silva P and Epstein F H 1984 Renal ischemia in a new perspective *Kidney Int.* **26** 375-83

Buck S M *et al* 2004 Optochemical nanosensor PEBBLEs: photonic explorers for bioanalysis with biologically localized embedding *Curr. Opin. Chem. Biol.* **8** 540-6

Castellano F N and Lakowicz J R 1998 A water-soluble luminescence oxygen sensor *Photochem. Photobiol.* **67** 179-83

Cater D B, Geraltini S, Marina F and Silver I 1961 Changes in oxygen tension in brain and somatic tissues induced by vasodilator and vasoconstrictor substances *Proc. R. Soc.* B **155** 136-57

Chance B, Noka S, Warren W and Yurtsever G 2005 Mitochondrial NADH as the bellwether of tissue O_2 delivery *Adv. Exp. Biol.*

Med. **566** 231-62

Chance B and Williams G R 1955 The respiratory chain and oxidative phosphorylation *J. Biol. Chem.* **217** 429-38 Clark H A, Hoyer M, Philbert M A and Kopelman R 1999 Optochemical nanosensors for chemical analysis in living cells *Anal. Chem.* **71** 4831-6

Coogan M P *et al* 2010 Probing intracellular oxygen by quenched phosphorescence lifetimes of nanoparticles containing polyacrylamide-embedded [Ru(dpp(SO_3Na)$_2$)$_3$]Cl_2 *Photochem. Photobiol. Sci.* **9** 103-9

DeGraaf B A and Demas J N 2005 Luminescence-based oxygen sensors *Reviews in Fluorescence* vol 2 ed C Geddes and J R Lakowicz (New York: Springer) pp 125-51

Devor A *et al* 2011 'Overshoot' of O_2 is required to maintain baseline tissue oxygenation at locations distal to blood vessels *J. Neurosci.* **31** 13676-81

D'Mello R, Hill S and Poole R K 1996 The cytochrome bd quinol oxidase in *Escherichia coli* has an extremely high oxygen affinity and two oxygen-binding haems: implications for regulation of activity *in vivo* by oxygen inhibition *Microbiology* **142** 755-63

Draaijer A, Sanders A and Yerritsen H C 1995 Fluorescence lifetime imaging, a new tool in confocal microscopy *Handbook of Biological Confocal Microscopy* 2nd edn ed J B Pawley (New York: Plenum) pp 491-505

Elson D *et al* 2004 Time-domain fluorescence lifetime imaging applied to biological tissue *Photochem. Photobiol.* **3** 795-801

Fernandez-Moreira V *et al* 2010 Uptake and localisation of rhenium fac-tricarbonyl polypyridyls in fluorescent cell imaging-experiments *Org. Biomol. Chem.* **8** 3888-901

Gitler C and Danon A (eds) *Cellular Implications of Redox Signalling* (London: Imperial College Press) p 427

Jones D P and Mason H S 1978 Gradients of O_2 concentration in hepatocytes *J. Biol. Chem.* **253** 4874-80

Lemar K M, Aon M A, Cortassa S, O'Rourke B, Muller C T and Lloyd D 2007 Diallyl disulphide depletes glutathione in Candida albicans: oxidative-stress mediated cell death studies by two-photon microscopy *Yeast* **24** 695-706

Lloyd D 2002 Noninvasive methods for the investigation of organisms at low oxygen levels *Adv. Appl. Microbiol.* **51** 155-83

Lloyd D, Coogan M P and Pope S J A 2011 Novel metal-based luminophores for biological imaging *Reviews in Fluorescence 2010* ed C D Geddes (New York: Springer) pp 15-44

Lloyd D, Mellor H and Williams J L 1983 Oxygen affinity of the respiratory chain of *Acanthamoeba castellanii Biochem. J.* **214** 47-51

Millet C O M, Lloyd D, Williams C F and Cable J 2010 *In vitro* culture of the diplomonad fish parasite *Spironucleus vortens* reveals unusually fast doubling time and a typical biphasic growth *J. Fish Dis.* **34** 71-3

Morris K J, Roach M S, Xu W, Demas J N and DeGraff B A 2007 Luminescence lifetime standards for the nanosecond to microsecond range and oxygen quenching of Ru(II) *Anal. Chem.* **79** 9310-4

Murphy M P 2009 How mitochondria produce reactive oxygen species *Biochem. J.* **417** 1-13

Paila Y D, Kombrabail M, Krishnamoorthy G and Chattopadhyay A 2011 Oligomerizarion of serotonin$_{1A}$ receptor in live cells: a time-resolved fluorescence anisotropy study *J. Phys. Chem.* B **115** 11439-47

Periasamy A *et al* 1996 Time-resolved fluorescence lifetime imaging microscopy using a picosecond pulsed tuneable dye laser system *Rev. Sci. Instrum.* **67** 3722-31

Podgorski G T, Longmuir I S, Knopp J A and Benson D M 1981 Use of an encapsulated fluorescent probe to measureintracellular PO_2 *J. Cell. Physiol.* **107** 329-34

Poulsen A K, Andersen A Z, Brasen J C, Sharff-Poulsen A

M and Olsen L F 2008a Probing glycolytic and membrane
potential oscillations in *Saccharomyces cerevisiae*
Biochemistry **47** 7447-84

Poulsen A K, Arleth L, Almdalk K and Scharff-Poulsen A M 2008b
Unusually large acrylamide induced effect on the droplet size
in AOT ∕Brij30 water-in-oil emulsions *J. Colloid Interface Sci.*
306 143-53

Poulsen A K, Sharff-Poulsen A M and Olsen L F 2007 Horseradish
peroxidase embedded in polyacrylamide nanoparticles enable
optical detection of reactive oxygen species *Anal. Biochem.*
366 29-36

Ramshesh V K 2007 Luminescence lifetime imaging microscopy by
confocal pinhole shifting (LLIM-CPS) *PhD Thesis* University
of North Carolina at Chapel Hill, NC, USA

Ramshesh V K and Lemasters J J 2008 Pinhole shifting lifetime
imaging microscopy *J. Biomed. Opt.* **13** 064001

Schindler F 1964 Oxygen kinetics in the cytochrome-oxygen
reaction *PhD Thesis* University of Pennsylvania (University
Microfilms Inc., Ann Arbor, MI)

Suhling K, French P M and Phillips D 2004 Time resolved
fluorescence microscopy *Photochem. Photobiol. Sci.*
4 13-22

Thorp-Greenwood F L *et al* 2011 A 'Sleeping Trojan Horse' which
transports metals into cells localises in nucleoli and has
potential for bionodal fluorescence ∕PET imaging *Chem.
Commun.* **47** 3096-8

Vanderkooi J M, Erecinska M and Silver I A 1991 Oxygen in
mammalian tissue: methods of measurement and affinities of
various reactions *Am. J. Physiol.* **260** C1131-50

Vanderkooi M, Maniara G, Green T J and Wilson D F 1987 An
optical method for the measurement of dioxygen concentration
based upon quenching of phosphorescence *J. Biol. Chem.*
262 3476-82

Vaughan W M and Weber G 1970 Oxygen quenching of
pyrene butyric acid fluorescence in water *Biochemistry*
9 464-73

Vinogradov S A, Jenkins W I W T, Evans S M, Koch C
and Wilson D F 1996 Non invasive imaging of the distribution
oxygen in tissue *in vivo* using near infrared phosphors *Biophys.
J.* **70** 1609-17

Watts R J and Crosby G A 1971 Spectroscopic characterization of
complexes of ruthenium (II) and iridium (II) with 4,4 diphenyl 2,2
bipyridine and 4,7-diphenyl-1,10-pehenanthroline *J. Am.
Chem. Soc.* **93** 3184-8

Whalen W J and Nair P 1967 Intracellular pO_2 and its regulation in
resting skeletal muscle on the guinea pig *Circ. Res.*
21 251-61

Wilhelm E, Battino O R and Woodcock R J 1977 Low pressure
solubility of gases in liquid water *Chem. Rev.* **77** 219-50

Wittenberg B A and Wittenberg J B 1989 Transport of oxygen in
muscle *Ann. Rev. Physiol.* **51** 857-78

Zhong W, Uravama P and Mycek M A 2003 Lifetime modulation of
a ruthenium-based dye in living cells: the potential for oxygen
sensing *J. Phys. D: Appl. Phys.* **36** 1689-95